

## REVIEW ARTICLE

# Zika virus infection from a newborn point of view. TORCH or TORZiCH?

Adriana TAHOTNÁ<sup>1</sup>, Jana BRUCKNEROVÁ<sup>1</sup>, Ingrid BRUCKNEROVÁ<sup>2</sup>

<sup>1</sup>Faculty of Medicine Comenius University in Bratislava, Slovakia

<sup>2</sup>Neonatal Department of Intensive Medicine, Medical Faculty, Comenius University in Bratislava and National Institute of Children's Diseases

ITX110418A01 • Received: 30 September 2018 • Accepted: 21 December 2018

## ABSTRACT

Zika virus (ZIKV) belongs to the group of viruses called arboviruses. Congenital Zika syndrome is a new disease with infectious teratogenic aetiology. The clinical symptoms are divided into morphological and functional. Most severe complication is the foetal brain disruption sequence that includes severe microcephaly, anomalies of the eyes and congenital contractions of joints. The aim of this paper was to review available facts about Zika virus infection from a newborn point of view in a form of the summary of all important information. Zika virus infection is a problem of past, present and future. Epidemics may occur because of global climate changes, also in countries where natural conditions for life of mosquitos are not present. This clearly indicates the need to continue developing of vaccines and specific antiviral drugs. Until this happens, we must adhere individual preventive measures. Zika virus has proven to us how it can affect the health of adults and neonates but also thinking of healthy people. Newborns with microcephaly on the front pages of the media caused in 2015 panic and fear around the world – for this reason education of people is necessary. Due to serious congenital disorders associated with ZIKV infection and global impact of virus we suggest modifying old acronym TORCH for new TORZiCH to accent the position of Zika virus.

**KEY WORDS:** newborn; Zika virus; complications; diagnosis; treatment

**ABBREVIATIONS:** **AMC:** arthrogryposis multiplex congenita; **BAEPs:** brainstem auditory evoked potentials; **CSF:** cerebrospinal fluid; **CMV:** cytomegalovirus; **FBDS:** Foetal brain disruption sequence; **GBS:** Guillain-Barré syndrome; **HSV:** herpes simplex virus; **ICH:** immunohistochemistry; **NAAT:** nucleic acid amplification test; **PRNT:** plaque reduction neutralization test; **TORCH:** most common vertically transmitted pathogens; **ZIKV:** virus Zika

## Introduction

Zika virus infection is a disease caused by virus Zika (ZIKV). In 2016, WHO declared ZIKV infection a public health emergency of international concern. Despite the great effort of scientists, we do not have an effective, specific therapy or vaccine yet. This is a summary of all important information about ZIKV infection from a comprehensive view.

Zika virus belongs to the group of viruses called arboviruses (arthropod-borne viruses). According to International Committee on Taxonomy of Viruses is ZIKV classified in genus *Flavivirus*, the family *Flaviviridae*. Viral particle is composed from nucleocapsid (+ssRNA

and C protein) and lipid bilayer (with glycoproteins M and E). It has very similar replicative cycle as other types of flaviviruses – after attaching to the receptor of host cell enters the cell through endocytosis. There are several entry factors, for example TAM family of receptor tyrosine kinases (TYRO3, AXL, and MER), T cell immunoglobulin, TIM proteins, C-type lectin receptors and the phosphatidylserine receptors (Perera-Lecoin *et al.*, 2014). Viral RNA is used for synthesis of polyprotein and it replicates itself on the surface of endoplasmic reticulum. Polyprotein is divided into three structural (C, E and M protein) and seven non-structural proteins (Bolatti *et al.*, 2010). Epidermal fibroblasts, epidermal keratinocytes and immature dendritic cells are more susceptible for ZIKV infection (Musso & Gubler, 2016).

## History

Virus itself does not have long history, because it was discovered in 1947 in Uganda during research for yellow fever virus and named after the forest where it was

Correspondence address:

**Prof. Ingrid Brucknerová, MD., PhD.**

Neonatal Department of Intensive Medicine  
Comenius University in Bratislava and  
National Institute of Children's Diseases  
Limbova 1, 833 40 Bratislava, Slovakia  
E-MAIL: [ingrid.brucknerova@fmed.uniba.sk](mailto:ingrid.brucknerova@fmed.uniba.sk)

discovered (Musso & Gubler, 2016). ZIKV was the first time isolated from human (ten years old Nigerian girl) in 1954 (MacNamara, 1954). First outbreak was in 2007 in Yap State – it is one of four states in the Federated States of Micronesia, located in the Western Pacific. In 2013, 28 000 of people were infected during outbreak in French Polynesia followed by the spread to the islands in Oceania, including New Caledonia, Cook Islands and Easter Island. The first cases of infection in America were reported in 2014 in northeastern Brazil. For first months of 2015, the infection has rapidly spread across Brazil (Musso & Gubler, 2016).

According to WHO situation report, there is 84 countries with evidence of vector-borne ZIKV transmission and 64 countries where the competent vector is established but with no documented past or current ZIKV transmission. 13 countries have reported evidence of person-to-person transmission of ZIKV and 31 countries have reported microcephaly or other CNS malformations potentially associated with ZIKV infection. 23 countries have reported increased incidence of Guillain-Barré syndrome (GBS) and/or laboratory confirmation of ZIKV infection among GBS cases (WHO, 2017).

#### Transmission

The most common method is vector-borne transmission, mostly by the bite of an infected *Aedes* species mosquito. These are distributed around the world, but we can find them mostly in subtropical and tropical areas. The virus continues to spread geographically to areas where competent vectors are present. ZIKV has two different geographical lines – African and Asian, so it circulates in two different cycles – sylvatic and urban. Sylvatic cycle is between monkeys and tropical mosquitos (for example *Aedes africanus*, *Aedes furcifer-taylori*, etc.) mostly in Africa. Urban cycle is between human and domestic mosquitos (for example *Aedes aegypti* or *Aedes albopictus*) mostly in Asia (Weaver *et al.*, 2016). The most important mosquitos in transmission are *Aedes africanus*, *Aedes aegypti*, *Aedes albopictus* and *Aedes hensilli*. First isolation of ZIKV from mosquito *Aedes africanus* has been made in 1948, Uganda (Dick *et al.*, 1952).

Other methods are from mother to child (during pregnancy or around the time of birth), through sexual intercourse (vaginal, anal and oral sex) and blood transfusion. Transmission methods as organ transplantations or laboratory exposure are currently being investigated.

Transplacental transmission has been confirmed using RT-PCR for detection of ZIKV RNA in amniotic fluid of symptomatic pregnant women (Oliveira Melo *et al.*, 2016). First case of perinatal infection has been reported during outbreak in French Polynesia in 2013 (Besnard *et al.*, 2014). Zika fever is sexually transmitted disease, virus was isolated from semen of symptomatic patient with hematospermia (Musso *et al.*, 2015) and can be passed through sex from infected person to his or her partner, even if the infected person does not have symptoms. Transmission by blood derivatives was confirmed in Brazil (Motta *et al.*, 2016). The number of reported cases of ZIKV

transmission by blood products is low, even in countries with outbreaks. However, Zika virus may be present in the blood of the patient within 4 weeks after the onset of the symptoms of infection. ECDC recommends people who have been in endemic or risk areas should postpone donation of blood for at least 28 days (ECDC, 2016).

#### Symptoms

Approximately 80% of patients with ZIKV infection are asymptomatic. The most common symptoms are fever, exanthema, headache, arthritis and/or joint pain and/or muscle pain, conjunctivitis and fatigue. In tropical areas is very common that patient infected with ZIKV had been previously infected with other disease (e.g. malaria), then is very difficult to find right diagnosis (Musso & Gubler, 2016).

ZIKV can damage cells of central nervous systems directly or indirectly (through immune mechanisms). In case of transplacental infection, ZIKV infects neural progenitor cells or neural cells of retina and causes congenital Zika syndrome. In case of adult infection, ZIKV can cause paralysis due to myelitis (damage of motor neurons) or GBS. GBS or acute inflammatory demyelinating polyradiculoneuropathy is autoimmune disorder, the association between ZIKV and GBS is very well documented. One of the best evidences comes from a case control study during the outbreak in French Polynesia (Cao-Lormeau *et al.*, 2016).

#### Congenital Zika syndrome

Congenital Zika syndrome is a new disease with infectious teratogenic aetiology. The clinical symptoms that characterize this syndrome we can divide into morphological and functional. Functional anomalies are associated with a neurological deficit and can vary in severity. Morphological changes include: anomalies of the skull, brain and eyes and congenital joints contractions.

Foetal brain disruption sequence (FBDS) include severe microcephaly, prominent occipital bone, overlapping cranial sutures and redundant scalp skin, in addition to severe neurological impairment. There is extreme craniofacial disproportion with overlapping and depression of frontal bones and parietal bones. FBDS is probably a result of decreased intracranial pressure and loss in brain volume. Some of brain anomalies can be detected prenatally with ultrasonography or magnetic resonance imaging. Anomalies of brain include: increased fluid spaces (ventricular and extra-axial), diffuse subcortical calcifications, hypoplasia or aplasia of the *corpus callosum*, marked cortical thinning with abnormal gyral patterns (most consistent with polymicrogyria), decreased myelination and cerebellar or cerebellar vermis hypoplasia. The most common anomalies of eyes are microphthalmia, iris coloboma, cataracts, intraocular calcifications and posterior ocular findings (Moore *et al.*, 2017).

Microcephaly is the most important sign of congenital Zika syndrome. It is a birth defect in which occipitofrontal size of head is less than -2 standard deviation for a given age and gender, severe microcephaly is less than -3 standard deviation (according to the American Academy

of Neurology and the Practice Committee of the Child Neurology Society). Primary microcephaly occurs during pregnancy at around 32 weeks of the gestation period, when the brain fails to grow – this is caused by a gradual decrease in the production of neurons. In secondary microcephaly neonate has normal brain size at birth but failure to grow subsequently due to the loss of dendritic connections (Woods, 2004). Precise molecular mechanism of ZIKV-induced microcephaly remains elusive. During the first trimester of pregnancy virus spreads into human neural progenitor cells and surface AXL protein is important for facilitating entry. Signalling pathways in host cells are altered, mostly TLR3-mediated immune network is changed and upregulation of apoptosis plus downregulation of neurogenesis in hNPCs lead to the death of the developing neurons. Genetic, environmental, immunological and physiological factors determine transmission of ZIKV in utero and they are also involved in neurotropism (Faizan *et al.*, 2016).

Congenital contractions of joints in foetuses or infants with congenital ZIKV infection can involve one joint or multiple joints (called arthrogyriposis multiplex congenita, AMC). AMC is clinically manifested by stiffening of the joints, especially of the knees, hips and wrists. The appearance of newborns is compared to wooden dolls (Dungl *et al.*, 2005). The contours of the limbs are prolonged, cylindrical with highlighted skin algae (Sosna *et al.*, 2001). AMC may be associated with pes equinovarus, luxation of the hips and “waiter-tip” wrist position (Dungl *et al.*, 2005).

### Diagnostic methods

Scientists around the world try to understand all details about pathogenesis or immunobiology of the ZIKV and the key is adequate diagnostics, but available diagnostic methods are still limited. Only laboratory methods can confirm ZIKV infection because there is no pathognomic sign for ZIKV infection to distinguish it from other infections. Diagnosis can be made directly (evidence of viral RNA) or indirectly (evidence of antibodies). Different clinical situations and appropriate diagnostic methods with samples are described in Table 1. Up-to-date diagnostic recommendations are posted on the website <https://www.cdc.gov/zika/>.

RT-PCR, serology and virus isolation are used to identify RNA virus and viral proteins. The best method is using RT-PCR because of high specificity and sensitivity, whereas virus isolation is gold standard but requires laboratories with cell cultures. Evidence of viral RNA during acute infection by RT-PCR or NAAT provides more specific results than antibodies, but the virus can be detected only within a short time interval. There is no reference frame for initiating diagnostics (Landry & St. George, 2017).

ELISA and plaque reduction neutralization test (PRNT) are mostly used to diagnose antibodies. Diagnosis of neutralizing antibodies by PRNT has a higher specificity than ELISA detection of IgM (Saeed *et al.*, 2016). Unfortunately, the main problem of antibody diagnosis is cross-reactivity with other flaviviruses. After previous or current flavivirus infection, or even after vaccination, false positives or

**Table 1.** Possible diagnostic methods in different clinical situations according to Landry & St George, 2017 (modified).

Clinical Situations	Samples	Methods	Comments
Acute infection	serum	NAAT, IgM	NAAT is more definitive than serology if positive
	whole blood	NAAT	
	urine	NAAT	urine has higher viral load than serum, detection is possible for 14 days or longer
Recent exposure (2–12 weeks)	serum	IgM	IgM is present 2–12 weeks after acute infection
	whole blood	NAAT	positive IgM results must be confirmed with PRNT (because of cross-reactivity between flaviviruses)
Past infection	serum	IgG	possible cross-reactivity, interpretation of results can be extremely difficult
Congenital infection (foetus)	maternal serum/whole blood	IgM, IgG, NAAT	negative maternal results exclude foetal infection, unless sample is taken too soon after exposure to detect IgM or too late to detect RNA
	amniotic fluid	NAAT	positive result suggests foetal infection
Congenital infection (newborn)	maternal serum/whole blood	IgM, NAAT	
	infant serum, whole blood, urine or CSF	IgM, NAAT	necessary to obtain infant serum within 2 days of birth
	placenta, umbilical cord	NAAT, histopathology, ICH	
Congenital infection (postmortem)	fresh or formalin-fixed tissue	NAAT, histopathology, ICH	
Testing of blood donors	blood	NAAT	detection of acute viremia

NAAT– nucleic acid amplification test; PRNT– plaque reduction neutralization test; CSF– cerebrospinal fluid; ICH– immunohistochemistry

uninterpretable results are often generated. Flaviviruses with potential cross-reactivity with ZIKV antibodies are following: Dengue fever virus type 1–4, Yellow fever virus, West-Nile virus, St. Louis encephalitis, Japanese encephalitis virus and Powassan virus (Saeed *et al.*, 2016).

Detection of risk for the foetus is made primary by testing of the mother. When a baby is born to a mother with confirmed or suspected ZIKV infection, serum and whole blood of newborn, placenta, umbilical cord (plus cerebrospinal fluid if obtained for another reason) should be sent for ZIKV IgM, RT-PCR and histopathology, as appropriate (Landry & St George, 2017). Interpretation of results in newborns is described in Table 2.

It is necessary to know epidemiological history of all flavivirus diseases and vaccinations for using suitable diagnostic method and interpreting the results. This information must be provided together with the sample of biological material, also with standard data and other important information such as: date of onset of the disease, date of sampling and description of clinical signs.

ZIKV infection can be classified (Table 3) as probable (patient meets clinical and epidemiological criteria or meets laboratory criteria for probable case) or confirmed (patient meets laboratory criteria for confirmed case).

Clinical criteria are – any patient with a rash and/or fever and at least one of the following symptoms: joint pain, muscle pain, non-purulent conjunctivitis or hyperaemia.

**Table 2.** Interpretation of results from neonate’s blood, urine or CSF for evidence of congenital ZIKA virus infection (Russell, 2016).

Methods		Congenital ZIKA virus infection
RT-PCR (DNA)	ELISA (IgM)	
+	+/-	confirmed
-	+	probable
-	-	negative

**Table 3.** Diagnostic criteria for ZIKA virus infection according to Public Health Authority of the Slovak Republic, 2016.

	Criteria			
	Epidemiological	Clinical	Laboratory (for probable case)	Laboratory (for confirmed case)
probable ZIKA virus infection	+	+	-	-
	-	-	+	-
confirmed ZIKA virus infection	-	-	-	+

**Table 4.** Clinical manifestation of vertically transmitted infection according to Li *et al.*, 2016.

	CMV	toxoplasmosis	rubella	HSV	ZIKV
microcephaly	++	+	-	++	+++
calcifications	++	++	-	+	++
hydrocephalus	+	++	-	+	+
chorioretinal disease	++	++	-	+	++
systemic disease	+	-	++	++	-

CMV- cytomegalovirus; HSV- herpes simplex virus; ZIKV- Zika virus

Epidemiological criteria are – travelling in ZIKV areas two weeks before first symptoms, sexual intercourse with a person with confirmed case of infection or sexual intercourse with a person who has been in the ZIKV area in the last four weeks.

Laboratory criteria for the diagnosis of probable case is the detection of specific IgM antibodies in the serum.

Laboratory criteria for the diagnosis of confirmed case is at least one of following: detection of ZIKV nucleic acid, detection of ZIKV antigen, isolation of ZIKV, detection of serum specific IgM antibodies plus confirmation with virus-neutralization assay (Public Health Authority of the Slovak Republic, 2016).

**Differential diagnostics**

Symptoms of Zika virus infection may not be present at all, on the other hand the infection may manifest by wide range of non-specific symptoms – differential diagnostics based on clinical presentation is impossible task. Therefore, laboratory methods mostly serological tests are necessary. Infections need to be distinguished from Zika including the following: Dengue fever and chikungunyai virus, rubella, measles and parvoviruses, enteroviruses, adenoviruses and alphaviruses, leptospirosis, rickettsial infections, group A Streptococcal infection, African tick bite fever and relapsing fever and malaria (Sládečková & Rozinová, 2017).

The top in differential diagnosis for any sick neonate is the acronym TORCH – it refers to the most common vertically transmitted pathogens:

- Toxoplasmosis,
- Others (syphilis, group B Streptococcus, Listeria, Candida, etc.),
- Rubeola,
- Cytomegalovirus,
- Herpes simplex virus.

Zika virus is now considered to be part of TORCH infections (Li *et al.*, 2016). Different clinical manifestations of

vertically transmitted infection are described in Table 4. Complications may include microcephaly, periventricular calcifications, chorioretinal disease, hydrocephalus, growth retardation, hepatosplenomegaly, jaundice, thrombocytopenia and other systemic disease (Li *et al.*, 2016).

### Therapy

No approved specific antiviral therapy is available yet. Adult asymptomatic patients and patients with uncomplicated illness do not even require specific therapy. Therapeutic strategies are only symptomatic: analgesic, antipyretics, adequate hydration, plenty of rest and therapy of neurological complications. Acetaminophen is recommended to reduce fever and pain. Aspirin is contraindicated due to risk of a bleeding and Rey's syndrome in children. Non-steroidal anti-rheumatic drugs are also contraindicated due to the increased risk of haemorrhagic syndrome. Infected patients should be isolated during the first days of infection to avoid further mosquito bites.

If ZIKV infection of mother is laboratory confirmed and neonate has signs of congenital Zika syndrome, it is necessary to perform: routine physical examination, including head circumference, birth length, birth weight, gestational age assessment, head ultrasound, laboratory tests for congenital ZIKV infection, neurological examination, brainstem auditory evoked potentials (BAEPs), ophthalmologic examination of the retina, full blood count, metabolic and liver panels.

Consultation with the following specialists should be considered: infectious disease specialist to distinguish other congenital infections (for example syphilis, toxoplasmosis, rubella, CMV infection, or herpes simplex virus), neurologist for comprehensive neurologic examination and consideration of other evaluations (neuroimaging and electroencephalography), ophthalmologist for comprehensive eye exam, clinical geneticist for evaluation of other causes of congenital anomalies and confirmation of the clinical phenotype, early intervention and developmental specialists, family and supportive services, endocrinologist (thyroid testing and evaluation of hypothalamic or pituitary dysfunction), lactation specialist, nutritionist, gastroenterologist, or speech or occupational therapist (evaluation of dysphagia, management of feeding issues), orthopaedist, physiatrist, or physical therapist (the management of AMC, hypertonía, clubfoot etc.) and pulmonologist or otolaryngologist (CDC, 2017).

### Prevention

Currently, no vaccine is available to prevent ZIKV infection but NIAID has multiple vaccine candidates to prevent Zika virus infection in development and research programmes (NIAID, 2017). The most important way to prevent ZIKV infection is to protect yourself from mosquito bites. Sexual protection (using condoms) and testing of blood donors in risk areas are also necessary. Blood donation is contraindicated 28 days after returning from risk country. All travellers are encouraged to check

whether the country where the person is traveling is a risk country (with reported occurrence of the transmission ZIKV). Pregnant women and women planning pregnancy should postpone unnecessary journeys to risk countries. In risk countries it is recommended to take preventive measures to prevent mosquito bites: using repellents; children older than 2 months, pregnant and breastfeeding women should use repellents containing N, N-diethyl-m-toluamide, wearing suitable clothes (long sleeves and long pants, light colours), using mosquito nets, avoiding areas infested with mosquitoes (Public Health Authority of the Slovak Republic, 2016).

### Conclusion

Zika virus infection is a problem of past, present and future. Epidemics may occur because of global climate changes, also in countries where natural conditions for life of mosquitos are not present. This clearly indicates the need to continue developing of vaccines and specific antiviral drugs. Until this happens, we must adhere to individual preventive measures. Zika virus has proven to us how it can affect the health of adults and neonates but also thinking of healthy people. Newborns with microcephaly on the front pages of the media caused in 2015 panic and fear around the world – for this reason education of people is necessary. Due to serious congenital disorders associated with ZIKV infection and global impact of virus we suggest modifying old acronym TORCH for new TORZiCH to accent the position of Zika virus.

### REFERENCES

- Besnard M, Lastère S, Teissier A, Cao-Lormeau VM, Musso D. (2014). Evidence of perinatal transmission of Zika virus, French Polynesia, December 2013 and February 2014. *Euro Surveill* **19**(13): pii: 20751.
- Bollati M, Alvarez K, Assenberg R, Baronti C, Canard B, Cook S, Coutard B, Decroly E, de Lamballerie X, Gould EA, Grard G, Grimes JM, Hilgenfeld R, Jansson AM, Malet H, Mancini EJ, Mastrangelo E, Mattevi A, Milani M, Moureau G, Neyts J, Owens RJ, Ren J, Selisko B, Speroni S, Steuber H, Stuart DI, Unge T, Bolognesi M. (2010). Structure and functionality in flavivirus NS-proteins: Perspectives for drug design. *Antiviral Res* **87**(2): 125–148
- Cao-Lormeau VM, Blake A, Mons S, Lastere S, Roche C, Vanhomwegen J, Dub T, Baudouin L, Teissier A, Larre P, Vial AL, Decam C, Choumet V, Halstead SK, Willison HJ, Musset L, Manuguerra JC, Despres P, Fournier E, Mallet HP, Musso D, Fontanet A, Neil J, Ghawché F. (2016). Guillain-Barré Syndrome outbreak associated with Zika virus infection in French Polynesia: a case-control study. *Lancet* **387**(10027): 1531–1539.
- CDC. National Center for Emerging and Zoonotic Infectious Diseases (NCEZID). Division of Vector-Borne Diseases (DVBD). (2017). [cit. 2017-08-30]. <https://www.cdc.gov/zika/hc-providers/infants-children/evaluation-testing.html#clinicianresources>
- Dick GWA, Kitchen SF, Haddowab AJ (1952) Zika virus (I). Isolations and serological specificity. *Trans R Soc Trop Med Hyg* [online]. **46**(5): 509–20.
- Dungl P, *et al.* (2005). *Ortopedie*. 1<sup>st</sup> ed. Praha: Grada Publishing.
- ECDC. (2016). How is Zika virus transmitted? [online]. [cit. 2018-07-19]. <https://ecdc.europa.eu/en/publications-data/how-zika-virus-transmitted>
- Faizan MI, Abdullah M, Ali S, Naqvi IH, Ahmed A, Parveen S. (2016). Zika Virus-Induced Microcephaly and Its Possible Molecular Mechanism. *Intervirolgy* **59**(3): 152–158
- Landry ML, St George K. (2017). Laboratory Diagnosis of Zika Virus Infection. *Arch Pathol Lab Med* **141**(1): 60–67.

- Li H, Saucedo-Cuevas L, Shresta S, Gleeson JG3. (2016). The Neurobiology of Zika Virus. *Neuron* **92**(5): 949–958.
- MacNamara FN. (1954). Zika virus: report on three case of human infection during an epidemic of jaundice in Nigeria. *Trans R Soc Trop Med Hyg* **48**(2): 139–45.
- Moore CA, Staples JE, Dobyns WB, Pessoa A, Ventura CV, Fonseca EB, Ribeiro EM, Ventura LO, Neto NN, Arena JF, Rasmussen SA. (2017). Characterizing the Pattern of Anomalies in Congenital Zika Syndrome for Pediatric Clinicians. *JAMA Pediatr* **171**(3): 288–295.
- Motta IJ, Spencer BR, Cordeiro da Silva SG, Arruda MB, Dobbin JA, Gonzaga YB, Arcuri IP, Tavares RC, Atta EH, Fernandes RF, Costa DA, Ribeiro LJ, Limonte F, Higa LM, Voloch CM, Brindeiro RM, Tanuri A, Ferreira OC Jr. (2016). Evidence for Transmission of Zika Virus by Platelet Transfusion. *N Engl J Med* **375**(11): 1101–1103.
- Musso D, Roche C, Robin E, Nhan T, Teissier A, Cao-Lormeau VM. (2015). Potential sexual transmission of Zika virus. *Emerg Infect Dis* **21**(2): 359–61.
- Musso D, Gubler DJ. (2016). Zika Virus. *Clin Microbiol Rev* **29**(3): 487–524.
- NIAID. Zika Virus Vaccines [online]. 2017 [cit. 2017-08-29]. <https://www.niaid.nih.gov/diseases-conditions/zika-vaccines>
- Oliveira Melo AS, Malinge G, Ximenes R, Szejnfeld PO, Alves Sampaio S, Bispo de Filippis AM. (2016). Zika virus intrauterine infection causes fetal brain abnormality and microcephaly: tip of the iceberg? *Ultrasound Obstet Gynecol* **47**(1): 6–7.
- Perera-Lecoin M, Meertens L, Carnec X, Amara A. (2014). Flavivirus entry receptors: an update. *Viruses* **6**(1): 69–88.
- Public Health Authority of the Slovak Republic. Updated Guideline of the SR's Principal Hygiene Regarding Zika Virus [online]. 2016 [cit. 2017-04-20]. [http://www.uvzsr.sk/docs/info/epida/Aktualizovane\\_usmernenie\\_hlavneho\\_hygienika\\_SR\\_v\\_suvlosti\\_s\\_virusom\\_Zika.pdf](http://www.uvzsr.sk/docs/info/epida/Aktualizovane_usmernenie_hlavneho_hygienika_SR_v_suvlosti_s_virusom_Zika.pdf)
- Russell K, Oliver SE, Lewis L, Barfield WD, Cragan J, Meaney-Delman D, Staples JE, Fischer M, Peacock G, Oduyebo T, Petersen EE, Zaki S, Moore CA, Rasmussen SA. (2016). Update: Interim Guidance for the Evaluation and Management of Infants with Possible Congenital Zika Virus Infection - United States, August 2016. *MMWR Morb Mortal Wkly Rep* **65**(33): 870–878.
- Saeed RJM, Samaneh B, Sepideh JM, Raheleh G, Fatemeh GP, Seyed ASA. (2016). Zika virus: A review of literature. *Asian Pac J Trop Biomed* **6**(12): 989–994.
- Sládečková V, Rozinová E. (2017). Zika virus – an overview of the current situation. *InVitro* **5**(1): 66–70.
- Sosna A, et al. (2001). *Základy ortopedie*. 1. vydání. Praha: Triton. ISBN 80-7254-202-8.
- Weaver SC, Costa F, Garcia-Blanco MA, Ko AI, Ribeiro GS, Saade G, Shi PY, Vasilakis N. (2016). Zika virus: History, emergence, biology, and prospects for control. *Antiviral Res* **130**: 69–80.
- WHO. Emergencies: Zika virus situation reports [online]. 2017 [cit. 2018-07-19]. <http://www.who.int/emergencies/zika-virus/situation-report/en/>
- Woods CG. (2004). Human microcephaly. *Curr Opin Neurobiol* **14**(1): 112–7.

## REVIEW ARTICLE

# Medicinal plants and natural products can play a significant role in mitigation of mercury toxicity

Sanjib BHATTACHARYA

West Bengal Medical Services Corporation Ltd., GN 29, Sector V, Salt Lake City, Kolkata, West Bengal, India

ITX110418A02 • Received: 01 June 2018 • Accepted: 11 August 2018

## ABSTRACT

Mercury is a heavy metal of considerable toxicity. Scientific literature reveals various plants and plant derived natural products, *i.e.*, phytochemicals, which can alleviate experimentally induced mercury toxicity in animals. The present review attempts to collate those experimental studies on medicinal plants and phytochemicals with ameliorative effects on mercury toxicity. A literature survey was carried out by using Google, Scholar Google, Scopus and Pub-Med. Only the scientific journal articles found in the internet for the last two decades (1998–2018) were considered. Minerals and semi-synthetic or synthetic analogs of natural products were excluded. The literature survey revealed that in pre-clinical studies 27 medicinal plants and 27 natural products exhibited significant mitigation from mercury toxicity in experimental animals. Clinical investigations were not found in the literature. Admissible research in this area could lead to development of a potentially effective agent from the plant kingdom for clinical management of mercury toxicity in humans.

**KEY WORDS:** mercury; ascorbic acid; natural products; oxidative stress; quercetin

## Introduction

The heavy metals are generally characterized as inorganic elements having specific gravity five times of that of water. Almost all the environmental components including biosphere have been consistently threatened by excessive contamination of heavy metals continuously released from various sources. Different heavy metals have been reported to generate adverse effects in diverse ways (Singh *et al.* 2014).

Mercury is a substantially toxic heavy metal which is widely distributed in nature. It exists in the environment in three chemical forms: elemental mercury (poisonous as vapor), organic mercury (methyl mercury and ethyl mercury), and inorganic mercury (mercuric mercury). All these forms have toxic health effects. Mercury and its related compounds are circulated and concentrated in soil and distributed into the air via burning of fossil fuels, industrial furnaces or active volcanos. It then comes back

to the soil, water bodies or living organisms. Recycling from atmospheric outflow, deposition in water reservoirs and bioaccumulation or biomagnifications in plants, animals and humans complete the mercury cycle in the environment (Rafati-Rahimzadeh *et al.* 2014).

Subjection to mercury occurs in two ways: through environmental and occupational exposure. Human exposure to mercury specifically takes place via consumption of mercury contaminated food, especially sea fish, water, dental care procedures (using amalgams in endodontics), using mercury based instruments (thermometers and sphygmomanometers), occupational exposure (e.g. mining) and others (using fluorescent light bulbs and batteries, industrial wastes/effluents). Mercury has no known beneficial effects in the human body yet it elicits different ill effects in the body according to its chemical forms. However, several reports point to a beneficial hormetic response promoted by mercury at a low dose in various *in vitro* and *in vivo* models (Helmcke & Aschner, 2010; Heinz *et al.* 2012; Zhang *et al.* 2013; Tan *et al.* 2018).

Exposure to mercury compounds leads to toxic effects on cardiovascular, pulmonary, urinary, gastrointestinal, neurological systems and skin, which might become fatal. Different forms of mercury affect different vital organs of the body, causing damage or failure of these organs

Correspondence address:

**Dr. Sanjib Bhattacharya M. Pharm., PhD.**

West Bengal Medical Services Corporation Ltd., GN 29, Sector V, Salt Lake City, Kolkata 700091, West Bengal, India.

TEL.: +91 9874331777 • FAX +91 33-40340400

E-MAIL: sakkwai@yahoo.com

crucial for the body, which might cause the death of the individual. Mercury toxicity has been a serious environmental public health hazard worldwide provoking several disastrous incidents like Minamata disease in Japan during 1950–1960 (Bernhoft, 2012; Mostafalou & Abdollahi, 2013).

The toxic effects of mercury in the human body and their conventional managements using putative complexing or chelating agents have so far been well studied and reviewed earlier (Bernhoft, 2012; Sabarathinam *et al.*, 2016). But there is no comprehensive account in the studies on alternative options for counteracting mercury toxicity.

The use of medicinal plants and natural products for treatment of ailments is as old as mankind (Kumar *et al.*, 2015). The major merits of traditional or plant based medicine seem to be their perceived efficacy, low incidence of serious adverse reactions and comparatively low cost (Bhattacharya & Halder, 2012a, b). Literature survey reveals that for the last 12 years only experimental research has been surged in pursuit of medicinal plants and their constituents, i.e. phytochemicals that could mitigate mercury toxicity in experimental animals. Various medicinal plants and natural products afforded significant alleviation from experimentally induced mercury toxicity in animal models. The objective of the present review is to overview and summarize apposite preclinical research findings in this arena.

## Review methodology

Internet associated literature survey was carried out by using Google, Scholar Google, Scopus and Pub-Med database search. Only the scientific journal articles published and/or abstracted in internet during the last two decades (1998–2018) were considered here. The experimental pre-clinical studies on medicinal plants (crude, semi-pure or enriched extracts thereof) and the constituents acquired from plants (including fixed and essential oils) were selected. Combination of phytochemicals was regarded as a separate study. Minerals and semi-synthetic or synthetic analogs of natural products were excluded from the present extent of compilation and review.

## Results

Twenty-seven (27) medicinal plants were reported to possess ameliorative effect on mercury toxicity in experimental models of sub-chronic mercury toxicity. The details are summarized in Table 1. A substantial number of the studied plants are indigenous to the Indian subcontinent. These include certain putative medicinal plants recognized in Ayurveda, the traditional system of Indian medicine and worldwide, namely *Zingiber officinalis*, *Bacopa monnieri*, *Tribulus terrestris*, *Allium sativum*, *Camellia sinensis*, *Vitis vinifera*, *Ocimum sanctum* and *Curcuma longa*. The major dietary plants

include *Camellia sinensis*, *Vitis vinifera*, *Zanthoxylum piperitum*, *Triticum aestivum*, *Curcuma longa*, *Zingiber officinalis* and *Allium sativum*. Most of the plants possess both dietary and medicinal values/usages.

The crude extracts of dried plant materials using suitable solvents like ethanol are used for the studies. In case of *Camellia sinensis* (tea leaf), *Rheum palmatum* (rhubarb), *Zanthoxylum piperitum* (Japanese/Korean pepper) and *Vitis vinifera* (grape seed) a specific chemical constituent or active principle enriched extracts were employed and found to have beneficial effects in ameliorating multiple organ toxicities in rodents.

Twenty seven (27) plant derived natural products were found to demonstrate alleviative effects on mercury induced sub-chronic toxicity, mostly in intact rodent models. The details are given in Table 2. Among them two are vitamins, namely ascorbic acid (vitamin C) and  $\alpha$ -tocopherol (vitamin E) and one is a pro-vitamin A ( $\beta$ -carotene). Two are fixed oils, viz. pomegranate oil, moringa oil; and two are essential oils namely argan oil and *Selinum vaginatum* oil. Ascorbic acid,  $\alpha$ -tocopherol and quercetin are also used as reference compounds in the above mentioned studies on medicinal plant extracts for comparison/validation of experiments.  $\beta$ -carotene and  $\alpha$ -tocopherol co-administration showed prominent ameliorative effect by recuperating oxidative stress, indicating the likelihood of this combination for clinical regimen.

Except the cells/cell lines or *in vitro/ex vivo* studies, most common *in vivo* intact models include rodents like mice and rats. Most commonly studied parameters are hematological and antioxidative parameters (biomarkers). Parameters specific for organs include those of liver, kidney, heart, brain, testes, with the liver and brain being the most common. Histopathological studies of these target organs were also performed in some cases. Measurement of mercury contents in concerned tissues was performed in a few cases. Mercury chelating activity *in vitro* was determined in one case. Urinary excretion study of mercury or its metabolites was not performed. Mercuric chloride ( $\text{HgCl}_2$ ) was used most routinely as toxicant followed by methyl mercury ( $\text{CH}_3\text{Hg}$ ).

## Discussion

Mercury toxicity is known and has been reported historically. It results in multi-organ toxicity depending on age, organ and exposure factors. Chelating agents and combinations thereof and certain symptomatic supportive treatments have been conventionally utilized in treatment of mercury toxicity along with advocating avoiding environmental or occupational mercury exposure. Most of the investigators do not appear very confident to advocate any alternative options like supplementation of herbals or antioxidants in management of mercury toxicity; nevertheless, elicitation of oxidative stress by creation of free radicals during the metabolism of mercury in the body is considered to be one of the pertinent mechanisms of mercury toxicity (Rafati-Rahimzadeh *et al.*, 2014; Aflanie, 2015).

**Table 1.** Medicinal plants with mercury toxicity ameliorative potential.

Sl. No.	Botanical name	Plant Part/ Extracts used	Toxicant used	Experimental model	Organ(s)/system/ cell line involved	Reference(s)
1	<i>Zingiber officinale</i>	Rhizome	HgCl <sub>2</sub>	Rats	Liver, kidney	Joshi <i>et al.</i> , 2017a
2	<i>Paullinia cupana</i>	Fruit	CH <sub>3</sub> Hg	Round worm ( <i>Caenorhabditis elegans</i> )	Whole organism	Aranes <i>et al.</i> , 2016
3	<i>Annona coriacea</i>	Leaf	HgCl <sub>2</sub>	<i>Staphylococcus aureus</i> , <i>Escherichia coli</i> , and <i>Pseudomonas aeruginosa</i>	Whole organism (cells)	Júnior <i>et al.</i> , 2016
4	<i>Lygodium venustum</i>	Aerial parts	HgCl <sub>2</sub>	<i>Escherichia coli</i>	Whole organism (cells)	Figueredo <i>et al.</i> , 2016
5	<i>Rheum palmatum</i>	Total anthraquinone extract of root	HgCl <sub>2</sub>	Rats	Kidney	Gao <i>et al.</i> , 2016
6	<i>Triticum aestivum</i>	Aerial parts	HgCl <sub>2</sub>	Rats	Liver, Haematological	Lakshmi <i>et al.</i> , 2014
7	<i>Dendropanax morbifera</i>	Leaf	(CH <sub>3</sub> ) <sub>2</sub> Hg	Rats	Brain	Kim <i>et al.</i> , 2015
8	<i>Zanthoxylum piperitum</i>	Glycoprotein (ZPDC)	HgCl <sub>2</sub>	Mice	Liver, murine hepatocytes	Lee <i>et al.</i> , 2014
9	<i>Solanum sessiliflorum</i>	Fruit	CH <sub>3</sub> Hg	Rats	Testes	Frenedoso <i>et al.</i> , 2014
9	<i>Acacia arabica</i>	Gum	HgCl <sub>2</sub>	Rats	Kidney	Gado & Aldahmash, 2013
10	<i>Bacopa monnieri</i>	Aerial parts	CH <sub>3</sub> Hg	Rats	Brain	Sumathi <i>et al.</i> , 2012; Ayyathan <i>et al.</i> , 2015
11	<i>Camellia sinensis</i>	Leaf polyphenol extract	HgCl <sub>2</sub>	Rats	Kidney	Liu <i>et al.</i> , 2011
12	<i>Allium sativum</i>	Bulb	CH <sub>3</sub> Hg	Human	Peripheral leukocytes	Abdalla <i>et al.</i> , 2010
13	<i>Allium sativum</i>	Bulb	CH <sub>3</sub> Hg	Rats	Brain	Bellé <i>et al.</i> , 2009
14	<i>Tribulus terrestris</i>	Fruit	HgCl <sub>2</sub>	Mice	Kidney, Liver	Kavitha <i>et al.</i> , 2006; Jagadeesan <i>et al.</i> , 2005; Jagadeesan & Kavitha, 2006
15	<i>Ginkgo biloba</i>	Leaf	HgCl <sub>2</sub>	Rats	Brain, lung, liver, and kidney	Sener <i>et al.</i> , 2007
16	<i>Eruca sativa</i>	Seeds	HgCl <sub>2</sub>	Rats	Kidney	Alam <i>et al.</i> , 2007
17	<i>Ocimum sanctum</i>	Leaf	HgCl <sub>2</sub>	Onion ( <i>Allium cepa</i> )	Root tip cells (meristems)	Babu & Uma Maheswari, 2006
18	<i>Ocimum sanctum</i>	Leaf	HgCl <sub>2</sub>	Mice	Hematological, Liver	Sharma <i>et al.</i> , 2002
19	<i>Halimeda incrassata</i>	Whole plant	CH <sub>3</sub> Hg	Rats, Mice	Hematological, GT1-7 mouse, hypothalamic cells	Linares <i>et al.</i> , 2004
19	<i>Juglans sinensis</i>	Leaf	HgCl <sub>2</sub>	Rabbits	Kidney	Ahn <i>et al.</i> , 2002
20	<i>Vitis vinifera</i>	Seed proanthocyanidin extract	CH <sub>3</sub> Hg	Rats	Brain	Yang <i>et al.</i> , 2012
21	<i>Curcuma longa</i>	Rhizome	HgCl <sub>2</sub>	Rats	Liver	Joshi <i>et al.</i> , 2017b
22	<i>Artemisia absinthium</i>	Aerial parts	HgCl <sub>2</sub>	Rats	Brain	Hallal <i>et al.</i> , 2016
23	<i>Hygrophila auriculata</i>	Whole plant	HgCl <sub>2</sub>	Rat	Liver	Sridhar <i>et al.</i> , 2013
24	<i>Eugenia jambolana</i>	Leaf	HgCl <sub>2</sub>	<i>Escherichia coli</i> , lettuce ( <i>Lactuca sativa</i> ) seeds	–	Sobral-Souza <i>et al.</i> , 2014
25	<i>Eugenia uniflora</i>	Leaf	HgCl <sub>2</sub>	<i>Escherichia coli</i> , lettuce ( <i>Lactuca sativa</i> ) seeds	–	Cunha <i>et al.</i> , 2016
26	<i>Psidium guajava</i> var. <i>pomifera</i>	Leaf	HgCl <sub>2</sub>	Yeast ( <i>Saccharomyces cerevisiae</i> )	–	Pinho <i>et al.</i> , 2017
27	<i>Launaea taraxacifolia</i>	Leaf	HgCl <sub>2</sub>	Rats	Brain	Owoeye & Arinola . 2017

**Table 2.** Natural products with mercury toxicity ameliorative potential.

Sl. No.	Name	Toxicant used	Experimental Model	Organ(s)/System/ Cell line involved	Reference(s)
1	6-gingerol	HgCl <sub>2</sub>	Rats	Liver, Kidney	Joshi <i>et al.</i> , 2017a
2	<i>Moringa oleifera</i> oil	HgCl <sub>2</sub>	Rats	Testes	Abarikwu <i>et al.</i> , 2017
3	Schisandrin B	HgCl <sub>2</sub>	Rats	Kidney	Liu <i>et al.</i> , 2011
4	<i>Bixin</i>	CH <sub>3</sub> Hg	Rats	Liver, Hematological	Barcelos <i>et al.</i> , 2012
5	Norbixin	CH <sub>3</sub> Hg	Rats	Liver, Hematological	Barcelos <i>et al.</i> , 2012
6	β-carotene	HgCl <sub>2</sub>	Nile tilapia ( <i>Oreochromis niloticus</i> )	Hematological	Elseady <i>et al.</i> , 2013
7	β-carotene + α-Tocopherol	CH <sub>3</sub> HgCl	Mice	Liver, Brain, Kidney	Andersen & Andersen, 1993
8	α-Tocopherol	HgCl <sub>2</sub>	Mice	Testes	Rao & Sharma, 2001
9	α-Tocopherol	HgCl <sub>2</sub>	Rats	Liver, Kidney, Brain	Agarwal <i>et al.</i> , 2010a
10	α-Tocopherol	CH <sub>3</sub> Hg	Rats	Fetus	Abd El-Aziz <i>et al.</i> , 2012
11	Ascorbic acid	HgCl <sub>2</sub>	Human	Leucocytes	Rao <i>et al.</i> , 2001
12	Ascorbic acid	HgCl <sub>2</sub>	Olive flounder ( <i>Paralichthys olivaceus</i> )	Kidney	Lee <i>et al.</i> , 2016
13	Ascorbic acid	HgCl <sub>2</sub>	Rats	Spleen, Hematological	Ibegbu <i>et al.</i> , 2014
14	Astaxanthin	HgCl <sub>2</sub>	Rats	Kidney	Augusti <i>et al.</i> , 2008
15	Quercetin	HgCl <sub>2</sub>	Rats	Kidney	Shin <i>et al.</i> , 2015
16	Quercetin	CH <sub>3</sub> Hg	Rats	Hepatocytes, Leucocytes	Barcelos <i>et al.</i> , 2011a
17	Quercetin	HgCl <sub>2</sub>	Human	Leucocytes	Barcelos <i>et al.</i> , 2011b
18	Lycopene	HgCl <sub>2</sub>	Rats	Kidney, Liver	Augusti <i>et al.</i> , 2007; Yang <i>et al.</i> , 2011; Deng <i>et al.</i> , 2012
19	Lycopene	HgCl <sub>2</sub>	Mice	Hematological	Cavusoglu <i>et al.</i> , 2009
20	Curcumin	HgCl <sub>2</sub>	Rats	Liver, Kidney, Brain, Testes	Agarwal <i>et al.</i> , 2010b; Tamer & Saad, 2013; García-Niño & Pedraza-Chaverrí, 2014; Joshi <i>et al.</i> , 2017b, Liu <i>et al.</i> , 2017
21	Coumarin	HgCl <sub>2</sub>	Human	Peripheral lymphocytes	Patel & Rao, 2015
22	Andrographolide	HgCl <sub>2</sub>	Human	Peripheral lymphocytes	Patel & Rao, 2015
23	Fisetin	CH <sub>3</sub> Hg	Rats	Fetus brain	Jacob & Thangarajan, 2017
24	Naringin	HgCl <sub>2</sub>	Human	Leucocytes	Harisa <i>et al.</i> , 2014
25	Luteolin	HgCl <sub>2</sub> and C <sub>9</sub> H <sub>9</sub> HgNaO <sub>2</sub> S*	Human	Mast cells	Asadi <i>et al.</i> , 2010
26	Luteolin	HgCl <sub>2</sub>	Mice	Liver	Yang <i>et al.</i> , 2016
27	Luteolin	HgCl <sub>2</sub>	Rats	Liver	Zhang <i>et al.</i> , 2017
28	Myricetin	CH <sub>3</sub> Hg	Mice	Brain	Franco <i>et al.</i> , 2010
29	Thymol	HgCl <sub>2</sub>	Human	Hepatocarcinoma (HepG2) cell line	Shettigar <i>et al.</i> , 2015
30	Vitamin K	CH <sub>3</sub> Hg	Rats	Brain	Sakaue <i>et al.</i> , 2011
31	Berberine	HgCl <sub>2</sub>	Rats	Brain, Liver, Kidney	Othman <i>et al.</i> , 2014; Moneim, 2015
32	Diallylsulphide	HgCl <sub>2</sub>	Rats	Brain	Ansar, 2015
33	Pomegranate oil	HgCl <sub>2</sub>	Rats	Kidney	Boroushaki <i>et al.</i> , 2014
34	Hydroxytyrosol	HgCl <sub>2</sub>	Human	Erythrocytes and neuroblastoma	Officioso <i>et al.</i> , 2016
35	Glucan	C <sub>9</sub> H <sub>9</sub> HgNaO <sub>2</sub> S*, Hg(O <sub>2</sub> CCH <sub>3</sub> ) <sub>2</sub> †	Mice	Immunological	Vetvicka & Vetvickova 2009
36	<i>Selinum vaginatum</i> oil	CH <sub>3</sub> Hg	Rats	Brain	Thiagarajan <i>et al.</i> , 2018
37	Argan oil	HgCl <sub>2</sub>	Rats	Liver	Necib <i>et al.</i> , 2013

\* Thiomersal, † Mercury (II) acetate.

Higher plants, whether dietary or medicinal, and their constituents traditionally possessed an overriding impact in drug discovery and served as the basis of premature medicines (Das *et al.*, 2013; Bhattacharya & Haldar, 2011). There is ample literature currently being available on usefulness of medicinal plants and constituents thereof against experimental mercury and other heavy metal/metalloid poisonings (Bhattacharya, 2017; 2018). Such reports of mercury are comparatively few as compared to those of lead, arsenic and cadmium. From the present literature survey it appears that medicinal plants have played a significant role in mitigation of experimentally induced mercury toxicity in animals. The crude or semi-pure plant extracts in general, exhibit antioxidant activities and thus show toxicity abrogative potential in reducing mercury induced oxidative insult. Besides, modulation of apoptosis is another less reported way of amelioration of mercury-induced organ toxicity by medicinal plant extracts. Mercury chelating property of plant extract *in vitro* is the least reported possible mechanism of protective effect operative along with antioxidant activity. Most of the literature neither discuss their possible clinical utility or ability in decreasing body mercury burden nor execute any endeavor to identify, isolate or characterize the active constituent(s). This is the major limitation of most of these works.

The present literature probe revealed that nearly all of the medicinal plants and natural products possessing preclinical mercury toxicity alleviative effects simultaneously revealed considerable innate antioxidant property by repression of mercury-induced oxidative stress by multimodal elevation of endogenous enzymatic and non-enzymatic fortification systems that resulted in mitigation of mercury-induced toxicity in animals. The 27 natural products tested are entrenched nutraceuticals or dietary supplements and these are all well described as natural antioxidants. This indicates the beneficial role of antioxidant supplementation and strongly corroborates the exhortation of antioxidant therapy to humans. At the experimental stage, a segment of researchers opines this respect (Patrick, 2002; Gupta *et al.*, 2015; Officioso *et al.*, 2016). Notwithstanding, the benefits of these compounds at organic and cellular level require validation in human subjects with mercury toxicity. So far no clinical study was found in the scientific literature where medicinal plants or phytochemicals suppressed any kind of mercury toxicity in humans. The inherent toxicity of mercury may be the limiting factor here.

Mercury chelating activity of plant extract *in vitro*, reported in a recent study (Pinho *et al.*, 2017) appears to be a novel protective mechanism which requires further studies involving concurrence *in vivo*. Few plant extracts showing mercury toxicity protective effects in bacterial and plant models exhibited *in vitro* iron chelating effects along with antioxidant properties (Sobral-Souza *et al.*, 2014; Cunha *et al.*, 2016). Such plants should be further investigated for possible mercury chelating potential in pre-clinical set up.

Recent reviews suggest that people, who are at risk of arsenic, lead and cadmium exposure, should consume vitamin and antioxidant rich food on a regular basis for prevention of possible toxicity (Zhai *et al.*, 2015; Bhattacharya, 2017; 2018). So far there is no work on the effect of dietary supplementation of edible or medicinal plants and/or their bioactive constituents in animals or humans with long-term and environmentally-relevant low levels of mercury exposure. Research work should be formulated in this facet.

The most studied natural products like ascorbic acid,  $\alpha$ -tocopherol, quercetin,  $\beta$  carotene (Figures 1–4) in rodents require further comprehensive clinical

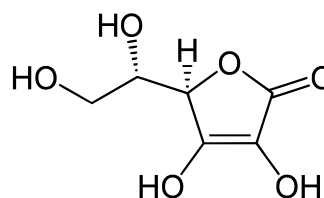


Figure 1. Vitamin C (ascorbic acid).

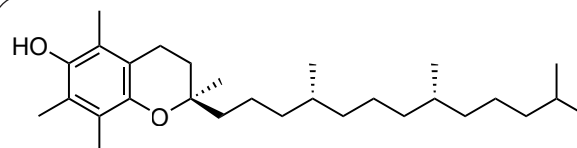


Figure 2. Vitamin E ( $\alpha$  tocopherol).

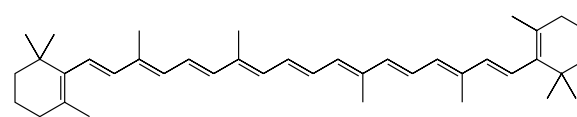


Figure 3. Beta carotene.

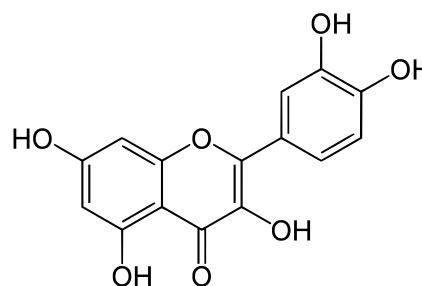


Figure 4. Quercetin.

exploitation. More of such pre-clinically worthy phytochemicals could be introduced for clinical studies. These agents could be used alone, in combination, or concomitantly with mainstream or newer chelating agents. These agents thus may aid in disease reversal or may serve as auxiliary, complementary or disease modifying agents and hence could help in palliative therapy by reducing the patient's agonies.

It is therefore hypothesized that the present facts and findings, although demonstrated principally in lower animal models, will have sustainable ameliorative potential against mercury toxicity and possible preventive mitigation to those subjects potentially susceptible to environmental mercury exposure. These apparently introductory studies could serve as pivot for further investigation which may lead to discovery of any potentially useful agent in clinical management of mercury toxicity in humans in due course, which may act by a distinct mode other than synthetic chelation, like modulation of oxidative stress, gene regulation or apoptosis. The material explored and presented in the current concise review appears to be quite motivating for further mechanistic pre-clinical and definitively designed clinical studies on dietary and medicinal plants and natural products in particular, for management of mercury toxicity hazard in humans.

**Declaration of interest.** *The author reports no conflict of interest. The author alone is responsible for the content and writing of this paper.*

## REFERENCES

- Abarikwu SO, Benjamin S, Ebah SG, Obilor G, Agbam G. (2017). Oral administration of *Moringa oleifera* oil but not coconut oil prevents mercury-induced testicular toxicity in rats. *Andrologia* **49**: e12597.
- Abd El-Aziz GS, El-Fark MM, Saleh HA. (2012). The prenatal toxic effect of methylmercury on the development of the appendicular skeleton of rat fetuses and the protective role of vitamin E. *Anat Rec (Hoboken)* **295**: 939–949.
- Abdalla FH, Bellé LP, De Bona KS, Bitencourt PE, Pigatto AS, Moretto MB. (2010). *Allium sativum* L. extract prevents methyl mercury-induced cytotoxicity in peripheral blood leukocytes (LS). *Food Chem Toxicol* **48**: 417–421.
- Aflanite I. (2015). Effect of heavy metal on malondialdehyde and advanced oxidation protein products concentration: A focus on arsenic, cadmium, and mercury. *J Med Bioeng* **4**: 332–337.
- Agarwal R, Goel SK, Behari JR. (2010b). Detoxification and antioxidant effects of curcumin in rats experimentally exposed to mercury. *J Appl Toxicol* **30**: 457–68.
- Agarwal R, Goel SK, Chandra R, Behari JR. (2010a). Role of vitamin E in preventing acute mercury toxicity in rat. *Environ Toxicol Pharmacol* **29**: 70–78.
- Ahn CB, Song CH, Kim WH, Kim YK. (2002). Effects of *Juglans sinensis* Dode extract and antioxidant on mercury chloride-induced acute renal failure in rabbits. *J Ethnopharmacol* **82**: 45–49.
- Alam MS, Kaur G, Jabbar Z, Javed K, Athar M. (2007). *Eruca sativa* seeds possess antioxidant activity and exert a protective effect on mercuric chloride induced renal toxicity. *Food Chem Toxicol* **45**: 910–20.
- Andersen HR, Andersen O. (1993). Effects of dietary alpha-tocopherol and beta-carotene on lipid peroxidation induced by methyl mercuric chloride in mice. *Pharmacol Toxicol* **73**: 192–201.
- Ansar S. (2015). Pretreatment with diallylsulphide modulates mercury-induced neurotoxicity in male rats. *Acta Biochimica Polonica* **62**: 599–603.
- Arantes LP, Peres TV, Chen P, Caito S, Aschner M, Soares FA. (2016). Guarana (*Paullinia cupana* Mart.) attenuates methylmercury-induced toxicity in *Caenorhabditis elegans*. *Toxicol Res (Camb)* **5**: 1629–1638.
- Asadi S, Zhang B, Weng Z, Angelidou A, Kempuraj D, Alysandratos KD, Theoharides TC. (2010). Luteolin and thiosalicylate inhibit HgCl<sub>2</sub> and thimerosal-induced VEGF release from human mast cells. *Int J Immunopathol Pharmacol* **23**: 1015–1020.
- Augusti PR, Conterato GM, Somacal S, Einfeld L, Ramos AT, Hosomi FY, Graça DL, Emanuelli T. (2007). Effect of lycopene on nephrotoxicity induced by mercuric chloride in rats. *Basic Clin Pharmacol Toxicol* **100**: 398–402.
- Augusti PR, Conterato GM, Somacal S, Sobieski R, Spohr PR, Torres JV, Charão MF, Moro AM, Rocha MP, Garcia SC, Emanuelli T. (2008). Effect of astaxanthin on kidney function impairment and oxidative stress induced by mercuric chloride in rats. *Food Chem Toxicol* **46**: 212–219.
- Ayyathan DM, Chandrasekaran R, Thiagarajan K. (2015). Neuroprotective effect of Brahmi, an ayurvedic drug against oxidative stress induced by methyl mercury toxicity in rat brain mitochondrial-enriched fractions. *Nat Prod Res* **29**: 1046–1051.
- Babu K, Uma Maheswari KC. (2006). *In vivo* studies on the effect of *Ocimum sanctum* L. leaf extract in modifying the genotoxicity induced by chromium and mercury in *Allium* root meristems. *J Environ Biol* **27**: 93–95.
- Barcelos GR, Angeli JP, Serpeloni JM, Grotto D, Rocha BA, Bastos JK, Knasmüller S, Júnior FB. (2011b). Quercetin protects human-derived liver cells against mercury-induced DNA-damage and alterations of the redox status. *Mutat Res* **726**: 109–115.
- Barcelos GR, Grotto D, Serpeloni JM, Aissa AF, Antunes LM, Knasmüller S, Barbosa F Jr. (2012). Bixin and norbixin protect against DNA-damage and alterations of redox status induced by methylmercury exposure *in vivo*. *Environ Mol Mutagen* **53**: 535–541.
- Barcelos GR, Grotto D, Serpeloni JM, Angeli JP, Rocha BA, de Oliveira Souza VC, Vicentini JT, Emanuelli T, Bastos JK, Antunes LM, Knasmüller S, Barbosa F Jr. (2011a). Protective properties of quercetin against DNA damage and oxidative stress induced by methylmercury in rats. *Arch Toxicol* **85**: 1151–1157.
- Bellé LP, De Bona KS, Abdalla FH, Pimentel VC, Pigatto AS, Moretto MB. (2009). Comparative evaluation of adenosine deaminase activity in cerebral cortex and hippocampus of young and adult rats: effect of garlic extract (*Allium sativum* L.) on their susceptibility to heavy metal exposure. *Basic Clin Pharmacol Toxicol* **104**: 408–413.
- Bernhoft RA. (2012). Mercury toxicity and treatment: a review of the literature. *J Environ Public Health* **2012**: Article ID 460508.
- Bhattacharya S, Haldar PK. (2011). *Trichosanthes dioica* root extract induces tumor proliferation and attenuation of antioxidant system in albino mice bearing Ehrlich ascites carcinoma. *Interdiscip Toxicol* **4**: 184–90.
- Bhattacharya S, Haldar PK. (2012a). *Trichosanthes dioica* root possesses stimulant laxative activity in mice. *Nat Prod Res* **26**: 952–957.
- Bhattacharya S, Haldar PK. (2012b). Protective role of the triterpenoid-enriched extract of *Trichosanthes dioica* root against experimentally induced pain and inflammation in rodents. *Nat Prod Res* **26**: 2348–2352.
- Bhattacharya S. (2017). Medicinal plants and natural products in amelioration of arsenic toxicity: a short review. *Pharm Biol* **55**: 349–354.
- Bhattacharya S. (2018). The role of medicinal plants and natural products in melioration of cadmium toxicity. *Oriental Pharm Exp Med* **18** (3): pp 177–186
- Borouhaki MT, Mollazadeh H, Rajabian A, Dolati K, Hoseini A, Paseban M, Farzadnia M. (2014). Protective effect of pomegranate seed oil against mercuric chloride-induced nephrotoxicity in rat. *Ren Fail* **36**: 1581–1586.
- Cavusoglu K, Oruc E, Yapar K, Yalcin E. (2009). Protective effect of lycopene against mercury-induced cytotoxicity in albino mice: pathological evaluation. *J Environ Biol* **30**: 807–814.
- Cunha FAB, Pinho AI, Santos JFS, Sobral-Souza CE, Leite NF, Albuquerque RS, Tintino SR, Costa JGM, Matias EFF, Boligon AA, Waczuk EP, Rocha JBT, Posser T, Coutinho HDM, Quintans-Junior LJ, Franco JL. (2016). Cytoprotective effect of *Eugenia uniflora* L. against the waste contaminant mercury chloride. *Arabian J Chem* <http://dx.doi.org/10.1016/j.arabjc.2016.04.018>.
- Das SK, Bhattacharya S, Kundu A. (2013). Rationalized design, synthesis and pharmacological screening of amino acid linked spiro pyrrolidino oxindole analogs through environment friendly reaction. *J Adv Pharm Technol Res* **4**: 198–205.
- Deng Y, Xu Z, Liu W, Yang H, Xu B, Wei Y. (2012). Effects of lycopene and proanthocyanidins on hepatotoxicity induced by mercuric chloride in rats. *Biol Trace Elem Res* **146**: 213–223.
- Elseday Y, Zahran E. (2013). Ameliorating effect of  $\beta$ -carotene on antioxidant response and hematological parameters of mercuric chloride toxicity in Nile tilapia (*Oreochromis niloticus*). *Fish Physiol Biochem* **39**: 1031–1041.

- Figueredo FG, Lima LF, Morais-Braga MF, Tintino SR, Farias PA, Matias EF, Costa JG, Menezes IR, Pereira RL, Coutinho HD. (2016). Cytoprotective effect of *Lygodium venustum* Sw. (Lygodiaceae) against mercurium chloride toxicity. *Scientifica* (Cairo) **2016**: 4154265.
- Franco JL, Posser T, Missau F, Pizzolatti MG, Dos Santos AR, Souza DO, Aschner M, Rocha JB, Dafre AL, Farina M. (2010). Structure-activity relationship of flavonoids derived from medicinal plants in preventing methylmercury-induced mitochondrial dysfunction. *Environ Toxicol Pharmacol* **30**: 272–278.
- Frenedoso da Silva R, Missassi G, dos Santos Borges C, Silva de Paula E, Hornos Carneiro MF, Grotto D, Barbosa Junior F, De Grava Kempinas W. (2014). Phytoremediation potential of Maná-Cubiu (*Solanum sessiliflorum* Dunal) for the deleterious effects of methylmercury on the reproductive system of rats. *Biomed Res Int* **2014**: 309631.
- Gado AM, Aldahmash BA. (2013). Antioxidant effect of Arabic gum against mercuric chloride-induced nephrotoxicity. *Drug Des Devel Ther* **7**: 1245–1452.
- Gao D, Zeng LN, Zhang P, Ma ZJ, Li RS, Zhao YL, Zhang YM, Guo YM, Niu M, Bai ZF, Xiao XH, Gao WW, Wang JB. (2016). Rhubarb anthraquinones protect rats against mercuric chloride (HgCl<sub>2</sub>)-induced acute renal failure. *Molecules* **21**: 298.
- García-Niño WR, Pedraza-Chaverrí J. (2014). Protective effect of curcumin against heavy metals-induced liver damage. *Food Chem Toxicol* **69**: 182–201.
- Gupta VK, Siddiqi NJ, Singh S, Agrawal A, Sharma B. (2015). Phytochemicals mediated remediation of neurotoxicity induced by heavy metals. *Biochem Res Int* **2015** Article ID 534769.
- Hallal N, Kharoubi O, Benyettou I, Tair K, Ozaslan M, Aoues AEK. (2016). *In vivo* amelioration of oxidative stress by *Artemisia absinthium* L. administration on mercuric chloride toxicity in brain regions. *J Biol Sci* **16**: 167–177.
- Harisa GI, Mariee AD, Abo-Salem OM, Attia SM. (2014). Erythrocyte nitric oxide synthase as a surrogate marker for mercury-induced vascular damage: the modulatory effects of naringin. *Environ Toxicol* **29**: 1314–1422.
- Heinz GH, Hoffman DJ, Klimstra JD, Stebbins KR, Kondrad SL, Erwin CA. (2012). Hormesis associated with a low dose of methylmercury injected into mallard eggs. *Arch Environ Contam Toxicol* **62**: 141–144.
- Helmcke KJ, Aschner M. (2010). Hormetic effect of methylmercury on *Caenorhabditis elegans*. *Toxicol Appl Pharmacol* **248**: 156–64.
- Ibegbu AO, Micheal A, Abdulrazaq AA, Daniel B, Sadeeq AA, Peter A, Hamman WO, Umana UE, Musa SA. (2014). Ameliorative effect of ascorbic acid on mercury chloride induced changes on the spleen of adult wistar rats. *J Exp Clin Anatomy* **13**: 60–65.
- Jacob S, Thangarajan S. (2017). Effect of gestational intake of fisetin (3,3',4',7-Tetrahydroxyflavone) on developmental methyl mercury neurotoxicity in F1 generation rats. *Biol Trace Elem Res* **177**: 297–315.
- Jagadeesan G, Kavitha AV, Subashini J. (2005). FT-IR Study of the influence of *Tribulus terrestris* on mercury intoxicated mice, *Mus musculus* liver. *Trop Biomed* **22**: 15–22.
- Jagadeesan G, Kavitha AV. (2006). Recovery of phosphatase and transaminase activity of mercury intoxicated *Mus musculus* (Linn.) liver tissue by *Tribulus terrestris* (Linn.) (Zygophyllaceae) extract. *Trop Biomed* **23**: 45–51.
- Joshi D, Mittal DK, Shukla S, Srivastav SK, Dixit VA. (2017b). *Curcuma longa* Linn. extract and curcumin protect CYP 2E1 enzymatic activity against mercuric chloride-induced hepatotoxicity and oxidative stress: A protective approach. *Exp Toxicol Pathol* **69**: 373–382.
- Joshi D, Srivastav SK, Belemkar S, Dixit VA. (2017a). *Zingiber officinale* and 6-gingerol alleviate liver and kidney dysfunctions and oxidative stress induced by mercuric chloride in male rats: A protective approach. *Biomed Pharmacother* **91**: 645–655.
- Júnior JG, Coutinho HD, Boris TC, Cristo JS, Pereira NL, Figueiredo FG, Cunha FA, Aquino PE, Nascimento PA, Mesquita FJ, Moreira PH, Coutinho ST, Souza IT, Teixeira GC, Ferreira NM, Farina EO, Torres CM, Holanda VN, Pereira VS, Guedes MI. (2016). Chemical characterization and cytoprotective effect of the hydroethanol extract from *Annona coriacea* Mart. (Araticum). *Pharmacognosy Res* **8**: 253–257.
- Kavitha AV, Jagadeesan G. (2006). Role of *Tribulus terrestris* (Linn.) (Zygophyllaceae) against mercuric chloride induced nephrotoxicity in mice, *Mus musculus* (Linn.). *J Environ Biol* **27**: 397–400.
- Kim W, Kim DW, Yoo DY, Jung HY, Kim JW, Kim DW, Choi JH, Moon SM, Yoon YS, Hwang IK. (2015). Antioxidant effects of *Dendropanax moribifera* Léveillé extract in the hippocampus of mercury-exposed rats. *BMC Complement Altern Med* **15**: 247.
- Kumar RBS, Kar B, Dolai N, Karmakar I, Bhattacharya S, Halder PK. (2015). Antitumor activity and antioxidant status of *Streblus asper* bark against Dalton's ascitic lymphoma in mice. *Interdiscip Toxicol* **8**: 125–130.
- Lakshmi BV, Sudhakar M, Nireesha G. (2014). Modification of mercury-induced biochemical alterations by *Triticum aestivum* Linn in rats. *Indian J Physiol Pharmacol* **58**: 423–436.
- Lee J, Lee SJ, Lim KT. (2014). Preventive effects of ZPDC glycoprotein (24 kDa) on hepatotoxicity induced by mercury chloride *in vitro* and *in vivo*. *Cell Biochem Funct* **32**: 520–529.
- Lee JH, Moniruzzaman M, Yun H, Lee S, Park Y, Bai SC. (2016). Dietary vitamin C reduced mercury contents in the tissues of juvenile olive flounder (*Paralichthys olivaceus*) exposed with and without mercury. *Environ Toxicol Pharmacol* **45**: 8–14.
- Linares AF, Loikkanen J, Jorge MF, Soria RB, Novoa AV. (2004). Antioxidant and neuroprotective activity of the extract from the seaweed, *Halimeda incrassata* (Ellis) Lamouroux, against *in vitro* and *in vivo* toxicity induced by methyl-mercury. *Vet Hum Toxicol* **46**: 1–5.
- Liu W, Xu Z, Li H, Guo M, Yang T, Feng S, Xu B, Deng Yu. (2017). Protective effects of curcumin against mercury-induced hepatic injuries in rats, involvement of oxidative stress antagonism, and Nrf2-ARE pathway activation. *Hum Exp Toxicol* **36**: 949–966.
- Liu W, Xu Z, Yang H, Deng Y, Xu B, Wei Y. (2011). The protective effects of tea polyphenols and schisandrin B on nephrotoxicity of mercury. *Biol Trace Elem Res* **143**: 1651–1665.
- Moneim AEA. (2015). The neuroprotective effect of berberine in mercury-induced neurotoxicity in rats. *Metab Brain Dis* **30**: 935–42.
- Mostafalou S, Abdollahi M. (2013). Environmental pollution by mercury and related health concerns: Renote of a silent threat. *Arh Hig Rada Toksikol* **64**: 179–181.
- Necib Y, Bahi A, Zerizer S. (2013). Amelioration of mercuric chloride toxicity on rat liver. With argan oil and sodium selenite supplements. *Int J Pharm Bio Sci* **4** (B): 839–849.
- Officioso A, Tortora F and Manna C. (2016). Nutritional aspects of food toxicology: mercury toxicity and protective effects of olive oil hydroxytyrosol. *J Nutr Food Sci* **6**: 539.
- Othman MS, Safwat G, Aboulkhair M, Abdel Moneim AE. (2014). The potential effect of berberine in mercury-induced hepatorenal toxicity in albino rats. *Food Chem Toxicol* **69**: 175–181.
- Owoeye O, Arinola GO. (2017). A vegetable, *Launaea taraxacifolia*, mitigated mercuric chloride alteration of the microanatomy of rat brain. *J Diet Suppl* **14**: 613–625.
- Patel TA, Rao MV. (2015). Ameliorative effect of certain antioxidants against mercury induced genotoxicity in peripheral blood lymphocytes. *Drug Chem Toxicol* **38**: 408–414.
- Patrick L. (2002). Mercury toxicity and antioxidants: part I: role of glutathione and alpha-lipoic acid in the treatment of mercury toxicity. *Alt Med Rev* **7**: 456–471.
- Pinho AI, Oliveira CS, Lovato FL, Waczuk EP, Piccoli BC, Boligon AA, Leite NF, Coutinho HDM, Posser T, Da Rocha JBT, Franco JL. (2017). Antioxidant and mercury chelating activity of *Psidium guajava* var. *pomifera* L. leaves hydroalcoholic extract. *J Toxicol Environ Health A* **80**: 1301–1313.
- Rafati-Rahimzadeh M, Rafati-Rahimzadeh M, Kazemi S Moghadamnia AA. (2014). Current approaches of the management of mercury poisoning: need of the hour. *DARU J Pharm Sci* **22**: 46.
- Rao MV, Chinoy NJ, Suthar MB, Rajvanshi MI. (2001). Role of ascorbic acid on mercuric chloride-induced genotoxicity in human blood cultures. *Toxicol In Vitro* **15**: 649–654.
- Rao MV, Sharma PS. (2001). Protective effect of vitamin E against mercuric chloride reproductive toxicity in male mice. *Reprod Toxicol* **15**: 705–12.
- Sabarathinam J, Vishnu Riya V, Gayathri R. (2016). Mercury poisoning and management: a systematic review. *Asian J Pharm Clin Res* **9**: 8–12.
- Sakae M, Mori N, Okazaki M, Kadowaki E, Kaneko T, Hemmi N, Sekiguchi H, Maki T, Ozawa A, Hara S, Arishima K, Yamamoto M. (2011). Vitamin K has the potential to protect neurons from methylmercury-induced cell death *in vitro*. *J Neurosci Res* **89**: 1052–1058.
- Sener G, Sehirli O, Tozan A, Velioglu-Ovunc A, Gedik N, Omurtag GZ. (2007). *Ginkgo biloba* extract protects against mercury(II)-induced oxidative tissue damage in rats. *Food Chem Toxicol* **45**: 543–50.
- Sharma MK, Kumar M, Kumar A. (2002). *Ocimum sanctum* aqueous leaf extract provides protection against mercury induced toxicity in Swiss albino mice. *Indian J Exp Biol* **40**: 1079–1082.
- Shettigar NB, Das S, Rao NB, Rao SB. (2015). Thymol, a monoterpene phenolic derivative of cymene, abrogates mercury-induced oxidative stress resultant cytotoxicity and genotoxicity in hepatocarcinoma cells. *Environ Toxicol* **30**: 968–980.

- Shin YJ, Kim JJ, Kim YJ, Kim WH, Park EY, Kim IY, Shin HS, Kim KS, Lee EK, Chung KH, Lee BM, Kim HS. (2015). Protective effects of quercetin against HgCl<sub>2</sub>-induced nephrotoxicity in Sprague-Dawley rats. *J Med Food* **18**: 524–534.
- Singh KP, Bhattacharya S, Sharma P. (2014). Assessment of heavy metal contents of some Indian medicinal plants. *American-Eurasian J Agric Environ Sci* **14**: 1125–1129.
- Sobral-Souza CE, Leite NF, Cunha FAB, Pinho AI, Albuquerque RS, Carneiro JNP, Menezes IRA, Costa JGM, Franco JL, Coutinho HDM. (2014). Cytoprotective effect against mercury chloride and bioinsecticidal activity of *Eugenia jambolana* Lam. *Arabian J Chem* **7**: 165–170.
- Sridhar MP, Nandakumar N, Rengarajan T, Balasubramanian MP. (2013). Amelioration of mercuric chloride induced oxidative stress by *Hygrophila auriculata* (K.Schum) Heine via modulating the oxidant – antioxidant imbalance in rat liver. *J Biochem Tech* **4**: 622–627
- Sumathi T, Shobana C, Christinal J, Anusha C. (2012). Protective effect of *Bacopa monniera* on methyl mercury-induced oxidative stress in cerebellum of rats. *Cell Mol Neurobiol* **32**: 979–87.
- Tamer M, Saad M. (2013). Effect of curcumin on some heavy metals induced renal and testicular injuries in male rats. *Egyptian J Hosp Med* **53**: 770–781.
- Tan Q, Liu Z, Li H, Liu Y, Xia Z, Xiao Y, Usman M, Du Y, Bi H, Wei L. (2018). Hormesis of mercuric chloride-human serum albumin adduct on N9 microglial cells via the ERK/MAPKs and JAK/STAT3 signaling pathways. *Toxicol* **408**: 62–69.
- Thiagarajan K, Gamit N, Mandal S, Ayyathan DM, Chandrasekaran R. (2018). Amelioration of methylmercury induced neural damage by essential oil of *Selinum vaginatum* (Edgew) C. B. Clarke. *Pak J Pharm Sci* **31**: 399–404.
- Vetvicka V, Vetvickova J. (2009). Effects of glucan on immunosuppressive actions of mercury. *J Med Food* **12**: 1098–104.
- Yang D, Tan X, Lv Z, Liu B, Baiyun R, Lu J, Zhang Z. (2016). Regulation of Sirt1/Nrf2/TNF- $\alpha$  signaling pathway by luteolin is critical to attenuate acute mercuric chloride exposure induced hepatotoxicity. *Scientific Reports* **6**: 37157.
- Yang H, Xu Z, Liu W, Deng Y, Xu B. (2011). The protective role of procyanidins and lycopene against mercuric chloride renal damage in rats. *Biomed Environ Sci* **24**: 550–559.
- Yang H, Xu Z, Liu W, Wei Y, Deng Y, Xu B. (2012). Effect of grape seed proanthocyanidin extracts on methylmercury-induced neurotoxicity in rats. *Biol Trace Elem Res* **147**: 156–164.
- Zhai Q, Narbad A, Chen W. (2015). Dietary strategies for the treatment of cadmium and lead toxicity. *Nutrients* **7**: 552–571.
- Zhang H, Tan X, Yang D, Lu J, Liu B, Baiyun R, Zhang Z. (2017). Dietary luteolin attenuates chronic liver injury induced by mercuric chloride via the Nrf2/NF- $\kappa$ B/P53 signaling pathway in rats. *Oncotarget* **8**: 40982–40993.
- Zhang Y, Lu R, Liu W, Wu Y, Qian H, Zhao X, Wang S, Xing G. (2013). Hormetic effects of acute methylmercury exposure on GRP78 expression in rat brain cortex. *Dose-Response* **11**: 109–120.

## ORIGINAL ARTICLE

# Assessment of the time-dependent dermatotoxicity of mechlorethamine using the mouse ear vesicant model

Benedette J. CUFFARI<sup>1</sup>, Hemanta C Rao TUMU<sup>1</sup>, Maria A. PINO<sup>1,2</sup>, Blase BILLACK<sup>1</sup>

<sup>1</sup>Department of Pharmaceutical Sciences, College of Pharmacy and Health Sciences, St. John's University, Jamaica, NY, USA;

<sup>2</sup>Department of Clinical Specialties, NYIT College of Osteopathic Medicine, Old Westbury, NY, USA

ITX110418A03 • Received: 21 June 2018 • Accepted: 07 December 2018

## ABSTRACT

Mechlorethamine (HN2) is an alkylating agent and sulfur mustard gas mimetic which is also used in anticancer therapy. HN2 is associated with skin inflammation and blistering which can lead to secondary infections. The purpose of the present study was to investigate the time-dependent dermatotoxicity of HN2 using the mouse ear vesicant model (MEVM). To this end, our operational definition of dermatotoxicity included tissue responses to HN2 consistent with an increase in the wet weights of mouse ear punch biopsies, an increase in the morphometric thickness of H&E stained ear sections and histopathologic observations including tissue edema, inflammatory cell infiltration and vesication. The ears of male Swiss Webster mice were topically exposed to a single dose of HN2 (0.5  $\mu\text{mol}/\text{ear}$ ) or DMSO vehicle (5  $\mu\text{l}/\text{ear}$ ) or left untreated (naive). Mice were then euthanized at 15 min, 1, 2, 4, 8 or 24 hr following HN2 exposure. Compared to control ears, mouse ears exposed to HN2 at all time points showed an increase in wet weights, morphometric thickness, edema, inflammatory cell infiltration and signs of vesication. The incidence in tissue vesication sharply increased between 4 and 8 hr after exposure, revealing that tissue vesication is well established by 8 hr and remains elevated at 24 hr after exposure. It is noteworthy that, compared to control ears, mouse ears treated with DMSO vehicle alone also exhibited an increase in wet weights and morphometric thickness at 15 min, 1, 2 and 4 hr following treatment; however, these vehicle effects begin to subside after 4 hr. The results obtained here using the MEVM provide a more holistic understanding of the kinetics of vesication, and indicate that time points earlier than 24 hr may prove useful not only for investigating the complex mechanisms involved in vesication but also for assessing the effects of vesicant countermeasures.

**KEY WORDS:** mechlorethamine; mouse ear vesicant model; MMP-9; dermatotoxicity; vesication

## Introduction

Mechlorethamine (HN2) is a prototype nitrogen mustard (NM) that shares a similar structure and toxicity profile with the chemical warfare agent sulfur mustard (SM) (Korkmaz *et al.*, 2006; Shakarjian *et al.*, 2010). HN2 is widely used as a surrogate to study and mimic the effects of SM under laboratory conditions (Composto *et al.*, 2018; Lulla *et al.*, 2014; Malaviya *et al.*, 2015; Sunil *et al.*, 2011; Tumu *et al.*, 2018).

Due to the presence of the highly reactive chloroethyl side chains in both compounds, both SM and NM readily interact with a wide variety of macromolecules including

proteins and nucleic acids. Upon absorption into the aqueous components of the body, SM and NM transform into the reactive intermediates ethylene sulfonium and ethylene immonium ions, respectively. These reactive intermediates cause direct injury to tissues through their interaction with proteins and DNA, particularly through their ability to form both bifunctional DNA interstrand cross links and monofunctional DNA adducts which can subsequently block DNA replication and lead to cell cycle arrest (Kehe *et al.*, 2009). Moreover, HN2 and SM have been reported to alkylate cytoskeletal proteins such as keratin 5 and keratin 14 in epidermal keratinocytes and to affect proteins in the extracellular matrix such as laminin-332 (Shakarjian *et al.*, 2010). Laminin-332 is regarded as a supramolecular bridge between the basal keratinocytes of the epidermis and the underlying dermis (Kiritsi *et al.*, 2013). In addition, sulfhydryl groups, such as those found in key cellular enzymes or in reduced glutathione (GSH) are a common site for protein and peptide

Correspondence address:

**Blase Billack**

Department of Pharmaceutical Sciences, St. John's University, 8000 Utopia Parkway, Jamaica, NY 11439, USA

FAX + 718-990-1877

E-MAIL: billackb@stjohns.edu

alkylation by mustards (Kehe *et al.*, 2009; Korkmaz *et al.*, 2006; Shakarjian *et al.*, 2010).

Part of the toxicity of SM and HN2 may stem from depletion of cellular glutathione stores which, in turn, leads to the intracellular accumulation of reactive oxygen species (ROS) and oxidative DNA damage (Crater and Kannan, 2007; Pant and Lomash, 2016; Paromov *et al.*, 2007). The combination of oxidative DNA damage and direct DNA alkylation leads to strand breaks and activates polymerases such as poly(adenosine diphosphate-ribose) polymerase (PARP). When PARPs react with cellular proteins following exposure to SM, a marked depletion in nicotinamide adenine dinucleotide (NAD<sup>+</sup>) and adenosine triphosphate (ATP) has been observed. The depletion of NAD<sup>+</sup> is associated with reduced glucose consumption and lactate formation, whereas low ATP levels contribute to necrotic cell death (Kehe *et al.*, 2009). Thus, following exposure to SM and subsequent overactivation of PARP, ATP is depleted and degradative enzymes including matrix metalloproteinases (MMPs) and serine proteases are released and thus contributing to tissue destruction (Kehe *et al.*, 2009).

The vesicant actions of SM or HN2 are likely due, at least in part, to the upregulation of MMPs capable of degrading extracellular macromolecules and contributing to epidermal:dermal detachments (Shakarjian *et al.*, 2010). To this end, topically applied SM led to the expression of MMP-9 in a 3D-skin model (Ries *et al.*, 2009), while mouse ears topically exposed to SM (Shakarjian *et al.*, 2006) or HN2 (Tumu *et al.*, 2018) exhibited an increase in MMP-9 expression relative to control tissues MMP-9, also increased in mustard-exposed rat lungs (Sunil *et al.*, 2011; Malaviya, *et al.*, 2010) and mustard-exposed corneas (Gordon *et al.*, 2016).

Despite several decades of research, a highly efficacious countermeasure to SM toxicity in humans has yet to be developed. Moreover, the process of tissue vesication, also known as epidermal:dermal detachment remains to be fully characterized. The main purpose of this study was to use the SM surrogate HN2 to better understand the process of tissue vesication and to investigate the approximate time when subepidermal blister formation occurs after HN2 exposure. This knowledge is necessary for the development of antidotes aimed at reducing the vesicant activity of HN2. The mouse ear vesicant model (MEVM) was used here to investigate the time-dependent dermatotoxicity of HN2 *in vivo*. The dermatotoxic endpoints investigated included tissue edema, as determined by measurement of tissue wet weights and thickness, tissue expression of MMP-9, as determined by immunohistochemistry (IHC), and vesication, as determined from light microscopy of H&E stained tissue sections.

## Materials and methods

### Chemicals, reagents, and other materials

Mechlorethamine hydrochloride (HN2) was purchased from Pfaltz & Bauer (Waterbury, CT; Cat # 55-86-7).

Dimethyl sulfoxide (DMSO) was obtained from J.T. Baker (Philipsburg, NJ; Cat# 67-68-5). A dose of 0.5 μmol/ear HN2 was used in the present study. DMSO was used as the vehicle for HN2 due to its ability to readily penetrate the skin.

Eosin (Cat # CA95057-848), hematoxylin (Cat # CA95057-844), xylene (Cat # CA95057-822), histology grade 100% ethanol (Cat # CA95057-828) and Paraplast X-tra (Cat # 15159-486 -1 kg) were purchased from VWR International (West Chester, PA). Buffered formalin (1:10 dilution, already diluted) (Cat # 23-245-685) was purchased from Fisher Scientific (Nazareth, PA). Permount was purchased from Fisher Scientific (Fairlawn, NJ; Cat# SP15-500). Isoflurane (Cat # 029405) was purchased from Henry Schein (Dublin, OH). Slides and cover glasses were also purchased from VWR International (Radnor, PA; Cat# 16004-386 and Cat # 48382-136, respectively). Vectastain ABC Rabbit IgG Kit (Cat # PK-6101) and Antigen Unmasking Solution (Citrate Based) (Cat # H-3300) were both purchased from Vector Laboratories (Burlingame, CA). Phosphate buffered saline (PBS) (10X) liquid concentrate was obtained from EMD Millipore (Gibbstown, NJ; Cat # 6505-OP). Tris Buffered Saline (TBS) (10X) was purchased from VWR International (West Chester, PA; Cat # 10128-548). The 100% n-butanol was purchased from EMD Millipore (Billerica, MA; Cat # BX1777-6). Tween-20 was purchased from VWR International (Solon, OH; Cat # 97062-332). 30% Hydrogen Peroxide (H<sub>2</sub>O<sub>2</sub>) was purchased from VWR International (Mississauga, ON, Cat # BDH7690-1).

### Animal studies

The protocol for this research was approved by the Institutional Animal Care and Use Committee (IACUC) of St. John's University and the animals were cared for in accordance with the guidelines established by the U.S. Department of Agriculture (USDA). Outbred male Swiss Webster mice were purchased from Taconic farms (Germantown, NY). All mice were kept and maintained in the AAALAC-accredited Animal Care Center at St. John's University (Queens, NY). Animals were allowed to adjust to the new environment for at least 2–3 days before use. All animals were housed in groups of 2–4 per cage in temperature and humidity regulated rooms with 12 hour day and 12 hour night cycles. The total number of mice that were used for the HN2 time course study was 72.

The MEVM has been utilized previously to investigate various histopathological parameters of skin exposed to mustards (Brinkley *et al.*, 1989; Casillas *et al.*, 1997, 2000; Dahir *et al.*, 2002). Common skin responses that are evaluated using the MEVM include edema, hyperplasia, dermal:epidermal separation (vesication), inflammatory cell infiltration and epidermal necrosis. In particular, the strength of the MEVM is that allows for a quantitative measure of vesication.

### Test solutions and reagents

(a) HN2 solution: mechlorethamine hydrochloride in the amount of 0.0192 g (molecular weight: 192.52) was

dissolved in 1 ml of DMSO to obtain a 0.100 M of HN2. When 5 µl of this solution is applied to the inner surface of a mouse ear, it is equal to a HN2 dose of 0.5 µmol/ear. This dose has previously been used by our lab to induce the formation of subepidermal microblisters in Swiss Webster mice (Lulla *et al.*, 2014; Tumu *et al.*, 2018).

(b) Other reagents. *Vehicle*: a 5 µl volume of DMSO was applied to the ears that served as controls in vehicle control tissues. *Buffered formalin solution (1:10 dilution)*: Neutral buffered formalin (8 ml) was used for fixation of each ear punch. *Dehydration alcohol solutions*: Histology grade dehydration ethanol 100% was diluted with distilled and deionized water to obtain 30%, 60%, 70% and 95% ethanol concentrations. *Hematoxylin staining solution*: Ready-made hematoxylin (H) solution purchased from VWR was used to stain the nuclei of the tissue sections. *Eosin staining solution*: Ready-made eosin (E) solution purchased from VWR was used to stain the cytoplasm of the tissue sections.

#### HN2 time course study

Wild type, male Swiss Webster mice weighing between 25–30 g were separated into different groups. For HN2 treated mice, the right ears were treated with a 5 µl volume of 0.100 M HN2, while the left ears served as test controls and received a 5 µl volume of DMSO. For mice treated with DMSO only, the right ears were treated with a 5 µl volume of DMSO, while the left ears were left untreated (naive). Next, at 15 min, 1 hr, 2 hr, 4 hr, 8 hr or 24 hr after exposure to HN2 or DMSO only, blood was collected from anesthetized mice via close chested cardiac puncture. Animals were then euthanized in a carbon dioxide (CO<sub>2</sub>) chamber and ear tissue samples were collected using an 8 mm biopsy punch and weighed on an analytical balance. The ear samples were then transferred to 20 ml vials with 8–10 ml neutral buffered formalin for 18–24 hr before dehydration and embedding in paraffin. Tissue sections of 5 µm thickness were sectioned using a standard rotary microtome, placed in a water bath at 40 °C that also contained few drops of 5% gelatin. Sections were lifted from the water onto the slides and dried overnight. The next day, slides without visible tissue section tears were selected for staining with H & E using a standard staining protocol.

#### Morphometric analysis

Ear thickness was measured using the camera of a Motic BA210 microscope and Motic Image plus 2.0 software. The H & E stained sections were measured under a total magnification of 40× with software calibrated measurements. Thickness of the ear tissues was measured by drawing several perpendicular lines from one side of the tissue to the other side. Nine such lines were drawn on each section and equally spaced along the section and the average distance from one epidermis to the other epidermis was determined. Two duplicate slides for each ear were used in the morphometric analysis. In total, the average of eighteen measurements was taken for each ear sample.

#### Histopathological evaluation

A Zeiss Axio Scope A1 microscope equipped with Axiocam 506 color camera and Zeiss Zen 2.3 software was used for obtaining light microscopy images of immunohistochemistry (IHC) and H & E stained tissues. Stained tissues were evaluated for vesication (epithelial detachment) using a “+” or “-” system by three blinded investigators. Each blinded investigator was instructed to assign a positive score for vesication (+) if the tissue section was found to possess at least one epidermal:dermal detachment. It should be noted that two different tissue sections from each ear punch were scored by each of the three blinded scorers, leading to a total of six scores per ear sample. Lastly, an ear sample was counted as “+” for vesication when at least four of the combined six scores for a particular ear sample were in agreement.

#### IHC for MMP-9

IHC for MMP-9 was carried out as described previously (Tumu *et al.*, 2018).

#### Statistical analysis

All results are presented as the mean ± SEM for 6 or 12 ear samples, depending on the experiment. Statistical significance for wet weight and morphometric analysis was tested between groups using a one-way ANOVA followed by Newman-Keuls multiple comparison post hoc analysis and GraphPad Prism® version 5.0 software.

## Results

For each time point studied there were two groups of mice (N=6 per group). In the first group, mouse ears were treated with HN2 (0.5 µmol/ear) on the right ear and DMSO on the left ear. In the second group, mouse ears were treated with DMSO on the right ear, with the left ear untreated (naive). Mice were euthanized at 15 min, 1 hr, 2 hr, 4 hr, 8 hr or 24 hr following exposure to HN2 or DMSO.

Tissue biopsy wet weights were used as a rudimentary indicator of edema. It is noteworthy that when ear tissues treated with DMSO vehicle alone were compared to untreated naive ear tissues, significant increases in tissue biopsy wet weights were observed at 15 min (1.47 fold vs. naive), 1 hr (1.84 fold vs. naive) and 2 hr (1.78 fold vs. naive) following topical application, as well as at 4 hr (1.46 fold vs. naive), but not at 8 hr (1.14 fold vs. naive) or 24 hr (1.01 fold vs. naive) (Figure 1). When ear punch biopsies were obtained from mice treated with HN2 and compared to those obtained from mice treated with DMSO alone, significant increases in tissue wet weights were observed at 15 min (1.19 fold vs. DMSO), 1 hr (1.17 fold vs. DMSO), 2 hr (1.53 fold vs. DMSO), 4 hr (2.01 fold vs. DMSO), 8 hr (3.05 fold vs. DMSO) and 24 hr (2.84 fold vs. DMSO) (Figure 1). Thus, ear swelling was observed to be time-dependent, with maximum swelling observed 8 hr after topical application of HN2.

Morphometric thickness of ear tissues was then assessed using light microscopy. Compared to tissue

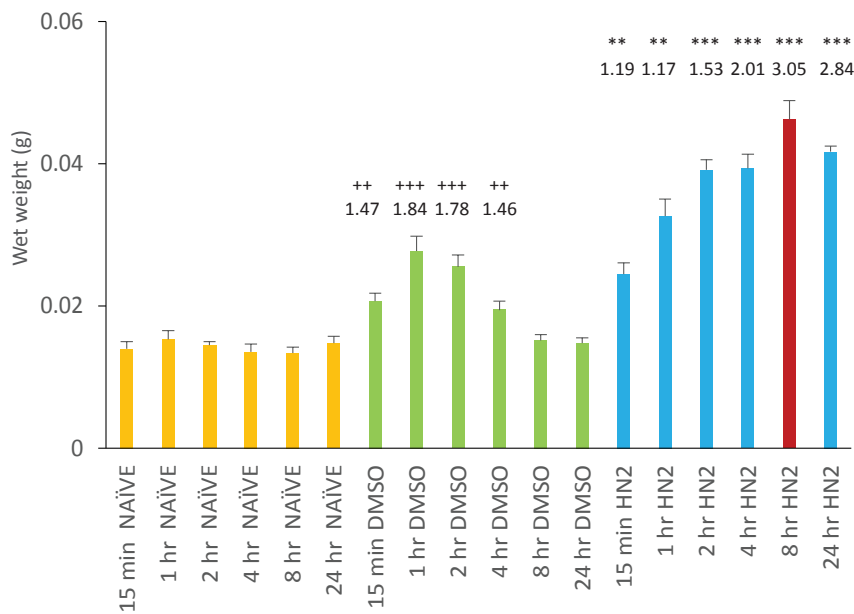


**Figure 1.** Wet weight analysis of ear punches obtained from male Swiss Webster mice. Ears were treated with either HN2 (0.5  $\mu\text{mol}/\text{ear}$ ) or DMSO or left untreated (naïve) and euthanized at 15 min, 1 hr, 2 hr, 4 hr, 8 hr or 24 h following topical exposure. Statistical differences were observed between naïve tissues and DMSO only treated ears at 15 min and 4 hr after treatment which were significant at  $++p<0.01$ , whereas DMSO only treated ears were significantly different from naïve tissues at 1 hr or 2 hr at  $+++p<0.001$ . Note that fold changes relative to naïve are indicated above each bar. Statistical differences between HN2 and DMSO groups at 15 min and 1 hr were significant at  $**p<0.01$ , whereas HN2 treated ears were significantly different from DMSO treated ears 2 hr, 4 hr, 8 hr and 24 hr at  $***p<0.001$ . Note that fold changes relative to DMSO only are indicated above each bar. Data represent average weights  $\pm$  SEM.

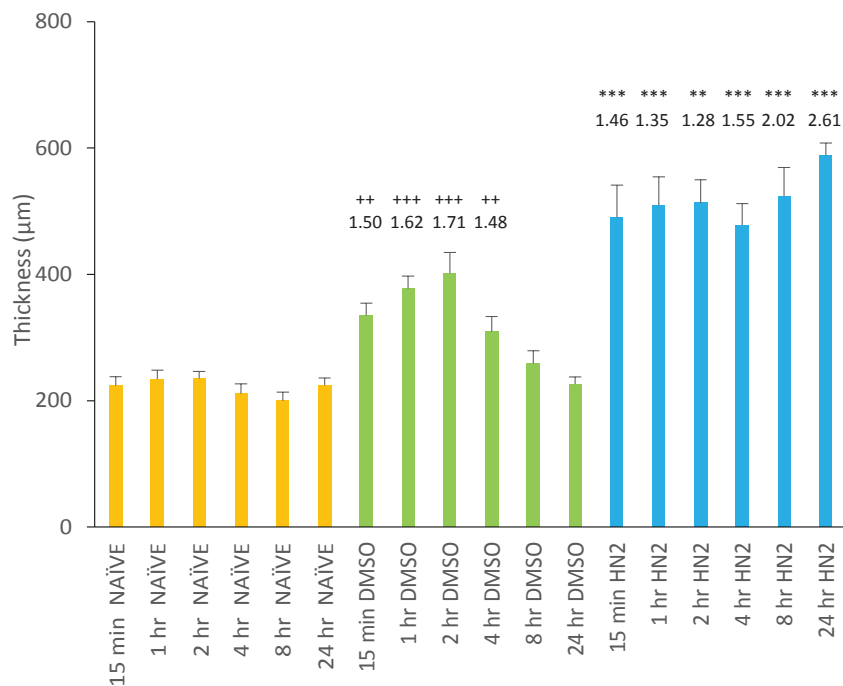


**Figure 2.** Morphometric analysis of ear punches obtained from male Swiss Webster mice. Ears were treated with either HN2 (0.5  $\mu\text{mol}/\text{ear}$ ) or DMSO or left untreated (naïve) and euthanized at 15 min, 1 hr, 2 hr, 4 hr, 8 hr or 24 h following topical exposure. Statistical differences were observed between naïve tissues and DMSO only treated ears 15 min and 4 hr after treatment which were significant at  $++p<0.01$ , whereas DMSO only treated ears were significantly different from naïve tissues at 1 and 2 hr after treatment at  $+++p<0.001$ . Note that fold changes relative to naïve are indicated above each bar. Statistical differences between HN2 treated ear tissues and DMSO only treated ears ear tissues were significant at 15 min, 1 hr and 2 hr at  $**p<0.01$  and at 4 hr, 8 hr and 24 hr following HN2 exposure at  $***p<0.001$ . Note that fold changes relative to DMSO only are indicated above each bar. Data represent average weights  $\pm$  SEM.

sections from naïve ears, those treated with DMSO vehicle alone showed a significant increase in morphometric thickness at 15 min (1.50 vs. naïve), 1 hr (1.62 vs. naïve), 2 hr (1.71 fold vs. naïve) and 4 hr (1.48 fold vs. naïve) but not at 8 hr (1.30 fold vs. naïve,  $p=0.052$ ) or 24 hr (1.00 fold vs. naïve) (Figure 2). When ear punch biopsies were obtained from mice treated with HN2 and compared to ear punch biopsies obtained from mice treated with DMSO alone, significant increases in morphometric thickness were observed at 15 min (1.46 fold vs. DMSO), 1 hr (1.35 fold vs. DMSO), 2 hr (1.28 fold vs. DMSO), 4 hr (1.55 fold vs. DMSO), 8 hr (2.02 fold vs. DMSO) and 24 hr (2.61 fold vs. DMSO) (Figure 2). Morphometric thickness analysis therefore revealed that ear swelling was time-dependent, occurring in as little as 15 min with maximum tissue thickness observed 24 hr after topical application of HN2.

Histopathologic assessment of H&E stained ear tissues demonstrated that untreated naïve ears exhibited two epidermal cell layers, representing the external and internal surfaces of the ear, both approximately one cell in thickness; moreover, these sections showed normal cartilage and sebaceous glands (Figure 3, Panels A and B; Figure 4, Panels A and B). Tissues that were treated with HN2 and then harvested after 15 min (Figure 3, Panel D), 1 hr (Figure 3, Panel F), 2 hr (Figure 3, Panel H), 4 hr (Figure 4, Panel D), 8 hr (Figure 4, Panel F) or 24 hr (Figure 4, Panel H) showed a time-dependent increase in tissue edema and infiltrating immune cells, with minor tissue injury evident in as little as 15 min after HN2 exposure and severe edema and inflammatory cell infiltrates observed at time points  $\geq 1$  hr. Maximum injury, including the presence of epidermal:dermal detachments, was observed at time points  $\geq 8$  hr. Note that the present study did not examine tissue responses beyond 24 hr.

Compared to naïve ears, ear tissues treated with DMSO alone and collected 15 min after exposure showed a slight increase in tissue swelling (Figure 3, Panel C). The effects of DMSO after topical application to mouse ear skin became more pronounced at 1 hr (Figure 3, Panel E), 2 hr (Figure 3, Panel G) and 4 hr (Figure 4, Panel C), with tissue sections showing edema and increased inflammatory cells at these time points. The worst injury caused by exposure to DMSO alone was observed 2 hr after topical application (Figure 3, Panel G). Ear samples treated topically with DMSO and collected after 8 hr (Figure 4, Panel E) or 24 hr (Figure 4, Panel G) looked similar to naïve ear tissues (Figure 4, Panels A and B). Thus the effects of DMSO alone on tissue edema were transient and subsided by 8 hr after treatment. Moreover, ears treated with HN2 showed more severe tissue injury at every time point than ears treated with DMSO alone. All in all, the light micrographs supported the data obtained from wet weight and morphometric tissue thickness analyses (see Figures 1 and 2).

To investigate the extent to which DMSO or HN2 affects tissue expression of MMP-9, IHC was performed on ear punch biopsies collected 15 min, 1, 2, 4, 8 or 24 hr after topical application (Figure 5 and Figure 6). Whereas naïve ear tissues showed very low expression of MMP-9

(Figure 5, Panels A and B; Figure 6, Panels A and B), ear tissues treated topically with HN2 showed a time-dependent increase in its expression. To this end, MMP-9 was initially observed near the HN2 exposed side of the dermis at 15 min (Figure 5, Panel D) and 1 hr (Figure 5, Panel F) after exposure, but then found to be expressed throughout the tissue and specifically within infiltrating inflammatory cells at 2 hr (Figure 5, Panel H) and 4 hr (Figure 6, Panel D) following HN2 exposure. MMP-9 staining remained elevated throughout the tissue at 8 hr (Figure 6, Panel F) and 24 hr (Figure 6, Panel H) after HN2 exposure, with expression observed not only within inflammatory cells but also in extracellular regions.

Treatment of mouse ears with DMSO alone had an unexpected transient effect on MMP-9 expression which was not observed to persist beyond 4 hr. To this end, when compared to naïve ear tissues (Figure 5, Panels A and B) or ear tissues exposed to DMSO alone and collected 15 min later (Figure 5, Panel C), ear samples obtained at 1 hr after topical application of DMSO exhibited slightly higher expression of MMP-9 within the dermis (Figure 5, Panel E). By 2 hr after DMSO exposure, ear sections showed abundant expression of MMP-9 in both the epidermis and the infiltrating immune cells (Figure 5, Panel G) which persisted until 4 hr after DMSO exposure (Figure 6, Panel C). Ear samples treated topically with DMSO and collected after 8 hr (Figure 6, Panel E) or 24 hr (Figure 6, Panel G) looked similar to naïve ear tissues.

All in all, the tissue expression of MMP-9 in ears treated with HN2 (0.5  $\mu\text{mol}/\text{ear}$ ) at 4, 8 and 24 hr after topical application (Figure 6, Panels D, F and H, respectively) was dramatically increased compared to tissue expression observed at earlier time points including 15 min, 1 hr and 2 hr (Figure 5, Panels D, F and H, respectively). A transient increase in tissue expression of MMP-9 was observed after topical exposure to DMSO at early time points (1 hr, 2 hr and 4 hr) which was not observed at time points  $\geq 8$  hr.

Inspection of H&E sections prepared from ear tissues exposed to HN2 and harvested after 15 min, 2 hr or 4 hr revealed vesication in 16.7% of ears. Ears treated with HN2 and collected after 1 hr did not show any signs of vesication. Ears exposed to HN2 and harvested 8 hr later exhibited vesication in 66.7% of the samples. Ears exposed to HN2 and collected 24 hr later showed vesication in 83.3% of the ears (Table 1; Figure 4, Panel H). Ears exposed to DMSO alone did not show vesication.

## Discussion

Previous studies using the MEVM to investigate mustard toxicity have examined ear tissues for signs of injury at time points such as 6, 12, 18 or 24 hr after exposure (Casillas *et al.*, 1997; Dachir *et al.*, 2002; Shakarjian *et al.*, 2006; Tumu *et al.*, 2018), or have included even later time points such as 72, 120 or 168 h after exposure (Dachir *et al.*, 2002; Shakarjian *et al.*, 2006; Tewari-Singh *et al.*, 2013). In the present study, we investigated the effects of HN2 on the ear skin of male Swiss Webster mice at

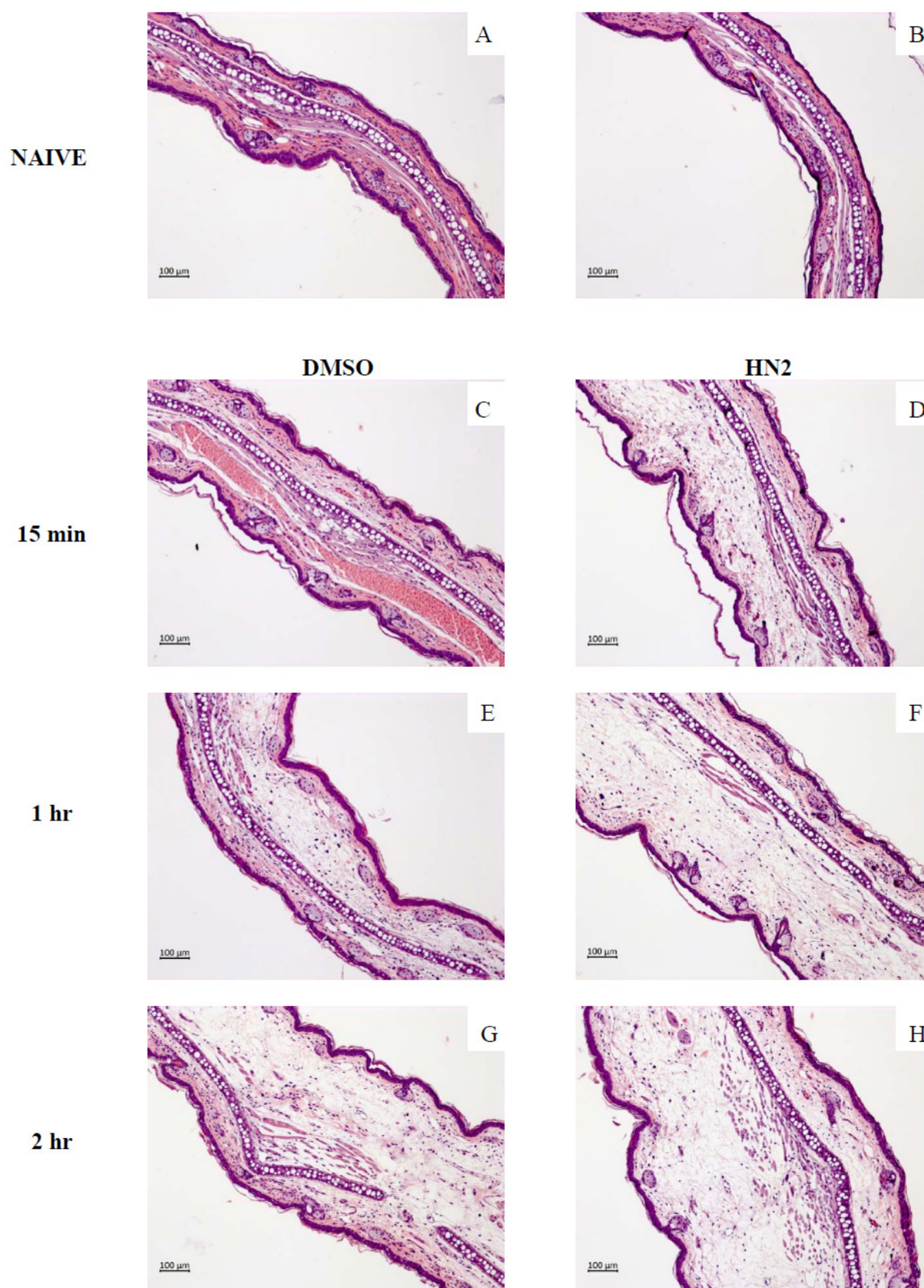


**Figure 3.** Representative light micrographs of H & E stained ear tissue sections obtained from male Swiss Webster mice. Panels A and B represent untreated (naïve) ear tissues. Panels C, E and G represent ears treated with the vehicle DMSO only, and Panels D, F and H represent ears treated with HN2 (0.5 µmol/ear) at 15 min, 1 hr and 2 hr, respectively. Total magnification used is 100X. Scale bars on the micrographs represent a length of 100 µm.

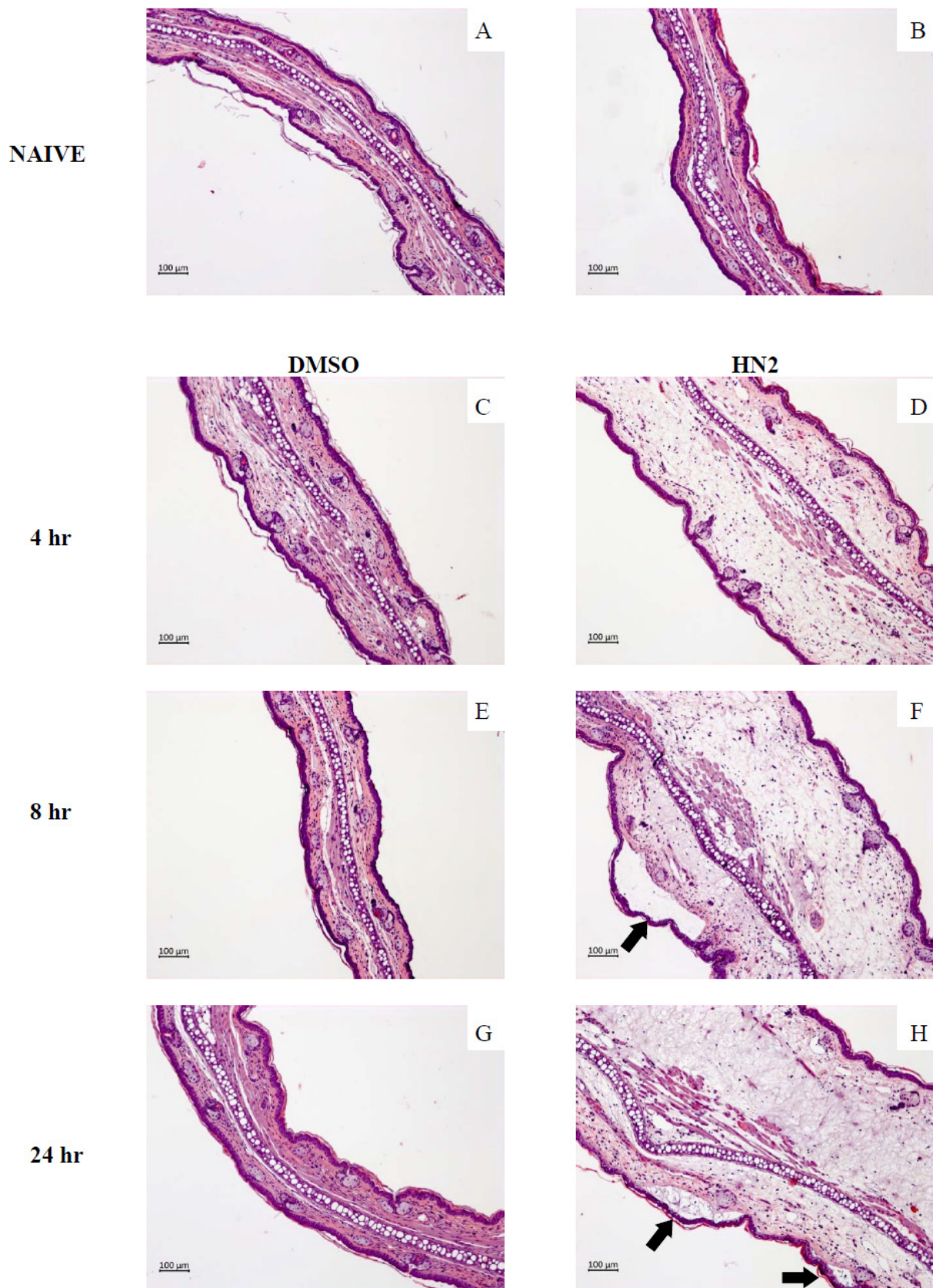


**Figure 4.** Representative light micrographs of H & E stained ear tissue sections obtained from male Swiss Webster mice. Panels A and B represent untreated (naïve) ear tissues. Panels C, E and G represent ears treated with the vehicle DMSO only, and Panels D, F and H represent ears treated with HN2 (0.5 µmol/ear) at 4 hr, 8 hr and 24 hr, respectively. Note the presence of epidermal:dermal detachments in Panels F and H as indicated by the black arrows. Total magnification used is 100X. Scale bars on the micrographs represent a length of 100 µm.

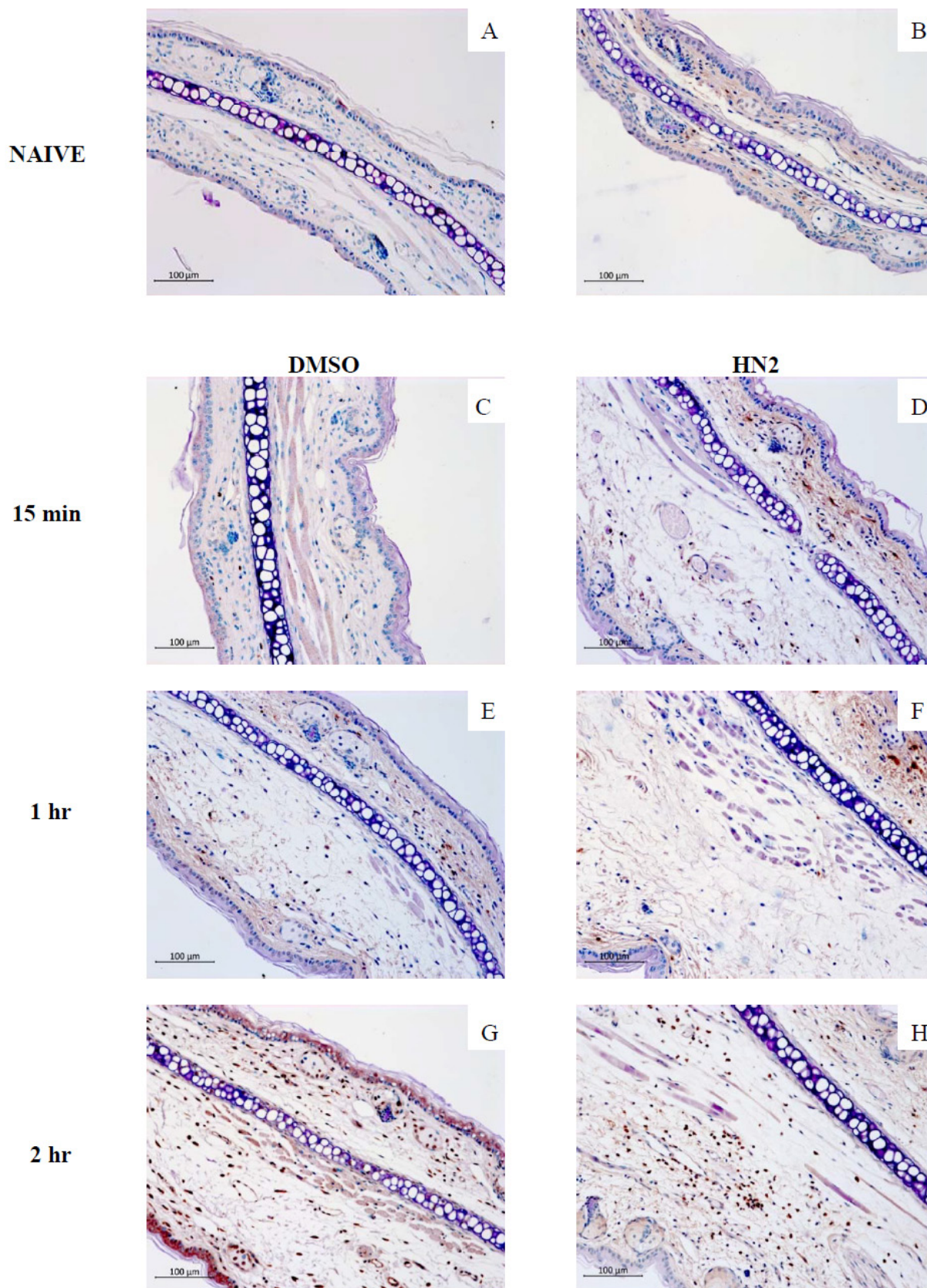


**Figure 5.** Representative light micrographs of IHC staining for MMP-9 in ear tissue sections obtained from male Swiss Webster mice. Panels A and B represent untreated (naïve) ear tissues. Panels C, E and G represent ears treated with the vehicle DMSO only, and Panels D, F and H represent ears treated with HN2 (0.5 µmol/ear) at 15 min, 1 hr and 2 hr, respectively. Total magnification used is 200×. Scale bars on the micrographs represent a length of 100 µm.

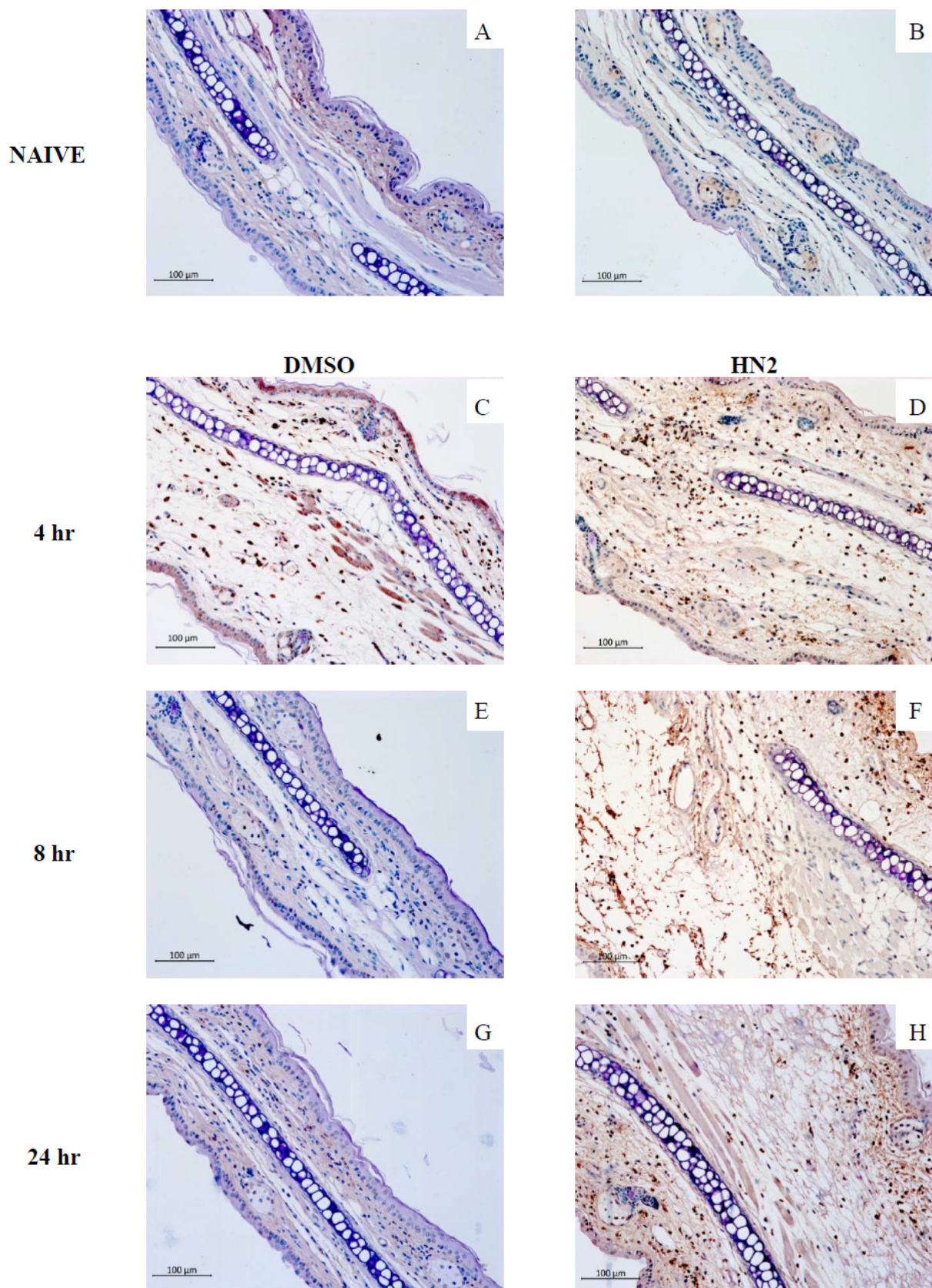


**Figure 6.** Representative light micrographs of IHC staining for MMP-9 in ear tissue sections obtained from male Swiss Webster mice. Panels A and B represent untreated (naïve) ear tissues. Panels C, E and G represent ears treated with the vehicle DMSO only, and Panels D, F and H represent ears treated with HN2 (0.5 µmol/ear) at 4 hr, 8 hr and 24 hr, respectively. Total magnification used is 200×. Scale bars on the micrographs represent a length of 100 µm.

**Table 1.** Vesication/epidermal:dermal detachments in ear punches obtained from male Swiss Webster mice at 15 min, 1 h, 2 h, 4 h, 8 h and 24 h after topical exposure to HN2 or DMSO.

Time Point	Treatment	% Vesication	N (# of ears)
15 min	Naïve (untreated)	0%	6
15 min	DMSO (5 µl/ear)	0%	12
15 min	HN2 (5 µmol/ear)	16.7%	6
1 h	Naïve	0%	6
1 h	DMSO	0%	12
1 h	HN2	0%	6
2 h	Naïve	0%	6
2 h	DMSO	0%	12
2 h	HN2	16.7%	6
4 h	Naïve	0%	6
4 h	DMSO	0%	12
4 h	HN2	16.7%	6
8 h	Naïve	0%	6
8 h	DMSO	0%	12
8 h	HN2	66.7%	6
24 h	Naïve	0%	6
24 h	DMSO	0%	12
24 h	HN2	83.3%	6

15 min, 1 hr, 2 hr, 4 hr and 8 hr following HN2 exposure. Mice ears were also collected at the 24 hr time point after HN2 exposure to serve as a positive control.

To our knowledge, few studies have investigated the dermatotoxicity of HN2 at time points earlier than 6 hr using the MEVM. One recent study (Composto *et al.*, 2018) examined epidermal responses to HN2 applied topically to the dorsal skin of mice. In that study, the time points evaluated included 15 min, 30 min, 45 min, 1 hr, 2 hr, 3 hr, 6 hr, 12 hr and 24 hr. The epidermis of the mice was removed at the respective time points and analyzed for dermatotoxicity by H&E staining, immunohistochemistry of 8-oxo-dG and Western Blot analysis for pH2A.X, poly ADP-ribose (pADPr), heme oxygenase-1 (HO-1) and proteins modified by 4-hydroxyl nonenal (4HNE). The results of that study demonstrated that HN2 exposure led to skin inflammation and edema as early as 12 hr, a significant increase in pH2A.X, pADPr, HO-1 and 4HNE as early as 15 min and an increase in the epidermal expression of 8-oxo-dG by 6 hr. However, no signs of vesication were assessed in that study and the gross injury, as shown by light microscopy of H&E tissue sections, was relatively minor. Thus it appears that our study is the first report of vesication by HN2 at time points as early as 15 min following exposure.

The vehicle used here to dissolve HN2 was DMSO. The tissue penetration of DMSO is attributed to an increase in diffusion through the stratum corneum by disruption of the membrane barrier function. This disruption by DMSO has been hypothesized to result from

aprotic interactions occurring with intercellular lipids, the reversible distortion of lipid head groups which allows for a more permeable packing arrangement, and the formation of solvent microenvironments within the tissue that enable the solute to be extracted from the vehicle (Capriotti & Capriotti, 2012). Compared to other vehicles, DMSO has been shown to exhibit a greater solubilizing effect on less soluble agents, and its ability to enhance the penetration of a given drug subsequently allows for a greater concentration of the drug to be delivered to the membrane barrier.

In the present study, DMSO applied topically to the mouse ear as a vehicle control resulted in transient tissue edema, as observed by wet weight and morphometric thickness analyses and light microscopy at 15 min, 1 hr, 2 hr and 4 hr. The swelling of ears exposed to DMSO observed here may be attributed to its initial penetration through the mouse ear skin and absorption into the dermis; however, after 4 hr the ear swelling by DMSO subsides and becomes similar to that which is exhibited by untreated naïve ear tissues. Thus, DMSO vehicle, while not inert, did not interfere with the assessment of inflammation or vesication. Until now, we have not known of this DMSO effect, as our previous studies in the MEVM have been carried out ≥12 hr after HN2 exposure. Although the swelling by DMSO subsides after 4 hr, it may be useful to investigate alternate vehicles that could be used to dissolve HN2 for treatment on the mouse ear tissue. For example, Composto and colleagues (2018) dissolved 20 µmol of HN2 in a solution that was 80% acetone and 20% water; forty times higher than the concentration of 0.5 mol HN2 used in the present study. Despite using a much higher concentration of HN2, no evidence of vesication was demonstrated in their study, which may be attributed to a poor ability of the acetone:water vehicle to distribute HN2 into the skin. If this is correct, then vesication by HN2 may require penetration into the dermis, which is achieved with DMSO, but not with acetone or water. Further study will be required to confirm our hypothesis. In addition, whereas Composto *et al.* (2018) exposed the dorsal skin of mice to HN2 in an acetone:water vehicle, it would be interesting to investigate whether the same HN2 formulation exhibits vesication in the MEVM. The use of an acetone mixture poses the risk of evaporation and precipitation on the epidermal surface, which may impact the accurate penetration of the drug into the skin. The use of DMSO in the present study therefore ensures that the full dose of HN2 is delivered into the mouse ear and allows for the presence of vesication to be evaluated.

The results of our study determined that HN2 causes a significant increase in edema in terms of wet weight and morphometric thickness as early as 15 min following HN2 exposure. It should be noted that while both wet weight and morphometric thickness measurements of HN2-treated ear tissues were significant at all time points, the two assays did not match exactly, as demonstrated by the greater increase in ear wet weight observed at 8 hr than at 24 hr, as opposed to the observation of a greater increase

in morphometric thickness at 24 hr than at 8 hr. The differences observed between the two assays may point to differences in assay sensitivity which should be taken into consideration; however, the ease of determining tissue wet weight as a preliminary index of tissue edema is a great advantage, especially when compared to the more cumbersome tissue preparation required for H&E staining and morphometric thickness analysis. Thus, both assays are complementary and useful in determining the extent by which HN2 induces ear edema. It is noteworthy that both edema and vesication were observed as early as 15 min following HN2 exposure; with a sharp increase in vesication detected between 4 to 8 hr following HN2 exposure. It can therefore be concluded that a 0.5 µmol/ear dose of HN2 in the MEVM results in a time-dependent tissue injury that is accompanied by significant vesication in as little as 8 hr after HN2 exposure.

Matrix metalloproteinases (MMPs) are capable of degrading extracellular matrix proteins and modifying various non-matrix substrates such as cytokines and chemokines. SM exposure leads to upregulation of MMP-9 in a 3D-skin model (Ries *et al.*, 2009) and also *in vivo* (Shakarjian *et al.*, 2006). In the present investigation, the tissue expression of MMP-9 was increased by DMSO vehicle alone up through 4 hr; however, the tissue expression induced by DMSO was transient, confined within immune cells, and returned to baseline levels by 8 hr after vehicle exposure. On the other hand, ear tissues exposed to HN2 exhibited time-dependent accumulation of MMP-9 positive immune cells within the dermis as well as release of MMP-9 into the extracellular matrix. This also correlated with the high incidence of vesication observed at time points ≥8 hr after HN2 exposure.

The results of this study provide a more holistic understanding of the process of vesication and reveal useful information for future investigation aimed at identifying potential antidotes to mustard toxicity. For example, previous work in our lab has applied various potential antidotes to HN2-exposed ears at 15 min, 4 hr and 8 hr following initial exposure, with tissues harvested at 12 hr and 24 hr following exposure (Tumu *et al.*, 2018). By utilizing the information provided by the present study, it may be useful to apply countermeasure treatments at alternative time points such as 1 hr, 2 hr and 4 hr after HN2 exposure, as significant tissue swelling and inflammation are already observed at these earlier time points. Additionally, future studies may look to euthanizing mice at 8 hr following treatment(s), as the extent of vesication induced by HN2 begins to plateau by this point, and only increases slightly up to 24 hr. Moreover, the present study sets the stage to investigate DNA damage and other factors involved in the process of vesication and early stages in HN2 injury.

Altogether, the data obtained in the HN2 study demonstrate that:

DMSO vehicle is not inert and affects the mouse ear tissue at early time points (15 min, 1, 2 and 4 hr) after topical application, but not at later time points (8 and 24 hr).

The process of vesication begins as soon as 15 min after topical exposure to HN2 and is significantly upregulated between 4 and 8 hr.

High incidence of vesication (>50%) is time-dependent and associated with accumulation of MMP-9 protein expression in mouse ear tissue. Tissue abundance of MMP-9 increases significantly 2 hr after HN2 exposure, showing expression both within immune cells at 2, 4, 8 and 24 hr, as well extracellular expression at 8 and 24 hr.

These data have established a useful platform for mechanistic studies aimed at better understanding the process of vesication by mustards and the role of MMP-9 therein.

## Acknowledgements

This work was funded by the Department of Pharmaceutical Sciences, St. John's University. Part of this work was presented at the 23<sup>rd</sup> Interdisciplinary Toxicological Conference (TOXCON) in the Slovak Republic (June 2018). The authors thank Trishaal J.R. Rao for thoughtful comments pertaining to the revision of this manuscript.

## Declaration

All authors declare no financial activities or financial holdings that could be perceived as constituting a conflict of interest.

## REFERENCES

- Brinkley FB, Mershon MM, Yaverbaum S, Doxzon BF, Wade JV. (1989). The Mouse Ear Model as an *In Vivo* Bioassay for the Assessment of Topical Mustard (HD) Injury. In Proceedings of the 1989 Medical Defense Review. pp. 595–602.
- Capriotti K, & Capriotti JA. (2012). Dimethyl sulfoxide: history, chemistry and clinical utility in dermatology. *Journal of Clinical and Aesthetic Dermatology* **5(9)**: 24–6.
- Casillas RP, Mitcheltree LW, Stemler FW. (1997). The mouse ear model of cutaneous sulfur mustard injury. *Toxicology Mechanisms and Methods* **7(4)**: 381–397.
- Casillas RP, Kiser RC, Truxall J, Singer AW, Shumaker SM, Niemuth N, Ricketts KM, Mitcheltree LW, Castrejon LR, Blank J. (2000). Therapeutic approaches to dermatotoxicity by sulfur mustard I. modulation of sulfur mustard-induced cutaneous injury in the mouse ear vesicant model. *Journal of Applied Toxicology* **20**: S145–S151.
- Composto GM, Arunachalam T, Laskin DL, Heck DE, Laskin JD, Joseph LB. (2018). Oxidative stress and DNA damage in mouse epidermis following exposure to nitrogen mustard. *The Toxicologist: Proceedings of the 57<sup>th</sup> Annual Meeting of the Society of Toxicology* **162**: 312 (Abstract 2283).
- Crater J, Kannan S. (2007). Molecular mechanism of nitrogen mustard induced leukocyte(s) chemotaxis. *Medical Hypotheses* **68(2)**: 318–319.
- Dachir S, Fishbeine E, Meshulam Y, Sahar R, Amir A, Kadar T. (2002). Potential anti-inflammatory treatments against cutaneous sulfur mustard injury using the mouse ear vesicant model. *Human and Experimental Toxicology* **21(4)**: 197–203.
- Gordon MK, DeSantis-Rodrigues A, Hahn R, Zhou P, Chang Y, Svoboda KK, Gerecke DR. (2016). The molecules in the corneal basement membrane zone affected by mustard exposure suggest potential therapies. *Annals of the New York Academy of Sciences* **1378(1)**: 158–165.

- Kehe K, Balszuweit F, Steinritz D, Thiermann H. (2009). Molecular toxicology of sulfur mustard-induced cutaneous inflammation and blistering. *Toxicology* **263**(1): 12–19.
- Korkmaz A, Yaren H, Topal T, Oter S. (2006). Molecular targets against mustard toxicity: Implication of cell surface receptors, peroxynitrite production, and PARP activation. *Archives of Toxicology/Archiv Für Toxikologie* **80**(10): 662–70.
- Kiritzi D, Has C, Bruckner-Tuderman L. (2013). Laminin 332 in junctional epidermolysis bullosa. *Cell adhesion & migration* **7**(1): 135–41.
- Lulla A, Reznik S, Trombetta L, Billack B. (2014). Use of the mouse ear vesicant model to evaluate the effectiveness of ebselen as a countermeasure to the nitrogen mustard mechlorethamine. *Journal of Applied Toxicology* **34**(12): 1373–8.
- Malaviya R, Sunil VR, Cervelli JA, Anderson DR, Holmes WW, Conti ML, Gordon RE, Laskin JD, Laskin DL. (2010). Inflammatory effects of inhaled sulfur mustard in rat lung. *Toxicology and Applied Pharmacology* **248**(2): 89–99.
- Malaviya R, Sunil VR, Venosa A, Verissimo VL, Cervelli JA, Vayas KN, Hall L, Laskin JD, Laskin D. (2015). Attenuation of nitrogen mustard-induced pulmonary injury and fibrosis by anti-tumor necrosis factor- $\alpha$  antibody. *Toxicological Sciences* **148**(1): 71–88.
- Pant SC, Lomash V. (2016). Sulphur Mustard Induced Toxicity, Mechanism of Action and Current Medical Management. *Defence Life Science Journal* **1**(1): 07-17, DOI: 10.14429/dlsj.1.10089
- Paromov V, Suntres Z, Smith M, Stone WL. (2007). Sulfur mustard toxicity following dermal exposure: Role of oxidative stress, and antioxidant therapy. *Journal of Burns and Wounds* **7**: e7.
- Ries C, Popp T, Egea V, Kehe K, Jochum M. (2009). Matrix metalloproteinase-9 expression and release from skin fibroblasts interacting with keratinocytes: Upregulation in response to sulphur mustard. *Toxicology* **263**(1): 26–31.
- Shakarjian MP, Bhatt P, Gordon MK, Chang YC, Casbohm SL, Rudge TL., Kiser CR, Sabourin C, Casillas RP, Ohman-Strickland PA, Riley DJ, Gerecke DR. (2006). Preferential expression of matrix metalloproteinase-9 in mouse skin after sulfur mustard exposure. *Journal of Applied Toxicology* **26**(3): 239–246.
- Shakarjian MP, Heck DE, Gray JP, Sinko PJ, Gordon MK, Casillas RP, Heindel ND, Gerecke DR, Laskin D, Laskin JD. (2010). Mechanisms mediating the vesicant actions of sulfur mustard after cutaneous exposure. *Toxicological Sciences: An Official Journal of the Society of Toxicology* **114**(1): 5–19.
- Sunil VR, Patel KJ, Shen J, Reimer D, Gow AJ, Laskin JD, Laskin DL. (2011). Functional and inflammatory alterations in the lung following exposure of rats to nitrogen mustard. *Toxicology and Applied Pharmacology* **250**(1): 10–18.
- Tumu H, Cuffari B, Pino MA, Pietka-Ottlik M, Billack B. (2018). Ebselen oxide attenuates mechlorethamine dermatotoxicity in the mouse ear vesicant model. *Drug and Chemical Toxicology* 2018 Sep **26**: 1–12. doi: 10.1080/01480545.2018.1488858. [Epub ahead of print]; PMID: 30257109

## ORIGINAL ARTICLE

# Antiproliferative, neurotoxic, genotoxic and mutagenic effects of toxic cyanobacterial extracts

Enver Ersoy ANDEDEN<sup>1</sup>, Sahlan OZTURK<sup>2</sup>, Belma ASLIM<sup>3</sup>

<sup>1</sup> Molecular biology and genetics, Life sciences, Nevsehir Haci Bektas Veli, Nevsehir, Turkey

<sup>2</sup> Environmental Engineering, Faculty of Engineering-Architecture, Life sciences, Nevsehir Haci Bektas Veli, Nevsehir, Turkey

<sup>3</sup> Biology, Faculty of Science, Life sciences, Gazi, Ankara, Turkey

ITX110418A04 • Received: 15 August 2017 • Accepted: 13 January 2018

## ABSTRACT

Cyanobacteria are the rich resource of various secondary metabolites including toxins with broad pharmaceutical significance. The aim of this work was to evaluate the antiproliferative, neurotoxic, genotoxic and mutagenic effects of cyanobacterial extracts containing Microcystin-LR (MCLR) *in vitro*. ELISA analysis results showed that MCLR contents of five cyanobacterial extracts were 2.07 ng/mL, 1.43 ng/mL, 1.41 ng/mL, 1.27 ng/mL, and 1.12 ng/mL for *Leptolyngbya* sp. SB1, *Phormidium* sp. SB4, *Oscillatoria earlei* SB5, *Phormidium* sp. SB2, Uncultured cyanobacterium, respectively. *Phormidium* sp. SB4 and *Phormidium* sp. SB2 extracts had the lowest neurotoxicity (86% and 79% cell viability, respectively) and *Oscillatoria earlei* SB5 extracts had the highest neurotoxicity (47% cell viability) on PC12 cell at 1000 µg/ml extract concentration. *Leptolyngbya* sp. SB1 and *Phormidium* sp. SB2 showed the highest antiproliferative effect (92% and 77% cell death) on HT29 cell. On the other hand, all concentrations of five toxic cyanobacterial extracts induced DNA damage between 3.0% and 1.3% of tail intensity and did not cause any direct mutagenic effect at the 1000 µg/plate cyanobacterial extracts. These results suggest that cyanobacteria-derived MCLR is a promising candidate for development of effective agents against colon cancer.

**KEY WORDS:** Cyanobacteria; Microcystin-LR; HT29 cells; HeLa cells; PC12 cells

## Introduction

Cyanobacteria have been known as harmful to a large number of living organisms because of the production of toxic compounds, of which microcystines (MCs) commonly occur in freshwater blooms worldwide (Falconer & Humpage 2005; Dietrich *et al.*, 2008). The cyanobacterial toxins can be grouped by toxic effects on humans and animals as irritant toxins, dermatotoxins, neurotoxins, cytotoxins, and hepatotoxins (Kerbrat *et al.*, 2010; Nan *et al.*, 2011). The microcystines (MCs) are potent hepatotoxic cyclic heptapeptides produced by some of the cyanobacterial genera such as *Microcystis*, *Anabaena*, *Leptolyngbya*, *Oscillatoria*, *Phormidium* and *Planktothrix* (Izaguirre *et al.*, 2007; Frazao *et al.*, 2010; Wood *et al.*, 2010a; Shishido *et al.*, 2013). Several studies showed that

Microcystin-LR (MCLR) is produced by some of the *Leptolyngbya* sp. (Gantar *et al.*, 2009), *Phormidium* sp. (Teneva *et al.*, 2005; Shishido *et al.*, 2013), *Oscillatoria tenius* (El Herry *et al.*, 2008) and *Oscillatoria agardii* (Luukkainen *et al.*, 1993) strains. To date, a large number of variants of MCs (e.g. MCLR, MCYR, MCRR, MCLA, MCLW, MCLF) have been identified (Lürling & Faassen 2013; Palagama *et al.*, 2017). MCLR is the most abundant variant of all MCs in natural waters (Dietrich & Hoeger, 2005). Intracellular toxicity of MCs is characterized by inhibition of serine/threonine protein phosphatase 1 (PP1) and PP2 catalytic subunits, glutathione depletion and production of reactive oxygen species (ROS) (Gupta *et al.*, 2003). Furthermore, inhibition of protein phosphatases 1 and 2A causes hyperphosphorylation and aggregation of tau protein leading to neuronal degenerative changes and apoptosis, similar as those observed in the brains of Alzheimer patients (Li *et al.*, 2012).

Previous studies have indicated that MCs are able to accumulate in the brains of some animals and cause neurotoxicity (Cazenave *et al.*, 2008; Metcalf *et al.*, 2009).

Correspondence address:

**Sahlan Ozturk**

Environmental Engineering, Faculty of Engineering-Architecture, Life sciences, Nevsehir Haci Bektas Veli, Nevsehir, Turkey

E-MAIL: [ahlan.ozturk@nevsehir.edu.tr](mailto:ahlan.ozturk@nevsehir.edu.tr)

Reduction in brain size was demonstrated in progeny of Swiss Albino mice subjected to cyanobacterial extract containing MCs (Falconer *et al.*, 1988). Meng *et al.* (2011) showed that MCLR lead to damage on cytoskeleton system via hyperphosphorylation of tau and the 27-kDa heat-shock protein (HSP27) in neuroendocrine PC12 cell line.

While most of the researches have been based on toxicity of cyanobacterial metabolites, some studies have revealed that some cyanobacterial species produced anti-inflammatory and anticarcinogenic compounds (Singh *et al.*, 2011). In 2008, the International Agency for Research on Cancer (IARC) estimated that 12.4 million were new cancer cases and about 7.6 million people died due to this disease worldwide (Boyle & Levin, 2008). Synthetic drugs used for several cancer therapies influence quickly dividing normal cells in the patient body causing certain other major irreversible adverse effects (Nooter & Herweijer, 1991; Naumovski *et al.*, 1992). Therefore, the investigation of different natural products for finding a new pharmacological agent is valuable both as a source of potential chemotherapeutic drugs and as a measure of safety (Nascimento *et al.*, 2013). Cytotoxicity, genotoxicity and mutagenicity studies can also help in assessing the effect and safety of natural products as new pharmacological agents (Romero-Jimenez *et al.*, 2005).

From the pharmacological point of view, MCs can be qualified as potential candidate in cancer drug development. MCs cause cellular damage following uptake through organic anion transporting polypeptides (OATP) and there are certain OATPs expressed prominently in cancer tissue as compared to normal tissue (Monks *et al.*, 2007; Sainis *et al.*, 2010). Recently, Kounnis *et al.* (2015) reported that MCLR showed cytotoxic activity against BxPC-3 and MIA PACA-2 pancreatic cancer cell lines expressing the OATP1B1 and OATP1B3 membrane transporters. Also Meickle *et al.*, (2009) have confirmed toxic compounds from *Lyngbya* sp. to show effective cytotoxic activity to KB carcinoma cells, HT29 colorectal adenocarcinoma cells and IMR-32 neuroblastoma cells.

The present study was carried out to evaluate the neurotoxic, and antiproliferative effects of five toxic

cyanobacterial extracts which belong to *Leptolyngbya* sp., *Oscillatoria earlei*, *Phormidium* sp., *Phormidium* sp. and *Uncultured cyanobacterium* strains on ngF-differentiated PC12 cell, both human cervical adenocarcinoma cell line (HeLa) and human colorectal adenocarcinoma cell lines (HT29). The extracts were also investigated for their genotoxic and mutagenic effects to determine the possible mechanisms of cell death elicited by the extracts. This paper is the first report evaluating the genotoxic, mutagenic, neurotoxic and anticancer effects of the cyanobacterial extracts containing MCLR.

## Materials and methods

### Preparation of cyanobacterial extracts

The total biomass of 20 cyanobacterial isolates cultured in 500 ml of BG11 liquid medium (Rippka *et al.*, 1979) under continuous illumination (75  $\mu\text{M}$  photons  $\text{m}^{-2} \text{s}^{-1}$ ), at 25 °C for 30 days, were collected and rinsed twice with deionized distilled water and then dried at 60 °C. The dried algal biomass was powdered and 200 mg of dry algal powder was suspended in 10 ml of methanol. The suspension was kept at 50 °C in an incubator for three days. During this period, samples were taken away to ultrasonicate (20 KHZ) in cold water bath for one minute, twice a day. After three days, methanol extracts were centrifuged at 5000 rpm for 15 min at 5 °C, and the pellet was removed. One ml of supernatant was transferred to another tube for ELISA analysis. The methanol was evaporated from the remaining supernatant and the residue of cyanobacterial extracts and used for assays of neurotoxic and antiproliferative effect, genotoxicity, and mutagenicity.

### ELISA analysis

Microcystin content was determined by an indirect competitive ELISA using an Envirologix QuantiPlate Test Kit for microcystins (Envirologix EP-022, Inc., Portland, Maine, USA), according to the manufacturer's instructions. Absorbance was read at 450 nm using a microplate reader. The microcystin contents measured in this paper were expressed as Microcystin-LR equivalents, and all the analysis was performed in two repetitions. In order to detect MCLR content,  $B_0\%$  values for each sample and MCLR standards (0.16, 0.60 and 2.5 ng/ml) was calculated with the following formula  $B_0\% = (\text{average OD of calibrator or sample}) / (\text{average OD of negative control}) \times 100$  and then a logarithmic curve was obtained using  $B_0\%$  values of each MCLR standards (Figure 1).

### DNA extraction, amplification and sequencing

DNA extraction was performed using CTAB method (Doyle & Doyle 1990) with minor modifications. PCR reactions were carried out in a total volume of 50  $\mu\text{l}$  containing 100 ng of genomic DNA, 2 $\times$  PCR master mix (Thermo Scientific, K0171) and 100 mM of cyanobacterial specific primers, Cya359F, Cya781Ra and Cya781Rb (Nübel *et al.*, 1997). Amplification was performed in a thermocycler using the following protocol; initial denaturation at 94 °C

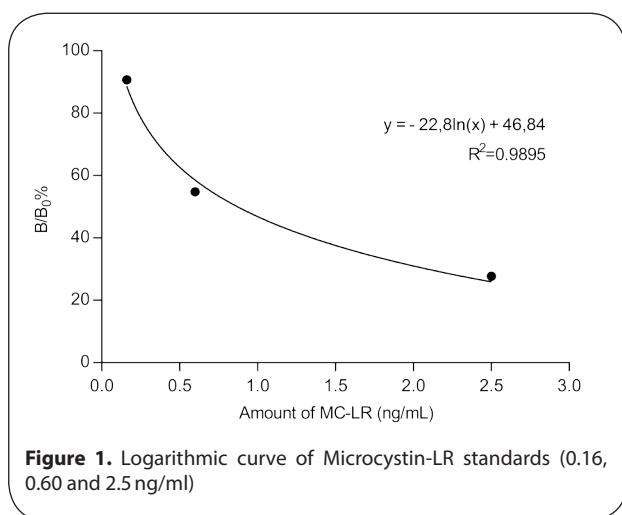


**Figure 1.** Logarithmic curve of Microcystin-LR standards (0.16, 0.60 and 2.5 ng/ml)

for 5 min followed by 30 cycles of 1 min denaturation at 94 °C, 1 min at 60 °C and 1 min extension at 72 °C, and a final extension period of 7 min at 72 °C. PCR products were checked by 2% agarose gel electrophoresis with ethidium bromide staining and UV illumination, and then sequenced commercially using the CYA359F primer. The 16S rRNA gene sequences were compared to sequences in the NCBI database (<http://www.ncbi.nlm.nih.gov/>) using Basic Local Alignment Search Tool (BLAST) (<http://www.ncbi.nlm.nih.gov/BLAST/>).

#### Cell cultures

PC12 cells (ATCC CRL-1721) are derived from a transplantable rat pheochromocytoma and represent a valuable model for neuronal differentiation. PC12 cells were cultured in Dulbecco's modified Eagle medium (DMEM) with 10% horse serum (HS), 10% fetal bovine serum (FBS), 100 IU/ml penicillin, 100 µg/ml streptomycin and 2 mM L-glutamine in a humidified CO<sub>2</sub> (5%) incubator at 37 °C (Ciofani *et al.*, 2010). Cells were differentiated for four days using 100ng/ml nerve growth factor (NGF) (Haq *et al.*, 2007). HeLa (human cervical cancer) (CCL-2™) and HT29 (human colon cancer) (HTB-38™) cell lines, the most commonly used for testing agents that may have antiproliferative effect, were purchased from ATCC. Cell lines were cultured in DMEM medium at 37 °C with 10% fetal bovine serum (FBS), 100 IU/ml penicillin, 100 µg/ml streptomycin and 2 mM L-glutamine under atmosphere of 95% air and 5% CO<sub>2</sub> in a 75 ml flask. The medium was changed every two days (Khanavi *et al.*, 2010; Priyadarsini *et al.*, 2010).

#### Neurotoxic and antiproliferative effect assays

For neurotoxic and antiproliferative effect testing, the cells were seeded in 96-well plates (10,000 cells per well) and incubated with increasing concentrations of cyanobacterial extracts (250, 500 and 1000 µg/ml) for 24 h. After incubations, cell viability was quantitatively measured with WST-1 assay (Cayman Chemical) (Lin *et al.*, 2010). Cell cultures were treated with 200 µl of culture medium added with 20 µl WST-1 mixture. The cells were incubated for 2 h at 37 °C in a CO<sub>2</sub> (5%) incubator and the absorbance of each sample was measured using microplate reader at wavelength of 450 nm (Epoch, BioTek) (Ciofani *et al.*, 2010). The neurotoxicity (according to % cell viability) was determined using the following formula: Cell Viability% = [Abs (sample)/Abs (control)] × 100 (Wen *et al.*, 2012). The antiproliferative effect was determined using the following formula: antiproliferative effect% = 1 – [Abs (sample)/Abs (control)] × 100 (Wang *et al.*, 2006).

#### Genotoxicity assay

For this test, the blood samples were obtained from Gazi University Hospital Blood Center. Blood lymphocytes isolated from healthy donors (ages 25 to 30, healthy, not using any alcohol, non-smoker, not under any medication and no radiological examination within the prior 3 months) were used for determining genotoxic effects of cyanobacterial toxins. Human lymphocytes were isolated using Biocoll separating solution according to the procedures of Sierens

*et al.*, (2001). In order to isolate human lymphocytes, the blood samples heparinized were mixed with Biocoll separating solution and then centrifuged at 3000 rpm at 25 °C for 20 min. After density gradient, lymphocyte cells were collected. The collected cells were washed with PBS. The genotoxicity was tested by exposure of human lymphocytes at various concentrations of extracts (250 µg/ml, 500 and 1000 µg/ml methanolic extract of cyanobacteria) at 37 °C for 1 h. A negative (phosphate buffer saline, PBS) and a positive control (50 µM H<sub>2</sub>O<sub>2</sub> for 15 min.) were also maintained. The slides were left in ice-cold alkaline solution (10M NaOH, 0.2M EDTA, pH>13) for 20 min, and then electrophoresis was conducted at 25 V, 300 mA for 20 min. After electrophoresis, each slide was stained with 50 µl of 20 µg/ml ethidium bromide. The slides were viewed using a fluorescent microscope (Olympus) equipped with an excitation filter (546 nm) and a barrier filter (590 nm) at 400× magnification. The tail length (µm), tail moment and tail intensity (%) of 100 comets on each slide were examined, using specialized Image Analysis System (Comet Assay III, Perceptive Instruments Ltd., UK) (Cestari *et al.*, 2004). DNA tail damage% = 100 × (Tail DNA density/Cell DNA density) (Behravan *et al.*, 2011). The comet analysis was carried out with three parallels in two repetitions.

#### Mutagenicity testing

Ames test was employed as a standard plate incorporation assay with *Salmonella typhimurium* strain TA100 without S9. Sodium azide (SA) and dimethyl sulfoxide (DMSO) were used as positive control and negative control, respectively. 500 µl phosphate buffer, 100 µl methanol extracts for each concentration (500 and 1000 µg/ml), and 100 µl cell suspension (1–2 × 10<sup>9</sup> cells/ml) were added to 2 ml top agar (kept at 45 °C) and vortexed for 3 s. The mixture was overlaid on the minimal glucose agar plates, and plates were incubated at 37 °C for 72 h. After the incubation period, the number of revertant bacterial colonies on each plate was counted (Lupi *et al.*, 2009).

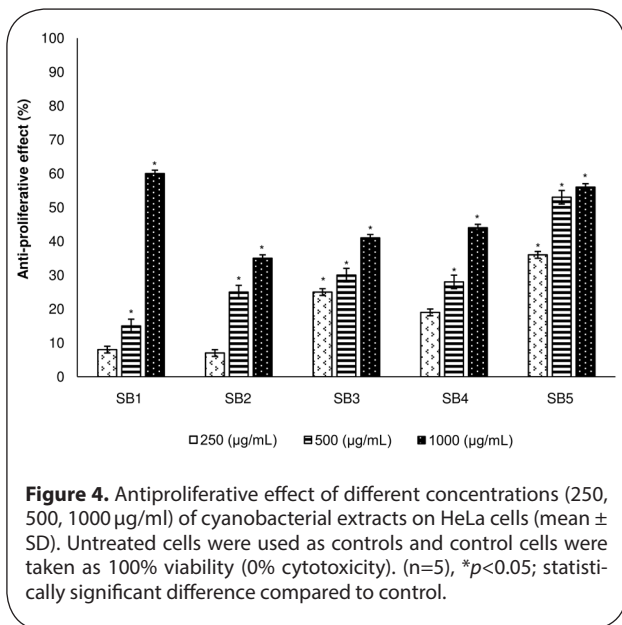
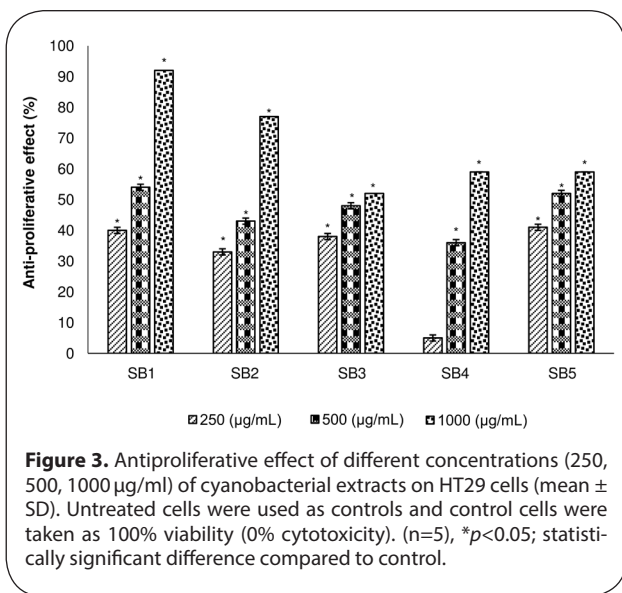
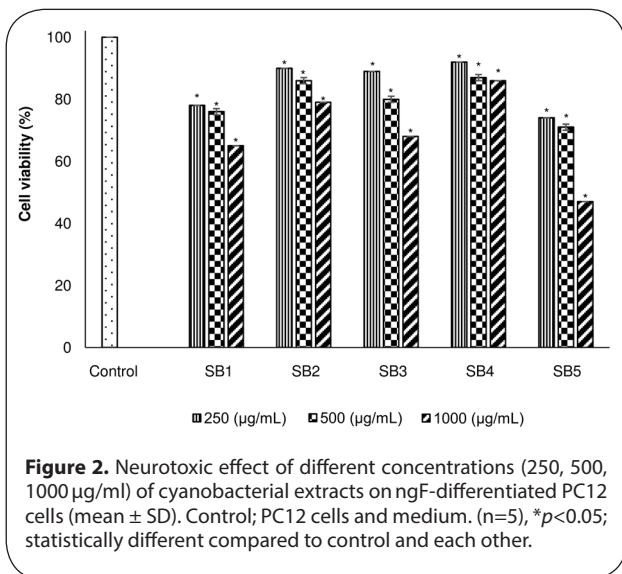
#### Statistical analysis

All data obtained from antiproliferative, neurotoxic, genotoxic and mutagenic effects analysis results were analyzed statistically by analysis of variance (ANOVA) and Tukey's post-test was used to identify statistical significance for  $p < 0.05$ . Results are submitted as mean value ± standard deviation (n=5 for the WST-1 assays, n=3 for all other analyses) (Ciofani *et al.*, 2010).

## Results

#### Toxin-producing cyanobacterial isolates

The five cyanobacterial isolates were selected according to the toxin production among 20 isolates from various fresh waters in Turkey (data not shown). Toxin-producing isolates were identified based on their 16S rRNA gene region sequence. The sequences were first analyzed at NCBI (<http://www.ncbi.nlm.nih.gov/>) databases using BLAST



(blastn) tool and corresponding sequences were downloaded. They displayed a similarity of  $\geq 98\%$  to a cultured cyanobacterium in the NCBI GenBank databases. Five toxic cyanobacterial isolates were identified as follows: *Leptolyngbya* sp., *Oscillatoria earlei*, *Phormidium* sp., *Phormidium* sp. and *Uncultured cyanobacterium* based on morphologic observations using light microscopy and 16S rRNA gene sequences. Accession numbers and similarity (%) of sequences are presented in Table 1. A total of 20 cyanobacterial isolates were analyzed by ELISA. Five of the 20 isolates produced Microcystine-LR. Microcystine contents of the five toxic strains are listed in Table 2. The minimum Microcystine-LR content was found in the strain *Uncultured cyanobacterium* SB3 (1.12 ng/ml) and the maximum in *Leptolyngbya* sp. SB1 (2.07 ng/ml).

### Neurotoxic effect of cyanobacterial extracts

Cyanobacteria-derived Microcystine-LR (microcystine-leucine arginine) is a typically potent hepatotoxin, and also known to be neurotoxic (Meng *et al.*, 2011; Li *et al.*, 2015). In this study, the extracts of five cyanobacterial isolates contained MCLR indicated concentration-dependent neurotoxic effect. Toxic effects of cyanobacterial extracts showed to differ significantly ( $p < 0.05$ ) from each other and control. Neurotoxic effect of toxic cyanobacterial extracts (1000 µg/ml) were determined as *Phormidium* sp. SB4 (86%) < *Phormidium* sp. SB2 (79%) < *Uncultured cyanobacterium* SB3 (68%) < *Leptolyngbya* sp. SB1 (65%) < *Oscillatoria earlei* SB5 (47%), based on cell viability. The extract of *Oscillatoria earlei* SB5 showed the highest neurotoxic effect (47% cell viability), and the extract of *Phormidium* sp. SB4 showed the lowest neurotoxic effect (86% cell viability) on ngF-differentiated PC12 cells. The results obtained are given in Figure 2.

### Antiproliferative effects of cyanobacterial extracts

The two different human cancer cell lines were tested for the in vitro antiproliferative bioactivity of the extracts. The cyanobacterial extracts showed an antiproliferative effect on HeLa and HT29 cells. The treated cells differed significantly ( $p < 0.05$ ) from control cells (untreated). All of cyanobacterial extracts exhibited higher antiproliferative effect against HT29 colon cancer cell line HeLa cervix cancer cell line. Furthermore, these five cyanobacterial extracts induced concentration-dependent antiproliferative effect through loss of viability. The best concentration in destroying the cancer cells was 1000 µg/ml of cyanobacterial extracts which had the highest antiproliferative effects compared to the other three concentrations. HT29 cells exposed to *Leptolyngbya* sp. SB1 and *Phormidium* sp. SB2 extracts showed 92% and 77% cell death, respectively, as presented in Figure 3. *Leptolyngbya* sp. SB1 and *Oscillatoria earlei* SB5 extracts showed a high antiproliferative effect on HeLa cells, 60% and 56% cell death, respectively, as given in Figure 4.

### In vitro DNA damage of cyanobacterial extracts

The genotoxic effects of cyanobacterial extracts were determined with human lymphocyte cells by

Comet Assay. Positive control (50  $\mu\text{M}$   $\text{H}_2\text{O}_2$ ) induced approximately 25% DNA damage. All concentrations of cyanobacterial extracts induced DNA damage between 3.0 and 1.3, according to the percentage of tail intensity (Table 3). Interestingly, the cyanobacterial extracts-treated lymphocyte cells were approximately 8 or 19 fold less DNA damaging than  $\text{H}_2\text{O}_2$  treated (Figure 5). Although there was not enough tail density difference between negative control and cyanobacterial extracts-treated lymphocyte cells, it was found that as increasing concentrations of extracts, the DNA tail damage was also increasing. According to comet test results, if the ratio of tail length to head length is below 5% it is accepted that there is no DNA damage (Yen *et al.*, 2001) This showed that the cyanobacterial extracts do not induce significant DNA damage in comparison to positive controls treated with  $\text{H}_2\text{O}_2$ .

### Mutagenicity of cyanobacterial extracts

The Ames test was utilized to determine the mutagenicity of cyanobacterial extracts (500 and 1000  $\mu\text{g}/\text{plate}$ ) in this study. In the Ames test, *Salmonella typhimurium* strains were used carrying different mutations in the operon coding for histidine, and TA100 tester strains served to detect mutagens causing base-pair substitutions (Huang *et al.*, 2007). The mutagenicity assays showed that none of the cyanobacterial extracts induced any significant increase in the number of revertant colonies, indicating the absence of any mutagenic activity on *Salmonella typhimurium* TA100 cells. The results obtained from studies on the mutagenic potential of cyanobacterial extracts are presented in Table 4.

### Discussion

Previous studies have suggested that MCs have a cytotoxic effect and tumor-promoting activity mediated by inhibition of protein phosphatases 1 and 2A (Humpage *et al.*, 2000; Lone *et al.*, 2015). Moreover, Cyanobacteria-derived Microcystine-LR (MCLR) has been proposed as potential neurotoxic compound by several studies (Feurstein *et al.*, 2009, 2010; Wang *et al.*, 2009; Meng *et al.*, 2011; Hu *et al.*, 2016). On the other hand, in spite of its tumor-promoting activity, earlier studies have suggested that MCLR may be utilized for cancer treatment as an anticancer agent (Monks *et al.*, 2007; Obaidat *et al.*, 2012). MCLR uptake is mediated by various organic anion-transporting polypeptides (OATPs) (Komatsu *et al.*, 2007; Monks *et al.*, 2007). Monks *et al.*, (2007) demonstrated that MCs cause cytotoxicity in OATP1B1 and OATP1B3 expressing HeLa cells. This study ensured a potential clue for the usage of MCs as anticancer agents for tumors expressing the OATP transporters. Besides, Lankoff *et al.* (2003) reported that MCLR induce the formation of abnormal mitotic spindles similar to taxol which is an antimetabolic compound used to treat cancers, especially breast and ovarian cancers.

In the present study, we investigated antiproliferative, neurotoxic, genotoxic and mutagenic effects

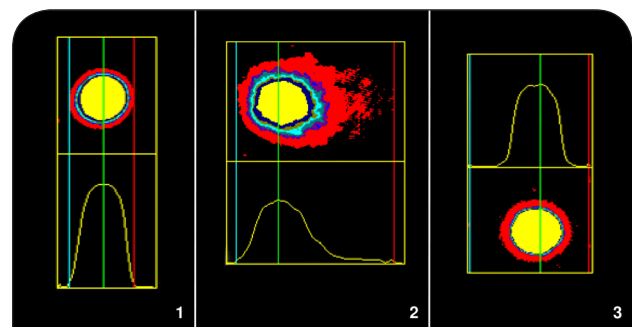


**Figure 5.** Fluorescence images of comet assay. DNA damage was detected in human lymphocyte cells exposed to (1) PBS (negative control), (2) 50  $\mu\text{M}$   $\text{H}_2\text{O}_2$  (positive control), and (3) *Leptolyngbya* sp. SB1 extract (1000  $\mu\text{g}/\text{ml}$  concentration).

**Table 1.** Sources and 16S rRNA-based identification of cyanobacterial isolates. The highest similarities to the sequences in GenBank and Accession numbers are shown.

Code	GenBank No	Cyanobacteria species	Homology (%)	Source
SB1	JX088103.1	<i>Leptolyngbya</i> sp. CAWBG532	98	Tatlarin/ Nevsehir
SB2	KU740243.1	<i>Phormidium</i> sp. CBC	99	Böyükören/ Nevsehir
SB3	KF856318.1	Uncultured cyanobacterium clone 4BF1C	99	Yalıntaş/ Nevsehir
SB4	KR872396.1	<i>Phormidium</i> sp. KO02	99	Böyükören/ Nevsehir
SB5	KF487296.1	<i>Oscillatoria earlei</i> S11	98	Tatlarin/ Nevsehir

**Table 2.** Microcystine-LR contents of cyanobacterial extracts based on ELISA assay.

Cyanobacterial extracts	B/B <sub>0</sub> %*	Estimation of MCLR content (ng/ml)
<i>Leptolyngbya</i> sp. (SB1)	30.29	2.07
<i>Phormidium</i> sp. (SB2)	41.26	1.27
Uncultured cyanobacterium (SB3)	44.07	1.12
<i>Phormidium</i> sp. (SB4)	38.60	1.43
<i>Oscillatoria earlei</i> (SB5)	38.82	1.41

\*: Mean optical density of test sample or control sample  $\div$  mean optical density of negative control  $\times$  100.

of cyanobacterial extracts containing MCLR on HeLa cells, HT29 cells, PC12 cells, human lymphocyte cells, and also *Salmonella typhimurium* TA100 cells. Our results demonstrated that MCLR content of five of the 20 cyanobacterial extracts were 2.07 ng/ml, 1.43 ng/ml, 1.41 ng/ml, 1.27 ng/ml, and 1.12 ng/ml for *Leptolyngbya* sp. SB1, *Phormidium* sp. SB4, *Oscillatoria earlei* SB5,

*Phormidium* sp. SB2, *Uncultured cyanobacterium* SB3, respectively. *Oscillatoria earlei* SB5 and *Leptolyngbya* sp. SB1 extracts had the highest neurotoxic effect while *Phormidium* sp. SB4 and SB2 extracts had the lowest neurotoxic effect at 1000 µg/ml concentration. Although

**Table 3.** DNA damage (tail length, tail moment, and tail intensity) in human lymphocyte cells exposed to cyanobacterial extracts according to Comet assay.

Agent	Conc. (µg/mL)	Tail length (µm)	Tail moment	Tail intensity(%)
*NC	–	12.0±1.2	0.3±0.0	0.5±0.2
**PC	–	50.4±0.6	24.0±0.2	25.0±1.7
<i>Leptolyngbya</i> sp. (SB1)	250	13.8±1.1	0.6±0.1	2.3±0.6
	500	19.5±1.0	0.8±0.1	2.7±0.2
	1000	20.8±0.0	1.0±0.1	3.0±0.1
<i>Phormidium</i> sp. (SB2)	250	25.4±0.4	0.9±0.2	1.3±0.1
	500	26.5±0.5	1.3±0.2	1.9±0.3
	1000	30.9±0.6	1.6±0.1	2.5±0.2
<i>Uncultured cyanobacterium</i> (SB3)	250	20.4±0.2	0.8±0.1	1.7±0.2
	500	25.2±0.4	1.3±0.2	2.0±0.0
	1000	29.5±0.6	1.8±0.2	2.4±0.2
<i>Phormidium</i> sp. (SB4)	250	16.0±0.3	0.7±0.2	1.4±0.3
	500	17.0±0.2	1.0±0.1	2.0±0.3
	1000	18.0±0.5	1.4±0.2	2.4±0.2
<i>Oscillatoria earlei</i> (SB5)	250	19.0±0.6	1.0±0.2	1.7±0.3
	500	24.0±0.8	1.4±0.2	2.2±0.3
	1000	30.8±0.7	1.8±0.1	2.9±0.4

\*: Negative control (PBS), \*\*: Positive control (50 µM H<sub>2</sub>O<sub>2</sub>), Mean ± SD (n=3), p<0.05; statistically significant difference compared to positive control.

**Table 4.** Mutagenic activities of cyanobacterial extracts on *Salmonella typhimurium* TA100.

Agent	Amount (µg/plate)	TA100 (revertant colony/plate)
*NC	10	244±7
**PC	10	967±6
<i>Leptolyngbya</i> sp. (SB1)	250	269±1
	500	328±11
<i>Phormidium</i> sp. (SB2)	250	272±3
	500	293±4
<i>Uncultured cyanobacterium</i> (SB3)	250	300±2
	500	321±6
<i>Phormidium</i> sp. (SB4)	250	293±1
	500	319±5
<i>Oscillatoria earlei</i> (SB5)	250	272±3
	500	297±1

\*: Negative control (only DMSO), \*\*: Positive control (Sodium azide), Mean±SD (n=3), p<0.05; statistically significant difference compared to positive control.

toxin content of *Oscillatoria earlei* SB5 extract (1.41 ng/ml) was lower than of *Leptolyngbya* sp. SB1 (2.07 ng/ml) and *Phormidium* sp. SB4 (1.43 ng/ml) extracts, neurotoxic effect of *Oscillatoria earlei* SB5 extract (47%) on PC12 cells was higher than *Leptolyngbya* sp. SB1 (65%) and *Phormidium* sp. SB4 extracts (86%) at 1000 µg/ml concentration based on cell viability. Furthermore, the neurotoxic effect of *Uncultured Cyanobacterium* SB3 extract (68%) defined as the lowest toxic isolate was higher than *Phormidium* sp. SB4 (86%) and *Phormidium* sp. SB2 (79%) extracts at 1000 µg/ml concentration. There was no direct correlation between MCLR toxin content and neurotoxic effect according to our results. In our opinion, the reason is that MCLR obtained from five toxic isolates may have different chemical variants of MCLR such as [Leu<sup>1</sup>], [Leu<sup>1</sup>, Glu(OCH<sub>3</sub>)<sup>6</sup>], [Leu<sup>1</sup>, Ser<sup>7</sup>], [D-Asp<sup>3</sup>], [Dha<sup>7</sup>] [D-Asp<sup>3</sup>, Z-Dhb<sup>7</sup>] e.g. (Shimizu *et al.*, 2013; Qi *et al.*, 2014) and this variation may be changed at the neurotoxic effect of cyanobacterial extracts.

*Leptolyngbya* sp. SB1 extract containing maximum MCLR (2.07 ng/ml) showed the highest antiproliferative effect on both HeLa (60% cell death) and HT29 cells (92% cell death). Although toxin content of *Phormidium* sp. SB2 extract (1.27 ng/ml) was lower than that of *Oscillatoria earlei* SB5 (1.41 ng/ml) and *Phormidium* sp. SB4 (1.43 ng/ml) extracts, antiproliferative effect of *Phormidium* sp. SB2 extract (77%) on HT29 cells was significantly higher than *Oscillatoria earlei* SB5 (59%) and *Phormidium* sp. SB4 extracts (59%) at 1000 µg/ml concentration. Moreover, antiproliferative effect of *Phormidium* sp. SB2 extract on HeLa cells was 42% less than on HT29 cell line. Consequently, some of five cyanobacterial extracts containing MCLR were shown different antiproliferative effect on HeLa and HT29 cells supporting that MCLR, as has been reported, exhibited different cytotoxicity in several cell types including HeLa and RKO cells (Zegura *et al.*, 2008; Niedermeyer *et al.*, 2014). Besides, Shimizu *et al.*, (2013) showed that differences in the amino acid constituents of MCLR were associated with differences in cytotoxic potential.

Because cyanobacterial extracts are potential agents for the development of biologically active molecules, it is also important to evaluate the genotoxic and mutagenic effects of these extracts. In this regard, the genotoxic effect of cyanobacterial extracts on human lymphocyte cells was assessed in this study and all concentrations of cyanobacterial extracts induced DNA damage according to the percentage of tail intensity. This showed that the cyanobacterial extracts do not induce DNA damage significantly. Also, we determined that cyanobacterial extracts did not show direct mutagenic effect on *Salmonella typhimurium* TA100 cells. Similarly to our results, several studies reported that cyanobacterial extracts containing cyanotoxins and pure MCLR did not induce reverse mutation in *S. typhimurium* strains (Wu *et al.*, 2006). In a contrary study, a strong mutagenic response which caused by microcystic cyanobacterial extract was shown using four *S. typhimurium* (TA97, TA98, TA100 and TA102) (Ding *et al.*, 1999).

In summary, our results showed that both neurotoxicity of *Leptolyngbya* sp. SB1 and *Phormidium* sp. SB2 cyanobacterial extracts were slightly lower on PC12 cells and highly antiproliferative on HT29 cells as well as lower genotoxicity and mutagenicity considering their potential pharmacological applications. Therefore we suggested that MCLR obtained from *Leptolyngbya* sp. SB1 and *Phormidium* sp. SB2 extracts may be used as an agent for treatment of colon cancer.

## Acknowledgements

The authors express their gratitude to the University of Nevsehir Hacı Bektaş Veli, Scientific Research Projects Unit (Project no: NEUBAP13F43) for their financial support.

## REFERENCES

- Behravan J, Mosafa F, Soudmand N, Taghiabadi E, Razavi BM, Karimi G. (2011). Protective effects of aqueous and ethanolic extracts of *Portulaca oleracea* L. aerial parts on H<sub>2</sub>O<sub>2</sub>-induced DNA damage in lymphocytes by comet assay. *J Acupunct Meridian Stud* **4**: 193–7.
- Boyle P, Levin B. (2008). World Cancer Report. Lyon: International Agency for Research on Cancer (IARC). WHO.
- Cazenave J, Nores MI, Miceli M, Díaz MP, Wunderlin DA, Bistoni MA. (2008). Changes in the swimming activity and the glutathione S-transferase activity of *Jenynsia multidentata* fed with microcystin-RR. *Water Res* **42**: 1299–307.
- Cestari MM, Lemos PMM, Ribeiro CAdO, Costa JRMA, Pelletier E, Ferraro MV, Mantovani MS, Fenocchio AS. (2004). Genetic damage induced by trophic doses of lead in the neotropical fish *Hoplias malabaricus* (Characiformes, Erythrinidae) as revealed by the comet assay and chromosomal aberrations. *Genet Mol Biol* **27**: 270–4.
- Ciofani G, Danti S, D'Alessandro D, Ricotti L, Moscato S, Bertoni G, Falqui A, Berrettini S, Petrini M, Mattoli V, Mencias A. (2010). Enhancement of neurite outgrowth in neuronal-like cells following boron nitride nanotube-mediated stimulation. *ACS nano* **4**: 6267–77.
- Dietrich D, Hoeger S. (2005). Guidance values for microcystins in water and cyanobacterial supplement products (blue-green algal supplements): a reasonable or misguided approach? *Toxicol Appl Pharmacol* **203**: 273–89.
- Dietrich DR, Fischer A, Michel C, Höger SJ. (2008). Toxin mixture in cyanobacterial blooms—a critical comparison of reality with current procedures employed in human health risk assessment. *Adv Exp Med Biol* **619**: 885–912.
- Ding WX, Shen HM, Zhu HG, Lee BL, Ong CN. (1999). Genotoxicity of microcystic cyanobacteria extract of a water source in China. *Mutat Res Genet Toxicol Environ Mutagen* **442**: 69–77.
- Doyle JJ. (1990). Isolation of plant DNA from fresh tissue. *Focus* **12**: 13–5.
- El Herry S, Fathalli A, Rejeb AJ, Bouaïcha N. (2008). Seasonal occurrence and toxicity of *Microcystis* spp. and *Oscillatoria tenuis* in the Lebna Dam, Tunisia. *Water Res* **42**: 1263–1273.
- Falconer IR, Humpage AR. (2005). Health risk assessment of cyanobacterial (blue-green algal) toxins in drinking water. *Int J Environ Res Public Health* **2**: 43–50.
- Falconer IR, Smith JV, Jackson AR, Jones A, Runnegar MT. (1988). Oral toxicity of a bloom of the cyanobacterium *Microcystis aeruginosa* administered to mice over periods up to 1 year. *J Toxicol Environ Health* **24**: 291–305.
- Feurstein D, Holst K, Fischer A, Dietrich DR. (2009). Oatp-associated uptake and toxicity of microcystins in primary murine whole brain cells. *Toxicol Appl Pharmacol* **234**: 247–55.
- Frazão B, Martins R, Vasconcelos V. (2010). Are known cyanotoxins involved in the toxicity of picoplanktonic and filamentous North Atlantic marine cyanobacteria? *Mar Drugs* **8**: 1908–19.
- Gantar M, Sekar R, Richardson LL. (2009). Cyanotoxins from black band disease of corals and from other coral reef environments. *Microb ecol* **58**: 856.
- Gupta N, Pant S, Vijayaraghavan R, Rao PL. (2003). Comparative toxicity evaluation of cyanobacterial cyclic peptide toxin microcystin variants (LR, RR, YR) in mice. *Toxicology* **188**: 285–96.
- Haq F, Anandan V, Keith C, Zhang G. (2007). Neurite development in PC12 cells cultured on nanopillars and nanopores with sizes comparable with filopodia. *Int J Nanomedicine* **2**: 107.
- Hu Y, Chen J, Fan H, Xie P, He J. (2016). A review of neurotoxicity of microcystins. *Environ Sci Pollut Res* **23**: 7211–9.
- Huang WJ, Lai CH, Cheng YL. (2007). Evaluation of extracellular products and mutagenicity in cyanobacteria cultures separated from a eutrophic reservoir. *Sci Total Environ* **377**: 214–23.
- Humpage AR, Hardy SJ, Moore EJ, Frosco SM, Falconer IR. (2000). Microcystins (cyanobacterial toxins) in drinking water enhance the growth of aberrant crypt foci in the mouse colon. *J Toxicol Environ Health* **61**: 155–65.
- Izaguirre G, Jungblut AD, Neilan BA. (2007). Benthic cyanobacteria (Oscillatoriaceae) that produce microcystin-LR, isolated from four reservoirs in southern California. *Water Res* **41**: 492–8.
- Kerbrat A-S, Darius HT, Pauillac S, Chinain M, Laurent D. (2010). Detection of ciguatoxin-like and paralyzing toxins in *Trichodesmium* spp. from New Caledonia lagoon. *Mar Pollut Bull* **61**: 360–6.
- Khanavi M, Nabavi M, Sadati N, Shams Ardekani M, Sohrabipour J, Nabavi SMB, Ghaeli P, Ostad NS. (2010). Cytotoxic activity of some marine brown algae against cancer cell lines. *Biol Res* **43**: 31–7.
- Komatsu M, Furukawa T, Ikeda R, Takumi S, Nong Q, Aoyama K, Akiyama S, Keppler D, Takeuchi T. (2007). Involvement of mitogen-activated protein kinase signaling pathways in microcystin-LR-induced apoptosis after its selective uptake mediated by OATP1B1 and OATP1B3. *Toxicol Sci* **97**: 407–16.
- Kounnis V, Chondrogiannis G, Mantzaris MD, Tzakos AG, Fokas D, Papanikolaou NA, Galani V, Sainis I, Briassoulis E. (2015). Microcystin LR shows cytotoxic activity against pancreatic cancer cells expressing the membrane OATP1B1 and OATP1B3 transporters. *Anticancer Res* **35**: 5857–65.
- Lankoff A, Banasik A, Obe G, Deperas M, Kuzminski K, Tarczynska M, Jurczak T, Wojcik A. (2003). Effect of microcystin-LR and cyanobacterial extract from Polish reservoir of drinking water on cell cycle progression, mitotic spindle, and apoptosis in CHO-K1 cells. *Toxicol Appl Pharmacol* **189**: 204–13.
- Li G, Yan W, Dang Y, Li J, Liu C, Wang J. (2015). The role of calcineurin signaling in microcystin-LR triggered neuronal toxicity. *Sci Rep* **5**: 11271.
- Li T, Ying L, Wang H, Li N, Fu W, Guo Z, Xu L. (2012). Microcystin-LR induces ceramide to regulate PP2A and destabilize cytoskeleton in HEK293 cells. *Toxicol Sci* **128**: 147–157.
- Lin ES, Chou HJ, Kuo PL, Huang YC. (2010). Antioxidant and antiproliferative activities of methanolic extracts of *Perilla frutescens*. *J Med Plant Res* **4**: 477–83.
- Lone Y, Koiri RK, Bhide M. (2015). An overview of the toxic effect of potential human carcinogen Microcystin-LR on testis. *Toxicol Rep* **2**: 289–96.
- Lupi S, Marconi S, Paiaro E, Fochesato A, Gregorio P. (2009). Mutagenicity evaluation with Ames test of hydro-alcoholic solution of terpenes. *J Prev Med Hyg* **50**: 170–4.
- Luukkainen R, Sivonen K, Namikoshi M, Fardig M, Rinehart KL, Niemela SI. (1993). Isolation and identification of eight microcystins from thirteen *Oscillatoria agardhii* strains and structure of a new microcystin. *Appl Environ Microbiol* **59**: 2204–2209.
- Lürling M, Faassen EJ. (2013). Dog poisonings associated with a *Microcystis aeruginosa* bloom in the Netherlands. *Toxins* **5**: 556–67.
- Meickle T, Matthew S, Ross C, Luesch H, Paul V. (2009). Bioassay-guided isolation and identification of desacetylmicrocolin B from *Lyngbya cf. polychroa*. *Planta Med* **75**: 1427–30.
- Meng G, Sun Y, Fu W, Guo Z, Xu L. (2011). Microcystin-LR induces cytoskeleton system reorganization through hyperphosphorylation of tau and HSP27 via PP2A inhibition and subsequent activation of the p38 MAPK signaling pathway in neuroendocrine (PC12) cells. *Toxicology* **290**: 218–29.
- Metcalfe JS, Codd GA. (2009). Cyanobacteria, neurotoxins and water resources: Are there implications for human neurodegenerative disease? *Amyotroph Lateral Sc* **10**: 74–8.

- Monks NR, Liu S, Xu Y, Yu H, Bendelow AS, Moscow JA. (2007). Potent cytotoxicity of the phosphatase inhibitor microcystin LR and microcystin analogues in OATP1B1-and OATP1B3-expressing HeLa cells. *Mol Cancer Ther* **6**: 587–98.
- Nan HB, Mcphail KL, Maier CS. (2011). Wewakamide A and guineamide G, cyclic depsipeptides from the marine cyanobacteria *Lyngbya semiplena* and *Lyngbya majuscula*. *J Microbiol Biotechnol* **21**: 930–6.
- Nascimento AKL, Melo-Silveira RF, Dantas-Santos N, Fernandes JM, Zucolotto SM, Rocha HAO, Scortecci KC. (2013). Antioxidant and antiproliferative activities of leaf extracts from *Plukenetia volubilis* Linneo (Euphorbiaceae). *J Evid Based Complementary Altern Med* **2013**: 1–10.
- Naumovski L, Quinn J, Miyashiro D, Patel M, Bush K, Singer SB, Graves D, Palzkill T, Arvin AM. (1992). Outbreak of ceftazidime resistance due to a novel extended-spectrum beta-lactamase in isolates from cancer patients. *Antimicrob Agents Chemother* **36**: 1991–6.
- Niedermeyer TH, Daily A, Swiatecka-Hagenbruch M, Moscow JA. (2014). Selectivity and potency of microcystin congeners against OATP1B1 and OATP1B3 expressing cancer cells. *PLoS one* **9**: e91476.
- Nooter K, Herweijer H. (1991). Multidrug resistance (mdr) genes in human cancer. *Br J Cancer* **63**: 663.
- Nübel U, Garcia-Pichel F, Muyzer G. (1997). PCR primers to amplify 16S rRNA genes from cyanobacteria. *Appl Environ Microbiol* **63**: 3327–32.
- Obaidat A, Roth M, Hagenbuch B. (2012). The expression and function of organic anion transporting polypeptides in normal tissues and in cancer. *Annu Rev Pharmacol Toxicol* **52**: 135–51.
- Palagama DS, West III RE, Isailovic D. (2017). Improved solid-phase extraction protocol and sensitive quantification of six microcystins in water using an HPLC-orbitrap mass spectrometry system. *Anal Methods* **9**: 2021–30.
- Priyadarsini RV, Murugan RS, Maitreyi S, Ramalingam K, Karunakaran D, Nagini S. (2010). The flavonoid quercetin induces cell cycle arrest and mitochondria-mediated apoptosis in human cervical cancer (HeLa) cells through p53 induction and NF-κB inhibition. *Eur J Pharmacol* **649**: 84–91.
- Qi Y, Bortoli S, Volmer DA. (2014). Detailed study of cyanobacterial microcystins using high performance tandem mass spectrometry. *J Am Soc Mass Spectrom* **25**: 1253–62.
- Rippka R, Deruelles J, Waterbury JB, Herdman M, Stanier RY. (1979). Generic assignments, strain histories and properties of pure cultures of cyanobacteria. *Microbiology* **111**: 1–61.
- Romero-Jiménez M, Campos-Sánchez J, Analla M, Muñoz-Serrano A, Alonso-Moraga Á. (2005). Genotoxicity and anti-genotoxicity of some traditional medicinal herbs. *Mutat Res Genet Toxicol Environ Mutagen* **585**: 147–55.
- Sainis I, Fokas D, Vareli K, Tzakos AG, Kounnis V, Briasoulis E. (2010). Cyanobacterial cyclopeptides as lead compounds to novel targeted cancer drugs. *Mar Drugs* **8**: 629–57.
- Shimizu K, Sano T, Kubota R, Kobayashi N, Tahara M, Obama T, Naoki S, Nishimura T, Ikarashi Y. (2013). Effects of the amino acid constituents of microcystin variants on cytotoxicity to primary cultured rat hepatocytes. *Toxins* **6**: 168–79.
- Shishido TK, Kaasalainen U, Fewer DP, Rouhiainen L, Jokela J, Wahlsten M, Fiore MF, Yunes JS, Rikkinen J, Sivonen K. (2013). Convergent evolution of [D-Leucine 1] microcystin-LR in taxonomically disparate cyanobacteria. *BMC Evol Biol* **13**: 86.
- Sierens J, Hartley JA, Campbell MJ, Leatham AJ, Woodside JV. (2001). Effect of phytoestrogen and antioxidant supplementation on oxidative DNA damage assessed using the comet assay. *Mutat Res/DNA Rep* **485**: 169–76.
- Singh RK, Tiwari SP, Rai AK, Mohapatra TM. (2011). Cyanobacteria: an emerging source for drug discovery. *J Antibiot* **64**: 401–12.
- Teneva I, Dzhambazov B, Koleva L, Mladenov R, Schirmer K. (2005). Toxic potential of five freshwater *Phormidium* species (Cyanoprokaryota). *Toxicon* **45**: 711–725.
- Wang M, Chan LL, Si M, Hong H, Wang D. (2009). Proteomic analysis of hepatic tissue of zebrafish (*Danio rerio*) experimentally exposed to chronic microcystin-LR. *Toxicol Sci* **113**: 60–69.
- Wang SL, Lin TY, Yen YH, Liao HF, Chen YJ. (2006). Bioconversion of shellfish chitin wastes for the production of *Bacillus subtilis* W-118 chitinase. *Carbohydr Res* **341**: 2507–15.
- Wen H, Dong C, Dong H, Shen A, Xia W, Cai X, Song Y, Li X, Li Y, Shi D. (2012). Engineered redox-responsive PEG detachment mechanism in PEGylated nano-graphene oxide for intracellular drug delivery. *Small* **8**: 760–9.
- Wood S, Heath M, McGregor G, Holland P, Munday R, Ryan K. (2010). Identification of a benthic microcystin producing *Planktothrix* sp. and an associated dog poisoning in New Zealand. *Toxicon* **55**: 897–903.
- Wu S, Xie P, Liang G, Wang S, Liang X. (2006). Relationships between microcystins and environmental parameters in 30 subtropical shallow lakes along the Yangtze River, China. *Freshw Biol* **51**: 2309–19.
- Yen G, Chen H, Peng H. (2001). Evaluation of the cytotoxicity, mutagenicity and antimutagenicity of emerging edible plants. *Food Chem Toxicol* **39**: 1045–53.
- Žegura B, Zajc I, Lah TT, Filipič M. (2008). Patterns of microcystin-LR induced alteration of the expression of genes involved in response to DNA damage and apoptosis. *Toxicon* **51**: 615–23.

ORIGINAL ARTICLE

# Novel pentacyclic triterpene isolated from seeds of *Euryale Ferox Salisb.* ameliorates diabetes in streptozotocin induced diabetic rats

Danish AHMED<sup>1</sup>, Mohd. Ibrahim KHAN<sup>1</sup>, Manju SHARMA<sup>2,3</sup>, Mohd. Faiyaz KHAN<sup>4</sup>

<sup>1</sup> Department of Pharmaceutical Sciences, Faculty of Health Sciences, Sam Higginbottom University of Agriculture, Technology & Sciences, Allahabad, Uttar Pradesh, INDIA

<sup>2</sup> Department of Pharmacology, Faculty of Pharmacy, Jamia Hamdard, New Delhi, India

<sup>3</sup> Hamdard Institute of Medical Sciences & Research (HIMSR), Jamia Hamdard, New Delhi, India

<sup>4</sup> Department of Clinical Pharmacy, College of Pharmacy, Prince Sattam Bin Abdulaziz University, Al-Kharj, Kingdom of Saudi Arabia

ITX110418A05 • Received: 14 November 2017 • Accepted: 17 March 2018

## ABSTRACT

The present research was carried out to study the effect of 2 $\beta$ -hydroxybetulinic acid 3 $\beta$ -oleiate (HBAO), a novel compound isolated from the seeds of *Euryale ferox salisb.* on glycemic control, antioxidant status and histopathological morphological alterations in the liver, pancreas, kidney and heart in streptozotocin induced type-2 diabetes in rats. HBAO was isolated from the seeds of *Euryale ferox salisb.* according to Lee. Isolation of the active principle HBAO was performed for the first time. To date there are no reports on the isolation and evaluation of 2 $\beta$ -hydroxybetulinic acid 3 $\beta$ -oleiate (HBAO) from *Euryale ferox salisb.* Assessment of different biochemical parameters like the effect of HBAO on glycemic control, plasma insulin, glycosylated hemoglobin, hepatic glucose-6-phosphate dehydrogenase, glucose-6-phosphatase and fructose-1-6-biphosphatase, hepatic hexokinase, lipid profile, antioxidant marker and histopathology of pancreas, liver and kidney examination was done at the end of the experimentation, i.e. on day 45. HBAO exhibited remarkable improvement in glycemic control, lipid levels, plasma insulin, glycogenic liver enzymes and antioxidant activity in diabetic rats, along with progressive enhancement of distortive histopathological morphology of liver, pancreas and kidney. The results strongly suggest that HBAO could be a potential therapeutic agent in diabetes.

**KEY WORDS:** Diabetes; *Euryale ferox salisb.*; HBAO

## ABBREVIATIONS:

**ANOVA:** Analysis of Variance, **CAT:** Catalase, **GPx:** Glutathione Peroxidase, **HBAO:** 2 $\beta$ -hydroxybetulinic acid 3 $\beta$ -oleiate, **HDL:** High Density Lipoprotein, **HE:** Hematoxylin and Eosin, **LDL:** Low Density Lipoprotein, **RNS:** Reactive Nitrogen Species, **ROS:** Reactive Oxygen Species, **SOD:** Superoxide dismutase, **STZ:** Streptozotocin, **T2DM:** Type-2 Diabetes Mellitus, **VLDL:** Very Low Density Lipoprotein

## Introduction

The prevalence of diabetes is increasing rapidly throughout the world. According to the International Diabetes Federation (IDF) 2015, it was estimated that there were 415 million adult diabetic patients worldwide (IDF Atlas, 2015). The country specific estimates showed India at number 2 position in terms of highest number of people (99.2 million) with diabetes after China with 109.6 million (IDF Atlas, 2015). Multiple pathophysiological defects are currently recognized in type-2 diabetes mellitus (T2DM): insulin resistance, impaired insulin secretion, impaired glucagon suppression, increased lipolysis, exaggerated hepatic glucose production, incretin deficiency, maladaptive renal glucose reabsorption and defects of central nervous system, which may include impaired dopaminergic tone and dysregulation of satiety (King *et al.*, 2012; Suraamornkul *et al.*, 2010; Yoon *et al.*, 2003). The regulation of blood glucose is complex and involves factors affecting the digestion and absorption of dietary

Correspondence address:

**Danish Ahmed**

Department of Pharmaceutical Sciences, Faculty of Health Science  
Sam Higginbottom University of Agriculture Technology and Sciences  
Post. Agriculture Institute  
Naini, Allahabad - 211007, (U.P.), India.  
TEL.: +91-9580001578  
E-MAIL: danish.ahmed@shiats.edu.in

carbohydrates, the regulation of hepatic glucose uptake and production, and the effectiveness of insulin to stimulate glucose uptake in insulin sensitive tissues, particularly skeletal muscle and adipose tissues. Type-2 diabetes is most commonly associated with obesity and insulin resistance. While the cause of insulin resistance is not fully understood, both genetic and environmental factors play a contributing role. Metabolic factors include intra-abdominal obesity, increased hepatic triglyceride content and increased plasma free fatty acid concentrations (Poretsky, 2010).

Free radicals are atoms or group of atoms that contain an unpaired electron in their valance shell. Reactive oxygen species (ROS) and reactive nitrogen species (RNS) are chemically reactive metabolites classified as free radicals owing to the presence of one unpaired electron in an oxygen atom and a nitrogen atom respectively (Maritim *et al.*, 2003). Larger amounts of NADH and FADH are produced in hyperglycemic conditions owing to glucose autoxidation. Diabetes not only increases the rate of ROS production but also lowers cellular anti-oxidant capacity. Earlier researchers demonstrated impaired antioxidant capacity in brains of streptozotocin-diabetic rats (Thannickal & Fanburg, 2000). There is a wealth of evidence to suggest that oxidative stress plays a key role in the development and progression of diabetic complications such as nephropathy, retinopathy, neuropathy, silent myocardial ischemia, or coronary artery disease.

Different in vitro and animal studies have shown that dietary antioxidants have beneficial effects on glucose metabolism and can help to prevent diabetes or related disorders (Ahmed *et al.*, 2015<sup>a</sup>). Such studies have attracted the attention of many researchers to develop and identify potential antioxidants. Several Indian medicinal plants are considered to have great antioxidant potential.

*Euryale ferox salisb.* is a perennial plant of the Nymphaeaceae family, which is native to eastern Asia. It is found from India to Korea and Japan (Ahmed *et al.*, 2015<sup>b</sup>). The seeds of *Euryale ferox salisb.* are considered for the treatment of circulatory, respiratory, digestive, excretory and respiratory system disorders (Ahmed *et al.*, 2015<sup>b</sup>). Some important research work has shown the beneficial properties of seeds of *Euryale ferox salisb.*, such as tonic, astringent properties, expectorant, emetic, cardiac stimulant and immune stimulant properties (Ahmed *et al.*, 2015<sup>b</sup>). *Euryale ferox* has been used as a crucial cash crop and as a valuable nutritive tonic in ancient medication for hundreds of years (Rai *et al.*, 2002). *Euryale ferox* seed exhibited positive potency in treating spermatorrhea, diarrhea, xerostomia and polydipsia. A review of several literature data has confirmed that the alcoholic as well as aqueous extract of *Euryale ferox* holds antioxidant activity (Sun *et al.*, 2011).

In our previous research work (Ahmed *et al.*, 2015<sup>b</sup>) we isolated another novel molecule 2 $\beta$ -hydroxybetulinic acid 3 $\beta$ -caprylate (HBAC) from *Euryale ferox salisb.* which depicted a prominent activity against distorted glycemic control, lipid level, hepatic gluconeogenic

enzymes and corrected the deformed histopathological alterations in liver, pancreas and kidney. This directed us to isolate another active principle from seeds of *Euryale ferox salisb.*

The aim of our present research work was to isolate a novel and imperative active principle from seeds of *Euryale ferox salisb.* and to study its diabetic, antioxidant, antihyperlipidemic, as well as hepatic and pancreatic protective action.

## Materials and methods

### General experimental procedure

The melting point was recorded on a melting point apparatus, Veego, Model No. MPI. NMR spectra were collected on Bruker Advance II 100 NMR spectrophotometer in DMSO, utilizing TMS as internal standard. Mass spectra were recorded on VG-AUTOSPEC spectrometer. UV spectra were determined on Shimadzu double-beam 210A spectrometer. FT-IR (in 2.0 cm<sup>-1</sup>, flat, smooth, Abex) were determined on Perkin Elmer – Spectrum RX-I spectrophotometer.

### Chemicals and reagents

Streptozotocin (STZ) was purchased from Sigma Aldrich (MO, USA). Span Diagnostics (Surat, India) had kindly gifted us free samples of kits, namely Glucose Kit, Triglyceride Kits and Cholesterol Kit. Silica gel for column chromatography was purchased from Nicholas, India. Glibenclamide was a generous gift from Ranbaxy, Gurgaon, India. All reagents/solvents used were of analytical grade.

### Plant material

Seeds of *Euryale ferox Salisb.* were collected in Allahabad district (India) in March-April 2014. With respect to voucher number: 11098/BOT/DOP/FHS/2014, seeds of *Euryale ferox salisb.* were botanically recognized by a botanist at the Department of Pharmaceutical Science, Faculty of Health Sciences, SHIATS, where the specimen voucher was deposited.

### Extraction and isolation

The sun dried and ground seed powders of *Euryale ferox salisb.* (2kg) were extracted according to Lee (Lee *et al.*, 2002). The extraction of powdered seed was done at 80 °C in 70% methanol for 3 hours. Filtration of the extract was accomplished with rotary evaporator (Buchi, India) under low pressure. The resultant residue was freeze dried at -80 °C. Then the whole extracts were extracted using separating funnel with dichloromethane, n-hexane, n-butanol and ethyl acetate in a stepwise method. The ethyl-acetate extract (27 g) was connected to a silica gel segment column chromatography and eluted with expanding measures of methanol to outfit the part containing compound 2 $\beta$ -hydroxybetulinic acid 3 $\beta$ -oleiate (HBAO). Fractions of *Euryale ferox salisb.* were collected by removing the solvents with rotary evaporator.

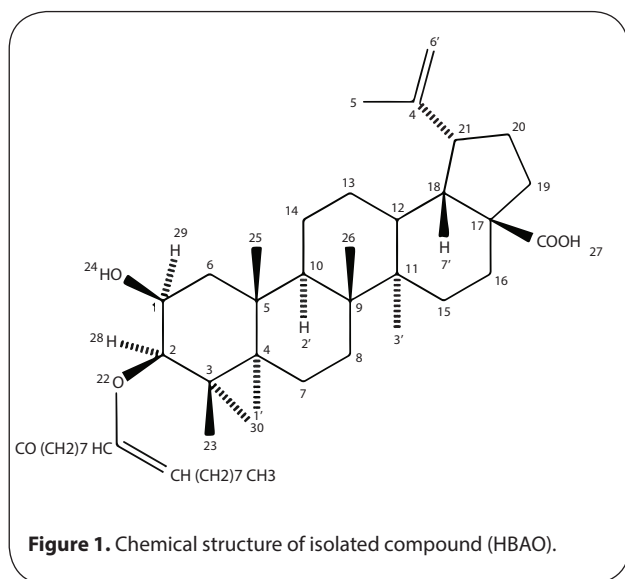
**Compound (2β-hydroxybetulinic acid 3β-oleiate) HBAO**

2β-hydroxybetulinic acid 3β-oleiate: 2β-hydroxybetulinic acid 3β-oleiate was obtained as yellow amorphous powder. [α]<sup>20</sup>-3°. IR max (KBr): 3419, 3275, 2919, 2850, 1725, 1687, 1635, 1464, 1388, 1376, 1273, 1238, 1194, 1108, 1032, 883, 720 cm<sup>-1</sup>, <sup>1</sup>HNMR (DMSO<sub>6</sub>):δ 5.32 (1H m1, H<sub>2</sub>-9'), 5.30 (1H, m1, H-10'), 4.68 (1H<sub>1</sub> brs, H<sub>2</sub>-29b) 4.22 (1H, d, J=5.3 Hz., H-3α), 3.76 (1H, ddd, J=5.3, 5.5, 8.5 Hz, H-2α), 2.27 (2H<sub>1</sub>, t, J=7.6 Hz., H<sub>2</sub>-2), 1.68 (3H, brs, Me-30), 1.25 (20H, brs, 10x CH<sub>2</sub>), 1.23 (3H, brs, Me-23), 0.92 (3H, brs, Me-24), 0.87 (3H, brs, Me-25), 0.84 (3H, t, J=6.3 Hz, Me-1'8), 0.77 (3H, brs, Me-27), 0.65 (3H, brs, Me-27), 2.96-1.30 (29H<sub>1</sub>, m<sub>1</sub>, 12xCH<sub>2</sub>, 5xCH. ESI MS mHz (rel. int.) 736 [M]<sup>+</sup> (C<sub>48</sub>H<sub>80</sub>O<sub>5</sub>) (12.6), 471 (57.5), 455, (71.3), 281 (8.4), 265 (8.7) (Table 1).

The compound, named 2β-hydroxybetulinic acid 3β-oleiate (HBAO) (Figure 1), showed positive test for triterpenoids and IR absorption bands for hydroxyl group (3419 cm<sup>-1</sup>), ester function (1725 cm<sup>-1</sup>), carboxylic group (3275, 1687 cm<sup>-1</sup>), unsaturation (1635 cm<sup>-1</sup>) and long aliphatic chain (720 cm<sup>-1</sup>). It had molecular ion peak at mHz 736, established on the basis of mass and <sup>13</sup>C NMR spectral data analysis which was consistent with the molecular formula of a triterpenic ester C<sub>48</sub>H<sub>80</sub>O<sub>5</sub>. The ion fragments generated at mHz 265 [CO(CH<sub>2</sub>)<sub>7</sub>CH=CH-(CH<sub>2</sub>)<sub>7</sub>CH<sub>3</sub>]<sup>+</sup>, 281 [OCO(CH<sub>2</sub>)<sub>7</sub>CH=CH(CH<sub>2</sub>)<sub>7</sub>CH<sub>3</sub>]<sup>+</sup>, 471 (M-265)<sup>+</sup> and 455 {M-281}<sup>+</sup> indicated that a pentacyclic triterpenoid was esterified with oleic acid. The <sup>1</sup>HNMR spectrum of the compound displayed two one-proton multiplets at δ5.32 and 5.30, assigned to vinylic H-9' and H-10' proton respectively. Two one-proton broad singlets at δ 4.68 and 4.55 were ascribed to methylene H<sub>2</sub>-29 protons. A one-proton doublet at δ 4.22 (J=5.3 Hz) and a one-proton triplet doublet at δ3.76 (J=5.3, 5.5 8.5 Hz) were attributed to α- oriented carbinol H-2 and oxygenated methine H-3 protons respectively. A two-proton triplet at δ 2.27 (J=7.6 Hz) was due to methylene H<sub>2</sub>-2' protons adjacent to the ester function. Six broad singlets at δ 1.68, 1.23, 0.92, 0.87, 0.77 and 0.65 and a triplet at δ 0.84 (J=6.5 Hz) , all

**Table 1.** <sup>13</sup>C NMR spectral data for compound 2β-hydroxybetulinic acid 3β-oleiate (HBAO).

Carbon (position)	<sup>13</sup> C NMR (DMSO6)
1	38.45
2	69.75
3	76.73
4	38.23
5	55.37
6	18.89
7	33.88
8	41.95
9	49.91
10	37.54
11	24.47
12	25.04
13	39.04
14	46.58
15	31.67
16	36.68
17	54.87
18	48.49
19	46.56
20	150.24
21	30.06
22	36.31
23	29.04
24	15.75
25	17.93
26	15.67
27	13.92
28	177.18
29	109.58
30	20.42
1'	174.43
2'	33.62
3'	31.66
4'	28.92
5'	28.84
6'	28.75
7'	27.55
8'	31.30
9'	129.66
10'	127.70
11'	30.89
12'	29.17
13'	29.17
14'	28.92
15'	27.12
16'	26.58
17'	22.09
18'	14.33



integrating for three protons each, were accounted correspondingly to C-30 methyl located on a vinylic carbon C-20, tertiary C-23, C-24, C-25, C-26 and C-27 methyl and primary C-18' methyl protons. The other methylene and methine protons were from  $\delta$  2.96 to 1.30.

The  $^{13}\text{C}$  NMR spectrum of compound exhibited signals for ester carbon at  $\delta$  177.18 (C-28), oxygenated methine carbons at  $\delta$  69.75 (C-2) and 76.33 (C-3), vinylic carbons at  $\delta$  150.24 (C-20), 109.58 (C-29), 129.66 (C-9') and 127.70 (C-10'), and methyl carbon between  $\delta$  29.04-13.92. The  $^1\text{H}$  and  $^{13}\text{C}$  spectral data of the triterpenic carbon framework were comparable with the lupe type triterpenic spectral values. On the basis of the above discussion, the structure of the compound was characterized as lup-20 (29)-en-2 $\beta$ -ol-3 $\beta$ -octadec-9'-enoate-28-oic acid. This is a new teriterpenic ester.

### Animals

All animals used as part of this experimentation got altruistic care in consistence with the standards of creature care defined by the Committee for the Purpose of Control and Supervision of Experiments on Animals (CPCSEA). Male wistar rats (200-250 g) were taken for this research. All the animals were kept under standard conditions of temperature ( $25\pm 1^\circ\text{C}$ ), relative humidity ( $55\pm 10\%$ ), 12hr/12hr light/dark cycle. The animals were fed standard pellet diet (Amrut rat feed, Pune) and water *ad libitum*. The trial

convention was affirmed by the Institutional Animal Ethical Committee of Adina Institute of Pharmaceutical Sciences, Sagar, MP, India (IAEC Reg. no. 1546/PO/a/11/CPCSEA).

### Experimental design

The male albino wistar rats were divided into experimental groups shown in Table 2.

Every morning the drugs were given orally to the animals using a catheter. The rats were categorized as per above distribution and on the 45<sup>th</sup> day of dosage, which was the end of the research plan, all the animals were fasted overnight with free access to water.

### Induction of diabetes

Wistar rats were infused intraperitoneally with STZ disintegrated in newly prepared 0.1 M citrate buffer at 60 mg/kg (Ahmed *et al.*, 2017) (pH=6.5). Animals of the control group received equal volume of vehicle. Blood glucose concentration was examined in all rats after 2 days of STZ administration. The rats were categorized as Diabetic with the blood glucose level exceeding 250 mg/dl.

To estimate the impact of HBAO on STZ induced diabetes mellitus rats, a few biochemical estimations were performed in all groups of tentatively instigated diabetic rats for the estimation of plasma glucose, plasma insulin, serum cholesterol, serum triglycerides, glycated hemoglobin (A1c), hepatic hexokinase, hepatic glucose-6-phosphate dehydrogenase, hepatic fructose-1-6-biphosphatase, superoxide dismutase (SOD), catalase (CAT) and glutathione peroxidase (GPx).

### Histological changes

Pancreas and hepatic tissues were removed from the body and preserved by fixing them in 10% neutral-buffered formalin, dehydrated by passing through series of alcohol and followed by sectioning into 4  $\mu\text{m}$  slices with the help of semi-automated rotary machine (model RM2245, Leica Microsystems, Wetzlar, Germany). Hematoxylin and eosin (HE) staining was done. Histological observation

**Table 2.** Experimental groups.

Group	Dose plan
Group 1	Normal control
Group 2	Normal + HBAO (60 mg/kg p.o.) continued for 45 days.
Group 3	Diabetic control (Infused with STZ 60 mg/kg i.p)
Group 4	Diabetic + HBAO (20 mg/kg p.o.) and continued for 45 days
Group 5	Diabetic + HBAO (40 mg/kg p.o.) and continued for 45 days.
Group 6	Diabetic + HBAO (60 mg/kg p.o.) and continued for 45 days
Group 7	Diabetic + Glibenclamide (10mg/kg p.o.) and continued for 45 days

**Table 3.** Effect of HBAO on plasma glucose level (mg/dl) and glycosylated hemoglobin (A1c) (in percentages) level in normal control and STZ-induced diabetic treated rats.

Groups	Plasma glucose level at different periods of time in normal control and STZ-induced diabetic treated rats			Glycosylated Hemoglobin (A1c) (%) at the end of therapy
	At start of therapy	On 22nd day of therapy	At the end of therapy (on 45th day)	
Group 1	93.78 $\pm$ 1.03	96.45 $\pm$ 1.003	97.80 $\pm$ 1.61	7.09 $\pm$ 0.02
Group 2	92.64 $\pm$ 0.86	93.54 $\pm$ 0.93	94.34 $\pm$ 1.34	7.13 $\pm$ 0.02
Group 3	290.6 $\pm$ 1.13 <sup>a</sup>	294.5 $\pm$ 1.22 <sup>a</sup>	326.9 $\pm$ 1.6 <sup>a</sup>	12.51 $\pm$ 0.15 <sup>a</sup>
Group 4	286.4 $\pm$ 1.17	265.4 $\pm$ 0.87	244.5 $\pm$ 0.98	11.52 $\pm$ 0.13
Group 5	284 $\pm$ 0.7	244.2 $\pm$ 2.14	153.8 $\pm$ 1.42*	9.606 $\pm$ 0.12*
Group 6	282 $\pm$ 0.66	206.1 $\pm$ 0.75	114.7 $\pm$ 1.46*	8.42 $\pm$ 0.18**
Group 7	280.3 $\pm$ 0.7	197.6 $\pm$ 1.14	104.3 $\pm$ 1.66*	7.46 $\pm$ 0.18***

The data are expressed as mean  $\pm$  SEM. The comparisons were made by one way ANOVA followed by Dunnett's test. \* $p$ <0.05 is considered significant when compared to the control group (0 h); \*\* $p$ <0.001 is considered very significant when compared to the control group (0 h); \*\*\* $p$ <0.001 is considered extremely significant when compared to the control group (0 h). <sup>a</sup> - compared to normal; \* - compared to diabetic control

was done to rectify the potency of HBAO against diabetes (Ahmed *et al.*, 2014). Imaging software for laboratory microscopy (Model No. DXIT 1200, Nikon, Japan) was used for photomicrography of each tissue.

### Statistical analysis

Data were given as the mean  $\pm$  SEM. All the data were statistically analyzed by one-way analysis of variance ANOVA, further followed by DUNNET's 't'test.  $p < 0.05$  was considered to be significant.

## Results

### Effect of HBAO on glycemic control

The data resulting from Table 3 and Figure 2 show that blood glucose level fed by normal diet (group 1) was constant in Wistar rats. In comparison to the normal group, the glucose level in STZ induced diabetic rats (group 3) was increased to a significant level ( $p < 0.001$ ). Furthermore, the level of glucose in (group 2), i.e. HBAO administered, was steady throughout 45 days, indicating that no hypoglycemic effect occurred with administration of the maximum dose of HBAO. In addition, the increasing dose of HBAO administered to the diabetic group showed that the lowering in blood glucose level in the drug treated group receiving HBAO=60 mg/kg p.o. was the best when compared to the diabetic control group, as well as in HBAO group receiving doses of 20 mg/kg p.o., 40 mg/kg p.o. and the group receiving the standard drug Glibenclamide.

### Effect of HBAO on glycosylated hemoglobin (A1c)

Glycosylated level was found to be normal with the group receiving HBAO 60 mg/kg without induced diabetes (Table 3). On the other hand, the group with STZ received diabetes when given HBAO doses in increasing manner, it depicts significance level of ( $p < 0.01$ ) lowering in glycosylated hemoglobin in the group that received HBAO with dose of 60 mg/kg p.o. as compared to the group 3, group 4, group 5 and the group received Glibenclamide (group 7).

### Effect of HBAO on level of plasma insulin

Table 4 and Figure 3 show that the insulin levels of untreated diabetic rats were considerably lower than those in normal rats. The increasing levels of HBAO administered results in significant enhancement in the level of plasma insulin in STZ induced diabetic rats. The maximum enhancement in the plasma insulin level was observed in HBAO treated rats that received a dose of 60 mg/kg p.o. for 45 days in comparison to all other HBAO receiving groups and also including the standard group receiving Glibenclamide.

### Effect of HBAO on hepatic glucose-6-phosphate dehydrogenase, glucose-6-phosphatase and fructose-1-6-biphosphatase

Table 5 and Figure 4A and 4B state clearly the activities of gluconeogenic enzymes with levels of glucose-6-phosphatase and fructose-1-6-biphosphatase significantly

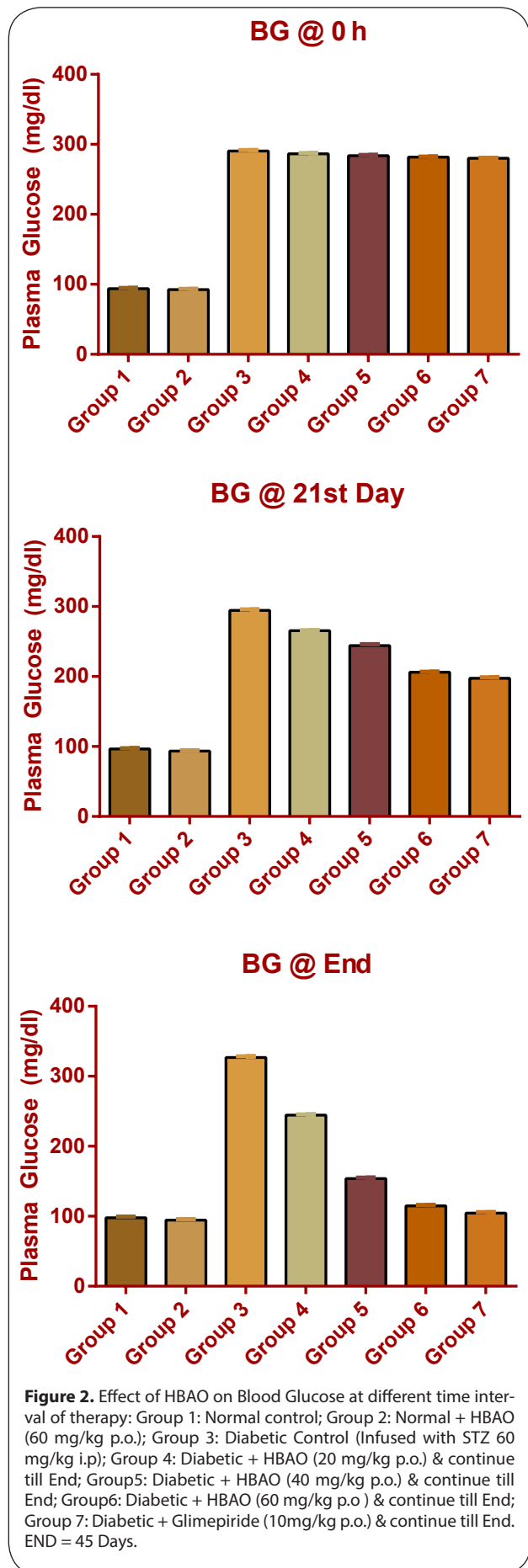


**Table 4.** Effect of HBAO on plasma insulin level in normal control and STZ-induced diabetic treated rats.

Groups	Plasma insulin ( $\mu\text{IU/ml}$ ) level at different periods of time in normal control and STZ-induced diabetic treated rats		
	At start of therapy	At 22 days of therapy	At the end of therapy (on 45th day)
Group 1	14.42 $\pm$ 0.20	15.37 $\pm$ 0.18	16.19 $\pm$ 0.13
Group 2	14.71 $\pm$ 0.15	14.67 $\pm$ 0.33	16.90 $\pm$ 0.34
Group 3	4.18 $\pm$ 0.004 <sup>a</sup>	4.81 $\pm$ 0.04 <sup>a</sup>	10.38 $\pm$ 6.65 <sup>a</sup>
Group 4	4.29 $\pm$ 0.01	4.86 $\pm$ 0.18	8.5 $\pm$ 0.16*
Group 5	4.34 $\pm$ 0.02	6.79 $\pm$ 0.06*	10.5 $\pm$ 0.14**
Group 6	4.49 $\pm$ 0.02	9.67 $\pm$ 0.17**	13.66 $\pm$ 0.17***
Group 7	4.82 $\pm$ 0.07	11.42 $\pm$ 0.19**	14.84 $\pm$ 0.27***

The data are expressed as mean  $\pm$  SEM. The comparisons were made by one way ANOVA followed by Dunnett's test. \* $p$ <0.05 is considered significant when compared to the control group (0 h); \*\* $p$ <0.001 is considered very significant when compared to the control group (0 h); \*\*\* $p$ <0.001 is considered extremely significant when compared to the control group (0 h). <sup>a</sup> – compared to normal; \* – compared to diabetic control

**Table 5.** Effect of HBAO on hepatic gluconeogenic enzymes in normal control and STZ-induced diabetic rats.

Groups	Biochemical estimations of hepatic enzymes			
	Glucose-6-phosphate dehydrogenase (units/min/mg of protein)	Glucose-6-phosphatase (units/min/mg of protein)	Fructose-1-6-biphosphatase (units/min/mg of protein)	Hepatic hexokinase (units/min/mg of protein)
Group 1	0.15 $\pm$ 0.005	0.03 $\pm$ 0.0007	0.01 $\pm$ 0.0003	0.24 $\pm$ 0.004
Group 2	0.15 $\pm$ 0.003	0.03 $\pm$ 0.001	0.017 $\pm$ 0.0007	0.212 $\pm$ 0.003
Group 3	0.04 $\pm$ 0.001 <sup>a</sup>	0.07 $\pm$ 0.0003 <sup>a</sup>	0.07 $\pm$ 0.002 <sup>a</sup>	0.11 $\pm$ 0.005 <sup>a</sup>
Group 4	0.05 $\pm$ 0.0008	0.07 $\pm$ 0.0005	0.065 $\pm$ 0.001	0.13 $\pm$ 0.006
Group 5	0.07 $\pm$ 0.001	0.18 $\pm$ 0.11	0.046 $\pm$ 0.001	0.16 $\pm$ 0.005
Group 6	0.09 $\pm$ 0.002**	0.04 $\pm$ 0.0003**	0.02 $\pm$ 0.001*	0.20 $\pm$ 0.001**
Group 7	0.12 $\pm$ 0.008***	0.03 $\pm$ 0.002***	0.02 $\pm$ 0.001***	0.21 $\pm$ 0.001***

The data are expressed as mean  $\pm$  SEM. The comparisons were made by one way ANOVA followed by Dunnett's test. \* $p$ <0.05 is considered significant when compared to the control group (0 h); \*\* $p$ <0.001 is considered very significant when compared to the control group (0 h); \*\*\* $p$ <0.001 is considered extremely significant when compared to the control group (0 h). <sup>a</sup> – compared to normal; \* – compared to diabetic control

( $p$ <0.01) increased in the group of diabetes induced STZ. On contrast, the activity of glucose-6-phosphate, dehydrogenase was significantly reduced in diabetic control rats. Moreover, HBAO given in the dose of 60 mg/kg depicts the best output compared to other doses.

#### Effect of HBAO on level of hepatic hexokinase

Diabetic group induced with STZ showed a prominently lower level of hexokinase. All other diabetic groups when given HBAO with increasing dose, i.e. 20, 40 60 mg/kg p.o., showed a marked ( $p$ <0.01) increment in the level of hexokinase. The best activity was observed at the dose of 60 mg/kg p.o. of HBAO as compared to the other groups (Table 5 and Figure 4C).

#### Effect of HBAO on levels of serum total cholesterol

The results from Table 6 and Figure 5A show that when STZ diabetic rats were treated with HBAO in increasing doses, i.e. 20, 40 60 mg/kg p.o., there was a significant ( $p$ <0.01) decrease in serum cholesterol level as compared to other groups and standard group having Glimepiride. The most favorable result was deduced with the group receiving HBAO with 60 mg/kg p.o., compared to the other groups.

#### Effect of HBAC on levels of serum HDL cholesterol

An increment with significant extent of ( $p$ <0.01) in serum HDL was seen when given to STZ diabetic rats with novel isolated HBAO, as compared to diabetic group as well as standard treated with Glimepiride (Table 6 and Figure 5C). HBAO in the dose of 60 mg/kg. p.o. treated in diabetes holds the best output of drug.

#### Effect of HBAO on levels of serum LDL cholesterol

The analysis of serum LDL was measured and as intelligible from (Table 6 and Figure 5D) diabetic rats had maximum level of serum LDL. When HBAO in different doses was incorporated in animals, the best diminishing serum LDL outcome was noticed with HBAO 60 mg/kg. compared to all other groups, as well as to standard Glimepiride.

#### Effect of HBAO on levels of serum VLDL cholesterol

There was an increased level of serum VLDL providing logically the affirmation that the diabetic rat had maximum level of serum VLDL and when the same diabetic rats were given HBAO at increased doses of 20, 40 60 mg/kg p.o., maximum serum VLDL decrease was noticed with HBAO 60 mg/kg. compared to all other groups as well as to standard Glimepiride.

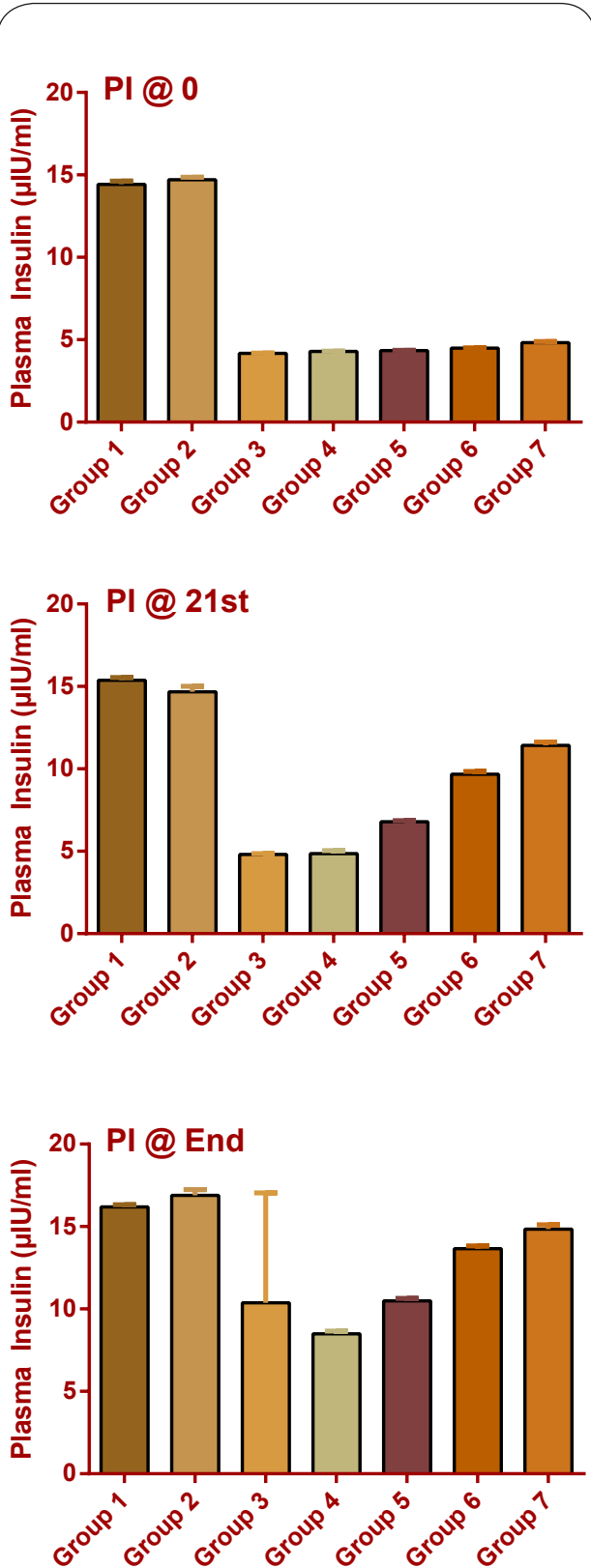


**Figure 3.** Effect of HBAO on Plasma Insulin at different time interval of therapy: Group 1: Normal control; Group 2: Normal + HBAO (60 mg/kg p.o.); Group 3: Diabetic Control (Infused with STZ 60 mg/kg i.p); Group 4: Diabetic + HBAO (20 mg/kg p.o.) & continue till End; Group5: Diabetic + HBAO (40 mg/kg p.o.) & continue till End; Group6: Diabetic + HBAO (60 mg/kg p.o.) & continue till End; Group 7: Diabetic + Glimpiride (10mg/kg p.o.) & continue till End. END = 45 Days.

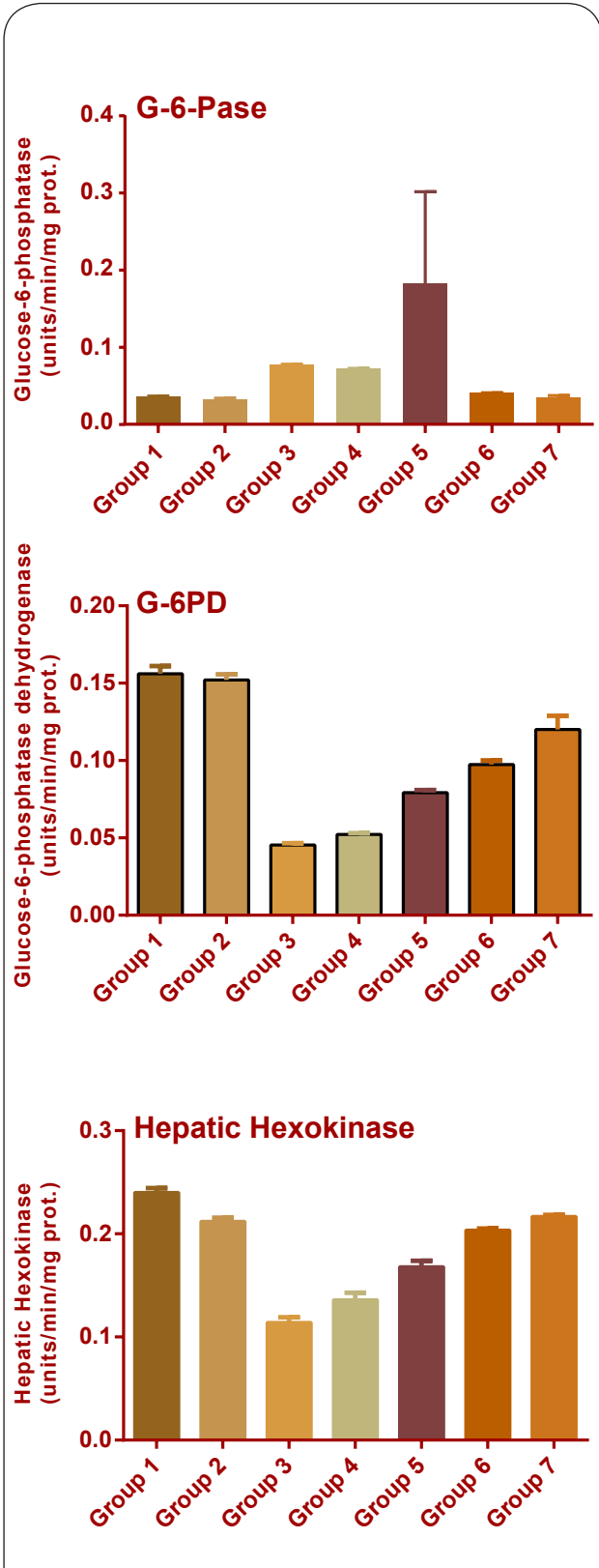


**Figure 4.** Effect of HBAO on Gluconeogenic hepatic enzymes at different time interval of therapy: Group 1: Normal control; Group 2: Normal + HBAO (60 mg/kg p.o.); Group 3: Diabetic Control (Infused with STZ 60 mg/kg i.p); Group 4: Diabetic + HBAO (20 mg/kg p.o.) & continue till End; Group5: Diabetic + HBAO (40 mg/kg p.o.) & continue till End; Group6: Diabetic + HBAO (60 mg/kg p.o.) & continue till End; Group 7: Diabetic + Glimpiride (10mg/kg p.o.) & continue till End. END = 45 Days.

**Effect of HBAO on serum triglyceride levels**

With the outcome of Table 6 and Figure 5B it is evident that STZ diabetic rats showed noticeable increase in triglyceride level of serum. Similarly to other parameters, here too HBAO with 60 mg/kg. resulted in better response compared to other dosage concentrations as well as to diabetic rats given Glimepiride.

**Effect of HBAO on superoxide dismutase (SOD), catalase (CAT) and glutathione peroxidase (GPx) activity**

As expected and as clear from Table 7 and Figure 6A, 6B and 6C, there was significantly decreased activity of SOD, CAT and GPx ( $p < 0.01$ ) in STZ induced diabetic rats compared to normal control rats. The dose of 60 mg/kg HBAO yielded the best result with significant level of ( $p < 0.01$ ) increased in SOD, CAT and GPx in comparison to other given concentrations and standard Glimepiride.

**Effect of HBAO on body weight variation**

Reduced body weight was observed to an extent compared to the normal group. HBAO showed a markedly increased body weight in the STZ induced diabetic rats with maximum weight gain in the group given 60 mg/kg HBAO (Table 8 and Figure 7).

**Effect of HBAO on histopathology of pancreas, kidney & liver***Pancreas*

Normal control animals displayed a typical histological design. Many rounded typical proportions of islet of Langerhans were discovered all around the pancreatic acini. Noticeable nuclei with very much systematic lobules with encompassing islet cells were found in typical control rats (Figure 8). The diabetic group showed spoiled cells of pancreatic islets and acini which consequently proved pancreatic  $\beta$ - cell damage and deteriorated with irregular vacuoles. HBAO treated to STZ induced group demonstrated distinct change of the cell injury, as apparent from the partial restoration of islet cells, diminished  $\beta$ -cell damage, more symmetrical vacuoles and an expansion in number of islet cells.

*Kidney*

Ascending & descending loops of Henle, collecting duct-tubules and prominent glomeruli were among the major morphological features of the kidney in the normal control group. The diabetic group showed deposition of crystals upon glomeruli as well as infiltration of red blood cells (Figure 9). The groups that received HBAO demonstrated the reversibility of the destruction resulting in retention of crystal deposited and cell regeneration.

*Liver*

Normal control groups exhibited influential hepatocytes with central vein along with portal triad (Figure 10). On the other hand, a clearly visible damaged central vein, hepatocytes and portal triad was observed in STZ induced diabetic rats. All the HBAO groups overturned the damage to liver cells.

**Discussion**

At present, traditional and complementary medicine has seen an upsurge in its popularity for the treatment of different diseases. India is endowed with a rich tradition of herbal medicines as is evident from the fact that the Susruta Samhita differentiated between genetically and acquired forms of diabetes and recommended many herbal medicines in different oral formulations for treatment of the disease. Recently, search for appropriate anti-hyperglycemic agents has focused on plants used in traditional medicine because of leads provided by natural products that may provide better treatment than currently used drugs.

In the main, a wide range of secondary metabolites and substances are synthesized by plants playing a key role for their pharmacological potentials. Alkaloids, triterpenoids and steroids were reported to have anti-diabetic activity already in ancient times (Erememisoglu *et al.*, 1995).

The present research depicts the isolation of a novel pentacyclic triterpene (Figure 1) isolated from the methanolic extract of *Euryale ferox salish.* seeds further

**Table 6.** Effect of HBAO on lipid profiles in normal control and STZ-induced diabetic treated rats.

Groups	Lipid Profiles			
	Total cholesterol (TC) (mg/dl)	LDL cholesterol (LDL-c) (mg/dl)	Triglycerides (mg/dl)	HDL cholesterol (HDL-c) (mg/dl)
Group 1	118.9±0.39	24.40±0.44	71.97±0.29	55.79±0.31
Group 2	115.4±2.24	23.76±0.61	72.10±0.49	54.25±0.27
Group 3	231.8±0.31 <sup>a</sup>	144.6±0.54 <sup>a</sup>	281.7±0.42 <sup>a</sup>	19.83±0.26 <sup>a</sup>
Group 4	218.1±0.47	134.0±0.58	211.6±0.57	27.07±2.3
Group 5	142.8±0.31	103.2±0.62	140.9±0.29	37.09±0.37
Group 6	121.4±0.48 <sup>***</sup>	37.10±0.54 <sup>**</sup>	84.17±1.16 <sup>***</sup>	49.14±0.18 <sup>***</sup>
Group 7	135.7±0.52 <sup>**</sup>	43.51±0.65 <sup>**</sup>	91.99±0.53 <sup>**</sup>	46.62±0.39 <sup>***</sup>

The data are expressed as mean ± SEM. The comparisons were made by one way ANOVA followed by Dunnett's test. \* $p < 0.05$  is considered significant when compared to the control group (0 h); \*\* $p < 0.001$  is considered very significant when compared to the control group (0 h); \*\*\* $p < 0.001$  is considered extremely significant when compared to the control group (0 h). <sup>a</sup> – compared to normal; \* – compared to diabetic control

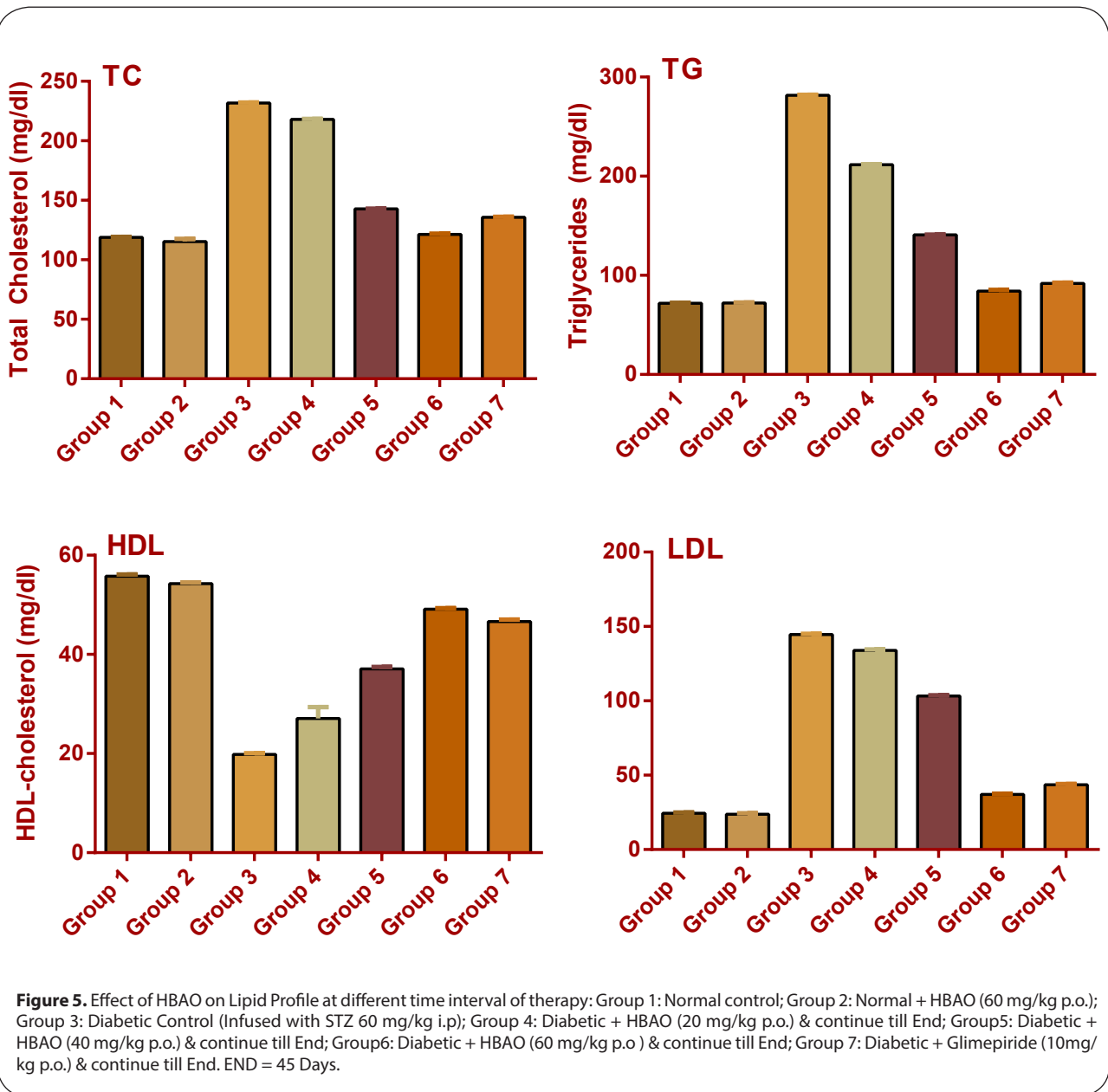


**Table 7.** Effect of HBAO on oxidative stress estimation in normal control and STZ-induced diabetic treated rats.

Groups	Oxidative stress parameters		
	Superoxide dismutase (SOD) (U/mg protein)	Catalase (CAT) (nM H <sub>2</sub> O <sub>2</sub> decomposed/min/g)	Glutathione peroxidase (GPx) (U/mg protein)
Group 1	11.10±0.28	83.24±0.87	13.11±0.41
Group 2	11.07±0.23	84.68±0.84	12.47±0.18
Group 3	3.15±0.04 a	26.89±0.31 a	5.62±0.082 a
Group 4	4.36±0.01	28.08±0.4	7.154±0.03
Group 5	7.32±0.05*	52.81±0.62*	9.69±0.12*
Group 6	9.214±0.04167**	71.88±0.2619**	10.64±0.04104**
Group 7	10.15±0.01428***	75.70±1.075***	11.73±0.1861**

The data are expressed as mean ± SEM. The comparisons were made by one way ANOVA followed by Dunnett’s test. \**p* < 0.05 is considered significant when compared to the control group (0 h); \*\**p* < 0.001 is considered very significant when compared to the control group (0 h); \*\*\**p* < 0.001 is considered extremely significant when compared to the control group (0 h). <sup>a</sup> – compared to normal; \* – compared to diabetic control

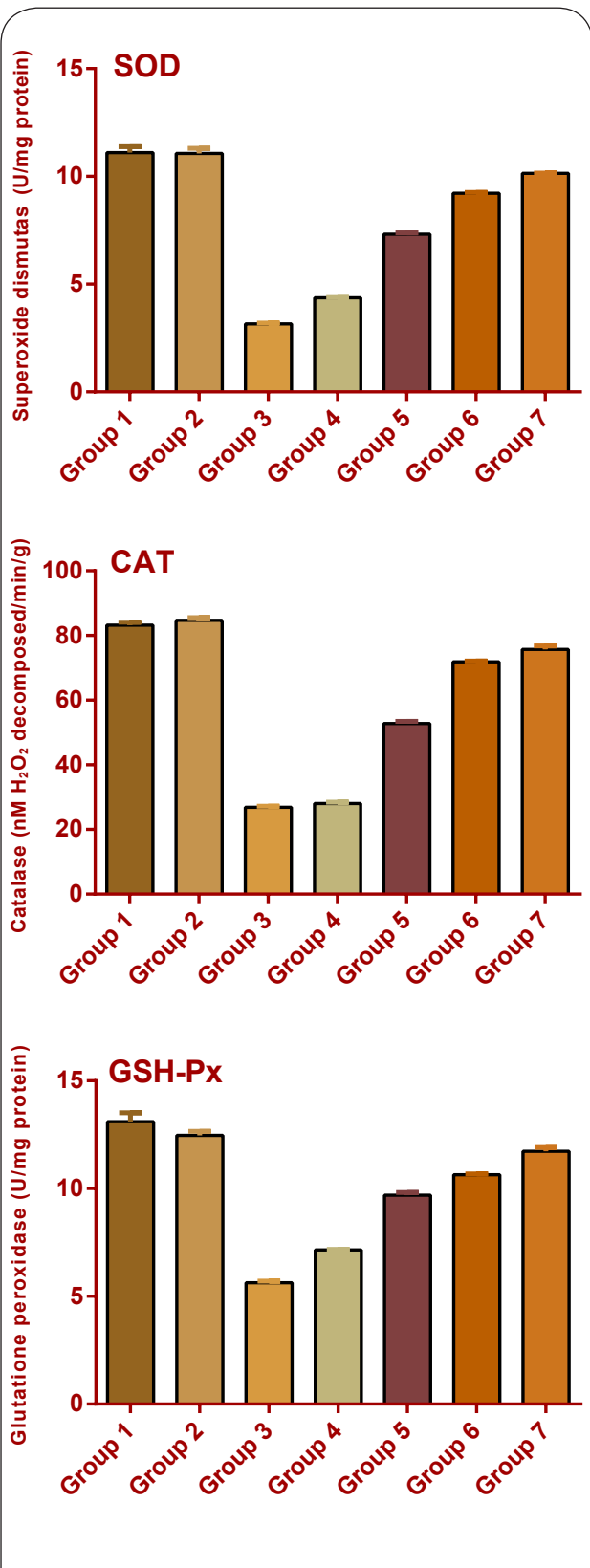


**Figure 6.** Effect of HBAO on Antioxidant marker enzymes at different time interval of therapy: Group 1: Normal control; Group 2: Normal + HBAO (60 mg/kg p.o.); Group 3: Diabetic Control (Infused with STZ 60 mg/kg i.p); Group 4: Diabetic + HBAO (20 mg/kg p.o.) & continue till End; Group5: Diabetic + HBAO (40 mg/kg p.o.) & continue till End; Group6: Diabetic + HBAO (60 mg/kg p.o.) & continue till End; Group 7: Diabetic + Glimperiride (10mg/kg p.o.) & continue till End. END = 45 Days.

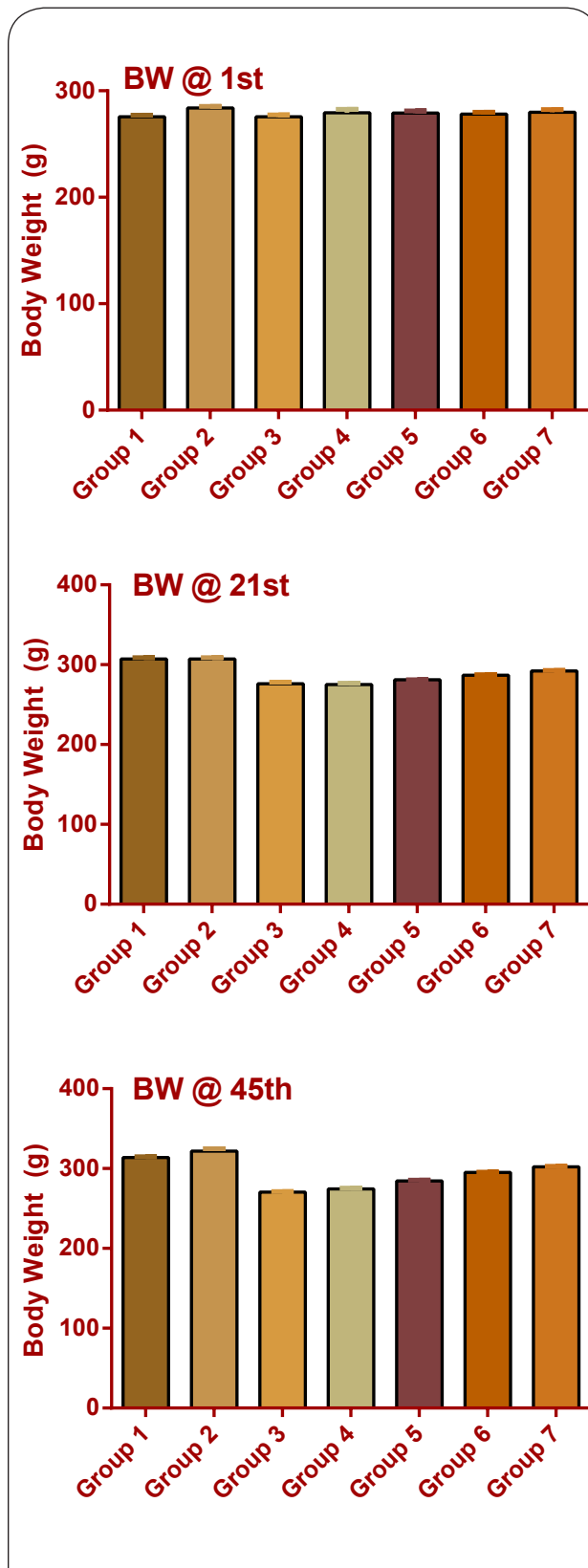


**Figure 7.** Effect of HBAO on Body Weight at different time interval of therapy: Group 1: Normal control; Group 2: Normal + HBAO (60 mg/kg p.o.); Group 3: Diabetic Control (Infused with STZ 60 mg/kg i.p); Group 4: Diabetic + HBAO (20 mg/kg p.o.) & continue till End; Group5: Diabetic + HBAO (40 mg/kg p.o.) & continue till End; Group6: Diabetic + HBAO (60 mg/kg p.o.) & continue till End; Group 7: Diabetic + Glimperiride (10mg/kg p.o.) & continue till End. END = 45 Days.

**Table 8.** Effect of HBAO on body weight (grams) in normal control and STZ-induced diabetic treated rats.

Groups	Body weight (g) at different time interval of experimentation		
	At start of therapy	At 22nd day of therapy	At end of therapy (45th Day)
Group 1	275.6±1.44	307±1.95	313.8±1.07
Group 2	283.8±1.59	307.2±1.56	321.8±3.18
Group 3	275.6±1.69 <sup>a</sup>	276±2.07 <sup>a</sup>	270.6±0.51 <sup>a</sup>
Group 4	279.4±3.20	275.2±1.74	274.6±0.87*
Group 5	279.2±1.83	281±0.32**	284.6±1.03**
Group 6	278.2±1.56	286.8±0.58**	295.2±0.374***
Group 7	279.8±2.65	292±0.71**	302±0.71***

The data are expressed as mean ± SEM. The comparisons were made by one way ANOVA followed by Dunnett's test. \*p< 0.05 is considered significant when compared to the control group (0 h); \*\*p< 0.001 is considered very significant when compared to the control group (0 h); \*\*\*p< 0.001 is considered extremely significant when compared to the control group (0 h). <sup>a</sup> – compared to normal; \* – compared to diabetic control

assessed for its anti-diabetic, antihyperlipidemic, anti-oxidant and hepatic and pancreas protective activity against STZ-induced diabetic rats. STZ causes partial apoptosis of pancreatic cells and induces an experimental model for type-2 diabetes mellitus and it also releases free radicals which distort the mitochondrial function of  $\beta$ -cells (Szkudelski, 2001). This made us to take on this model for the induction of diabetes. STZ interferes with the cellular metabolic oxidative mechanisms and produces severe and irreversible hyperglycemia, if given at higher doses (Mitra *et al.*, 1996). Results of acute toxicity studies clearly demonstrate no mortality in the isolated compound treated rats and the behavior of the compound treated rats also appeared to be normal. Until the end of the research work, none of the rat showed any toxic reaction or lethality. This confirms that the isolated novel compound is non-toxic nature.

Augmented levels of blood glucose and insulin confirmed that the STZ-induced diabetic model was well founded. Plasma glucose level was measured at regular intervals (0, 5, 12, 20, 28, 35 and 45<sup>th</sup> day) in normal, diabetic and the novel compound treated Wistar rats. Administration of the novel compound HBAO clearly revealed the hypoglycemic, antihyperlipidemic, anti-oxidant and hepato-pancreas protective effect. There is a gradual reduction of plasma glucose in almost all the doses when compared to diabetic control rats. Maximum reduction of plasma glucose was obtained with 60 mg/kg p.o dose of HBAO. Simultaneously, it was also observed that the plasma glucose level of normal rats was unaltered upon administration of HBAO. This corroborates the substantial normoglycemic effect of the isolated compound. The decrement of plasma glucose of the HBAO treated diabetic rats advocates that the novel isolated compound acts to reduce plasma glucose either by promoting uptake metabolism by inhibiting hepatic gluconeogenesis or by advancing the entry of glucose into muscle and adipose tissues through plausible mechanism of stimulation of regenerating and revitalizing the spared pancreatic  $\beta$ -cells (Bolkent *et al.*, 2000).

Increased glycation of protein has been discovered to be a consequence of diabetic complications. Hemoglobin and various proteins are glycated to a greater extent in diabetes (Keen & Jarrett, 1982). Among the glycated proteins, HbA<sub>1c</sub> is widely recognized as marker of glycation control and is considered a biological intermediate criterion for measurement of efficacy of diabetic therapy. In our research work, HBAO clearly prevents a significant increase in HbA<sub>1c</sub> with a simultaneous control of plasma glucose.

The two primary complementary events that equilibrate the glucose load are glycolysis and gluconeogenesis, which is exemplified by the partial or total deficiency of insulin. Suppression of hepatic gluconeogenesis and glycogenolysis, while enhancing hepatic glycogen synthesis, was carried out by insulin. A major site of endogenous glucose production is the liver, where production of glucose was accomplished by gluconeogenesis and glycogenolysis. Hydrolysis of glucose-6-phosphate to glucose was done by glucose-6-phosphatase (G-6 Pase), which is the final step of both hepatic gluconeogenesis and glycogenolysis. G-6 Pase is mainly expressed in liver, kidney and small intestine. Treatment with HBAO (60 mg/kg p.o.), causes no significant alterations. This suggests that HBAO may modulate glycogen biosynthesis by suppressing the activity of glucose-6-phosphatase and as a result decreases hepatic glycogen synthesis and storage. Insulin regulates the activity of glucose-6-phosphate dehydrogenase (G6PD). Levels of G6PD were found to be decreased in diabetic rats suggesting a lowered glucose metabolism through phosphogluconate oxidation pathway. Oral administration of HBAO (60 mg/kg p.o.) significantly restored the level of G6PD, indicating improved glucose utilization by the hepatic tissues. Fructose-bi-phosphatase (FBPase) regulates the hepatic glucose hemostasis and is mainly expressed in liver and kidney (Nordlie *et al.*, 1999; Mithieux, 2009). In diabetic rats the hepatic glucose production was found to be increased and is directly associated with impaired function and increased level of FBPase in the liver. Enhanced

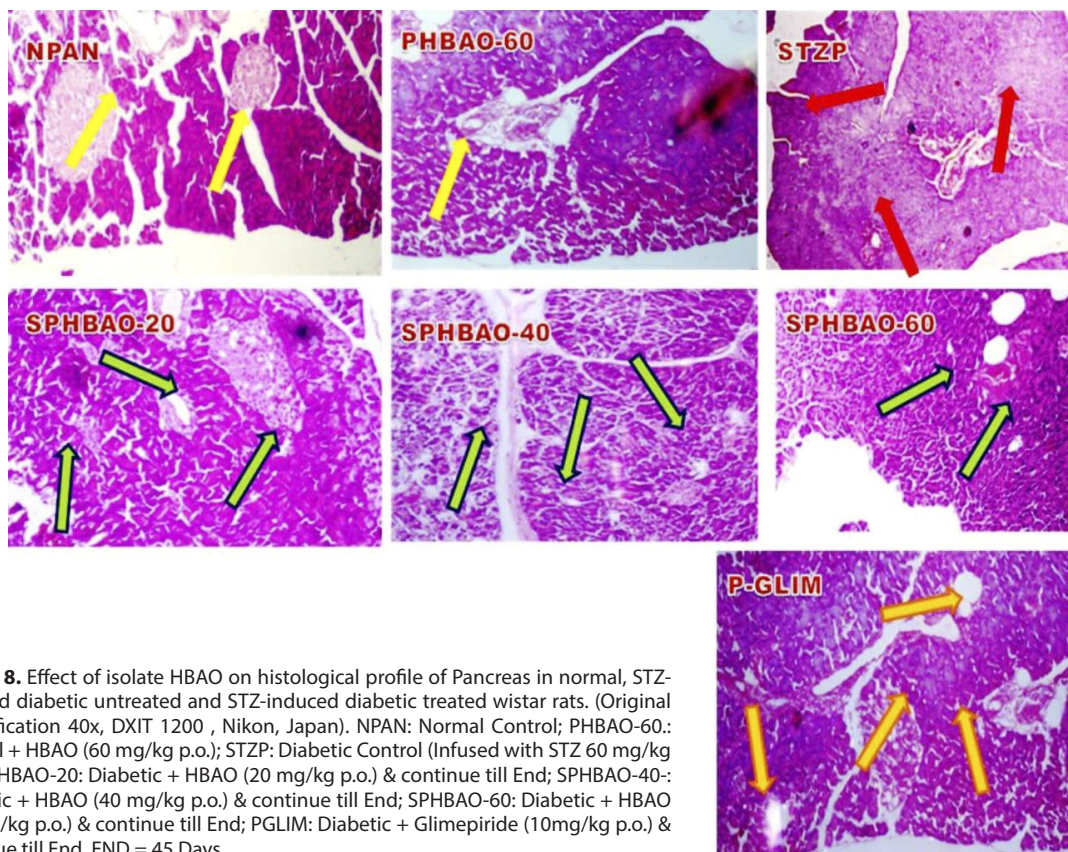


**Figure 8.** Effect of isolate HBAO on histological profile of Pancreas in normal, STZ-induced diabetic untreated and STZ-induced diabetic treated wistar rats. (Original magnification 40x, DXIT 1200 , Nikon, Japan). NPAN: Normal Control; PHBAO-60.: Normal + HBAO (60 mg/kg p.o.); STZP: Diabetic Control (Infused with STZ 60 mg/kg i.p); SPHBAO-20: Diabetic + HBAO (20 mg/kg p.o.) & continue till End; SPHBAO-40:- Diabetic + HBAO (40 mg/kg p.o.) & continue till End; SPHBAO-60: Diabetic + HBAO (60 mg/kg p.o.) & continue till End; PGLIM: Diabetic + Glimepiride (10mg/kg p.o.) & continue till End. END = 45 Days.

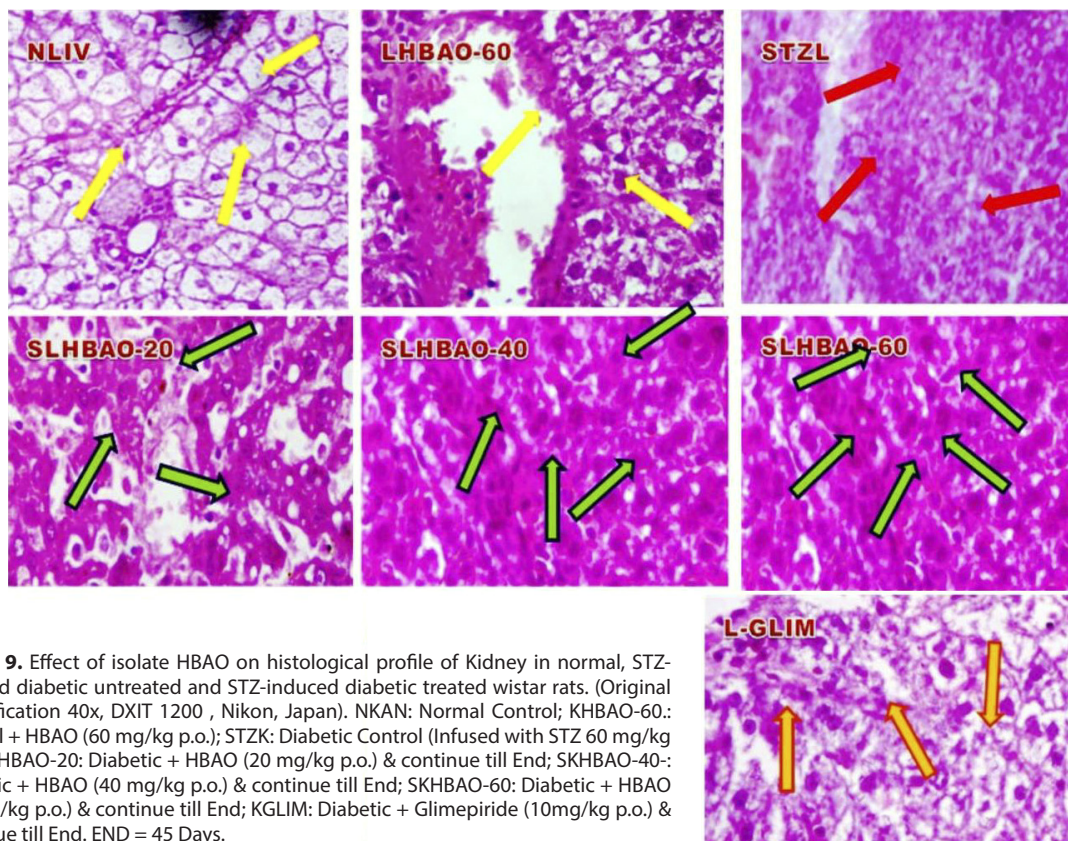


**Figure 9.** Effect of isolate HBAO on histological profile of Kidney in normal, STZ-induced diabetic untreated and STZ-induced diabetic treated wistar rats. (Original magnification 40x, DXIT 1200 , Nikon, Japan). NKAN: Normal Control; KHBAO-60.: Normal + HBAO (60 mg/kg p.o.); STZK: Diabetic Control (Infused with STZ 60 mg/kg i.p); SKHBAO-20: Diabetic + HBAO (20 mg/kg p.o.) & continue till End; SKHBAO-40:- Diabetic + HBAO (40 mg/kg p.o.) & continue till End; SKHBAO-60: Diabetic + HBAO (60 mg/kg p.o.) & continue till End; KGLIM: Diabetic + Glimepiride (10mg/kg p.o.) & continue till End. END = 45 Days.

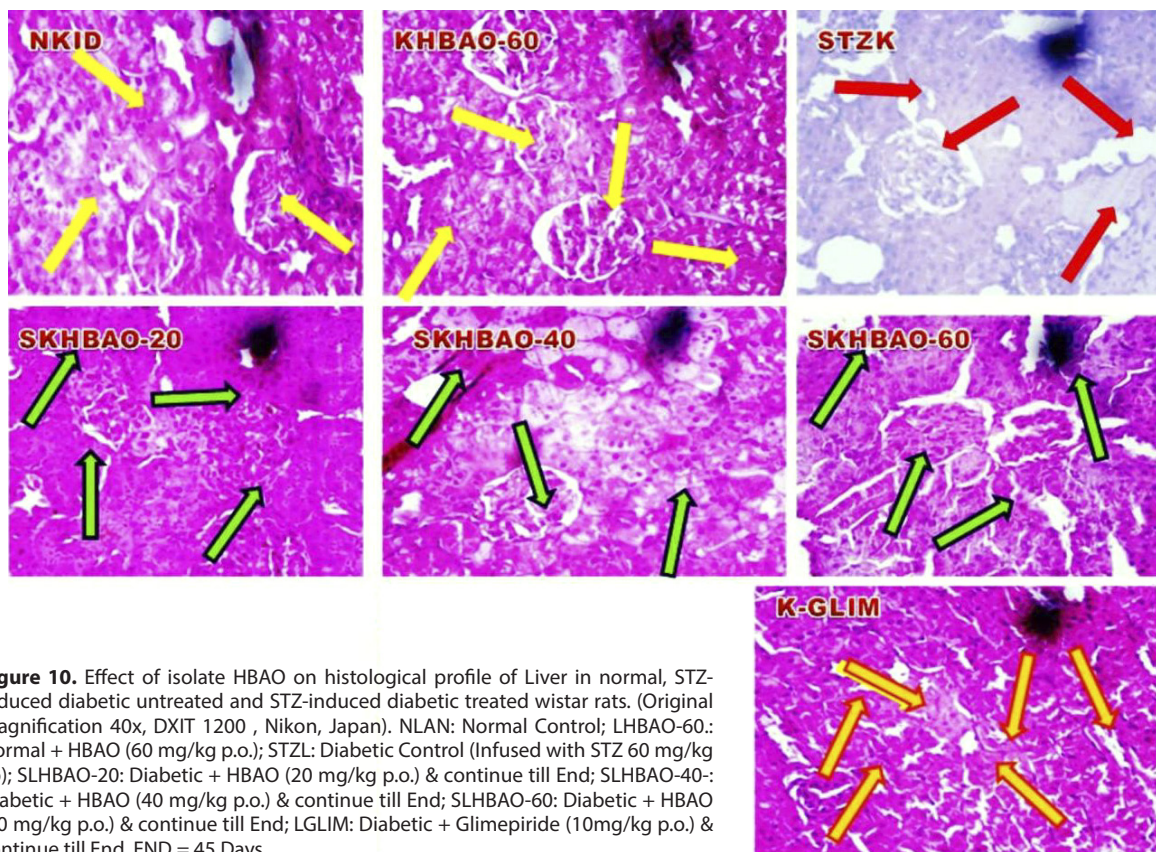


**Figure 10.** Effect of isolate HBAO on histological profile of Liver in normal, STZ-induced diabetic untreated and STZ-induced diabetic treated wistar rats. (Original magnification 40x, DXIT 1200, Nikon, Japan). NLAN: Normal Control; LHBAO-60.: Normal + HBAO (60 mg/kg p.o.); STZL: Diabetic Control (Infused with STZ 60 mg/kg i.p.); SLHBAO-20: Diabetic + HBAO (20 mg/kg p.o.) & continue till End; SLHBAO-40: Diabetic + HBAO (40 mg/kg p.o.) & continue till End; SLHBAO-60: Diabetic + HBAO (60 mg/kg p.o.) & continue till End; LGLIM: Diabetic + Glibenclamide (10mg/kg p.o.) & continue till End. END = 45 Days.

hepatic glucose production in STZ-induced diabetic rats is associated with dysregulation of these hepatic enzymes. Treatment of diabetic Wistar rats with HBAO (60mg/kg p.o.) clearly depicts the significant decline in the level of FBPase, which is escorted by reduction in hepatic glucose production. Hepatic hexokinase is an insulin independent enzyme in the glycolytic pathway and fundamental for glucose homeostasis. Reduction in hexokinase activity in STZ-induced diabetic rats may be due to deficiency of insulin, as insulin stimulates and activates hepatic hexokinase. Administration of HBAO (60mg/kg p.o) to STZ-induced diabetic rats significantly improved the activity of hexokinase, which in turn results in enhanced glucose utilization for energy production.

In diabetes mellitus, increased blood glucose level is accompanied with dyslipidemia which is characterized by increase in triglyceride (TG), total cholesterol (TC), LDL cholesterol and a decrease in HDL cholesterol (Gupta *et al.*, 2009). High level of TG, TC, LDL cholesterol are significant and major risk factors for cardiovascular disorders, while improved level of HDL cholesterol is associated with improvement in cardiovascular profile. HDL plays a key role in transfer of cholesterol from blood to liver by reverse cholesterol pathway (Wang *et al.*, 2010). Disturbed lipid profile was reversed after oral administration of HBAO. Thus HBAO has the potential to prevent atherosclerosis and coronary heart disease formation in STZ-induced diabetic rats.

Some important research indicates that chronic hyperglycemia mediated oxidative stress is a major risk factor for dysfunction of liver in diabetes (Evans *et al.*, 2002; Rochette *et al.*, 2014). In oxidative stress, free radicals are generated, associated with increased plasma glucose and liver dysfunction. In STZ-induced diabetic rats, a significant decrease in hepatic antioxidants including superoxide dismutase (SOD), catalase (CAT) and glutathione peroxidase (GPx) activities were observed. The role of SOD is imperative in eliminating reactive oxygen species (ROS) originating from peroxidative process in tissues of liver and scavenging superoxide radicals by converting them to less toxic H<sub>2</sub>O<sub>2</sub> and molecular oxygen (Packer *et al.*, 1978; Kaleem *et al.*, 2006). Upon administration of HBAO, the activity of SOD was significantly increased. In the present research work, a reduction in CAT activity was observed in STZ-induced diabetic rats. A reduction in CAT activity is primarily involved in the direct elevation of ROS, and might be associated with enhancement in oxidative stress in diabetes (Arulselvan & Subramanian, 2007). Our research work indicates a significant increase in CAT activity in HBAO treated STZ-induced diabetic rats. Another important enzyme, glutathione peroxidase (GPx), depicts a severe decline due to free radical induced inactivation and glycation of GPx in STZ-induced diabetic rats (Zhang & Tan, 2000). HBAO administration to STZ-induced diabetic rats increases GPx activities characteristic of insulin stimulatory activity of HBAO.

## Conclusion

The novelty of this study is that HBAO, a pentacyclic triterpene, is a novel compound found in *Euryale ferox salisb* seeds. Oral administration of HBAO alleviates glycaemic homeostasis and oxidative stress in STZ-induced diabetic rats, further HBAO normalized plasma glucose, glycosylated hemoglobin (HbA<sub>1c</sub>), hepatic gluconeogenic enzymes, plasma insulin, ameliorated pancreatic  $\beta$ -cell, hepatic and renal histology and  $\beta$ -cell functions, improving dyslipidemia and antioxidant enzymes in STZ-induced diabetic rats. Thus it can be concluded that HBAO derived from *Euryale ferox salisb* seeds may help prevent the important complications in diabetic rats and it might be a potential therapeutic candidate to combat diabetes.

## Authors' contributions

DA and MS developed and designed the study. DA and MIK performed the experiments. DA and MFK analyzed the data. DA and MIK wrote the manuscript. All authors finalized the reading and inputs of the manuscript.

## Acknowledgements

The authors wish to acknowledge SHUATS, Allahabad for providing necessary facilities and other documentary works.

## REFERENCES

- Ahmed D, Kumar V, Verma A, Gupta PS, Kumar V, Dhingra V, Mishra V, Sharma M. (2014). Antidiabetic, renal/hepatic/pancreas/cardiac protective and antioxidant potential of methanol/ dichloromethane extract of *Albizia Lebbeck* Benth. stem bark (ALEX) on streptozotocin induced diabetic rats. *BMC Comp. and Alt. Medicine*. **14**: 1–17.
- Ahmed D, Kumar V, Verma A, Shukla GS, Sharma M. (2015<sup>a</sup>). Antidiabetic, antioxidant, anti-hyperlipidemic effect of extract of *Euryale ferox salisb*. with enhanced histopathology of pancreas, liver and kidney in streptozotocin induced diabetic rats. *Springer Plus*. **4**: 1059–67.
- Ahmed D, Sharma M, Kumar V, Bajaj HK, Verma A. (2015<sup>b</sup>). 2 $\beta$ -hydroxybetulinic acid 3 $\beta$ -caprylate: an active principle from *Euryale ferox salisb*. seeds with antidiabetic, antioxidant, pancreas & hepatoprotective potential in streptozotocin induced diabetic rats. *Journal of Food Science and Technology*. **52**: 5427–5441.
- Ahmed D, Khan MI, Kaithwas G, Roy S, Gautam S, Singh M, Devi U, Yadav, R, Rawat J, Saraf S. (2017). Molecular docking Analysis and Antidiabetic activity of Rifabutin against STZ-NA induced diabetes in albino wistar rats. *Beni Suef Jour. of Basic and Applied Sci*. **6**: 269–284.
- Arulselvan P, Subramanian SP. (2007). Beneficial effects of *Murraya koenigii* leaves on antioxidant defense system and ultrastructural changes of pancreatic cells in experimental diabetes in rats. *Chem. Biol. Interact*. **165**: 155–64.
- Bolkent S, Yamardag R, Tabakogluoguz A, Ozsoyosacaon O. (2000). Effects of chord (*Beta vulgaris* L.Var.cicla) extract on pancreatic b- cells in Streptozotocin diabetic rats: a morphologic and biochemical study. *J. Ethnopharmacol*. **73**: 251–259.
- Erememisoglu A, Kelestimur F, Kokel AH, Utsun H, Tekol Y, Ustidal M. (1995). Hypoglycemic effect of *Zizyphus jujube* leaves. *J. Pharm. Pharmacol*. **47**: 72–74.
- Evans JL, Goldfine ID, Maddux BA, Grodsky GM (2002). Oxidative stress and stress-activated signaling pathways: A unifying hypothesis of type 2 diabetes. *Endocrine Reviews*. **23**: 599–622.
- Gupta S, Sharma SB, Bansal SK, Prabhu KM. (2009). Antihyperglycemic and hypolipidemic activity of aqueous extract of *Cassia auriculata* L. leaves in experimental diabetes. *J. Ethnopharm*. **123**: 499–503.
- IDF Atlas 2015: International Diabetes Federation, 2015.
- Kaleem M, Asif M, Ahmed QU, Bano B. (2006). Antidiabetic and antioxidant activity of *Annona squamosa* extract in streptozotocin-induced diabetic rats. *Singap. Med. J*. **47**: 670–5.
- Keen H, Jarrett J. Complications of diabetes, 1982; London: Edward Arnold.
- King GL, McNeely MJ, Thorpe LE, Mau MLM, Ko J, Liu LL, Sun A, Hsu WC, Chow EA. (2012). Understanding and addressing unique needs of diabetes in Asian Americans native Hawaiians and Pacific islanders. *Diabetes Care*. **35**: 1181–1188.
- Lee SE, Ju EM, Kim JH. (2002). Antioxidant activity of extracts from *Euryale ferox* seed. *Exp Mol. Med*. **34**: 100–106.
- Maritim AC, Sanders RA, Watkins JB. (2003). Diabetes, oxidative stress and antioxidants: a review. *J. Biochem. Molec. Toxicol*. **17**: 24–38.
- Mithieux G. (2009). A novel function of intestinal gluconeogenesis: Central signalling in glucose and energy homeostasis. *Nutrition*. **25**: 881–884.
- Mitra SK, Goupmadhavan S, Muralidhar TS, Seshadri SJ. (1996). Effect of D-400, a herbomineral formulation on liver glycogen content and microscopic structure of pancreas and liver in streptozotocin-induced diabetes in rats. *Indian J. Exp. Biol*. **34**: 964–967.
- Nordlie RC, Foster JD, Lange AJ. (1999). Regulation of glucose production by the liver. *Annu. Rev. Nutr*. **19**: 379–406.
- Packer JE, Slater TF, Willson RL. (1978). Reactions of the carbon tetrachloride related peroxy free radical with amino acids: pulse radiolysis evidence. *Life Sci*. **23**: 2617–20.
- Poretzky L. (ed.) Principles of Diabetes mellitus, Springer Science and Business Media 2010; 821–822.
- Rai UN, Tripathi RD, Vajpayee P, Jha V, Ali MB. (2002). Bioaccumulation of toxic metals (Cr, Cd, Pb and Cu) by seeds of *Euryale ferox salisb*. (Makhana). *Chemosphere*. **46**: 267–272.
- Rochette L, Zeller M, Cottin Y, Vergely C (2014). Diabetes, oxidative stress and therapeutic strategies. *Biochimica et Biophysica Acta*. **1840**: 2709–2729.
- Sun WK, Yuan H, Xu W, Qi L. (2011). Study on anti-oxidative activity of *Euryale ferox salisb*. shells extracts. *Sci. Technol. Food Ind*. **4**: 100–102.
- Suraamornkul S, Kwancharoen R, Ovarlamporn M, Rawdaree P, Bajaj M. (2010). Insulin clamp-derived measurements of insulin sensitivity and insulin secretion in lean and obese Asian type 2 diabetic patients. *Metabolic Syndrome and Related Disorder*. **8**: 113–118.
- Szkudelski T. (2001). The mechanism of alloxan and streptozotocin action in  $\beta$ -cells of the rat pancreas. *Physiol. Res*. **50**: 536–546.
- Thannickal VJ, Fanburg BL. (2000). Reactive oxygen species in cell signalling. *American Journal of Physiology - Lung Cellular and Molecular Physio*. **279**: L1005–L1028.
- Wang L, Zhang XT, Zhang HY, Yao HY, Zhang H. (2010). Effect of *Vaccinium bracteatum* Thunb. leaves extract on blood glucose and plasma lipid levels in streptozotocin-induced diabetic mice. *J. Ethnopharm*. **130**: 465–9.
- Yoon KH, Ko SH, Cho JH, Lee JM, Ahn YB, Song KH, Yoo SJ, Kang MI. (2003). Selective beta-cell loss and alpha-cell expansion in patients with type 2 diabetes mellitus in Korea. *The Journal of Clinical Endocrinology & Metabolism*. **88**: 2300–2308.
- Zhang XF, Tan BK. (2000). Anti-hyperglycemic and antioxidant properties of *Andrographis paniculata* in normal and diabetic rats. *Clin. Exp. Pharmacol. Physiol*. **27**: 358–63.

ORIGINAL ARTICLE

# Effect of AgNPs on the human reconstructed epidermis

Jana FRANKOVÁ<sup>1,2</sup>, Jana JURÁŇOVÁ<sup>1,2</sup>, Vojtěch KAMARÁD<sup>3</sup>, Bohumil ZÁLEŠÁK<sup>4</sup>, Jitka ULRICHOVÁ<sup>1,2</sup>

<sup>1</sup>Department of Medical Chemistry and Biochemistry, Faculty of Medicine and Dentistry, Hněvotínská 3, Olomouc, Czech Republic

<sup>2</sup>Institute of Molecular and Translational Medicine, Faculty of Medicine and Dentistry, Palacký University, Hněvotínská 5, Olomouc, Czech Republic

<sup>3</sup>Department of Histology and Embryology, Faculty of Medicine and Dentistry, Hněvotínská 3, Olomouc, Czech Republic

<sup>4</sup>Department of Plastic and Aesthetic Surgery, University Hospital Olomouc, I.P.Pavlova 6, Olomouc, Czech Republic

ITX110418A06 • Received: 21 November 2017 • Accepted: 23 February 2018

## ABSTRACT

Nanoparticles are utilized in a wide range of industries. The most studied silver nanoparticles (AgNPs) are used in medicine and also in several wound dressings due to their antimicrobial properties. The inflammatory response or potential morphological changes of skin cells after their application are not well known yet. In our study we used the model of human reconstructed epidermis (RHE), prepared in our laboratory, to evaluate whether the AgNPs penetrate through RHE, induce some morphological changes of keratinocytes or influence the production of pro-inflammatory cytokines (IL-6 and IL-8). After the application of three different concentrations (25 ppm, 2.5 ppm, 0.25 ppm) of AgNPs to RHE for 24 hours we verified that AgNPs did not affect the production of pro-inflammatory cytokines (IL-6 and IL-8) and neither did they influence the expression of keratin K14 and loricrin. The morphology of the cells was likewise unchanged. Based on these results we conclude that AgNPs do not have any negative effect on the morphological changes and do not increase the production of pro-inflammatory cytokines.

**KEY WORDS:** human reconstructed epidermis; AgNPs; IL-6; IL-8; loricrin; keratin K14

## Introduction

Nanoparticles display unique physical and chemical properties and can be used in numerous applications (Sondi & Salopek-Sondi, 2004). Due to their low toxicity to humans, and their antibacterial properties, silver and silver nanoparticles (AgNPs) are of interest in medicine and dermatology.

The establishment and application of alternative *in vitro* models for safety assessment is of growing interest of toxicology research today (Li *et al.*, 2017, Kandarova *et al.*, 2009). Some of the existing 3D models consist of one type of cells (e.g. reconstructed epidermis prepared of keratinocytes) (Mathes *et al.*, 2014). When keratinocytes grow on a solid surface, or on polycarbonate porous filter and were subjected to cyclic pressure treatment, they started to differentiate into a multilayer system with a protein expression pattern (keratins, fillagrin,

loricrin, *etc.*), which is typical of differentiated epidermis. Immunohistochemistry studies often monitor the abundance and distribution of these proteins within the given 3D model.

Cytokines are the key modulator of inflammation, participating in acute and chronic inflammation via a complex and sometimes seemingly contradictory network of interactions (Turner *et al.*, 2014, Ambrozova *et al.*, 2017). In response to physical and chemical stress, keratinocytes produce inflammatory cytokines such as interleukin 1 (IL-1), interleukin 6 (IL-6), interleukin 8 (IL-8), tumor necrotic factor  $\alpha$  (TNF- $\alpha$ ), *etc.* (Coquette *et al.*, 2013). The most frequently detected cytokines are IL-6 and IL-8. IL-6 is able to increase keratinocyte proliferation (Hänel *et al.*, 2013, Juráňová *et al.*, 2017) and may also enhance the barrier function of the skin (Wang *et al.*, 2004). However, the critical pro-inflammatory chemokine IL-8 participates in the initiation phase of cutaneous inflammation but does not correlate with cytotoxicity either as an irritant or sensitizer.

Based on the literature, we prepared an *in vitro* model of RHE that mimics normal human epidermis and is useful for toxicological testing. The aim of the study was to demonstrate the safety of AgNPs on the RHE model that simulated intact (healthy) epidermis.

Correspondence address:

Mgr. Jana Franková, PhD.

Palacky University, Department of Medical Chemistry and Biochemistry  
Faculty of Medicine and Dentistry, Hněvotínská 3,  
775 15 Olomouc, Czech Republic  
TEL.: +420 585 632 314 • FAX +420 585 632 302  
E-MAIL: frankova0@seznam.cz

## Materials and methods

### Preparation and characterization of AgNPs

AgNPs were prepared by Nano Trade Company (Czech Republic). In brief, AgNO<sub>3</sub> was dissolved in distilled water and NaBH<sub>4</sub> added under constant magnetic stirring. Formation of AgNPs occurred rapidly upon addition of NaBH<sub>4</sub> (Frankova *et al.*, 2016). The AgNPs were characterized by ultraviolet-visible (UV-VIS) spectroscopy (from 200 nm to 800 nm) and transmission electron microscopy (TEM). The analysis was performed using a JEOL JEM 2011 transmission electron microscope at an accelerating voltage of 100 kV. Photographs were taken with a Morada or Keen View II digital camera and the iTEM program (SIS, Olympus). Zeta Plus analyzer (Brookhaven) was used to measure the zeta potential. The silver nanoparticles used in our study had an average size of approximately 10 nm (more than 50%).

### Preparation of RHE model

The RHE was prepared using keratinocytes isolated from tissue sections of healthy volunteers with approval from the Ethical Committee of the University Hospital Olomouc and the patients' consent. After the third passage, the 500 µL of suspension of keratinocytes was seeded on special inserts (pore size 0.4 µm and surface of the insert 1.2 cm<sup>2</sup>) and allowed to grow under differentiation conditions for 14 days (Frankart *et al.*, 2012). After 14 days the 50 µL of AgNPs were applied on the top of RHE for 24 hours at either 25 ppm, 2.5 ppm or 0.25 ppm. These concentrations were used as they had been found to be non-toxic in previous experiments (Frankova *et al.*, 2016, Galandakova *et al.*, 2016). The RHE, only with the serum free medium (without AgNPs), was used as a negative control. Following the incubation period, we studied the histological changes of RHE and production of pro-inflammatory cytokines in collected medium (store at -80 °C).

### Histology and immunofluorescent staining

Following 24 hours of exposure to AgNPs, RHE was checked for morphological changes. RHE was then cut from the insert and fixed with Baker's solution for 1 hour followed by incubation in methanol and toluene. The fixed samples were embedded in paraffin. Sections were then cut and stained in hematoxylin and eosin, or with immunofluorescent antibodies, after deparaffinization. Differentiation markers were carried out with keratin 14 (1:500, Abcam) and loricrin (1:500, Abcam). The secondary antibody used was Alexa fluor 594 and 488 IgG (1:2000, Molecular Probes). Sections were mounted, covered and visualized by microscopy.

### Detection of IL-6 and IL-8

After the treatment of RHE with three different concentrations of AgNPs for 24 h, the levels of interleukins IL-6 and IL-8 were measured in the cell supernatant (Human Quantikine ELISA Kit, R&D Systems, Bio-Techne) according to the manufacturer's instructions.

## Results

### Characterization of AgNPs

AgNPs (1 ml) were diluted in 50 ml of distilled water for UV-VIS characterization (Figure 1a). Visualization of AgNPs by TEM is on figure 1 (Figure 1b). The silver colloid was characterized by strong absorption in the visible region (called the surface plasmon resonance band) at 400 nm. The position of the maximum and width of an absorption band provide information about the form, average size, and size distribution of NPs. The mean diameter of the AgNPs was 10±5 nm (>50% of the NPs) as confirmed by TEM. The pH of the AgNPs was found to be 7.1, with a zeta potential of -22 mV.

### Histological and immunofluorescent staining

We visualized RHE morphology by hematoxylin and eosin staining and by immunofluorescent staining for the detection of keratin 14 and loricrin. No morphological changes were observed between RHE treated with AgNPs at three different concentrations (25 ppm, 2.5 ppm, 0.25 ppm) and control RHE. However for the highest concentrations, AgNPs were visible on the top of RHE (Figure 2a, b, c and d). All RHE showed characteristic epidermal stratification consisting of fully differentiated epidermis. Distributions of two markers which are important for the function of the skin as a barrier, keratin 14 for the basal layer of epidermis and loricrin for terminal differentiation were unchanged after topical application of AgNPs (Figures 2e, f, g and h).

### Production of IL-6 and IL-8

We proposed that production of IL-6 and IL-8 could be affected by exposure to AgNPs. For this reason, the production of these cytokines was evaluated after 24 h incubation of RHE with AgNPs for all concentrations tested. We detected these two frequently studied cytokines by ELISA and found the same level of cytokines in medium

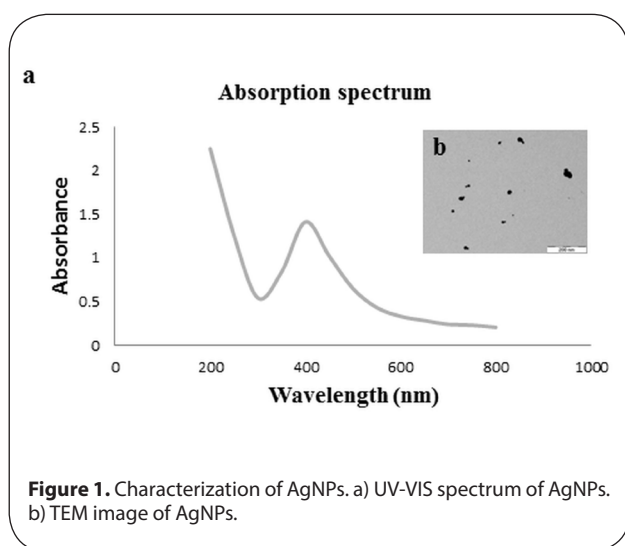
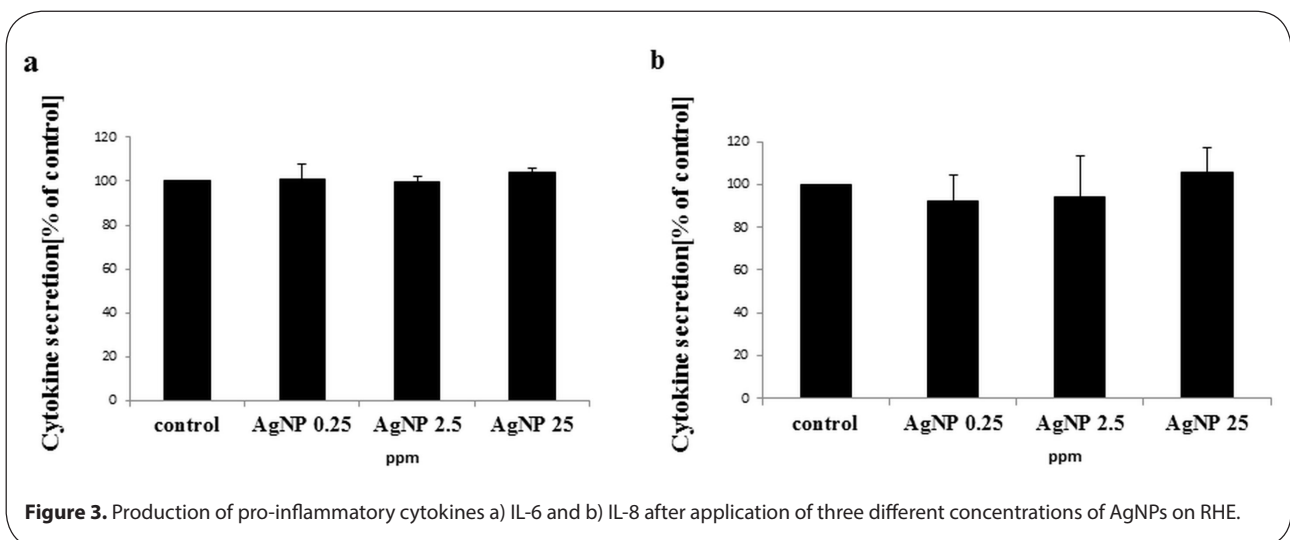
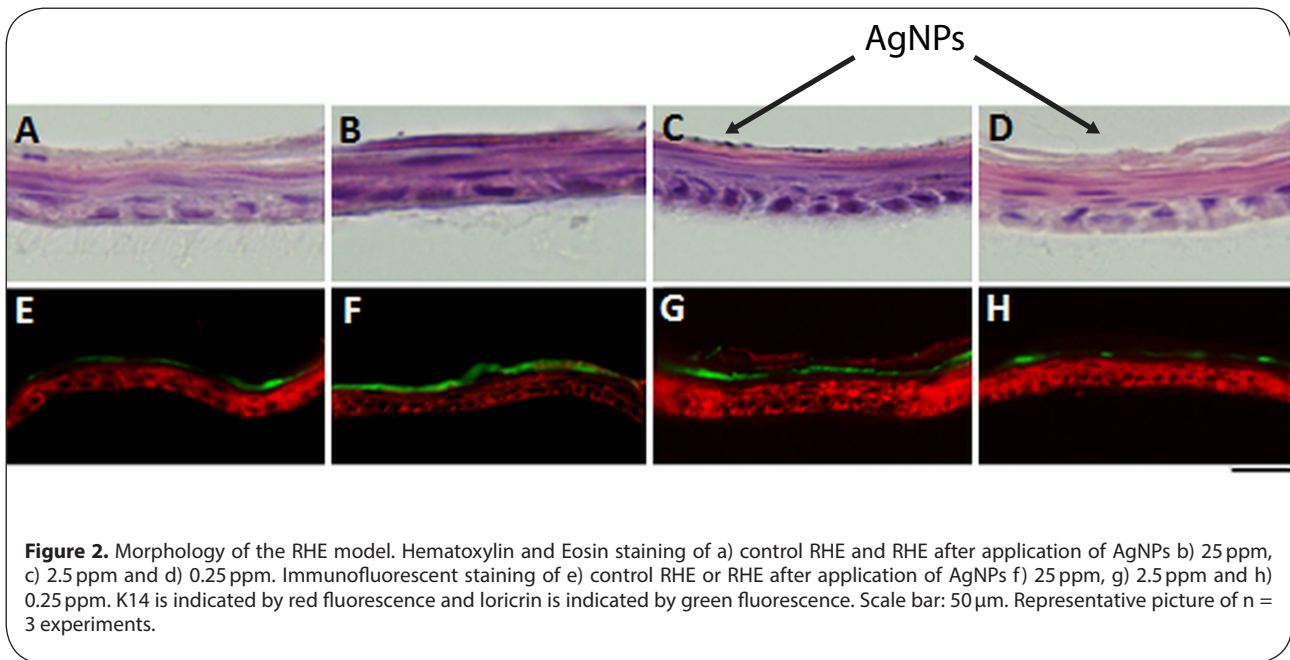


**Figure 1.** Characterization of AgNPs. a) UV-VIS spectrum of AgNPs. b) TEM image of AgNPs.



samples from treated RHE as in control RHE ( $p < 0.05$ ) (Figure 3).

## Discussion

RHE models have been validated for hazard prediction and are used for identifying irritant and cytotoxic properties of chemicals or natural substances. This highly differentiated multilayer model of human epidermis (Saito *et al.*, 2013) retains pro-inflammatory and immune regulatory functions (Mathes, 2014, Jung *et al.*, 2014).

Our RHE, derived from human skin tissue, exhibited the same cell layers as native human skin. It is divided into: stratum basale, stratum spinosum, stratum granulosum, stratum lucidum and the external layer of epidermis – stratum corneum. The basal layer is

composed of keratinocytes with highly expressed cyto-keratin 14 as a marker of dividing basal keratinocytes assisting in maintenance of the shape of keratinocytes and provides resistance to physical stress (Akhavan-Tavikoli *et al.*, 2017). The expression of cytokeratin 14 demonstrated that RHE was composed of normal skin keratinocytes. On the other hand, the expression of loricrin, a cross-linked envelope of keratinocytes (Jung *et al.*, 2014), which has a key role in keratinization of the skin (Akhavan-Tavikoli *et al.*, 2017), indicates that the stratum corneum serves as a functional physical barrier. Loricrin is initially expressed in the stratum granulosum and comprises 70% of the total protein mass of the cornified layer (Kim *et al.*, 2011).

AgNPs are incorporated into several wound dressings (e.g. Acticoat<sup>TM</sup> (Bhowmic & Koul, 2016) or PolyMem Silver<sup>®</sup>) with the size of the AgNPs released from the silver

hydrogel ranging from 2.1 nm to 15.6 nm, as determined by TEM (Boonkaew *et al.*, 2014). The results of studies characterizing which sizes of nanoparticles can penetrate the skin are far from consistent. Due to their small size, some particles could penetrate through the upper layers of the epidermis or into the deeper dermal layer and might influence the production of pro-inflammatory cytokines or affect the morphology of skin cells. Filon *et al.* (Filon *et al.*, 2015) postulated that the silver nanoparticles of 25 nm could penetrate through the intact skin, and Bianco *et al.* confirmed that smaller AgNPs (19 nm) were also able to penetrate through the skin (Bianco *et al.*, 2016). Our results, with RHE prepared from the skin tissue from three different volunteers and AgNPs with an average size of 10 nm, support the claim of Watkinson *et al.* that only nanoparticles below 1 nm are able to penetrate through intact skin (Watkinson *et al.*, 2013). Interaction between skin and nanoparticles (or certain irritants) may damage the stratum corneum and trigger the production of pro-inflammatory cytokines, which is followed by morphological changes. Our histological evaluation found that AgNPs have no negative influence on RHE and did not cause any morphological changes, but at the highest concentration AgNPs are visible at the top of the stratum corneum.

The interaction of AgNPs with skin cells is still under investigation. Following their application, AgNPs have first to penetrate the stratum corneum and reach the living cells below before a biological effect might be observed. If AgNPs could cause inflammation of the stratum corneum, release of pro-inflammatory cytokines would probably be detectable. For example kinases and cytokines, such as IL-1 $\alpha$ , IL-6, IL-8, PGE<sub>2</sub>, SKALP and HSP70, have been described to act as biomarkers of changes in metabolic activity and cytosolic leakage (Gibbs, 2009). IL-8 promotes the migration of dendritic cells and is a requirement of monocytes and neutrophils as key steps in the initiation phase of cutaneous inflammation (Coquette *et al.*, 2013) and could be linked to the product applied, either irritant or sensitizer. IL-6 is involved in the growth and differentiation of numerous cells. In addition, a deficiency in IL-6 causes a more pronounced reduction in barrier repair (Wang *et al.*, 2004). Not only does the inhibition of infiltration by inflammatory cells correspond to the reduced level of pro-inflammatory cytokines, but it is also known that various anti-inflammatory agents are effective in enhancing tissue repair and wound healing (Zhang *et al.*, 2014). We propose that if the production of pro-inflammatory cytokines is decreased (or unchanged), AgNPs should not be toxic. In our model of healthy epidermis, treated with AgNPs, we did not observe any deleterious effects on the production of pro-inflammatory cytokines IL-6 and IL-8.

In conclusion, AgNPs did not affect the production of IL-6 and IL-8, did not cause any morphological changes of RHE and may therefore be safe for further application. However for the full characterization of the mechanism of action of the AgNPs, or the metabolic pathways that are activated during their application, additional experiments are required.

## Acknowledgements

This paper was supported by grants: LF\_2017\_011, LF\_2018\_012, NPU I (LO1304), IGA 15-2776A and RVO 61989592. The authors are thankful to I. Travnickova for helping with histological analysis.

## REFERENCES

- Ambrozova N, Ulrichova J, Galandakova A. (2017). Models for the study skin wound healing. The role of Nrf2 and NF- $\kappa$ B. *Biomed Pap Med Fac Palacky Olomouc Czech Repub* **16**: 1–13.
- Akhavan-Tavakoli M, Fard M, Khanjani S, Zare S, Edalatkhah H, Mehrabani D, Zarnani AH, Shirazi H, Kazemnejad S. (2017). *In vitro* differentiation of menstrual blood stem cells into keratinocytes: A potential approach for management of wound healing. *Biologicals* **48**: 66–73.
- Bhowmic S, Koul V (2016). Assessment of PVA/silver nanocomposite hydrogel patch as antimicrobial dressing scaffold: Synthesis, characterization and biological evaluation. *Mater Sci Eng C Mater Biol Appl* **59**: 109–119.
- Bianco C, Visser MJ, Plutt OA, Svetlicic V, Pletikapic G, Jakasa I. (2016). Characterization of silver particles in stratum corneum of healthy subjects and atopic dermatitis patients dermally exposed to a silver-containing garment. *Nanotoxicology* **10**: 1480–1491.
- Boonkaew B, Kempf M, Kimble R, Supaphol L, Cuttle L. (2014). Antimicrobial efficacy of a novel silver hydrogel dressing compared to two common silver burn wound dressing: Acticoat™ and PolyMem Silver®. *Burns* **40**: 89–96.
- Coquette A, Berna N, Vandenbosch A, Rosdy M, De Wever B, Poumay Y. (2013). Analysis of interleukin-1 $\alpha$  (IL-1 $\alpha$ ) and interleukin-8 (IL-8) expression and release in *in vitro* reconstructed human epidermis for the prediction of *in vivo* skin irritation and/or sensitization. *Toxicol In Vitro* **17**: 311–321.
- Filon FL. (2015). Nanoparticles skin absorption: New aspects for a safety profile evaluation. *Regul Toxicol Pharm* **72**: 310–322.
- Frankart A, Malaise J, De Vuyst E, Minner F, de Rouvroit CL, Poumay Y. (2012). Epidermal morphogenesis during progressive *in vitro* 3D reconstruction at the air-liquid interface. *Exp Dermatol* **21**: 871–875.
- Frankova J, Pivodová J, Vágnerová H, Juráňová J, Ulrichová J. (2016). Effects of silver nanoparticles on primary cell cultures of fibroblasts and keratinocytes in a wound healing model. *J Appl Biomater Funct Mater* **14**(2): e137–e142.
- Galandáková A, Franková J, Ambrožová N, Habartová K, Pivodová V, Zálešák B, Šafářová K, Směkalová M, Ulrichová J. (2016) Effects of silver nanoparticles on human dermal fibroblasts and epidermal keratinocytes. *Hum Exp Toxicol* **35**(9): 946–957.
- Gibs S. (2009). *In vitro* Irritation Models and Immune Reactions. *Skin Pharmacol Physiol* **22**: 103–113.
- Hänel KH, Cornelissen C, Lüscher B, Baron JM. (2013). Cytokines and the skin barrier. *Int J Mol Sci* **14**(4): 6720–45.
- Jung MK, Lee SH, Jang WH, Jung HS, Heo Y, Park YH, Bae S, Lim KM, Seok SH. (2014). KeraSkin™ – VM: A novel reconstructed human epidermis model for skin irritation tests. *Toxicol In vitro* **28**: 742–750.
- Juráňová J, Franková J, Ulrichová J. (2017). The role of keratinocytes in inflammation. *J Appl Biomed* **15**: 169–179.
- Kandarova H, Hayden P, Klausner M, Kubilus J, Kearney P, Sheasgreen J. (2009). *In vitro* skin irritation testing: Improving the sensitivity of the EpiDerm skin irritation test protocol. *ATLA* **37** (6) : 671–689.
- Kim BE, Howell MD, Guttman E, Gilleaudeau PM, Cardinale IR, Boguniewicz M, Kreuger JG, Leung DYM. (2011). TNF- $\alpha$  downregulates filaggrin and loricrin through c-Jun N-terminal kinase: Role of TNF- $\alpha$  antagonists to improve skin barrier. *J Invest Dermatol* **131**: 1272–1279.
- Li N, Liu Y, Qiu J, Zhong L, Alépée N, Cotovio J, Cai Z. (2017). *In vitro* skin irritation assessment becomes a reality in China using a reconstructed human epidermis test method. *Toxicol In vitro* **41**: 159–167.
- Mathes SH. (2014). The use of skin models in drug development. *Adv Drug Deliv Rev* **69–70**: 81–102.
- Saito K, Nukada Y, Takenouchi O, Miyazawa M, Sakaguchi H, Nishiyama N. (2013). Development of a new *in vitro* skin sensitization assay (Epidermal Sensitization Assay; Epi SensA) using reconstructed human epidermis. *Toxicol In vitro* **27**: 2213–2224.

- Sondi I, Salopek-Sondi B. (2004). Silver nanoparticles as antimicrobial agent: a case study on *E. coli* as a model for Gram-negative bacteria. *J Colloid Interface Sci* **275**: 177–182.
- Turner D, Nedjai B, Hurst T, Pennington DJ. (2014). Cytokines and chemokines: At the crossroad of cell signalling and inflammatory disease. *Biochim Biophys Acta* **1843**: 2563–2582.
- Wang XP, Schunck M, Kallen KJ, Neumann C, Trautwein C, Rose – John S, Prokch S. (2004). The interleukin-6 cytokine system regulates epidermal permeability barrier homeostasis. *J Invest Dermatol* **123**: 124–131.
- Watkinson AC, Bunge AL, Hadgraft J, Lane ME. (2013). Nanoparticles do not penetrate human skin – a theoretical perspective. *Pharm Res* **30**(8): 1943–1946.
- Zhang S, Liu X, Wang H, Peng J, Wong KK. (2014). Silver nanoparticle-coated suture effectively reduces inflammation and improves mechanical strength at intestinal anastomosis in mice. *J Pediatr Surg* **49**: 606–613.

ORIGINAL ARTICLE

# Impact of quercetin on tight junctional proteins and BDNF signaling molecules in hippocampus of PCBs-exposed rats

Kandaswamy SELVAKUMAR<sup>1,2</sup>, Senthamilselvan BAVITHRA<sup>1</sup>, Gunasekaran KRISHNAMOORTHY<sup>3</sup>, Jagadeesan ARUNAKARAN<sup>1</sup>

<sup>1</sup> Department of Endocrinology, Dr. ALM Post Graduate Institute of Basic Medical Sciences, University of Madras, Chennai- 600113, India

<sup>2</sup> Department of Biochemistry, Kauvery Hospital, Luz church Road, Chennai 600004, Tamilnadu, India

<sup>3</sup> Department of Biochemistry, Rajas Dental College and Hospital, Tirunelveli-627105, Tamilnadu, India

ITX110418A07 • Received: 14 January 2018 • Accepted: 06 February 2018

## ABSTRACT

Polychlorinated biphenyls (PCBs) consist of a range of toxic substances which are directly proportional to carcinogenesis and tumor-promoting factors as well as having neurotoxic properties. Reactive oxygen species, which are produced from PCBs, alter blood–brain barrier (BBB) integrity, which is paralleled by cytoskeletal rearrangements and redistribution and disappearance of tight junction proteins (TJPs) like claudin-5 and occludin. Brain-derived neurotrophic factor (BDNF), plays an important role in the maintenance, survival of neurons and synaptic plasticity. It is predominant in the hippocampal areas vital to learning, memory and higher thinking. Quercetin, a flavonoid, had drawn attention to its neurodefensive property. The study is to assess the role of quercetin on serum PCB, estradiol and testosterone levels and mRNA expressions of estrogen receptor  $\alpha$  and  $\beta$ , TJPs and BDNF signaling molecules on the hippocampus of PCBs-exposed rats. Rats were divided into 4 groups of 6 each. Group I rats were intraperitoneally (i.p.) administered corn oil (vehicle). Group II received quercetin 50 mg/kg/bwt (gavage). Group III received PCBs (Aroclor 1254) at 2 mg/kg bwt (i.p.). Group IV received quercetin 50 mg/kg bwt (gavage) simultaneously with PCBs 2 mg/kg bwt (i.p.). The treatment was given daily for 30 days. The rats were euthanized 24 h after the experimental period. Blood was collected for quantification of serum PCBs estradiol and testosterone. The hippocampus was dissected and processed for PCR and Western blot; serum PCB was observed in PCB treated animals, simultaneously quercetin treated animals showed PCB metabolites. Serum testosterone and estradiol were decreased after PCB exposure. Quercetin supplementation brought back normal levels. mRNA expressions of estrogen  $\alpha$  and  $\beta$  were decreased in the hippocampus of PCB treated rats. TJPs and BDNF signalling molecules were decreased in hippocampus of PCB treated rats. Quercetin supplementation retrieved all the parameters. Quercetin alone treated animals showed no alteration. Thus in PCB caused neurotoxicity, quercetin protects and prevents neuronal damage in the hippocampus.

**KEY WORDS:** TJPs, BDNF, PCBs, Quercetin, GC-MS

## Introduction

Polychlorinated biphenyls (PCBs) are environmental toxicants widely used in electrical industry as coolants for transformers and capacitors (Safe, 1994). PCBs are lipophilic, resistant to biological decomposition and can accumulate in higher tropic levels through the food chain (Schneider *et al.*, 2007). Gonadal hormones exert profound influence in the brain of developing and adult vertebrates, regulating the survival of neurons, the differentiation of neurons and glial cells, plasticity and function

of synaptic contacts (McEwen *et al.*, 2001). Estradiol is a pleiotropic hormone that enhances plasticity and survival of the brain in multiple models of injury (Garcia-Segura, 2009). It acts as a neurotrophic and neuroprotective factor. Epidemiological studies have reported a positive alliance between testosterone level and cognition with relevance to the incidence of Alzheimer's disease. Testosterone is suggested to exert a protective effect on cognitive function (Muller *et al.*, 1996).

PCBs induced toxic manifestations are associated with the production of free radicals (Allen and Tresini, 2000), which can damage the cellular elements in the developing nervous system (Venkataraman *et al.*, 2007; Selvakumar *et al.*, 2012a,b,c). ROS are reported to damage almost all macromolecules of the cell including membrane polyunsaturated fatty acids, causing impairment of cellular

Correspondence address:

**Dr. Jagadeesan Arunakaran**

Department of Endocrinology

Dr. ALM. Post Graduate Institute of Basic Medical Sciences

University of Madras, Taramani, Chennai 600113, India

TEL.: +91-9444851005 • FAX: +91-8695873986

E-MAIL: j\_arunakaran@hotmail.com

functions (Shimada & Sawabe, 1983). This phenomenon is termed lipid peroxidation (LPO), which is considered an index of oxidative stress. The brain regions are highly rich in polyunsaturated fatty acids and thus highly susceptible to oxidative stress.

The blood-brain barrier (BBB) is maintained by the homeostasis of the central nervous system (CNS) micro-environment. The BBB acts as a physical and metabolic barrier because a complex tight junction system between adjacent endothelial cells restricts most paracellular movement of ions and solutes across the brain endothelium (Pardridge, 2002). TJ proteins are significant in maintaining polarity of the cell barrier and are involved in cellular signaling. Disruption of the integrity of this BBB has been associated with several central nervous system pathologies (Weiss *et al.*, 2009). TJPs form the most apical element of the junctional complex and are composed of an intricate complex of transmembrane, accessory, and cytoplasmic proteins that connect the TJPs to actin cytoskeleton and intracellular signaling systems (Abbott *et al.*, 2006). The transmembrane proteins occludin and claudin-5 form the primary seal of the TJPs, which bind to zonula occludens (ZO-1, ZO-2) the intracellular proteins that couple the TJPs to the actin cytoskeleton of endothelial cells (Abbott *et al.*, 2006). ALL-1 fusion partner at chromosome-6/ Afadin (AF6) is a multidomain actin-binding protein that serves as a scaffold protein between transmembrane proteins and the actin cytoskeleton (Boettner *et al.*, 2000). However, the mechanisms by which PCBs cause these neurotoxic effects are not fully understood. Reports suggest that age associated decreases in circulating estrogen in females may adversely affect the structural composition of tight junctions and compromise the integrity of the barrier counterparts (Bake & Sohrabji, 2004).

BDNF neurotrophin family members play a significant role in cell proliferation, differentiation, neuronal protection, and help in the regulation of synaptic function in the central nervous system (CNS) via stimulating key intracellular signaling cascades (Huang & Reichardt 2003; Numakawa *et al.* 2004). BDNF assist in maintenance, plasticity and homeostasis of the central and peripheral nervous systems (Genzer *et al.*, 2017). BDNF is known to be a strong survival-promoting factor against various insults. The molecular mechanisms of neurotrophin dependent survival when exposed to oxidative stress have been extensively studied. Furthermore, estrogens also regulate synaptic plasticity in addition to sex differentiation of the brain (Lee & Pfaff 2008; Brinton 2009; Tobet *et al.*, 2009) and were found to exert protective actions against oxidative stress (Simpkins *et al.*, 2010).

Activity-dependent changes in synaptic strength are considered mechanisms underlying learning and memory. One attractive candidate for modulating synaptic plasticity in learning and memory is BDNF (Tyler *et al.*, 2002; Yamada *et al.*, 2002), a member of the neurotrophin family, including nerve growth factor (NGF), neurotrophin-3 (NT-3), and NT-4/5. BDNF has been implicated in the modulation of synaptic function and plasticity (Schinder

& Poo 2000). There is a good correlation between BDNF mRNA expression and behavioral performance in various learning and memory tests (Tyler *et al.*, 2002; Yamada *et al.*, 2002). Thus, hippocampus-dependent learning in the Morris water maze, contextual fear, and passive avoidance tests are associated with a rapid and transient increase in BDNF mRNA expression in the hippocampus (Hall *et al.*, 2000; Tyler *et al.*, 2002; Yamada *et al.*, 2002). The role of BDNF in learning and memory has also been investigated with function-blocking anti-BDNF antibodies. Treatment with anti-BDNF antibodies causes impairment of memory in the water maze (Mu *et al.*, 1999). The tropomyosin receptor kinase (trk) trkB-CRE mutant mice show severe deficits in the stressful water maze test and partial impairment in the 8-arm maze test, but no changes in simple passive avoidance learning, suggesting a role for BDNF/TrkB receptor signaling in complex learning. The findings also imply that procedural long-term memory is relatively spared, whereas short-term plasticity within the hippocampus is impaired in trkB-CRE mutant mice. The role of BDNF and the development of synaptic architecture have thoroughly been studied (Wang *et al.*, 1995). Murray & Holmes (2011) found that BDNF activates Trk receptors which participate in the activation of many signaling cascades, including phospholipase c, phosphoinositol-3-kinase (PI3K) and Ras which are involved in neuronal survival and neurite growth. TrkB receptors use both PI3K and MAPK cascades for cell survival, while TrkA receptors depend mainly on PI3K.

Quercetin and associated flavonoids present in fruit and vegetable elicit neuroprotection in different models of oxidative death (Echeverry *et al.*, 2010). They have been reported to be strong oxygen radical scavengers and also good metal chelators. They were shown to scavenge superoxide in ischemia reperfusion injury. In addition, quercetin exerts its protective effect as chelator of divalent cations, free radical scavengers, as well as DNA damage protectors, and thus may be involved in preventing free radical-mediated cytotoxicity and lipid peroxidation (Zhang 2005). Pu *et al.* (2007) reported that quercetin increased brain GSH level, hydroxyl radical ( $\cdot\text{OH}$ ) scavenging capacity, and  $\text{Na}^+/\text{K}^+$  ATPases activity but decreased brain NOS activity and mitochondrial malondialdehyde content, which consequently reversed in the improvement of spontaneous behavior and cognitive performance and enhancement of brain inherent antioxidant capacity. Quercetin preserved the tight junctional protein integrity in endothelial and epithelial cells (Chuenkitiyanon *et al.*, 2010). Hence it is hypothesized that PCB exposure impairs BBB through TJP disruption and gonadal hormones *via* inducing ROS in rat brain. The present study was aimed at investigating the protective role of quercetin against adverse effects of PCBs on tight junctional proteins such as Oc1n, Cldn5, JAM-3, ZO-1, ZO-2, AF-6 and expression pattern of BDNF signaling molecules such as BDNF, TRKB, Ras, Raf, Mek-1, Mek-2, Erk-1, Erk-2 and CREB in the hippocampus. We analyzed serum testosterone, estradiol and also the level of PCBs. The mRNA expressions of estrogen  $\alpha$  and  $\beta$  in the hippocampus were also studied.

## Materials and methods

### Reagents

Aroclor 1254 was purchased from Chem Service, West Chester, PA, (USA). Quercetin, total RNA isolation reagent (TRI) and primers were purchased from Sigma–Aldrich Private Limited (USA). Superscript-III Reverse Transcriptase was purchased from Invitrogen, (USA) and QPCR Ready Mix was purchased from KAPA-Biosystem (USA). C18 columns (Bond Elute C18) cartridges were purchased from Agilent Technologies, Chennai. All other chemicals were purchased from Sisco Research Laboratories (SRL) Pvt. Ltd., Mumbai, India and were of analytical grade.

### Animals

Adult male albino rats of Wistar strain weighing about 180–200 g (age 90 days) were used in the present study which was approved by our ethical committee (Ref No. IAEC No 01/01/11- Experimental Set 3). Rats were maintained at room temperature (25 °C) and a normal light cycle (12 h light and 12 h dark) during the experiments. The animals were fed pellet diet (Amrut Laboratory Animal Feed, Maharashtra, India) and drinking water *ad libitum*.

### Experimental protocol

Rats were divided into 4 groups of 6 animals each and treatment was given for 30 days. Body weights of the animals were monitored throughout the experimental period. Group I received corn oil (vehicle) intraperitoneally (i.p.). Group 2 rats received quercetin (50 mg/kg bwt/day) (gavage) alone. Group 3 was subjected to i.p. treatment with PCBs (Aroclor 1254) (2 mg/kg bwt/ day). Group 4 received PCBs (2 mg/kg bw/day) (i.p.) simultaneously with quercetin (50 mg/kg bw/day) (gavage).

### Blood and tissue collection

24 hrs after the 30-day treatment, the rats were euthanized. Blood samples were collected in the vacutainer and allowed to clot and centrifuged at 5000 rpm for 20 min at 4 °C; the obtained serum was used for the analysis of testosterone, estradiol and estimation of PCB.

### Radioimmunoassay of Serum Testosterone and Estradiol

Serum testosterone was assayed using ImmuChem™ Testosterone double antibody RIA kit obtained from ICN Biomedicals, Inc, CA. The sensitivity of the testosterone was 0.4 pg/dl, the intra- and interassay coefficient of variations were 4–11% and 7.3–11%, respectively. The cross-reactivity of the testosterone antiserum with estradiol was 0.02%.

Estradiol was also assayed by solid-phase RIA kit obtained from DPC, USA. The sensitivity of the estradiol assay was 0.08 pg/dl. The intra- and interassay coefficient of variations were 4–7% and 4–8%, respectively and the cross reactivity of the estradiol antiserum with testosterone was 0.001%

### Assessment of PCBs in serum by gas chromatography and mass spectrometry (GC-MS)

GC/MS is a combination of two different analytical techniques, Gas Chromatography and Mass Spectrometry. GC/MS, with the use of internal standards, provides a multidimensional drug identification and quantitation procedure that is the leading confirmation method for forensic drug/toxicant testing (see Hajslova & Cajka, 2007).

### Sample preparation

The serum sample was collected from the control and the treated rats. The sample was diluted with dis.H<sub>2</sub>O and pretreated with water-1-propanol (85:15) and mixed and centrifuged at 10,000 rpm for 10mins. The C18 columns (Bond Elute C18) cartridges were purchased from Agilent Technologies, Chennai. The column was conditioned using 2 column volumes of methanol and 2 column volumes of water-1-propanol (85:15). Then the clear supernatant of the pretreated serum samples was aspirated through the column. After elution, the column was washed twice with 500 µl of water-1-propanol (85:15) and dried in a stream of air. The final elution was done using n-hexane four times to obtain PCB.

The GC-MS analysis was performed on a combined GC-MS instrument (ITQ 900 Model of Thermo Fisher Scientific (USA) using a HP-5 fused silica gel capillary column. The method to perform the analysis was designed for both GC and MS using the XCaliber Software provided with the machine. A 1 µl-aliquot of sample was injected into the column using a Programmed Temperature Vaporization (PTV) injector whose temperature was set at 275 °C. The GC program was initiated by a column temperature set at 60 °C for 5 min, increased to 300 °C at a rate of 8 C/min, held for 10 min. Helium was used as the carrier gas (1.5 ml/min). The mass spectrometer was operated in Electron Impact ionisation (EI) mode with mass source set at 200 °C. The chromatogram and spectrum of the peaks were visualized using Qual Browser software. The particular compounds present in the samples were identified by matching their mass spectral fragmentation patterns of the respective peaks in the chromatogram with those stored in the National Institute of Standards and Technology Mass Spectral database (NIST-MS, 1998) library.

### Total RNA isolation and RT-PCR

Total RNA was isolated from the hippocampus using TRI reagent following the method of Chomczynski & Sacchi (2006). 1 µg of total RNA was subjected to two-step RT-PCR. *First strand reaction:* Complementary DNA (cDNA) is made from mRNA template using dNTPs & reverse transcriptase (Superscript-III Reverse Transcriptase, Invitrogen, USA). The components were combined with a DNA primer in a reverse transcriptase buffer for an hour at 37 °C. *Second strand reaction:* After the reverse transcriptase reaction was complete, cDNA was generated from the original single strand mRNA, standard PCR was initiated. PCR Ready Mix DNA polymerase was

purchased from KAPA-Biosystem, (USA). PCR primers and conditions used in this study have been tabulated (see Table 1). The amplified products were separated by electrophoresis on 2% agarose gel and identified by ethidium bromide staining. Specificity was confirmed by the size of the amplified products with reference of 100 bp DNA ladder (Chromus Biotech, Chennai) and the band intensities were quantified by Quantity One Software, Bio-Rad, (USA).

**Western blotting analysis**

Tissue lysate was prepared with radio immuno precipitate assay buffer (RIPA) and protease inhibitor. Equal amounts of protein (60 µg) were electrophoresed on 10% SDS-PAGE. Following electrophoresis, separated proteins on SDS-PAGE gels were transferred on PVDF membrane (Millipore, USA). To block the nonspecific binding, the membranes were incubated with 5% skimmed milk for 2h. Membranes were probed with primary antibodies Ras and Raf, Cell signaling, (USA). Blots were incubated with horseradish peroxidase-conjugated secondary antibodies (1:10000). The bands were developed using ECL kit (Millipore, USA) in Chemi Doc image scanner from

Bio-Rad. The band intensity was quantified by Quantity One software, Bio Rad, (USA). The membranes were stripped and reprobed for β-actin (1:5000) as an internal control.

**Statistical analysis**

Data were analyzed using One-way analysis of variance (ANOVA), followed by Post Hoc test Student’s Newman-Keul’s test (SNK) with Graphpad Prism5 software. In all cases, *p*<0.05 was considered as statistically significant.

**Results**

**Effect of quercetin on serum PCBs levels in PCBs-exposed adult male rats**

The use of the ion-trap GC-MS done to estimate PCB residues in the serum samples of control, PCB treated and simultaneous PCB+quer treated rats. Ion-trap GC-MS estimation of PCB was made according to these two criteria: (i) retention time (RT) and relative absorbance (RA). Figure 1 Blank and control shows a double peak at around RT 25 and 30 min and RA at 60 and 100, respectively,

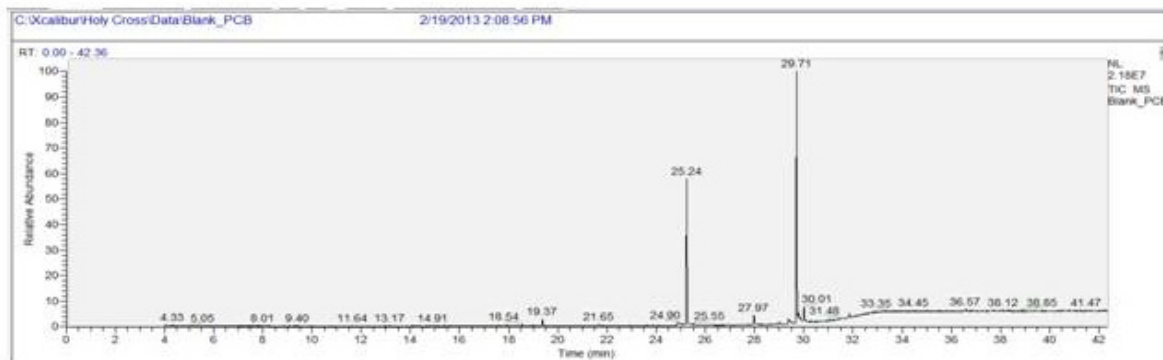
**Table 1.** Primer detail.

Target Gene	Primer Sequence (5'→3')	Amplicon size (bp)	Annealing Temp (°C)	GeneBank/ Accession Number
Ocln	Sense: TGGCGGAGAGATGCACGTTTCG Antisense: ACCGAAGCCGCTGCCGTAAG	247	55.2	NM_031329.2
Cldn5	Sense: CGTGACGGCGCAGACGACTT Antisense: TGCCTGAGCGCCGGTCAAG	194	57.8	NM_031701.2
Jam3	Sense: TCAAGGAGACTGGCCGGTTCG Antisense: GCCGAGGATAGCCCTCGCTCT	254	62.9	NM_001004269.1
ZO-1	Sense: GGCTACAGCCCAGGCGCATT Antisense: CCATGGGGCCCCCACATCAC	213	56.7	NM_001106266.1
ZO-2	Sense:TCCCGGACTACAGCCGTGG Antisense: GCCCGGACTAGACTCGGGG	208	59.1	NM_053773.1
AF-6	Sense: GCGATGGGCGAGGCTGAAACA Antisense: ATCAGGTGTCTCCGCTCCACAG	180	62.9	NM_001007754.1
β actin	Sense: TCCACCCGCGAGTACAACCTTC Antisense: GGGCCACACGACGCTCATTGTA	358	63.9	NM_031144.2
BDNF	Sense:TTGCCACAGCCCCAGGTGTGA Antisense: ACGCCTGTCACTGCGCCCTA	134	62.0	NM_012513.3
TRKB	Sense:ACTCTGCCAGCCCTCTCCACC Antisense: CGGCTTGAGCTGGCTGTTGGT	152	56.5	NM_012731.2
Ras	Sense:TGTGCTGTCTCTGACACAGGCT Antisense: TGGACTGGACTGGCTCCAGCA	118	55.7	NM_001105753.1
Raf	Sense:TGGGATTGGCTCGGGCTCCT Antisense:TGCGAAAACAGCCACCTCGT	137	55.7	NM_012639.2
Mek 1	Sense:GCTGGATGAGCAGCAGCGGA Antisense: CCACCATGCGACCCCGCAG	117	56.5	D14591.1
Mek 2	Sense:CATGGGGCTGTCTGCTGGTGG Antisense: TGGGGCTCTCCATCTGCCCC	120	56.5	D14591.1
Erk 1	Sense:ACCGGGACCTGAAGCCCTCC Antisense:GGCTCGGTACCAGCGTGTGG	146	62.9	NM_017347.2
Erk 2	Sense:CTCCTCGTCCCGATCGCCG Antisense:GGGCTCGACGCTTCGGTTA	100	58.6	NM_053842.1
CREB	Sense:TGATGCACCAGGGGTGCCAA Antisense:TGCTCCTCCCTGGGTAATGGC	142	55.7	NM_134443.1

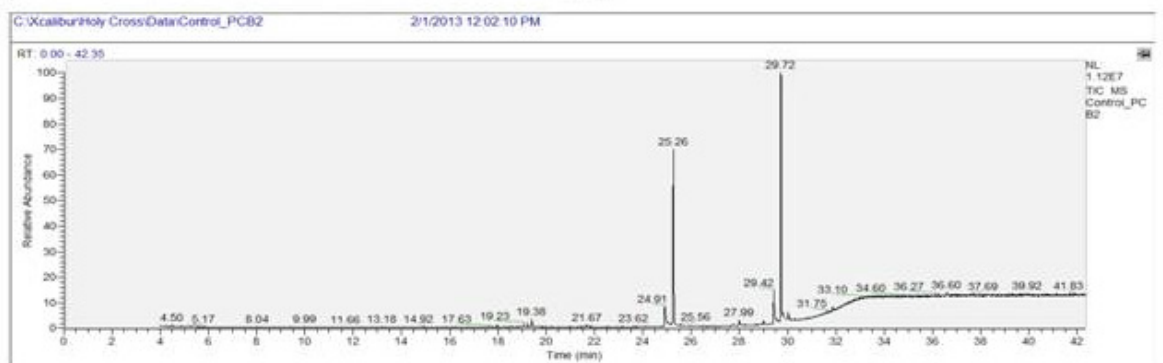
this indicates that there is no residue of PCBs in control treated rats which is similar to that blank and the peak is due to the solvent only. Figure1 PCB and PCB+quer,

shows the serum levels of PCBs in PCB treated rats, there is a peak at RT 33.6 min and with RA of 100. This may be due to the accumulation of PCB. Figure 1 d, shows the

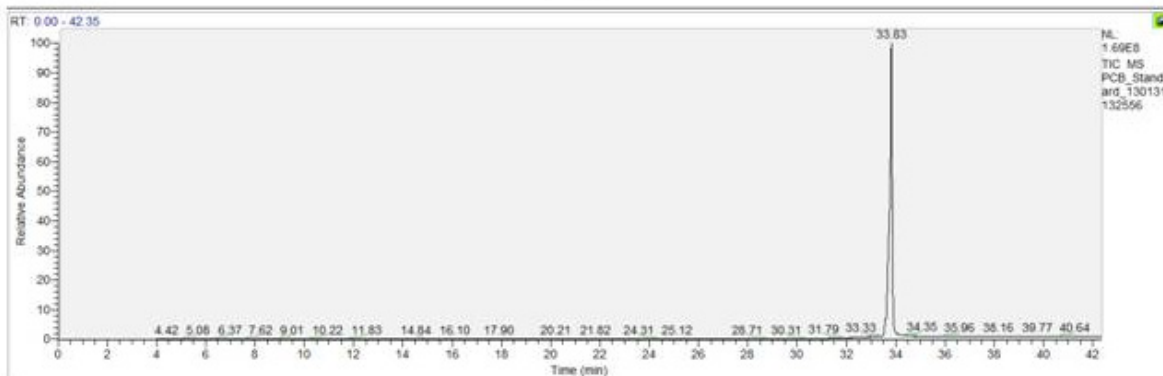
a. Blank



b. Control



c. PCB



d. PCB + Quer

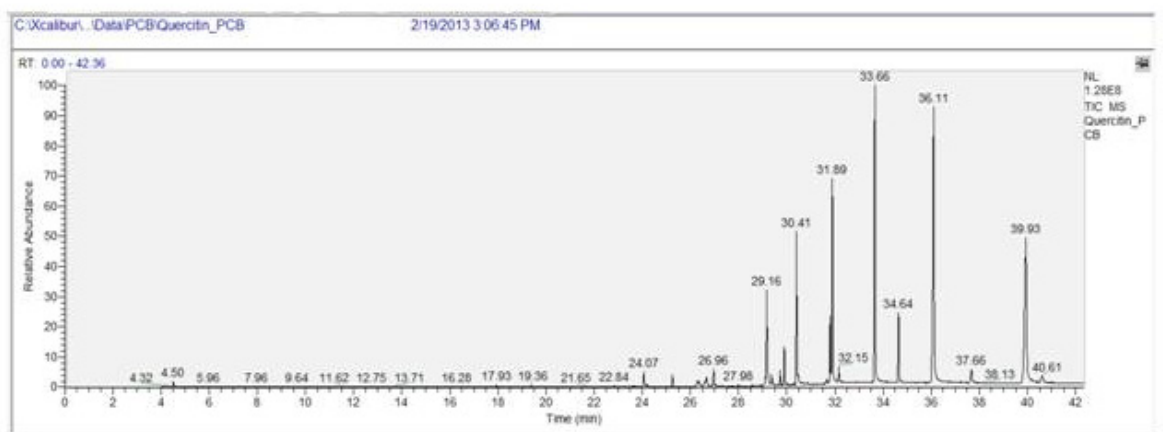


Figure 1. Effect of quercetin on serum PCBs leves in PCBs-exposed adult rats.

serum levels of PCBs in simultaneous PCB+Quer treated rat, there are lots of peak at around RT 25 to 40 min and RA from 10 to 100 this indicates that various metabolites of PCBs are present at this RT of serum of simultaneous quercetin treated rats.

#### Estimation of Serum testosterone and estradiol

Figure 2 shows serum testosterone and estradiol levels in control and PCB treated adult rats. The serum testosterone and estradiol concentrations were decreased in PCB administrated rats when compared to vehicle treated control animals. It had been retrieved in the simultaneous quercetin group as that of control. No alteration was observed in quercetin alone treated group.

#### Effect of quercetin on mRNA expression of estrogen receptor $\alpha$ and $\beta$ in hippocampus of PCBs-exposed adult male rats

The mRNA expression of ER $\alpha$  and ER $\beta$  were markedly reduced in the hippocampus of PCB treated rat while compared to control. The simultaneous supplementation of PCB+quercetin treatment retrieved the ER $\alpha$  and ER $\beta$  gene expression as that of control (Figure 3). Quercetin alone treatment shows no change.

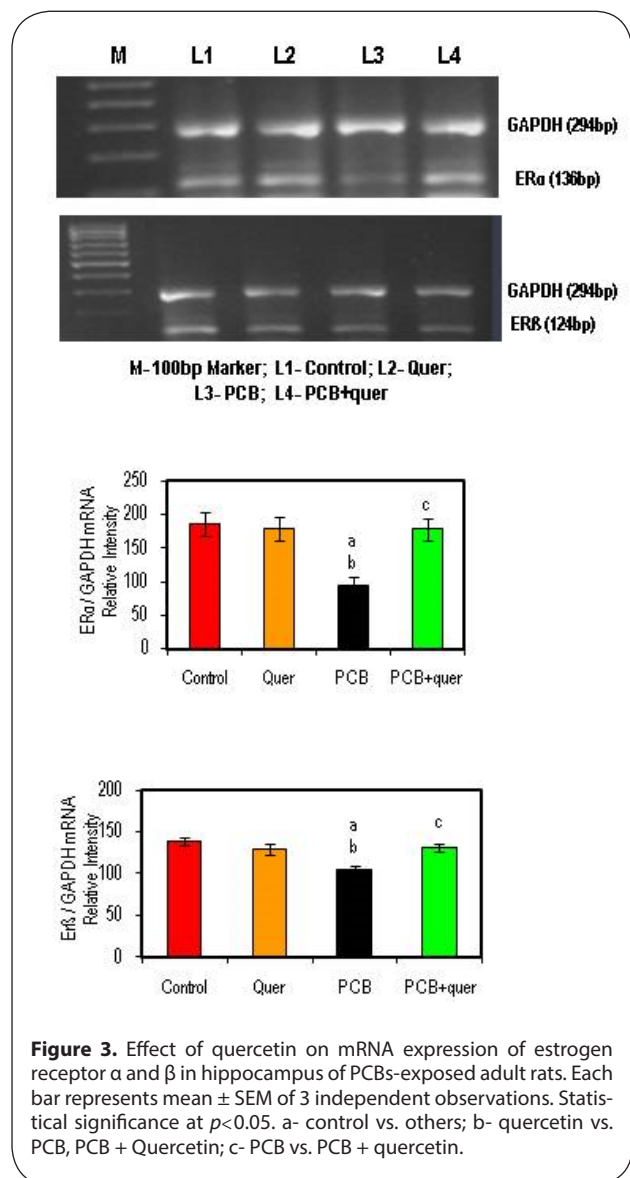
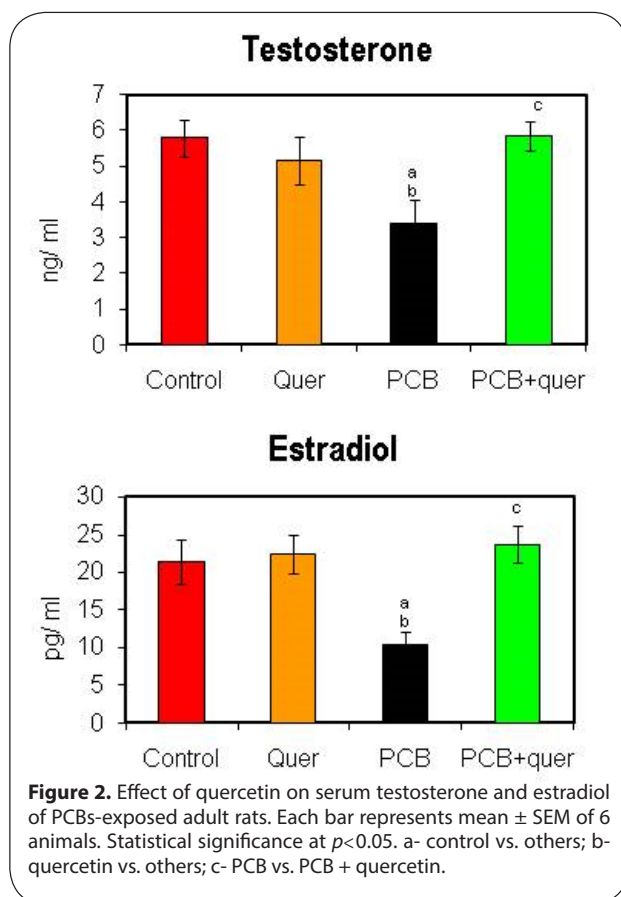
#### Effect of quercetin on mRNA expressions of (tight junctional proteins) Integral membrane and cytoplasmic accessory proteins in hippocampus of PCBs-exposed adult rats

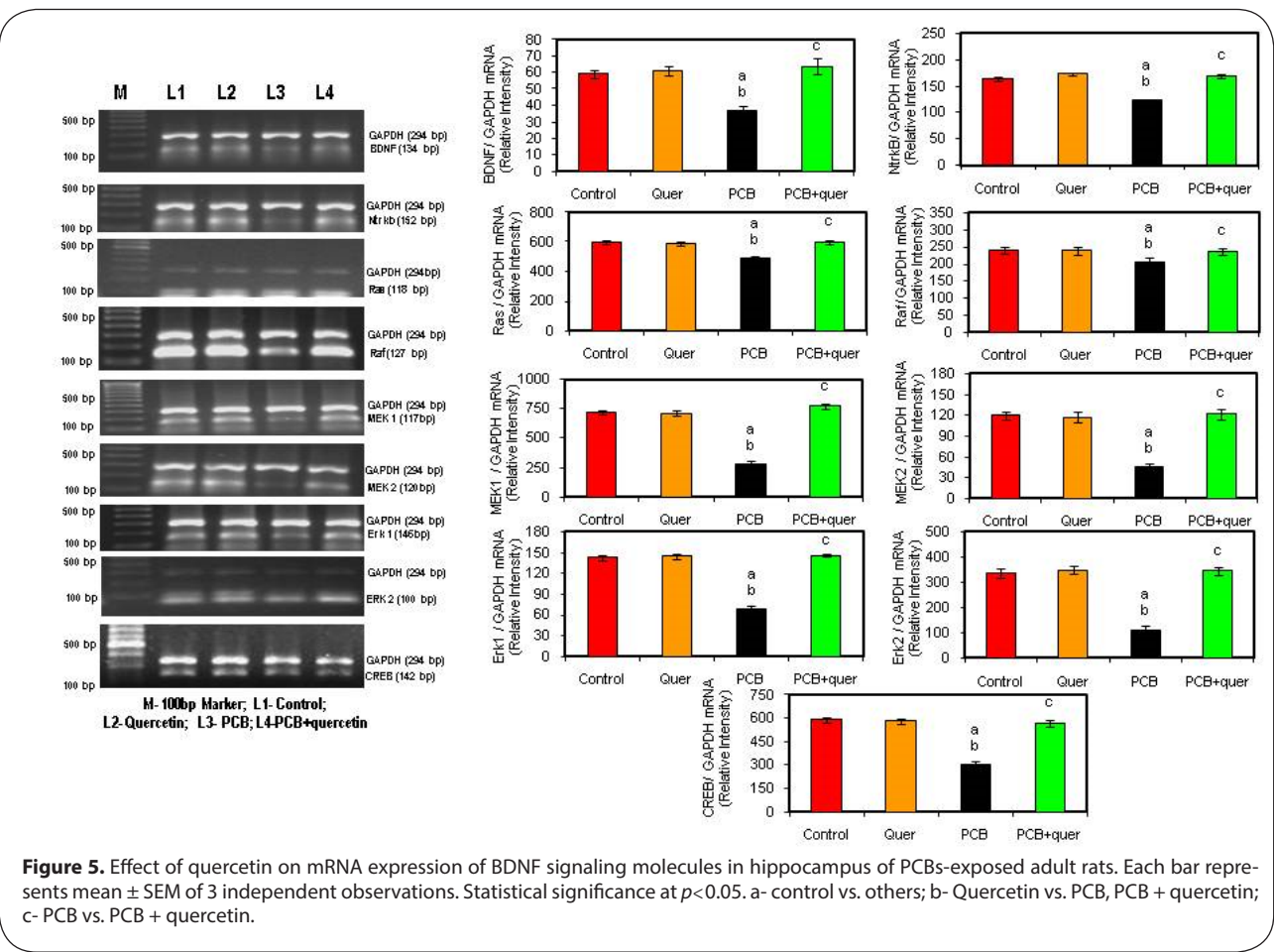
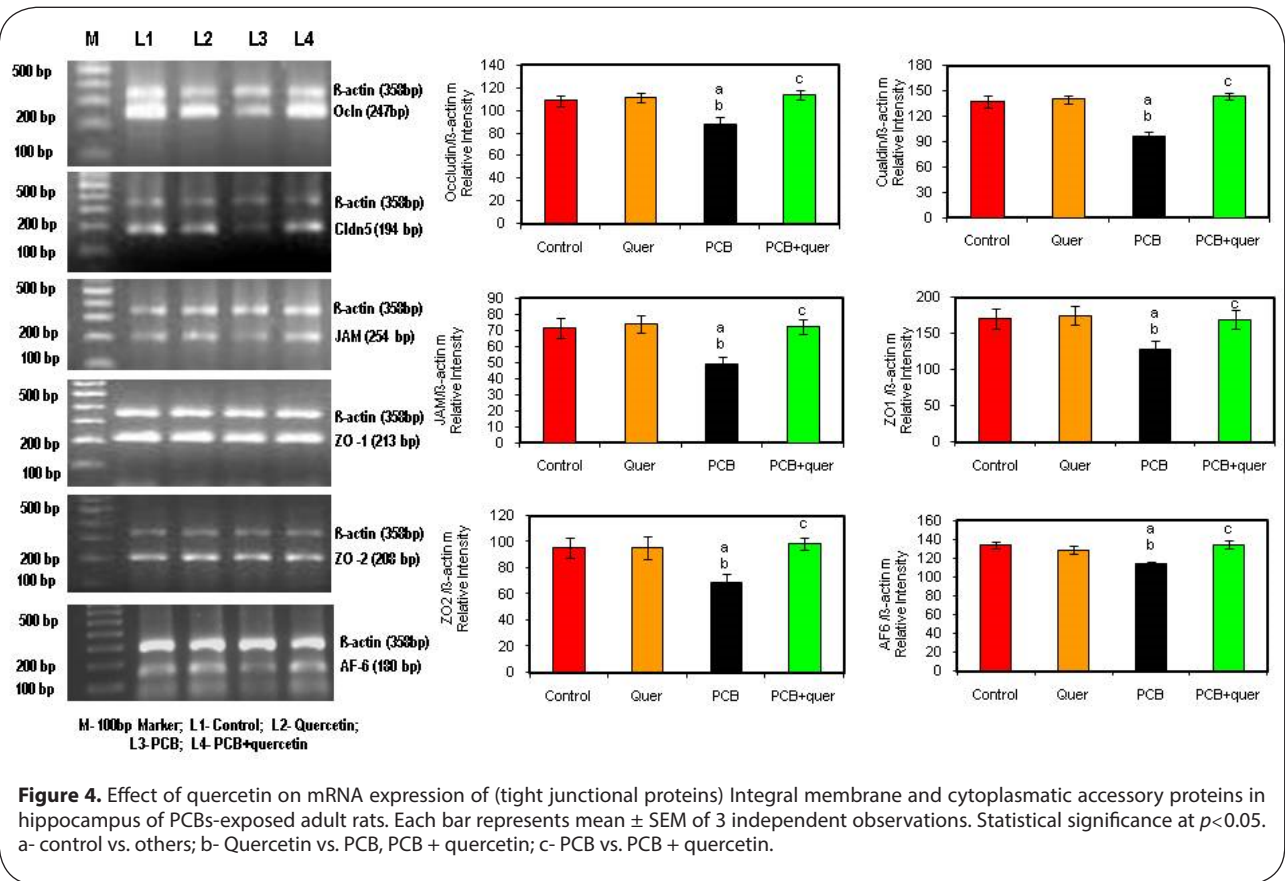
Figure 4 depicts the effect of quercetin on mRNA expression of Integral membrane protein Occludin (Ocln),

Claudin-5 (Cldn-5), cytoplasmic accessory proteins; Zona Occludens (ZO-1 and ZO-2) and AF-6 and Junction adhesion molecule (JAM-3) in hippocampus of PCBs-exposed adult male rats. Occludin, Claudin, Zona Occludens 1 and 2, AF 6 and Junction adhesion molecule mRNA expressions were decreased in PCBs-exposed rats while simultaneous supplementation of quercetin scavenges the ROS and decreases the degradation all the tight junctional proteins in hippocampus of PCBs-exposed adult male rats whereas simultaneous supplementation of quercetin brought levels back to normal. Quercetin alone didn't show any significant change.

#### Effect of quercetin on mRNA expressions of BDNF signaling molecules in hippocampus of PCBs-exposed adult rats

BDNF, a member of the nerve growth factor family, has been shown to increase synaptic strength, survival, and growth of mature neurons through activation of a transmembrane receptor (NTrkB). The ligand BDNF, gene expression is decreased in hippocampus after PCB





treatment (Figure 5). The simultaneous treatment of quercetin, a flavonoid brought back the level of BDNF expression to normal. The receptor NTrkB also get decreased in hippocampus of PCB treated rats, proclaiming the toxicity of PCB on neurotrophins and protective effect of quercetin against PCB induced toxicity.

Signal transduction cascades that underlie the actions of neurotrophic factors, including the phosphatidylinositol-3 kinase (PI3K)-Akt pathway and the Ras-mitogen-activated protein (MAPK) cascade. The MAPK cascade, which includes the extracellular signal regulated kinase (ERK), also supports cell survival and promotes synaptic plasticity by regulating several transcription factors, including the cyclic AMP response element binding protein (CREB). Figure 5 proclaims that the signaling molecules Ras, Raf, MAPK cascade were decreased during PCBs-treatment compared to control, whereas the quercetin treatment brought back the levels to normal. There is no difference in quercetin treated rats.

**Effect of quercetin on protein expression of Ras and Raf in hippocampus of PCBs-exposed adult male rats**

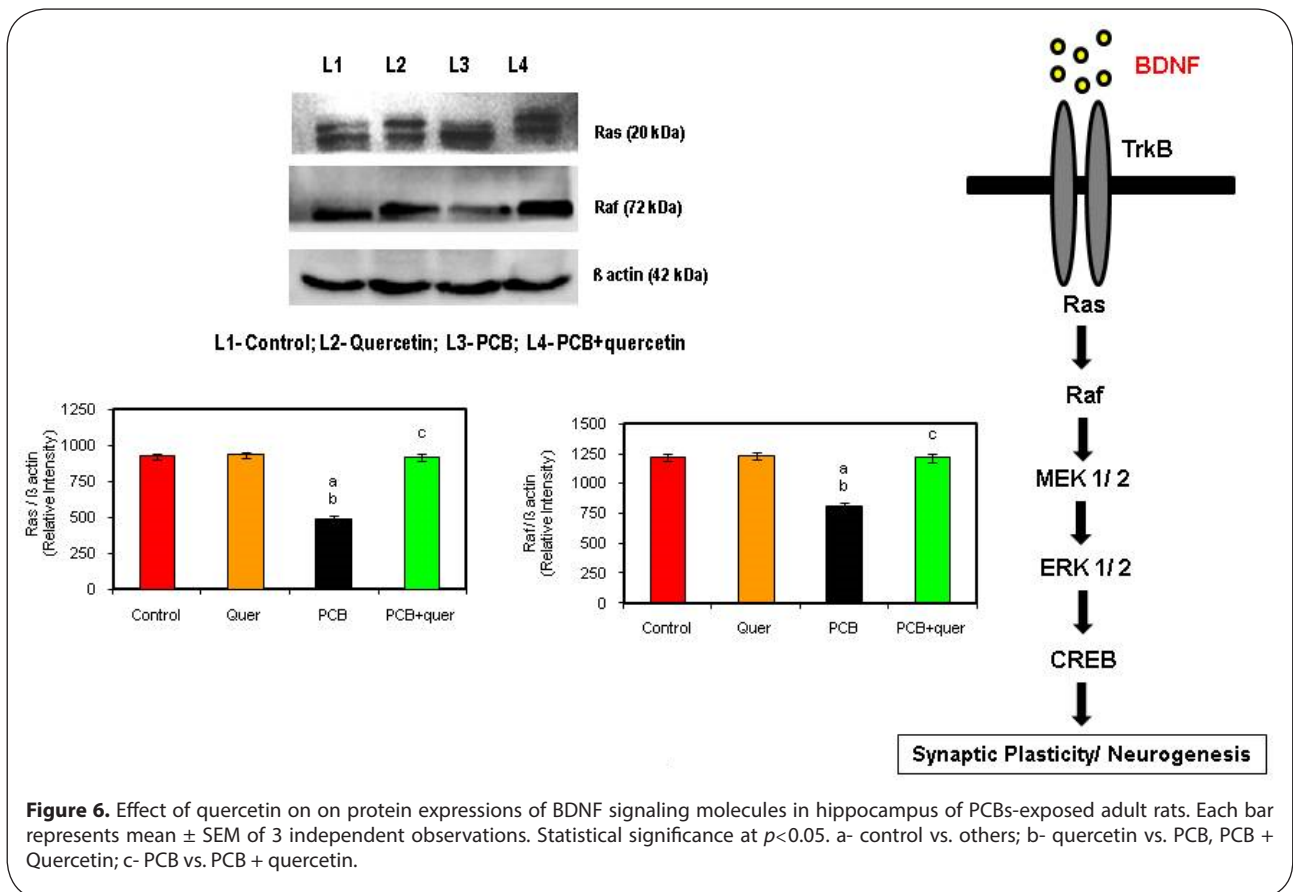
Ras and Raf proteins contribute to their aberrant regulation of growth stimulatory signaling pathways. Ras and Raf function as a relay switch that is positioned downstream of cell surface receptor tyrosine kinases and upstream of a cytoplasmic cascade of kinases that include the mitogen-activated protein kinases (MAPKs). During PCBs-treatment the Ras protein and its subsequent

downstream signaling molecule Raf also get decreased compared to control stating the inhibition of growth stimulatory signal by PCBs (Figure 6). The simultaneous quercetin treatment restored the levels and proved as a neuroprotectant.

**Discussion**

Previous studies in our laboratory also suggest that PCBs–quinones undergo redox cycling with the formation of ROS, thus becoming major source of oxidative stress in male Wistar rats. PCB-induced oxidative stress decreases the activities of antioxidant enzymes and disrupts the functional parameters in ventral prostate, testicular Leydig, Sertoli cells, and selected brain regions (Sridhar *et al.*, 2004; Murugesan *et al.*, 2005a; Venkataraman *et al.*, 2007, 2008; Bavithra *et al.*, 2012) and it can damage the cellular elements. Our recent study demonstrates that PCBs induced oxidative stress and apoptosis in the rat hippocampus (Selvakumar *et al.*, 2012a, b; 2013).

Quercetin is a strong oxygen radical scavenger and also a good metal chelator. It is believed to work *via* electron donation to directly detoxify free radicals, such as the highly toxic hydroxyl radicals. *In vitro* studies have suggested that quercetin has a potent inhibitory activity against production of nitric oxide and tumor necrosis factor in lipopolysaccharide stimulated Kupffer cells (Kawada *et al.*, 1998) Quercetin was shown to scavenge



superoxide in ischemia reperfusion injury (Huk *et al.*, 1998). The 4-oxo group and 2, 3- double bond in the c ring of quercetin is thought to play an important role in its neuroprotective effects in repeated cerebral ischemic model (Pu *et al.*, 2007). It was shown that the ROS produced by PCB had been scavenged by quercetin and protected the brain from neurodegeneration (Selvakumar *et al.*, 2012a,b).

The BBB is primarily formed by specialized brain endothelial cells (ECs), which form a tight seal due to the presence of well-developed tight junctions (TJ) that impede the entrance of circulating molecules and immune cells into the CNS (Pachter *et al.*, 2003). Loss of TJ proteins is commonly observed in neuroinflammatory and neurodegenerative disorders that are frequently associated with stroke (Brown & Davis, 2002), Alzheimer's disease (Fiala *et al.*, 2002), HIV-1 encephalitis (Persidsky *et al.*, 2006), and traumatic brain injury (Morganti-Kossmann *et al.*, 2002). The tight junctions (TJs) limit passive paracellular movement of solutes, ions, and water across the BBB. This barrier is variable and physiologically regulated, and its disruption contributes to human diseases (Powell, 1981). There is ample evidence that PCBs cause neurotoxicity in humans. The predominant mechanisms include alteration in TJ of human brain microvascular endothelial cells, intracellular signaling process and thyroid hormone metabolism (Kodavanti, 2005). PCB exposure induces TJ disruption of human brain microvascular endothelial cells, which may lead to perturbation of the BBB integrity (Eum *et al.*, 2008).

The ROS alter BBB integrity, which is paralleled by cytoskeleton rearrangements and redistribution and disappearance of TJ proteins (Schreibelt *et al.*, 2007). ROS, which are highly reactive molecules, are produced during monocyte migration and contribute to BBB injury and subsequent inflammation in the brain. In the present study, there is also decreased expression of tight junction protein in the microvascular endothelial cells in the hippocampus of PCB treated rats. Tight junctions (TJ) of the BBB are composed of an intricate combination of integral membrane proteins (Occludin Claudins and Junctional Adhesion Molecules [JAMs]) mediate cellular interaction between brain ECs and play a major role in TJ functioning and cytoplasmic accessory proteins [Zona Occludens (ZO-1, ZO-2) & AF6] provide a link between transmembrane TJ proteins and the actin cytoskeleton but also participate in intracellular signaling. This study prevails that the mRNA expression of Tight Junctional Proteins in the hippocampus significantly decreased at the PCB exposure. PCBs induced disruption of blood brain homeostasis, occurring predominantly by means of ROS induced tight junction disruption. The organization of TJ proteins occludin and ZO-1 is altered by exogenous ROS in brain ECs (Haorah *et al.*, 2007). ROS selectively activate signaling cascades involving RhoA, PI3 kinase, and protein kinase B (PKB/Akt) leading to rearrangements of the actin cytoskeleton and spatial redistribution and disappearance of occludin and claudin-5, inducing altered BBB integrity (Schreibelt *et al.*, 2007).

Previous studies in our laboratory showed neuronal damage, alteration of neuronal morphology of cerebral cortical layer, pyramidal cells of hippocampal layers and the Purkinjee cellular layer in the cerebellum after PCB exposure (Venkataraman *et al.*, 2010; Selvakumar *et al.*, 2012a). It may be due to enhanced free radical generation in PCB exposed animals. Pyknotic nuclei with predominant perineuronal spaces were observed in cortical layer due to enhanced lipid peroxidation. In the present study, down regulation of both integral membrane proteins and cytoplasmic accessory proteins mRNA expression were observed in PCBs treated group. The possible mechanism behind this is the ROS induced disruption. In the present study also disruption of hippocampal layer in CA4 was seen in PCB treated rats. Quercetin supplemented rats showed restoration of pyramidal cells. Degeneration of pyramidal cells in hippocampal layer may be due to enhanced free radical generation in PCB treated rats. Degeneration of cells was reduced in quercetin supplemented rats. Quercetin has been shown to possess genomic actions regulating the expression of several genes. Quercetin influences both antioxidant enzyme activity and cellular mRNA levels for these enzymes (Selvakumar *et al.*, 2013a).

Kevil *et al.* (2000) studied oxidative stress induced hyperpermeability and suggested it to be related to phosphorylation of occludin and ZO1 at the tyrosine residues, down regulation of occludin and activation of MAPK signaling pathways. The action of quercetin has been linked to a number of enzymes involved in proliferation and signal transduction pathways including PKC, tyrosine kinase, PI3 kinase, NF $\kappa$ B, and MPK family. Chuenkitiyanon *et al.* (2012) studied the protective effects of quercetin suggesting that it might involve altered MAPK activities, in particular the decrease in p38 MAP signaling on epithelial and endothelial barriers.

Estrogens have broad and profound effects on the structure and function of the CNS. Estradiol enhances cognition, memory and learning in the hippocampus (Yildirim *et al.* 2008). In the present study, serum testosterone and estradiol and the expression of ER $\alpha$  and ER $\beta$  were decreased after PCB exposure. The observed reduction in serum testosterone associated with decreased LH level was a result of diminished synthesis and secretion in rats subjected to PCB treatment (Murugesan *et al.* 2007). Our earlier studies also demonstrated that PCB treatment to adult male rats diminished Leydig cell LH receptor density (Murugesan *et al.* 2007). This was due to increased LPO and ROS in rats subjected to PCB. Andric *et al.* (2000) also reported that testosterone production was shown to be decreased by reduced activities of steroidogenic enzymes after PCBs exposure. The decreased serum estradiol may be due to impaired synthesis or enhanced metabolism, both of which are known to be influenced by PCB exposure. The synthesis of estradiol from testosterone depends on the activity of aromatase enzyme which was also shown to be decreased in PCB exposed male offspring (Hany *et al.* 1999). The study of aromatase enzyme is warranted. However simultaneous administration of

quercetin maintained both testosterone and estradiol to near normal levels.

PCB is a neurotoxic compound which gets metabolized into hydroxylated PCB in the biological system (Tilson and Kodavanti 1998). Hence we planned to estimate the PCB levels in the serum of PCB-exposed animals. The results suggested in the serum of simultaneous PCB+quer treated rats a peak representing phenol, which may be due to the metabolization of PCB in vivo condition itself. Hence the results obtained show metabolites of PCB. There are reports suggesting that quercetin increased the cytochrome P450 metabolizing enzymes which would have metabolized the PCB and the ROS produced during PCB metabolism is scavenged by the antioxidant property of quercetin. Compared to the PCB results with the treated ones, both contain phenols but the intensity of its presence differs. In the treated samples the phenol levels are very minute but there is a high and unique peak in PCB treated samples showing its abundant presence. Thus the present study proved that the accumulation of PCB as such found in the PCB-exposed animals was due to continuous exposure. However the PCB+quercetin treated rats showed metabolites of PCBs, pointing to the influence of cytochrome P450 enhancement by quercetin.

Protein levels of BDNF and mRNA are decreased in patients and animal models of neurodegenerative diseases (Gines *et al.* 2006). The level of TrkB receptor has also been decreased in the hippocampus after PCB treatment because PCB decreased the synaptic strength, survival and growth of hippocampal neurons. The actions of neurotrophic factors including PI3/Akt pathway and Ras – mitogen activated protein (MAPK) cascade (MEK1 and MEK2), which includes the extracellular signal regulated kinase (ERK1 and ERK2), also support cell survival and promote synaptic plasticity by regulating cyclic AMP response element binding protein (CREB) and were decreased after PCBs-exposure in the hippocampus. BDNF/TrkB signaling pathway plays a major role in memory processes. The binding of BDNF to its receptor tyrosine kinase B (TrkB) leads to dimerization and autophosphorylation of tyrosine residues in the intracellular domain of the receptor and subsequent activation of cytoplasmic signaling pathways including MAPK, PLC, PI3K (Kaplan & Miller 2000). Murray & Holmes (2011) reported that BDNF increased protein synthesis by enhancing translation initiation via multiple signaling pathways including PI3k/Akt. Ying *et al.* (2002) demonstrated that BDNF triggers long term potentiation in the hippocampus *in vivo* through MAPK.

In the present study, BDNF signaling molecules were decreased in the hippocampus of PCB exposed rats. Ras is a small GTP binding protein, which is the common upstream molecule of several signaling pathways including Raf/MEK/ERK. EGF receptor mediated Ras activation was reported in ROS induced neurodegenerative disorder. During the learning process, cyclic AMP CREB is activated in the hippocampus (Mizuno *et al.* 2002). Ras and its effectors may be appropriate targets for therapeutic intervention. Quercetin supplementation inhibited the

cell damage and prevented memory impairment and neuronal death. In addition to neurotrophic effects, regulation of synaptic plasticity is the primary function of BDNF. It induces several forms of synaptic plasticity in various brain areas including the hippocampus. Thus, BDNF is an attractive candidate molecule mediating learning and memory. Learning and memory behavior, anxiety and stress behavior evidence supports (Selvakumar *et al.*, 2013) that BDNF is essential for at least certain forms of learning and memory.

PCBs-induced free radicals altered calcium channel expressions in the hippocampus. Quercetin is a potent free radical scavenger. The 4-oxo group and 2,3, double bond in the C ring of quercetin is thought to play an important role in the neuroprotective effect in repeated cerebral ischemic model (Pu *et al.* 2007). The alterations of excitatory and inhibitory dopamine receptors are seen in PCBs treated rats, whereas quercetin treated rats show the normal conditions. Several drug candidates, which were found to attenuate deleterious symptoms in various models of neurodegenerative diseases, are reported to upregulate the expression of neurotrophic factors including BDNF (Kaplan & Miller 2000). Considering this, it seems significant to further investigate the probable mechanisms behind such neurotrophic factor upregulation. On the other hand, estrogenic survival promotion has also been well studied. Further investigation addressing how each ER contributes to neuronal protection against oxidative toxicity is required.

## Conclusion

To conclude, PCBs disrupt the gene expression of transmembrane tight junctional proteins (Occludin, Claudin-5 and JAM), cytoplasmic accessory tight junctional proteins (ZO-1, ZO-2 & AF-6), BDNF signaling molecules in the hippocampus and reduce the circulating gonadal hormone levels. Quercetin scavenges the PCBs induced ROS, thereby preventing transmembrane tight junctional proteins, cytoplasmic accessory tight junctional proteins in the hippocampus and maintaining the level of estradiol. thus protecting the BDNF signaling molecules in homeostasis. Thus quercetin might be clinically beneficial in reducing the potential threat to the brain system, particularly in the hippocampus.

## Acknowledgement

The financial assistance to Mr. K. Selvakumar, Senior Research Fellow, Department of Endocrinology from University Grants Commission- Research Fellowship in Science for Meritorious Students (UGC- RFSMS-SRF) programme is gratefully acknowledged.

## REFERENCES

- Anbalagan J, Kanagaraj P, Srinivasan N, Aruldas MM, Arunakaran J. (2003). Effect of polychlorinated biphenyl, Aroclor 1254 on rat epididymis. *Indian J Med Res* 118: 236–42.

- Andersen JK. (2004). Oxidative stress in neurodegeneration: cause or consequence? *Nat Med* **10** Suppl: S18–25
- Andric SA, Kostic TS, Stojilkovic SS, Kovacevic RZ. (2000). Inhibition of rat testicular androgenesis by a polychlorinated biphenyl mixture aroclor 1248. *Biol Reprod* **62**(6): 1882–8.
- Awad HM, Boersma MG, Vervoort J, Rietjens IM. (2000). Peroxidase-catalyzed formation of quercetin quinone methide-glutathione adducts. *Arch Biochem Biophys* **378**(2): 224–33.
- Bancroft LW, Peterson JJ, Kransdorf MJ, Nomikos GC, Murphey MD. (2002). Soft tissue tumors of the lower extremities. *Radiol Clin North Am* **40**(5): 991–1011.
- Bavithra S, Selvakumar K, Pratheepa Kumari R, Krishnamoorthy G, Venkataraman P, Arunakaran J. (2012). Polychlorinated biphenyl (PCBs)-induced oxidative stress plays a critical role on cerebellar dopaminergic receptor expression: ameliorative role of quercetin. *Neurotox Res* **21**(2): 149–59.
- Benjamins JA, Iwata R, Hazlett J. (1978). Kinetics of entry of proteins into the myelin membrane. *J Neurochem* **31**(4): 1077–85.
- Bishop NA, Lu T, Yankner BA. (2010). Neural mechanisms of ageing and cognitive decline. *Nature* **464**(7288): 529–35.
- Bossy-Wetzel E, Schwarzenbacher R, Lipton SA. (2004). Molecular pathways to neurodegeneration. *Nat Med* **10** Suppl: S2–9.
- Brinton RD. (2001). Cellular and molecular mechanisms of estrogen regulation of memory function and neuroprotection against Alzheimer's disease: recent insights and remaining challenges. *Learn Mem* **8**(3): 121–33.
- Brinton RD. (2009). Estrogen-induced plasticity from cells to circuits: predictions for cognitive function. *Trends Pharmacol Sci* **30**(4): 212–22.
- Brouwer A, Ahlborg UG, van Leeuwen FX, Feeley MM. (1998). Report of the WHO working group on the assessment of health risks for human infants from exposure to PCDDs, PCDFs and PCBs. *Chemosphere* **37**(9–12): 1627–43.
- Butterfield DA, Reed T, Newman SF, Sultana R. (2007). Roles of amyloid beta-peptide-associated oxidative stress and brain protein modifications in the pathogenesis of Alzheimer's disease and mild cognitive impairment. *Free Radic Biol Med* **43**(5): 658–77.
- Chomczynski P, Sacchi N. (2006). The single-step method of RNA isolation by acid guanidinium thiocyanate-phenol-chloroform extraction: twenty-something years on. *Nat Prot* **1**(2): 581–5.
- Chuenkitiyanon S, Pengsuparp T, Jianmongkol S. (2010). Protective effect of quercetin on hydrogen peroxide-induced tight junction disruption. *Int J Toxicol* **29**(4): 418–24.
- Devasagayam TP, Tarachand U. (1987). Decreased lipid peroxidation in the rat kidney during gestation. *Biochem Biophys Res Commun* **145**(1): 134–8.
- Egan MF, Weinberger DR, Lu B. (2003). Schizophrenia, III: brain-derived neurotrophic factor and genetic risk. *Am J Psychiatry* **160**(7): 1242.
- Faroon O, Jones D, de Rosa C. (2000). Effects of polychlorinated biphenyls on the nervous system. *Toxicol Ind Health* **16**(7–8): 305–33.
- Genzer Y, Chapnik N, Froy O. (2017). Effect of brain-derived neurotrophic factor (BDNF) on hepatocyte metabolism. *Int J Biochem Cell Biol*. **88**: 69–74.
- Gines S, Bosch M, Marco S, Gavalda N, Diaz-Hernandez M, Lucas JJ, Canals JM, Alberch J. (2006). Reduced expression of the TrkB receptor in Huntington's disease mouse models and in human brain. *Eur J Neurosci* **23**(3): 649–58.
- Gutteridge JM, Quinlan GJ. (1983). Malondialdehyde formation from lipid peroxides in the thiobarbituric acid test: the role of lipid radicals, iron salts, and metal chelators. *J Appl Biochem* **5**(4–5): 293–9.
- Habig WH, Pabst MJ, Fleischner G, Gatmaitan Z, Arias IM, Jakoby WB. (1974). The identity of glutathione S-transferase B with ligandin, a major binding protein of liver. *Proc Natl Acad Sci U S A* **71**(10): 3879–82.
- Hall J, Thomas KL, Everitt BJ. (2000). Rapid and selective induction of BDNF expression in the hippocampus during contextual learning. *Nature neuroscience* **3**(6): 533–5.
- Hansen LG. (1998). Stepping backward to improve assessment of PCB congener toxicities. *Environ Health Perspect* **106** Suppl 1: 171–89.
- Hany J, Lilienthal H, Sarasin A, Roth-Härer A, Fastabend A, Dunemann L, Lichtensteiger W, Winneke G. (1999). Developmental exposure of rats to a reconstituted PCB mixture or aroclor 1254: effects on organ weights, aromatase activity, sex hormone levels, and sweet preference behavior. *Toxicol Appl Pharmacol* **158**(3): 231–43.
- Harman D. (2006). Free radical theory of aging: an update: increasing the functional life span. *Ann NY Acad Sci* **1067**: 10–21.
- Heo HJ, Lee CY. (2004). Protective effects of quercetin and vitamin C against oxidative stress-induced neurodegeneration. *J Agric Food Chem* **52**(25): 7514–7.
- Huang EJ, Reichardt LF. (2003). Trk receptors: roles in neuronal signal transduction. *Annu Rev Biochem* **72**: 609–42.
- Kaplan DR, Miller FD. (2000). Neurotrophin signal transduction in the nervous system. *Curr Opin Neurobiol* **10**(3): 381–91.
- Krishnamoorthy G, Venkataraman P, Arunkumar A, Vignesh RC, Aruldas MM, Arunakaran J. (2007). Ameliorative effect of vitamins (alpha-tocopherol and ascorbic acid) on PCB (Aroclor 1254) induced oxidative stress in rat epididymal sperm. *Reprod Toxicol* **23**(2): 239–45.
- Kuiper GG, Enmark E, Pelto-Huikko M, Nilsson S, Gustafsson JA. (1996). Cloning of a novel receptor expressed in rat prostate and ovary. *Proc Natl Acad Sci U S A* **93**(12): 5925–30.
- Kurata K, Takebayashi M, Morinobu S, Yamawaki S. (2004). beta-estradiol, dehydroepiandrosterone, and dehydroepiandrosterone sulfate protect against N-methyl-D-aspartate-induced neurotoxicity in rat hippocampal neurons by different mechanisms. *J Pharmacol Exp Ther* **311**(1): 237–45.
- Lee AW, Pfaff DW. (2008). Hormone effects on specific and global brain functions. *J Physiol Sci* **58**(4): 213–20.
- Liu S, Mauvais-Jarvis F. (2010). Minireview: Estrogenic protection of beta-cell failure in metabolic diseases. *Endocrinology* **151**(3): 859–64.
- Mariussen E, Mørch Andersen J, Fønnum F. (1999). The effect of polychlorinated biphenyls on the uptake of dopamine and other neurotransmitters into rat brain synaptic vesicles. *Toxicol Appl Pharmacol* **161**(3): 274–82.
- Marklund S, Marklund G. (1974). Involvement of the superoxide anion radical in the autoxidation of pyrogallol and a convenient assay for superoxide dismutase. *Eur J Biochem* **47**(3): 469–74.
- Mizuno M, Yamada K, Maekawa N, Saito K, Seishima M, Nabeshima T. (2002). CREB phosphorylation as a molecular marker of memory processing in the hippocampus for spatial learning. *Behavioral brain research* **133**(2): 135–41.
- Mu JS, Li WP, Yao ZB, Zhou XF. (1999). Deprivation of endogenous brain-derived neurotrophic factor results in impairment of spatial learning and memory in adult rats. *Brain Res* **835**(2): 259–65.
- Murray PS, Holmes PV. (2011). An overview of brain-derived neurotrophic factor and implications for excitotoxic vulnerability in the hippocampus. *Int J Pept*. **2011**: 654085.
- Murugesan P, Kanagaraj P, Yuvaraj S, Balasubramanian K, Aruldas MM, Arunakaran J. (2005a). The inhibitory effects of polychlorinated biphenyl Aroclor 1254 on Leydig cell LH receptors, steroidogenic enzymes and antioxidant enzymes in adult rats. *Reprod Toxicol* **20**(1): 117–26.
- Murugesan P, Muthusamy T, Balasubramanian K, Arunakaran J. (2007). Effects of vitamins C and E on steroidogenic enzymes mRNA expression in polychlorinated biphenyl (Aroclor 1254) exposed adult rat Leydig cells. *Toxicology* **232**(3): 170–82.
- Murugesan P, Senthilkumar J, Balasubramanian K, Aruldas MM, Arunakaran J. (2005b). Impact of polychlorinated biphenyl Aroclor 1254 on testicular antioxidant system in adult rats. *Hum Exp Toxicol* **24**(2): 61–6
- Naidu PS, Kulkarni SK. (2004). Quercetin, a bioflavonoid, reverses haloperidol-induced catalepsy. *Methods Find Exp Clin Pharmacol*. **26**(5): 323–6.
- Numakawa T, Yagasaki Y, Ishimoto T, Okada T, Suzuki T, Iwata N, Ozaki N, Taguchi T, Tatsumi M, Kamijima K, Straub RE, Weinberger DR, Kunugi H, Hashimoto R. (2004). Evidence of novel neuronal functions of dysbindin, a susceptibility gene for schizophrenia. *Hum Mol Genet* **13**(21): 2699–708.
- Olton DS. (1979). Mazes, maps, and memory. *Am Psychol* **34**(7): 583–96
- Pick E, Keisari Y. (1980). A simple colorimetric method for the measurement of hydrogen peroxide produced by cells in culture. *J Immunol Methods* **38**(1–2): 161–70.
- Pratheepa Kumari R, Selvakumar K, Bavithra S, Zumaana R, Krishnamoorthy G, Arunakaran J. (2011). Role of quercetin on PCBs (Aroclor-1254) induced impairment of dopaminergic receptor mRNA expression in cerebral cortex of adult male rats. *Neurochem Res* **36**(8): 1344–52.
- Pu F, Mishima K, Irie K, Motohashi K, Tanaka Y, Orito K, Egawa T, Kitamura Y, Egashira N, Iwasaki K, Fujiwara M. (2007). Neuroprotective effects of quercetin and rutin on spatial memory impairment in an 8-arm radial maze task and neuronal death induced by repeated cerebral ischemia in rats. *J Pharmacol Sci* **104**(4): 329–34.
- Puntarulo S, Cederbaum AI. (1988). Increased microsomal interaction with iron and oxygen radical generation after chronic acetone treatment. *Biochim Biophys Acta* **964**(1): 46–52.

- Roegge CS, Seo BW, Crofton KM, Schantz SL. (2000). Gestational-lactational exposure to Aroclor 1254 impairs radial-arm maze performance in male rats. *Toxicol Sci* **57**(1): 121–30.
- Rotruck JT, Pope AL, Ganther HE, Swanson AB, Hafeman DG, Hoekstra WG. (1973). Selenium: biochemical role as a component of glutathione peroxidase. *Science* **179**(4073): 588–90.
- Schantz SL, Moshtaghian J, Ness DK. (1995). Spatial learning deficits in adult rats exposed to ortho-substituted PCB congeners during gestation and lactation. *Fundam Appl Toxicol* **26**(1): 117–26.
- Schinder AF, Poo M. (2000). The neurotrophin hypothesis for synaptic plasticity. *Trends Neurosci* **23**(12): 639–45.
- Selvakumar K, Bavithra S, Krishnamoorthy G, Venkataraman P, Arunakaran J. (2012a). Polychlorinated biphenyls-induced oxidative stress on rat hippocampus: a neuroprotective role of quercetin. *The Scientific World Journal* **2012**: 980314.
- Selvakumar K, Bavithra S, Suganthi M, Benson CS, Elumalai P, Arunkumar R, Krishnamoorthy G, Venkataraman P, Arunakaran J. (2012b). Protective role of quercetin on PCBs-induced oxidative stress and apoptosis in hippocampus of adult rats. *Neurochem Res* **37**(4): 708–21.
- Simpkins JW, Dykens JA. (2008). Mitochondrial mechanisms of estrogen neuroprotection. *Brain Res Rev* **57**(2): 421–30.
- Simpkins JW, Yi KD, Yang SH, Dykens JA. (2010). Mitochondrial mechanisms of estrogen neuroprotection. *Biochim Biophys Acta* **1800**(10): 1113–20.
- Sinha AK. (1972). Colorimetric assay of catalase. *Anal Biochem* **47**(2): 389–94.
- Staal GE, Visser J, Veeger C. (1969). Purification and properties of glutathione reductase of human erythrocytes. *Biochim Biophys Acta* **185**(1): 39–48.
- Tobet S, Knoll JG, Hartshorn C, Aurand E, Stratton M, Kumar P, Searcy B, McClellan K. (2009). Brain sex differences and hormone influences: a moving experience? *J Neuroendocrinol* **21**(4): 387–92.
- Tyler WJ, Alonso M, Bramham CR, Pozzo-Miller LD. (2002). From acquisition to consolidation: on the role of brain-derived neurotrophic factor signaling in hippocampal-dependent learning. *Learn Mem* **9**(5): 224–37.
- Venkataraman P, Krishnamoorthy G, Vengatesh G, Srinivasan N, Aruldas MM, Arunakaran J. (2008). Protective role of melatonin on PCB (Aroclor 1,254) induced oxidative stress and changes in acetylcholine esterase and membrane bound ATPases in cerebellum, cerebral cortex and hippocampus of adult rat brain. *Int J Dev Neurosci* **26**(6): 585–91.
- Venkataraman P, Muthuvel R, Krishnamoorthy G, Arunkumar A, Sridhar M, Srinivasan N, Balasubramanian K, Aruldas MM, Arunakaran J. (2007). PCB (Aroclor 1254) enhances oxidative damage in rat brain regions: protective role of ascorbic acid. *Neurotoxicology* **28**(3): 490–8.
- Venkataraman P, Sridhar M, Dhanammal S, Vijayababu MR, Arunkumar A, Srinivasan N, Arunakaran J. (2004). Effects of vitamin supplementation on PCB (Aroclor 1254)-induced changes in ventral prostatic androgen and estrogen receptors. *Endocr Res* **30**(3): 469–80.
- Vyas A, Mitra R, Shankaranarayana Rao BS, Chattarji S. (2002). Chronic stress induces contrasting patterns of dendritic remodeling in hippocampal and amygdaloid neurons. *J Neurosci* **22**(15): 6810–8.
- Wang T, Xie K, Lu B. (1995). Neurotrophins promote maturation of developing neuromuscular synapses. *J Neurosci* **15**(7 Pt 1): 4796–805.
- Williams CL, Barnett AM, Meck WH. (1990). Organizational effects of early gonadal secretions on sexual differentiation in spatial memory. *Behav Neurosci* **104**(1): 84–97.
- Yamada MK, Nakanishi K, Ohba S, Nakamura T, Ikegaya Y, Nishiyama N, Matsuki N. (2002). Brain-derived neurotrophic factor promotes the maturation of GABAergic mechanisms in cultured hippocampal neurons. *J Neurosci* **22**(17): 7580–5.
- Yildirim M, Janssen WG, Tabori NE, Adams MM, Yuen GS, Akama KT, McEwen BS, Milner TA, Morrison JH. (2008). Estrogen and aging affect synaptic distribution of phosphorylated LIM kinase (pLIMK) in CA1 region of female rat hippocampus. *Neuroscience* **152**(2): 360–70.
- Ying SW, Futter M, Rosenblum K, Webber MJ, Hunt SP, Bliss TV, Bramham CR. (2002). Brain-derived neurotrophic factor induces long-term potentiation in intact adult hippocampus: requirement for ERK activation coupled to CREB and upregulation of Arc synthesis. *J Neurosci* **22**(5): 1532–40.
- Zhao C, Dahlman-Wright K, Gustafsson JA. (2010). Estrogen signaling via estrogen receptor {beta}. *J Biol Chem* **285**(51): 39575–9.
- Zhu YS, Yen PM, Chin WW, Pfaff DW. (1996). Estrogen and thyroid hormone interaction on regulation of gene expression. *Proc Natl Acad Sci U S A* **93**(22): 12587–92.

ORIGINAL ARTICLE

# Mitochondrial respiratory chain inhibition and Na<sup>+</sup>K<sup>+</sup>ATPase dysfunction are determinant factors modulating the toxicity of nickel in the brain of indian catfish *Clarias batrachus* L.

Arpan Kumar MAITI<sup>1</sup>, Nimai Chandra SAHA<sup>2</sup>, Goutam PAUL<sup>3</sup>, Kishore DHARA<sup>4</sup>

<sup>1</sup> Department of Biological Sciences, School of Basic and Applied Sciences, Dayananda Sagar University, Shavige Malleshwara Hills, Kumaraswamy Layout, Bangalore, India

<sup>2</sup> Additional Director of Public Instruction, Govt. of West Bengal, Education Directorate, Bikash Bhavan, Salt Lake, Kolkata, India

<sup>3</sup> Environmental Physiology Laboratory, Department of Physiology, University of Kalyani, West Bengal, India

<sup>4</sup> Deputy Director of Fisheries, Gour Banga Zone, Govt. of West Bengal, Meen Bhavan, Mangal Bari, Malda, India

ITX110218A08 • Received: 16 June 2017 • Accepted: 17 March 2018

## ABSTRACT

Nickel is a potential neurotoxic pollutant inflicting damage in living organisms, including fish, mainly through oxidative stress. Previous studies have demonstrated the impact of nickel toxicity on mitochondrial function, but there remain lacunae on the damage inflicted at mitochondrial respiratory level. Deficient mitochondrial function usually affects the activities of important adenosinetriphosphatases responsible for the maintenance of normal neuronal function, namely Na<sup>+</sup>K<sup>+</sup>ATPase, as explored in our study. Previous reports demonstrated the dysfunction of this enzyme upon nickel exposure but the contributing factors for the inhibition of this enzyme remained unexplored. The main purpose of this study was to elucidate the impact of nickel neurotoxicity on mitochondrial respiratory complexes and Na<sup>+</sup>K<sup>+</sup>ATPase in the piscine brain and to determine the contributing factors that had an impact on the same. Adult *Clarias batrachus* were exposed to nickel treated water at 10% and 20% of the 96 h LC50 value (41 mg.l<sup>-1</sup>) respectively and sampled on 20, 40 and 60 days. Exposure of fish brain to nickel led to partial inhibition of complex IV of mitochondrial respiratory chain, however, the activities of complex I, II and III remained unaltered. This partial inhibition of mitochondrial respiratory chain might have been sufficient to lower mitochondrial energy production in mitochondria that contributed to the partial dysfunction of Na<sup>+</sup>K<sup>+</sup>ATPase. Besides energy depletion other contributing factors were involved in the dysfunction of this enzyme, like loss of thiol groups for enzyme activity and lipid peroxidation-derived end products that might have induced conformational and functional changes. However, providing direct evidence for such conformational and functional changes of Na<sup>+</sup>K<sup>+</sup>ATPase was beyond the scope of the present study. In addition, immunoblotting results also showed a decrease in Na<sup>+</sup>K<sup>+</sup>ATPase protein expression highlighting the impact of nickel neurotoxicity on the expression of the enzyme itself. The implication of the inhibition of mitochondrial respiration and Na<sup>+</sup>K<sup>+</sup>ATPase dysfunction was the neuronal death as evidenced by enhanced caspase-3 and caspase-9 activities. Thus, this study established the deleterious impact of nickel neurotoxicity on mitochondrial functions in the piscine brain and identified probable contributing factors that can act concurrently in the inhibition of Na<sup>+</sup>K<sup>+</sup>ATPase. This study also provided a vital clue about the specific areas that the therapeutic agents should target to counter nickel neurotoxicity.

**KEY WORDS:** mitochondrial respiratory chain, complex IV, sodium potassium ATPase, nickel, neurotoxicity

Correspondence address:

**Dr. Arpan Kumar Maiti**

Department of Biological Sciences  
School of Basic and Applied Sciences  
Dayananda Sagar University, Shavige Malleshwara Hills  
Kumaraswamy Layout, Bangalore, India -560078  
TEL.: +91-8861491925  
E-MAIL: arpankumar.maiti@gmail.com

## Introduction

Nickel (Ni) is an environmentally reactive toxic metal that exhibits a high degree of toxicity and carcinogenicity to living organisms including fishes (Brix *et al.*, 2004; Pane *et al.*, 2004). Previous studies have proposed oxidative stress as a possible mechanism involved in Ni cytotoxicity (Chen *et al.*, 2003; Ahmed *et al.*, 1999; Chen *et al.*, 1998). Among the various cell organelles, mitochondria

have been identified as a prime target for cytotoxic action of Ni, possibly through increased generation of reactive oxygen species (ROS) and the subsequent oxidative injuries. Mitochondrial dysfunction involving loss of mitochondrial membrane potential, reduced ATP generation and decreased mitochondrial DNA content have been reported in previous studies exposed to Ni toxicity (Xu *et al.*, 2015; He *et al.*, 2011; Xu *et al.*, 2010; Guan *et al.*, 2007; M'Bemba-Meka *et al.*, 2006; M'Bemba-Meka *et al.*, 2005; Bragadin & Viola, 1997). However, the impact of Ni toxicity on the mitochondrial respiratory complexes especially in piscine brain has remained uninvestigated. There is a high possibility of alteration of mitochondrial respiratory complexes in Ni cytotoxicity as alterations in other parameters of mitochondrial function have been reported in previous studies. Alteration in mitochondrial membrane potential is most likely to disrupt mitochondrial structure and function increasing the possibility of disruption of mitochondrial respiratory chain activity (Desagher & Martinou, 2000).

In the brain, among the membrane bound enzymes, Na<sup>+</sup>K<sup>+</sup>ATPase, a known major energy dependent heterodimeric enzyme, plays a crucial role in the maintenance of Na<sup>+</sup> and K<sup>+</sup> gradients across the cell membrane (Rakowski *et al.*, 1989). The inactivation of Na<sup>+</sup>K<sup>+</sup>ATPase often leads to diverse alterations in the neuron leading to functional deficits in the brain (Xiao *et al.*, 2002; DiPolo & Beauge, 1991; Lijnen *et al.*, 1986; Archibald & White, 1974). As Na<sup>+</sup>K<sup>+</sup>ATPase occupies central importance in maintaining brain function, in this study we have also tried to explore the impact of Ni-induced neurotoxicity on Na<sup>+</sup>K<sup>+</sup>ATPase and to elucidate the likely mechanisms involved in the inhibition of this particular enzyme. Inhibition of mitochondrial respiratory complexes upon Ni exposure may lead to diminution of energy production that can disrupt the normal functioning of Na<sup>+</sup>K<sup>+</sup>ATPase. In addition, oxidative stress induced factors may also contribute for the inhibition of this enzyme. Thus there may be involvement of several contributing factors that could act simultaneously for the inhibition of Na<sup>+</sup>K<sup>+</sup>ATPase. In our study, *Clarias batrachus* has been chosen as a working model as fishes are now considered to be more sensitive to transition metals and act as good alternative to mammalian models for studying metal neurotoxicity. In the present study, there were two main objectives – first, to study the impact of Ni neurotoxicity on both mitochondrial respiratory chain and Na<sup>+</sup>K<sup>+</sup>ATPase functions in the brain of *Clarias batrachus* and second, to determine the contributing factors that might lead to the suppression of mitochondrial respiratory chain and Na<sup>+</sup>K<sup>+</sup>ATPase functions in piscine brain upon Ni exposure.

## Materials and methods

### Chemicals

All common chemicals were of analytical grade. 2,6-dichlorophenolindophenol (DCPIP), rotenone, ubiquinol, cytochrome c, EGTA, phenyl-methanesulphonyl

fluoride (PMSF), JC-1 (5,5',6,6'-tetrachloro-1,1',3,3'-tetraethyl benzimidazolylcarbocyanine iodide) and diethylenetriaminepentacetic acid (DTPA) were purchased from Sigma Chemical Co.(USA). NADH, dimethyl sulphoxide (DMSO), sodium dodecyl sulphate (SDS), HEPES, 5,5V-dithiobis-2-nitrobenzoic acid (DTNB), dimethylformamide, trichloroacetic acid (TCA) and sucrose were from Sisco Research Laboratory (Mumbai, India).

### Animals, Grouping and Experimental protocol

Animal use protocols have been approved by the University of Kalyani Animal Care Committee in accordance with national guidelines. Healthy adult specimens of *Clarias batrachus* (60±1.19 g body weight, 15±0.79 cm in length) were collected from a single population from a local hatchery and were acclimatized for 2 weeks in dechlorinated tap water in large glass aquaria in the laboratory. They were fed *ad libitum* on alternate days and the water with requisite Ni salt was renewed after every 48 hr, leaving no fecal matter, unconsumed food or dead fish, if any. Prior to the commencement of the experiment, 96 h median lethal concentration (96 h LC<sub>50</sub>) of NiCl<sub>2</sub>.6H<sub>2</sub>O (E.Merck) was estimated by probit analysis (Finney, 1971) as in natural waters Ni<sup>2+</sup> is the dominant chemical species.

Adult *Clarias batrachus* were exposed to NiCl<sub>2</sub>.6H<sub>2</sub>O treated water at 10% (4.1 mg.l<sup>-1</sup>) and 20% (8.2 mg.l<sup>-1</sup>) of the 96 h LC<sub>50</sub> value (41 mg.l<sup>-1</sup>). Eight fishes were randomly assigned for each aquarium containing 30l of NiCl<sub>2</sub>.6H<sub>2</sub>O treated water, prepared in tap water (having dissolved oxygen 6.6 mg.l<sup>-1</sup>, pH 7.23, water hardness 23.8 mg.l<sup>-1</sup> and water temperature 26±2 °C). Identical groups of eight fish each were kept in separate aquaria containing 30l of plain dechlorinated tap water (without Ni salt) as controls. After each of the exposure periods of 20, 40 and 60 days, fishes from the respective experimental as well as control aquaria were sacrificed. Atomic absorption spectrometry was used to measure the exact concentration of Ni in experimental water during the course of 20, 40 and 60 days and was found to be very near to the desired concentration levels.

### Preparation of brain synaptosomal fraction

Each individual fish was killed, decapitated and the brain removed. The crude synaptosomal fraction was prepared by the method of Whittaker (1972). Briefly, the brain was cut into small pieces and minced with a sharp scalpel. Each minced brain was homogenized in a homogenizing buffer comprising of 9 volumes of 320 mM sucrose and 5 mM HEPES at pH 7.4 containing 0.1 mM phenylmethylsulphonyl fluoride. Post homogenization, the homogenate was centrifuged at 1000 × g for 10 min at 4°C. The supernatant obtained was collected and centrifuged at 12000 × g for 15 min. The supernatant obtained in this step was collected and stored for nitrite measurement. The remaining pellet was resuspended in the homogenizing buffer and was subjected to centrifugation at 12000 × g for 15 min. The final pellet was resuspended in the desired buffer and later utilized for measurement of lipid peroxidation, protein thiol, protein carbonyl and Na<sup>+</sup>K<sup>+</sup>ATPase.

### Assessment of lipid peroxidation

Lipid peroxidation was measured by the thiobarbituric acid assay (Ohkawa *et al.*, 1979). To each sample of 200 µl of synaptosomal suspension in 50 mM phosphate buffer, pH 7.4, was added in a sequence – 200 µl of 8.1% SDS, 1.5 ml of 20% acetic acid (pH 3.5), 1.5 ml of 0.85% TBA and 400 µl water followed by heating for 15 min in a boiling water bath. After cooling the tubes, the pink color developed was extracted with 5 ml of (1:15) n-butanol-pyridine. The organic layer was collected after centrifuging the tubes at 3000 rpm for 10 min. The absorbance was read at 532 nm and the amount of MDA calculated from the molar extinction coefficient of MDA-TBA adduct ( $\epsilon=1.56 \times 10^5 \text{ M}^{-1} \cdot \text{cm}^{-1}$ ).

### Assessment of protein carbonyl content

The protein carbonyl content of brain samples was assessed by 2,4-dinitrophenylhydrazine assay (Levine *et al.*, 1990; Shacter *et al.*, 1996). Briefly, the sample proteins were derivatized with 10 mM 2,4-dinitrophenylhydrazine (DNPH) for 15 min. This was followed by addition of TCA (20%) and pelleting of the protein and three successive washings of the pellet with ethanol-ethylacetate (1:1) to remove the excess DNPH. The derivatized protein was finally dissolved in protein dissolving solution containing 2% sodium dodecylsulphate (SDS) and optical density measured at 370 nm against the appropriate blank.

### Assessment of protein sulphhydryl (-SH) content

The free sulphhydryl content of protein sample was estimated using Ellman's reagent (Habeeb, 1972). The sample proteins were dissolved in a solution containing 2% SDS and 0.5% EDTA in 0.08 M phosphate buffer, pH 8.0. To this solution, 5 mM dithiobisnitrobenzoic acid (DTNB) solution was added and the absorbance of the yellow color was measured at 412 nm.

### Measurement of Na<sup>+</sup>K<sup>+</sup>ATPase activity

An aliquot (100 µl) of synaptosomal fraction containing 100–200 µg of protein was used for the assay of Na<sup>+</sup>K<sup>+</sup>ATPase activity in a reaction mixture containing 100 mM NaCl, 10 mM KCl, 6 mM MgCl<sub>2</sub> and 3 mM ATP in 25 mM Tris, pH 7.4 in the presence or absence of 2 mM ouabain as adapted from the method of Mallik *et al.* (2000). The activity of the enzyme was expressed as µmoles of inorganic phosphate liberated/mg protein/h.

### Immunoblotting of Na<sup>+</sup>K<sup>+</sup>ATPase

Synaptosomal fractions obtained from piscine brain as discussed earlier were utilized for the immunoblotting of Na<sup>+</sup>K<sup>+</sup>ATPase. The proteins were subjected to SDS-PAGE (8% acrylamide for resolving gel, 4% acrylamide for stacking gel) under conditions as described by Laemmli (1970). The proteins were then electrophoretically transferred onto PVDF membranes using a semi-dry electroblotting system. After transfer membranes were blocked with 10% skim milk in TTBS (0.05% tween 20 in tris-buffered saline: 20 mM.l<sup>-1</sup> Tris-HCl; 500 mM.l<sup>-1</sup> NaCl, pH 7.6) for 1 h before being incubated overnight at 4 °C with anti-NKA

antibody (α5, 1:400 dilution, DSHB, USA). The primary antibody was diluted in 1% bovine serum albumin in TTBS. The membranes were then incubated in goat anti-mouse horseradish peroxidase – conjugated secondary antibody (1:5000 dilution; Santa Cruz Biotechnology, USA) for 1 h at room temperature followed by band analysis.

### Isolation of piscine brain mitochondria

The brain mitochondrial fraction was isolated following the method of Berman & Hastings (1999), with minor modifications. Briefly, the brain was homogenized in 10 ml of buffer A (225 mM mannitol, 75 mM sucrose, 5 mM HEPES, 1 mM EGTA, 1 mg/ml BSA, pH 7.4). The homogenate was brought to 30 ml with the same buffer followed by centrifugation at 2000 g for 3 min at 4 °C. The supernatant was preserved and the pellet resuspended in 10 ml of buffer A followed by recentrifugation as earlier. The supernatants were pooled and centrifuged in 4 tubes at 12,000 g for 8 min. The pellet in each tube containing synaptosomes and mitochondria was treated with 10 ml of buffer A containing 0.02% digitonin to lyse the synaptosomes. The mitochondria were pelleted down by centrifugation at 12,000 g for 10 min. The mitochondrial pellet was washed again in buffer A without EGTA and BSA and resuspended in an appropriate buffer for further experimentation.

### Assessment of mitochondrial respiratory complexes

Frozen and thawed samples of mitochondrial suspension in 50 mM phosphate buffer, pH 7.4 (10–30 µg of protein), were used for mitochondrial complex I and complex IV enzyme assays. The activity of complex I was assayed by using ferricyanide as the electron acceptor as adapted from Hatefi (1978). The assay system at 30 °C contained 0.17 mM NADH, 0.6 mM ferricyanide, triton X-100 (0.1% v/v) in 50 mM phosphate buffer pH 7.4. The reaction was initiated by addition of mitochondrial suspension (10–30 µg protein) to the sample cuvette and the rate of oxidation of NADH was measured by the decrease in absorbance at 340 nm (Clark *et al.*, 1997).

Complex II (succinate-ubiquinone oxidoreductase) activity was performed using 2,6-dichlorophenolindophenol (DCPIP) as acceptor and succinate as donor. The reaction mixture contained 30 µg mitochondria, 25 mM potassium phosphate, 5 mM MgCl<sub>2</sub>, 2 mM KCN, 20 mM succinate, 3 µM antimycin A, 1 µM rotenone. 1 mM DCPIP was reincubated for 10 minutes at 37 °C the reaction was started with ubiquinone (0.1 mM) and the enzyme-catalyzed reduction of DCPIP to DCPIPH<sub>2</sub> was recorded for 5 min at 600 nm ( $\epsilon=21,000 \text{ M}^{-1}$ ) (Bo *et al.*, 2014).

Complex III (ubiquinone-ferricytochrome-c oxidoreductase) activity was measured by monitoring the reduction of cytochrome c at 550 nm in the assay medium (25 mM potassium phosphate, 5 mM MgCl<sub>2</sub>, 2 mM KCN, 2 µg/ml rotenone, pH 7.2). Cytochrome c (15 µM) and ubiquinol (0.1 mM) were added to the assay medium, and the nonenzymatic rate was recorded for 1 min. Then

mitochondria were added, and the increase in absorbance was recorded for 3 min (Bo *et al.*, 2014).

The activity of complex IV was assayed by following the oxidation of reduced cytochrome c (ferrocytochrome c) at 550 nm. Reduced cytochrome c (50  $\mu$ M) in 10 mM phosphate buffer pH 3097.4 was added to each of two 1 ml cuvettes. In the blank cuvette, ferricyanide (1 mM) was added to oxidize ferrocytochrome c and the reaction initiated in the sample cuvette by the addition of mitochondrial suspension (10–30  $\mu$ g protein). The rate of decrease of absorbance at 550 nm was measured at room temperature. The activity of the enzyme was calculated from the first-order rate constant taking into account the concentration of reduced cytochrome c in the cuvette and the amount of mitochondrial protein added (Wharton & Tzagoloff, 1967).

#### Assessment of mitochondrial ROS generation

The assessment of mitochondrial ROS generation was carried out by following the method of Dreiem *et al.* (2005), using DCFH-DA dye. DCF fluorescence values were corrected for protein levels and autofluorescence of the samples, according to the formula  $F_{co} = (F_{sa} - F_{bl}) / \text{protein}$ , where  $F_{co}$  is the corrected fluorescence value,  $F_{sa}$  is observed fluorescence in the sample and  $F_{bl}$  is observed fluorescence in the blank.

#### Assessment of mitochondrial ATP production

Mitochondrial ATP production was assessed by using luciferin-luciferase bioluminescent assay following the method of Hays *et al.* (2003). Mitochondrial samples were thawed and centrifuged at 10 000  $\times g$  for 5 min and the supernatant was used to determine ATP content. To prepare the luciferin-luciferase solution, 0.28 mg/ml luciferin and 1 mg/ml luciferase were combined with stabilizing buffer containing HEPES (0.025 M, pH 7.5). The sample supernatant of 10  $\mu$ l was added to 200  $\mu$ l of HEPES buffer and then 200  $\mu$ l of this solution was placed into cuvettes. Next, 100  $\mu$ l of luciferin-luciferase solution was added to each luminometer cuvette and placed in the luminometer. The results are expressed as nM ATP/mg protein.

#### Measurement of mitochondrial transmembrane potential

Aliquots of mitochondrial suspensions were incubated at 37 °C for 30 min in isotonic buffer A containing 10 mM pyruvate, 10 mM succinate and 1 mM ADP with 5  $\mu$ M JC-1 (5,5',6,6'-tetrachloro-1,1',3,3'-tetraethyl benzimidazolylcarbocyanine iodide, CS0760, Sigma-Aldrich). After incubation, the dyed mitochondria were collected by centrifugation, washed with isotonic buffer A to remove excess dye and resuspended in the same buffer in appropriate dilution, followed by measurement of fluorescence intensity ( $\lambda_{ex}$  490 nm,  $\lambda_{em}$  590 nm).

#### Assessment of caspase-3 and caspase-9 activities

Caspase-3 and caspase-9 assays were performed on the brain samples according to the manufacturer's protocol (Biovision, K106-100 and K119-100). The assays are based on spectrophotometric detection of the chromophore

p-nitroaniline (pNA) after cleavage from the labeled substrate DEVD-pNA (for caspase-3) and LEHD-pNA (for caspase-9) respectively. Initially the harvested brain tissue was homogenized using a Dounce homogenizer in lysis buffer followed by centrifugation at 10 000  $\times g$  for 10 min to obtain the supernatant. For post-protein estimation approximately 50  $\mu$ g protein was diluted to 50  $\mu$ l lysis buffer for each assay followed by addition of 50  $\mu$ l of 2 $\times$  reaction buffer (containing 10 mM DTT). To each sample 5  $\mu$ l of the 4 mM DEVD-pNA / LEHD-pNA substrate was added, followed by incubation at 37 °C for 1 hour. Post incubation samples were read at 405-nm using a 100- $\mu$ l micro quartz cuvette and the results are expressed as absorbance at 405 nm.

#### Protein assessment

The protein was assessed after solubilizing the membranes in 1% SDS by the method of Lowry *et al.* (1951).

#### Statistical analysis

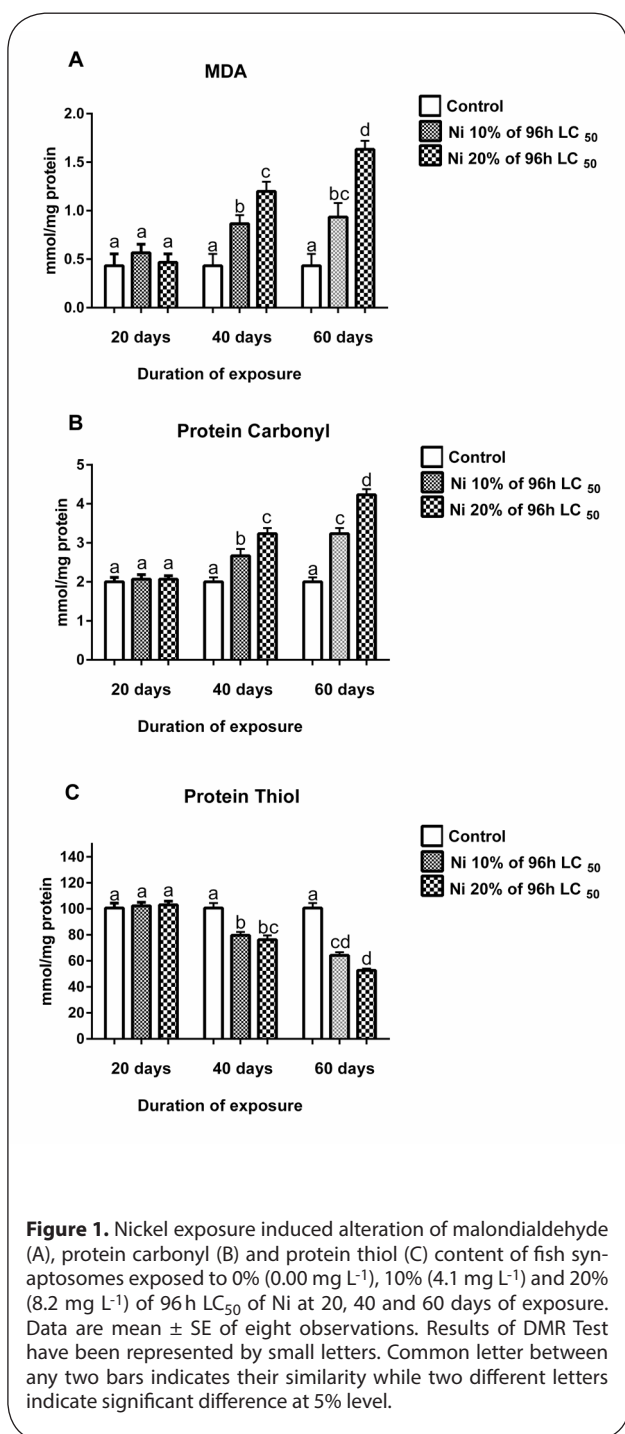
All data were subjected to Duncan's multiple range test (Duncan, 1955; Gomez & Gomez, 1984) to determine significant differences among means at 5% level of significance. In figures, data are mean  $\pm$  SEM of eight observations. Results of DMR Test have been represented by small letters. Common letter between any two bars (in figures) indicate their similarity while two different letters indicate significant difference at 5% level.

## Results

Nickel exposure increased lipid peroxidation and protein carbonyl content with reduced protein thiol level in fish synaptosomal fraction

The extent of lipid peroxidation in synaptosomal fraction was assessed by the amount of malondialdehyde (MDA), an important by-product of lipid peroxidation formed. It is apparent from the data presented in Figure 1A that among all the combinations of exposure of nickel with respect to duration and concentration of treatment, the combination of 60 days treatment with Ni 20% (of 96 h LC<sub>50</sub>) exposure recorded the highest increase in MDA production (nearly 4fold vs. control). However, a general tendency of increase in MDA production was observed in the synaptosomal fraction with successive increase in duration and concentration of Ni exposure (Figure 1A). Significant incorporation of protein carbonyl, an important marker of oxidative stress induced protein damage, was also noticed in the synaptosomal fraction of fish brain (Figure 1B). There was a gradual increase in carbonyl content in the synaptosomal fraction from 20 to 60 days duration of nickel treatment with respect to increasing concentrations of Ni (10% and 20% of 96 h LC<sub>50</sub> value) exposure. The highest incorporation of protein carbonyl in fish synaptosomal fraction was noticed at 60-day exposure period at Ni 20% (of 96 h LC<sub>50</sub>) treatment (nearly two fold vs. control). With the exception of 20-day treatment, in both 40- and 60-day

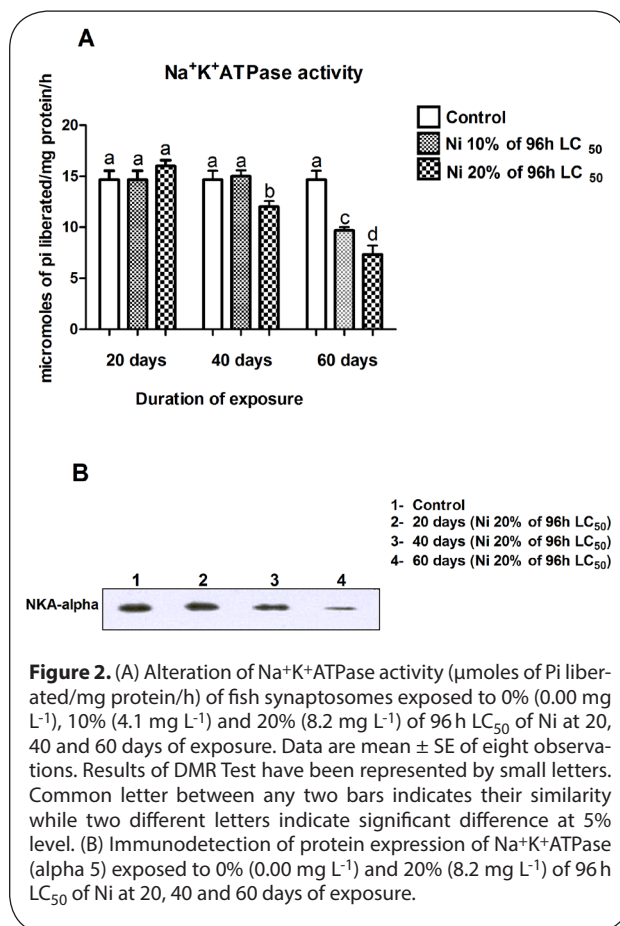
treatment periods, statistically significant differences in protein carbonyl incorporation was obtained among control (0% of 96 h LC<sub>50</sub>) and Ni treated (10% and 20% of 96 h LC<sub>50</sub> value) groups ( $p < 0.05$ ) (Figure 1B). Under our experimental conditions, a gradual loss of sulphhydryl (-SH) group content with increase in duration and concentration of Ni treatment was observed, as seen in Figure 1C. The maximum difference in -SH group content between control (0% of LC<sub>50</sub>) and its respective Ni treated groups (10% and 20% of 96 h LC<sub>50</sub> value) were observed in 60-day treatment period (by 38% and 45% respectively,  $p < 0.05$ ) (Figure 1C).



### Loss of Na<sup>+</sup>K<sup>+</sup>ATPase activity and protein expression in nickel treated fish synaptosomes

In Na<sup>+</sup>K<sup>+</sup>ATPase activity measurement, in case of 20 days of Ni exposure, though no statistically significant difference in enzyme activity was observed between control (0% of 96 h LC<sub>50</sub>) and Ni treated groups, yet in case of 40 day treatment, the Na<sup>+</sup>K<sup>+</sup>ATPase activity obtained at Ni 20% (of 96 h LC<sub>50</sub>) exposure was found to be significantly lower compared to the control (0% of 96 h LC<sub>50</sub>) and Ni 10% (of 96 h LC<sub>50</sub>) exposure (by 18% and 22% respectively,  $p < 0.05$ ) (Figure 2A). In 60-day duration of Ni exposure, at Ni 20% (of 96 h LC<sub>50</sub>) concentration, maximum decrease in Na<sup>+</sup>K<sup>+</sup>ATPase activity was observed, which was significantly lower compared to control (0% of 96 h LC<sub>50</sub>) and Ni 10% (of 96 h LC<sub>50</sub>) treated values (by 37% and 16% respectively,  $p < 0.05$ ) (Figure 2A).

However, considering the results obtained in the measurement of Na<sup>+</sup>K<sup>+</sup>ATPase activity, it was decided to focus solely on Ni 20% (of 96 h LC<sub>50</sub>) dosage in immunodetection study as this particular dosage had a profound impact on the activity of the enzyme at 20, 40 and 60 days of exposure period compared to Ni 10% (of 96 h LC<sub>50</sub>). The immunodetection of Na<sup>+</sup>K<sup>+</sup>ATPase indicated a gradual lowering of protein expression compared to control, as indicated by lowering of band intensity as the exposure period progressed from 20 days to 60 days; least band intensity was noticed in 60-day exposure period compared to other durations (Figure 2B).



Exposure to nickel caused mitochondrial dysfunction with suppression of mitochondrial respiratory complex IV in fish brain

In the mitochondrial respiratory enzyme complex studies, there was no diminution in mitochondrial complex I, II and III activities under Ni exposure (Figure 3A,B,C), however, significant inhibition of mitochondrial IV activity was observed in 40 and 60 days of exposure period (Figure 3D). In 60-day exposure period, significant difference in complex IV activities was observed between control (0% of 96 h LC<sub>50</sub>) and Ni treated groups (10% and 20% of 96 h LC<sub>50</sub> value) (by 26% and 37% respectively,  $p < 0.05$ ) (Figure 3D). In 40-day treatment period, the complex IV activity obtained at Ni 20% (of 96 h LC<sub>50</sub>) exposure was found to be significantly lower than the control (0% of 96 h LC<sub>50</sub>) value (by 19%,  $p < 0.05$ ) but insignificant to Ni 10% (of 96 h LC<sub>50</sub>) exposure (Figure 3D).

### Nickel treatment induced enhanced mitochondrial ROS generation accompanied by reduction of mitochondrial membrane potential and ATP generation

Regarding the status of energy generation in our experimental conditions, the present study has shown a decline in ATP generation in mitochondria. The drop in energy generation was profound in 60-day exposure period with significant difference observed between control (0% of 96 h LC<sub>50</sub>) and Ni treated groups (10% and 20% of 96 h LC<sub>50</sub> value) (by 20% and 37% respectively,  $p < 0.05$ ) (Figure 4A). In the 40-day exposure period, only significant difference was observed between control (0% of 96 h LC<sub>50</sub>) and Ni 20% (of 96 h LC<sub>50</sub> value) group (by 22%,  $p < 0.05$ ) (Figure 4A). Analysis of mitochondrial ROS generation clearly indicated the occurrence of oxidative stress upon Ni exposure with significant difference observed between control (0% of 96 h LC<sub>50</sub>) and Ni treated groups (10% and

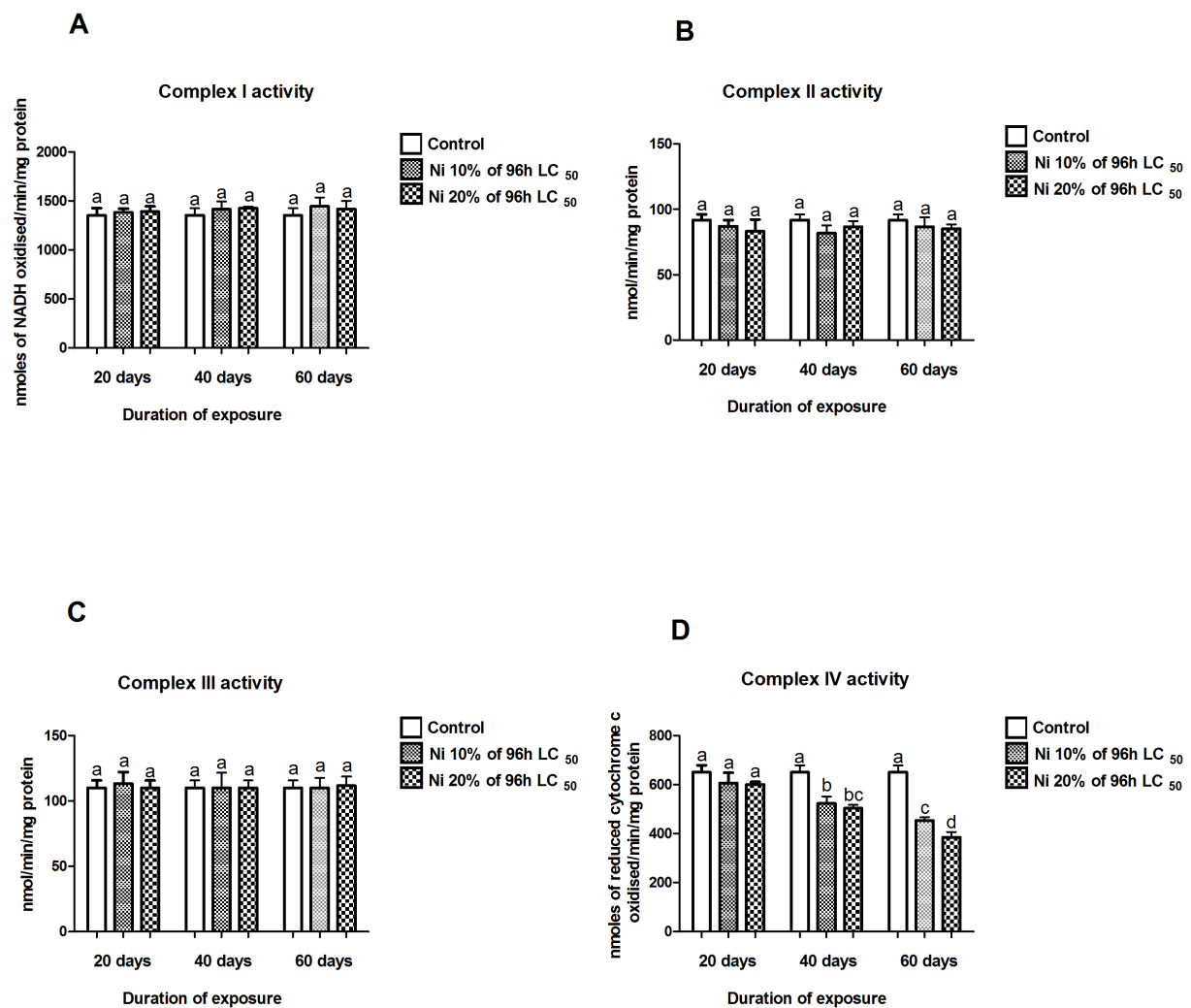


**Figure 3.** Impact of nickel exposure on mitochondrial complex I (A), complex II (B), complex III (C) and complex IV (D) of fish brain mitochondrial fraction exposed to 0% (0.00 mg L<sup>-1</sup>), 10% (4.1 mg L<sup>-1</sup>) and 20% (8.2 mg L<sup>-1</sup>) of 96 h LC<sub>50</sub> of Ni at 20, 40 and 60 days of exposure. Data are mean ± SE of eight observations. Results of DMR Test have been represented by small letters. Common letter between any two bars indicates their similarity while two different letters indicate significant difference at 5% level.

20% of 96 h LC<sub>50</sub> value) at 40 and 60 days of nickel treatment (Figure 4B). For mitochondrial membrane potential measurement, severe loss of membrane potential was observed during 40 and 60 days of nickel treatment with significant difference observed between control (0% of 96 h LC<sub>50</sub>) and Ni treated groups (10% and 20% of 96 h LC<sub>50</sub> value) at 40 and 60 days of nickel treatment (Figure 4C). The maximum loss of membrane potential of 34% was observed at Ni 20% (of 96 h LC<sub>50</sub>) exposure during 60 days treatment, indicating the maximum loss of mitochondrial function during nickel toxicity ( $p < 0.05$ ) (Figure 4C).

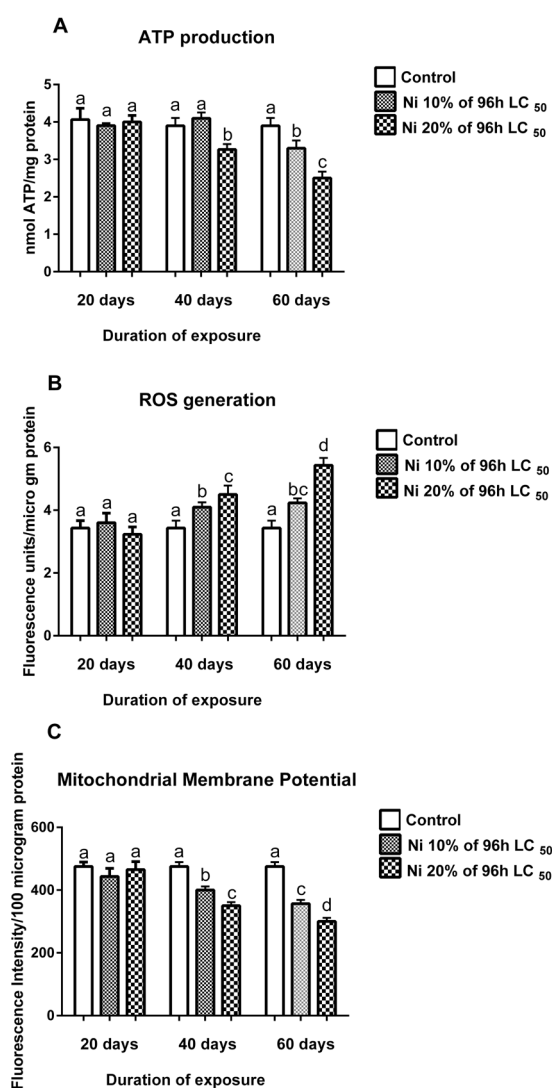


**Figure 4.** Variation of mitochondrial adenosine triphosphate (ATP) production (A), mitochondrial reactive oxygen species (ROS) generation (B) and mitochondrial membrane potential (C) of fish brain mitochondrial fraction exposed to 0% (0.00 mg L<sup>-1</sup>), 10% (4.1 mg L<sup>-1</sup>) and 20% (8.2 mg L<sup>-1</sup>) of 96 h LC<sub>50</sub> of Ni at 20, 40 and 60 days of exposure. Data are mean  $\pm$  SE of eight observations. Results of DMR Test have been represented by small letters. Common letter between any two bars indicates their similarity while two different letters indicate significant difference at 5% level.

#### Nickel exposure induced enhanced neuronal death as evidenced by enhanced caspase-3 and caspase-9 activities

In caspase-3 activity measurement, in case of 20 days of Ni exposure, though no statistically significant difference in enzyme activity was observed between control (0% of 96 h LC<sub>50</sub>) and Ni treated groups, however, in 40-day treatment, the caspase-3 activity obtained at Ni 20% (of 96 h LC<sub>50</sub>) exposure was found to be significantly higher compared to control (0% of 96 h LC<sub>50</sub>) (by 91%,  $p < 0.05$ ) (Figure 5A). In 60-day duration, significant increase in caspase-3 activity was observed at both Ni 10% and 20% (of 96 h LC<sub>50</sub>) exposure compared to control (0% of 96 h LC<sub>50</sub>) (by 101% and 117% respectively,  $p < 0.05$ ) (Figure 5A). A similar trend in activity was also observed for caspase-9 activity for 40 and 60 days of Ni exposure. Enhanced increase in caspase-9 activity was observed at 60-day exposure period at Ni 10% and 20% (of 96 h LC<sub>50</sub>) exposure compared to control (0% of 96 h LC<sub>50</sub>) (by 37% and 58% respectively,  $p < 0.05$ ) (Figure 5B).

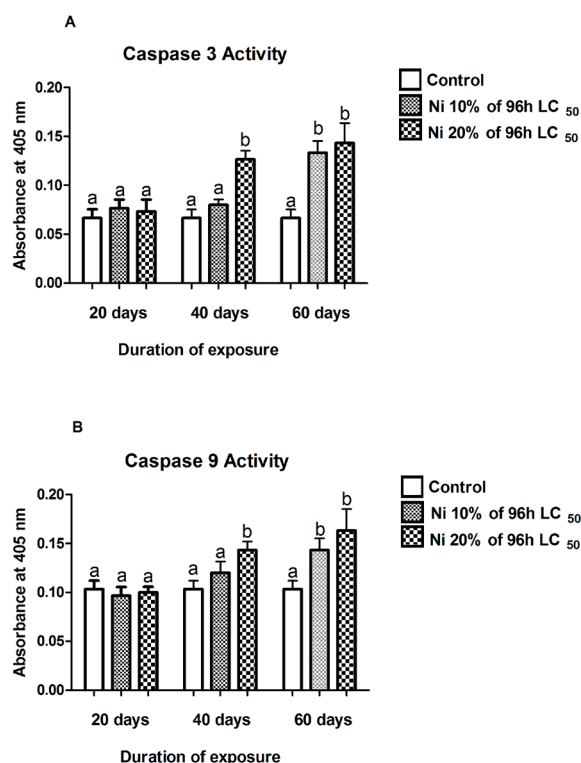


**Figure 5** Nickel exposure induced variation of caspase-3 (A) and caspase-9 (B) activities in piscine brain exposed to 0% (0.00 mg L<sup>-1</sup>), 10% (4.1 mg L<sup>-1</sup>) and 20% (8.2 mg L<sup>-1</sup>) of 96 h LC<sub>50</sub> of Ni at 20, 40 and 60 days of exposure. Data are mean  $\pm$  SE of eight observations. Results of DMR Test have been represented by small letters. Common letter between any two bars indicates their similarity while two different letters indicate significant difference at 5% level.

## Discussion

In our current study, the involvement of oxidative stress induced mechanisms following Ni exposure leading to partial inhibition of mitochondrial respiratory chain and Na<sup>+</sup>K<sup>+</sup>ATPase dysfunction were observed in the brain of Indian catfish *Clarias batrachus*. The brain is prone to oxidative stress because of its high O<sub>2</sub> uptake as it accounts for the vast amounts of energy required to maintain neuronal intracellular ion homeostasis in face of all the openings and closings of ion channels associated with the propagation of action potentials and neurosecretion (Halliwell, 2006). Besides, the availability of oxidizable substrates (like polyunsaturated fatty acids and catecholamines) and a deficient antioxidant defence system (low levels of catalase, glutathione peroxidase, and vitamin E) makes the brain more vulnerable to oxidative stress (Halliwell & Gutteridge, 1989). Among cell organelles, mitochondria are most prone to oxidative stress as mitochondrial oxidative phosphorylation is a major producer of ROS directly attacking its own membrane lipids, proteins, and nucleic acids (Chance *et al.*, 1979; Richter *et al.*, 1988). Exposure to trace elements like Ni as used in our study, amplifies the generation of reactive oxygen species even further. Earlier studies suggest that Ni exposure can disrupt mitochondrial function by decreasing membrane potential, reducing ATP generation and lowering mitochondrial DNA copy numbers and mtRNA transcript levels (Xu *et al.*, 2015; He *et al.*, 2011; Xu *et al.*, 2010). But the impact of Ni neurotoxicity on the individual mitochondrial respiratory complexes remains unexplored and uninvestigated. In the current study, we demonstrated for the first time that the activity of mitochondrial complex IV (cytochrome oxidase) in fish brain was significantly impaired with increase in time and concentration of Ni exposure, highlighting the sensitivity of piscine brain complex IV to Ni neurotoxicity. Mitochondrial complex I, II and III activities remained normal, however, the partial inhibition of complex IV was sufficient to lower the level of ATP generation in fish brain mitochondria, as seen in our study.

Regarding the cause of inhibition of complex IV activity, lipid peroxidation can be considered to be a major contributor. In our study increased generation of MDA in the fish synaptosomal fraction following Ni exposure has been observed, which is considered an important biomarker for lipid peroxidation. As respiratory enzyme complexes of the mitochondrial electron transport chain are embedded in the inner mitochondrial membrane, lipid peroxidation can cause a change in the lipid microenvironment of the membrane and thus the individual complexes of the mitochondrial respiratory chain may get affected in varying degrees. In our study, complex IV seems most affected and the direct involvement of lipid peroxidation in causing mitochondrial complex IV dysfunction cannot be ruled out. Besides, the numerous deleterious end-products of lipid peroxidation may also affect

complex IV of the mitochondrial respiratory chain. In support of this concept, Picklo *et al.* (1999) have already demonstrated the deleterious effects of byproducts of lipid peroxidation (namely 4-hydroxy-2-nonenal), altering the mitochondrial complex I and complex III linked respiration. Apart from lipid peroxidation, alteration of mitochondrial membrane potential, as observed in our current study, may also affect the functioning of mitochondrial complex IV activity as this respiratory complex is known to translocate protons from the mitochondrial matrix to intermembrane space, contributing to the proton gradient later utilized by ATP synthase for the generation of ATP (Marchi *et al.*, 2012; Desagher & Martinou, 2000). Moreover, the high sensitivity of complex IV to oxidizing agents may also result from the fact that complex IV contains heme groups and copper centers, all of which can be a site of direct ROS attack and their oxidative modifications can manifest with a decrease of enzymatic activity and dysfunction of the whole respiratory chain (Marchi *et al.*, 2012; Brown *et al.*, 1999; Bragadin & Radi, 1996; Cleeter *et al.*, 1994).

A deficient mitochondrial electron transport chain can have a direct impact on the activities of important adenosinetriphosphatases, namely Na<sup>+</sup>K<sup>+</sup>ATPase as explored in our study. Na<sup>+</sup>K<sup>+</sup>ATPase is an enzyme implicated in neuronal excitability, metabolic energy production, as well as in the uptake and release of catecholamines, serotonin, and glutamate (Liapi *et al.*, 2011; Lees *et al.*, 1990; Swann AC, 1984; Mata *et al.*, 1980). Our study clearly demonstrates the significant dysfunction of Na<sup>+</sup>K<sup>+</sup>ATPase activity and lowering of protein expression in fish brain. The degree of inhibition and lowering of protein expression increase with concentration and time of Ni exposure. This finding is in tune with that of Liapi *et al.* (2011), though in a different animal model, demonstrating a significant inhibition of Na<sup>+</sup>K<sup>+</sup>ATPase in rat brain following an *in vivo* short-term exposure of Ni. The Ni-induced inhibition of the piscine brain Na<sup>+</sup>K<sup>+</sup>ATPase as observed in this study is a novel finding as it highlights the neurotoxicological impact of long-term exposure of Ni mediated through oxidative stress. Like mitochondrial respiratory dysfunction, there may be involvement of several contributing factors that led to inhibition of Na<sup>+</sup>K<sup>+</sup>ATPase following Ni neurotoxicity. The conformation of Na<sup>+</sup>K<sup>+</sup>ATPase is likely to be severely altered by the structural and functional derangement of phospholipid bilayer of membranes in which this enzyme remains embedded. In addition, the lipid peroxidation-derived aldehyde products, namely 4-HNE, can also inflict severe damage to the normal conformation of this enzyme affecting its function (Miyake *et al.*, 2003; Zamai *et al.*, 2002). The loss of thiol (-SH) groups upon Ni exposure as observed in our study can be another important determining factor that leads to inhibition of this enzyme. Na<sup>+</sup>K<sup>+</sup>ATPase, being an -SH group containing enzyme, gets impaired due to Ni exposure, suggesting that -SH groups are essential for the enzyme activity. This finding is in conformity with earlier research reports that showed Ni toxicity causing

a decline in the thiol capacity of the cell (Petrushanko *et al.*, 2012; Chakrabarti & Bai, 1999; M'Bemba-Meka *et al.*, 2006). The fact that Na<sup>+</sup>K<sup>+</sup>ATPase is highly susceptible to oxidative attack can also be proved by an increase in lipid peroxidation induced protein carbonylation in the synaptosomal fraction as observed in our study. Such oxidative damaged proteins usually enter the degradation pathway in a cell indicating the measure of irreversible and unrepairable modification of proteins induced by oxidative stress (Nyström, 2005). Though direct evidence in favor of conformational changes of Na<sup>+</sup>K<sup>+</sup>ATPase upon nickel exposure has not been provided in this study, there remains a high chance of involvement of different contributory factors, like deficiency in ATP generation due to inhibition of mitochondrial complex IV, loss of thiol groups and lipid peroxidation derived metabolites, all contributing concurrently to the inhibition of Na<sup>+</sup>K<sup>+</sup>ATPase. These initial findings further encourage us to take up enzyme kinetics related work pertaining to Na<sup>+</sup>K<sup>+</sup>ATPase inhibition, which was not within the scope of the present study.

The direct implication of partial inhibition of mitochondrial respiratory chain and dysfunction of Na<sup>+</sup>K<sup>+</sup>ATPase is the neuronal death that was observed in the brain of *Clarias batrachus* in our study. To ascertain the occurrence of cell death upon Ni exposure, notably two cell death markers, i.e. caspase-3 and caspase-9, were studied as these markers are situated at pivotal junctions in cell death pathways. Interestingly, with the increase in duration and concentration of Ni exposure, enhanced activities of caspase-3 and caspase-9 were observed in the brain of *Clarias batrachus*, signifying the occurrence of neuronal death following Ni exposure.

Based on information obtained from this study and also from previous findings, it can be concluded that partial inhibition of mitochondrial respiratory chain and Na<sup>+</sup>K<sup>+</sup>ATPase dysfunction are the determinant factors modulating the toxicity of Ni in the brain of *Clarias batrachus* L. Though previous studies have dealt with the impact of Ni toxicity on mitochondrial function, there were certain lacunae concerning mitochondrial function especially at mitochondrial respiratory level which have been addressed in this study. Regarding the impact on Na<sup>+</sup>K<sup>+</sup>ATPase dysfunction, previous reports have demonstrated the dysfunction of this enzyme upon Ni exposure, however the factors contributing to the inhibition of this enzyme remained unexplored. Our current study clearly depicts the contributing factors that lead to the dysfunction of this enzyme, at the same time suggesting a possible link between mitochondrial dysfunction to that of Na<sup>+</sup>K<sup>+</sup>ATPase inhibition. So the rationale for targeting mitochondrial respiratory chain and Na<sup>+</sup>K<sup>+</sup>ATPase function in our study lies in the fact that the alterations in these basic functions can very well explain the loss of cell viability due to Ni neurotoxicity. In this connection, our study provides a vital clue about the specific areas that the therapeutic agents should target on in order to counteract the deleterious impact of Ni induced neurotoxicity.

## Acknowledgements

The authors are thankful to Dr D Mazumdar, Department of Agricultural Statistics, BCKV, West Bengal, India for extending useful suggestions in statistical analysis. The authors also thank Dr. Sunil More, Dean, School of Basic and Applied Sciences, Dayananda Sagar University, Bangalore, India for providing useful suggestions in manuscript preparation and assisting in reference collection.

## REFERENCES

- Ahmed S, Rahman A, Saleem M, Athar M, Sultana S. (1999). Ellagic acid ameliorates nickel induced biochemical alterations: diminution of oxidative stress. *Hum Exp Toxicol* **18**: 691–698.
- Archibald JT, White TD. (1974). Rapid reversal of internal Na<sup>+</sup> and K<sup>+</sup> contents of synaptosomes by ouabain. *Nature* **252**: 595–596.
- Berman SB, Hastings TG. (1999). Dopamine oxidation alters mitochondrial respiration and induces permeability transition in brain mitochondria: implications for Parkinson's disease. *J Neurochem* **73**: 1127–1137.
- Bo H, Kang W, Jiang N, Wang X, Zhang Y, Ji LL. (2014). Exercise-induced neuroprotection of hippocampus in APP/PS1 transgenic mice via upregulation of mitochondrial 8-oxoguanine DNA glycosylase. *Oxid Med Cell Longev*. **2014**: 834502
- Bragadin M, Viola E R. (1997). Ni<sup>++</sup> as a competitive inhibitor of calcium transport in mitochondria. *J Inorg Biochem* **66**: 227–229.
- Brix K V, Keithly J, DeFrost D K, Laughlin J. (2004). Acute and chronic toxicity of nickel to rainbow trout (*Oncorhynchus mykiss*). *Environ Toxicol Chem* **23**: 2221–2228.
- Brown GC. (1999). Nitric oxide and mitochondrial respiration. *Biochimica et Biophysica Acta* **1411**(2–3): 351–369.
- Chance B, Sies H, Boveris A. (1979). Hydroperoxide metabolism in mammalian organs. *Physiol Rev* **59**: 527–605.
- Cassina A, Radi R. (1996). Differential inhibitory action of nitric oxide and peroxynitrite on mitochondrial electron transport. *Arch Biochem Biophys* **328**(2): 309–316.
- Chakrabarti SK, Bai C. (1999). Role of oxidative stress in nickel chloride induced cell injury in rat renal cortical slices. *Biochem Pharmacol* **58**: 1501–1510.
- Chen CY, Wang YF, Lin YH, Yen SF. (2003). Nickel-induced oxidative stress and effect of antioxidants in human lymphocytes. *Arch Toxicol* **77**: 123–130.
- Chen CY, Huang YL, Lin TH. (1998). Association between oxidative stress and cytokine production in nickel-treated rats. *Arch Biochem Biophys* **356**: 127–132.
- Clark JB, Bates TE, Boakye P, Kuimov A, Land JM. (1997). *Investigation of mitochondrial defects in brain and skeletal muscle*. In: Turner A J, Bachelard H S, Editors. *Neurochemistry: A practical approach*. New York: Oxford University Press Inc., p151–74.
- Cleeter MW. (1994). Reversible inhibition of cytochrome c oxidase, the terminal enzyme of the mitochondrial respiratory chain, by nitric oxide Implications for neurodegenerative diseases. *FEBS Letters* **345** (1): 50–54.
- Cohen G, Farooqui R, Kesler N. (1997). Parkinson disease: a new link between monoamine oxidase and mitochondrial electron flow. *Proc Natl Acad Sci USA* **94**: 4890–4894.
- Demir TA, Akar T, Akyuz F, Isikli B, Kanbak G. (2005). Nickel and cadmium concentrations in plasma and Na<sup>+</sup>K<sup>+</sup>ATPase activities in erythrocyte membranes of the people exposed to cement dust emissions. *Environ Monit Assess* **104**: 437–444.
- Desagher S, Martinou JC. 2000. Mitochondria as the central control point of apoptosis. *Trends Cell Biol*. **10**(9): 369–77.
- DiPolo R, Beauge L. (1991). Regulation of Na-Ca exchange. An overview. *Annu NY Acad Sci* **639**: 100–111
- Dreiem A, Gertz CC, Seegal RF. (2005). The effects of methyl mercury on mitochondrial function and reactive oxygen species formation in rat striatal synaptosomes are age-dependent. *Toxicol Sci* **87**: 156–162.
- Dreiem A, Gertz CC, Seegal RF. (2005). The effects of methyl mercury on mitochondrial function and reactive oxygen species formation in rat striatal synaptosomes are age-dependent. *Toxicol Sci* **87**: 156–162.

- Duncan DB. (1955). Multiple range and multiple F tests. *Biometrics* **11**: 1–43.
- Finney DJ. (1971). *Probit analysis*. London: Cambridge University Press. p333–337.
- Gomez KA, Gomez AA. (1984). *Statistical procedures for agricultural research*. New York: 2<sup>nd</sup>ed. John Wiley and Sons. p162–169.
- Guan F, Zhang D, Wang X, Chen J. (2007). Nitric oxide and bcl-2 mediated the apoptosis induced by nickel (II) in human T hybridoma cells. *Toxicol Appl Pharmacol* **221**: 86–94.
- Habeeb AF. (1972). Reaction of protein sulphhydryl groups with Ellman's reagent. *Methods Enzymol* **25**: 457–464.
- Halliwell B, Gutteridge JMC. (1989). *Free radical in Biology and Medicine*. London: 2<sup>nd</sup> ed. Oxford University Press, Oxford, England.
- Halliwell B. (2006). Oxidative stress and neurodegeneration: where are we now? *J Neurochem* **97**(6): 1634–58.
- Hatefi Y. (1978). Preparation and properties of NADH: Ubiquinone oxidoreductase (complex I) E.C.1.6.5.3 *Methods Enzymol* **53**: 11–15.
- Hays AM, Lantz RC, Witten ML. (2003). Correlation between in vivo and in vitro pulmonary responses to jet propulsion fuel-8 using precision cut lung slices and a dynamic organ culture system. *Toxicol Pathol* **31**: 200–207.
- He MD, Xu SC, Lu YH, Li L, Zhong M, Zhang YW, Wang Y, Li M, Yang J, Zhang GB, Yu ZP, Zhou Z. (2011). L-carnitine protects against nickel-induced neurotoxicity by maintaining mitochondrial function in Neuro-2a cells. *Toxicol Appl Pharmacol*. **253**(1): 38–44.
- Laemmli UK. (1970). Cleavage of structural proteins during the assembly of the head bacteriophage T4. *Nature* **227**: 680–685.
- Liang FQ, Godley BF.(2003).Oxidative stress-induced mitochondrial DNA damage in human retinal pigment epithelial cells: a possible mechanism for RPE aging and age-related macular degeneration. *Exp Eye Res.* **76**(4): 397–403.
- Lees GJ, Lehmann A, Sandberg M, Hamberger A. (1990). The neurotoxicity of ouabain, a sodiumpotassium ATPase inhibitor, in the rat hippocampus. *Neurosci Lett* **120**: 159–162.
- Levine RL, Garland D, Oliver CN. (1990). Determination of carbonyl content in oxidatively modified proteins. *Methods Enzymol* **186**: 464–478.
- Liapi C, Zarros A, Theocharis S, Voumvourakis K, Anifantaki F, Gkrouzman E, Mellios Z, Skandali N, Al-Humadi H, Tsakiris S.2011.Short-term exposure to nickel alters the adult rat brain antioxidant status and the activities of crucial membrane-bound enzymes: neuroprotection by L-cysteine.*Biol Trace Elem Res.* **143**(3): 1673–81.
- Lijnen P, Hespel P, Lommelen G, Laermans M, M'Buyamba-Kabangu JR, Amery A. (1986). Intracellular sodium, potassium and magnesium concentration, ouabain-sensitive <sup>86</sup>Rb uptake and sodium-efflux and Na<sup>+</sup>K<sup>+</sup>-cotransport activity in erythrocytes of normal male subjects studied on two occasions. *Methods Find Exp Clin Pharmacol* **8**: 525–533.
- Lowry OH, Rosebrough NJ, Far AL, Randall RJ. (1951). Protein measurement with Folin-Phenol reagent. *J Biol Chem* **193**: 265–275.
- Luo J, Shi R. (2005). Acroline induced oxidative stress in brain mitochondria. *Neurochem Int* **46**: 243–252.
- Mallik BN, Adya HVA, Faisal M. (2000). Norepinephrine stimulated increase in Na<sup>+</sup>K<sup>+</sup>ATPase activity in the rat brain is mediated through alpha 1A adreno-receptor possibly by dephosphorylation of the enzyme. *J Neurochem* **74**: 1574–1578.
- Marchi S, Giorgi C, Suski JM, Agnoletto C, Bononi A, Bonora M, De Marchi E, Missiroli S, Patergnani S, Poletti F, Rimessi A, Duszynski J, Wieckowski MR, Pinton P. (2012). Mitochondria-ROS crosstalk in the control of cell death and aging. *J Signal Transduct* **2012**: 329635.
- Mata M, Fink DJ, Gainer H, Smith CB, Davidsen L, Savaki H, Schwartz WJ, Sokoloff L. (1980). Activity-dependent energy metabolism in rat posterior pituitary primarily reflects sodium pump activity. *J Neurochem* **34**: 213–215.
- M'Bemba-Meka P, Lemieux N, Chakrabarti SK. (2005). Role of oxidative stress, mitochondrial membrane potential and calcium homeostasis in nickel sulphate-induced human lymphocyte death in vitro. *Chem Biol Interact* **156**: 69–80.
- M'Bemba-Meka P, Lemieux N, Chakrabarti SK. (2006). Role of oxidative stress, mitochondrial membrane potential and calcium homeostasis in human lymphocyte death induced by nickel carbonate hydroxide in vitro. *Arch Toxicol* **80**: 405–420.
- M'Bemba-Meka P, Lemieux N, Chakrabarti S K. (2006). Role of oxidative stress, mitochondrial membrane potential and calcium homeostasis in nickel subsulfide-induced human lymphocyte death in vitro. *Sci Total Environ* **369**: 21–34.
- Miyake H, Kadoya A, Ohyashiki T. (2003). Increase in molecular rigidity of the protein cooperation of brain Na<sup>+</sup>K<sup>+</sup>ATPase by modification with 4-hydroxy-2-nonenal. *Biol Pharm Bull* **26**: 1652–1658.
- Nyström T. (2005). Role of oxidative carbonylation in protein quality control and senescence. *EMBO J.* **24**(7): 1311–7.
- Ohkawa H, Ohishi N, Yagi K. (1979). Assay for lipid peroxides in animal tissues by thiobarbituric acid reaction. *Anal Biochem* **95**: 351–358.
- Pane E F, Haque A, Goss G G, Wood CM. (2004). The physiological consequences of exposure to chronic, sublethal waterborne nickel in rainbow trout (*Oncorhynchus mykiss*): exercise vs resting physiology. *J Exp Biol* **207**: 1249–1261.
- Petrushanko IY, Yakushev S, Mitkevich VA, Kamanina YV, Ziganshin RH, Meng X, Anashkina AA, Makhro A, Lopina OD, Gassmann M, Makarov A, Bogdanova A. (2012). S-Glutathionylation of the Na,K-ATPase Catalytic  $\alpha$  Subunit Is a Determinant of the Enzyme Redox Sensitivity. *J Biol Chem* **287**(38): 32195–32205.
- Picklo MJ, Amarnath V, McIntyre JO, Graham DG, Montine TJ. (1999). 4-Hydroxy-2(E)-nonenal inhibits CNS mitochondrial respiration at multiple sites. *J Neurochem* **72**: 1617–24.
- Rakowski RF, Gadsby DC, deWeer P. (1989). Stoichiometry and voltage dependence of the sodium pump in voltage-clamped, internally dialyzed squid giant axon. *J Gen Physiol* **93**: 903–941.
- Richter C, Park JW, Ames BN.(1988). Normal oxidative damage to mitochondrial and nuclear DNA is extensive. *Proc Nat Acad Sci USA* **85**: 6465–6467.
- Rubanyi G, Bakos M, Hajdu K, Pataki T. (1982). Dependence of nickel-induced coronary vasoconstriction on the activity of the electrogenic Na<sup>+</sup>,K<sup>+</sup>-pump. *Acta Physiol Acad Sci Hung* **59**: 169–174.
- Swann AC. (1984). (Na<sup>+</sup>, K<sup>+</sup>)-adenosine triphosphatase regulation by the sympathetic nervous system: effects of noradrenergic stimulation and lesion *in vivo*. *J Pharmacol Exp Ther* **228**: 304–311.
- Wharton DC, Tzagoloff A. (1967). Cytochrome oxidase from beef heart mitochondria. *Methods Enzymol* **10**: 245–250.
- Whittaker V. (1972). *The Synaptosome*. In: Lajtha S, Editor. Hand book of neurochemistry. Plenum Press, New York, p327–364.
- Xiao AY, Wei L, Xia S, Rothman S, Yu SP. (2002). Ionic mechanism of quabain-induced concurrent apoptosis and necrosis in individual cultured cortical neurons. *J Neurosci* **22**: 1350–1362.
- Xu S, He M, Zhong M, Li L, Lu Y, Zhang Y, Zhang L, Yu Z, Zhou Z. (2015). The neuroprotective effects of taurine against nickel by reducing oxidative stress and maintaining mitochondrial function in cortical neurons. *Neurosci Lett.* **17**(590): 52–7.
- Xu SC, He MD, Zhong M, Zhang YW, Wang Y, Yang L, Yang J, Yu ZP, Zhou Z. (2010). Melatonin protects against Nickel-induced neurotoxicity in vitro by reducing oxidative stress and maintaining mitochondrial function. *J Pineal Res.* **49**(1): 86–94.
- Zamai TN, Titova NM, Zamai AS, Usol'tseva OS, Yulenkova OV, Shumkova DA. (2002). Effect of alcoholic intoxication on water content and activity of Na<sup>+</sup>K<sup>+</sup>ATPase and Ca-ATPase in rat brain. *Bull Exp Biol Med* **134**:541-543.
- Zhang Y, Marcillat O, Giulivi C, Ernster L, Davies KJA. (1990). The oxidative inactivation of mitochondrial electron transport chain components and ATPase. *J. Biol. Chem.* **265**: 16330-16336.

ORIGINAL ARTICLE

# Measurement of melamine migration from melamine-ware products by designed HPLC method and the effect of food-type on the level of migration

Ehsan HAGHI, Mahmood ALIMOHAMMADI, Attaollah SHAKOORI, Fariba RAZEGHI, Parisa SADIGHARA

*Environmental Health Engineering Department, School of Public Health, Tehran University of Medical Sciences, Tehran, Iran*

ITX110418A09 • Received: 30 July 2018 • Accepted: 19 August 2018

## ABSTRACT

Melamine-ware is widely used around the world. There is a public health concern as regards the safety of melamine when exposed to food. This study was carried out to measure the level of melamine migration in melamine-ware products by HPLC method and the effect of food-type on the level of melamine migration. In food control laboratories in Iran, there is no common method to measure and monitor melamine migration, hence a method using HPLC technique was adopted and validated to solve this problem. The validation results showed the reliability with 94.9% accuracy and 95.3% precision. Furthermore, the limit of detection (LOD) and quantification (LOQ) were 0.145 and 0.435 µg/ml, which for a new method were within acceptable ranges. Melamine migrations from 4 most available melamine wares were measured. Distilled water, 3% acetic acid and 15% ethanol were used as food simulant at 30 °C for 90 min. Although melamine migration occurred in all samples and acidic conditions had a significant effect, the values were not higher than the European standard (30 µg/ml). The study revealed that the HPLC method was valid and could be applied and developed to measure melamine migration. However, precautions should be considered while choosing melamine-ware utensil as long-term exposure to this substance has a negative effect on health, especially on the kidneys.

**KEY WORDS:** melamine; migration; HPLC; food type

## Introduction

Melamine, also known as tripolycyanamide or 2,4,6-triamino-1,3,5-triazine, is an industrial material used for the production of melamine resins (RAS, 2010; Johannes, 2005). It is generally used in the production of resins due to its durable thermosetting characteristic (Lokensgard & Richardson, 2003). Melamine ware is widely used around the world because of the toughness, heat resistance and low cost (RAS, 2010). It can decompose under high temperature; furthermore, factors such as temperature, acidity and frequent use significantly affect the level of melamine migration. This has raised concerns on the use

of melamine in packaging materials and utensils (Jacaab, 2007). The main safety concern regarding melamine-tableware is its possible migration into food (RAS, 2010) Direct contact with melamine can cause skin, eye and respiratory tract problems while (Jeong *et al.*, 2006) long-term exposure decreases fertility and high levels result in kidney damage (RAS, 2010; Kai-ching Hau *et al.*, 2009).

The No Observable Adverse Effects Level (NOAEL) of melamine was determined to be 63 mg/kg body weight/day, as to a 13-week toxicity assay by the National Toxicology Program (2009). The World Health Organization adopted a Take Daily Intake (TDI) of 0.2 mg/kg body weight/day. Few studies have been done to measure melamine migration and revealed that although the melamine-ware tested had low levels of migration, long term exposure can cause health problems (Kai-ching Hau *et al.*, 2009; WHO, 2009 Chik *et al.*, 2011) This study was carried out to measure the level of melamine migration in melamine-ware products using HPLC method and the effect of food-type on the level of migration.

Correspondence address:

**Dr. Parisa Sadighara**

Environmental Health Engineering Department  
School of Public Health, Tehran University of Medical Sciences  
Tehran, Iran

E-MAIL: sadighara@farabi.tums.ac.ir

## Materials and methods

### Materials and devices

Four samples of Iranian melamine-ware products were purchased from the market. In this study, 3% acetic acid, distilled water and 15% ethanol were used as food simulants under test conditions of 90°C for 30 min. Other materials used for the study were: Melamine Standard (99.0% purity) (Sigma-Germany Lot number: 1422105v), acetonitrile HPLC grid (Merck-Germany), deionized water HPLC quality, 3% acetic acid HPLC Grid (Merck, Germany). HPLC machine (American Agilent Technologies) and ultrasonic devices (Elma- Germany), Diode-array detector (DAD) with XBD-C18 column (4.6 × 250 mm 5-micro) was used to measure melamine migration. The size of particles was 5 µm, injection volume was 100 µl, mobile phase was 30% water + 70% ethanol, and the flow rate was 1 ml per minute. Melamine was determined at 220 nm wavelength (Chien *et al.*, 2011 )

### Calibration curve

The calibration curve with a range from 0.5 to 10 µg/ml was prepared in deionized distilled water. To determine retention time, injection was done at 30 min as pilot. Then 6 different concentrations of melamine standard solution (0.5, 1, 2, 2.5, 5 and 10 µg/ml) were injected into the HPLC column (in three replicates). The calibration curve was obtained by plotting area ratios of melamine standard against solvent concentration using Microsoft Excel 2013 software. The flow rate was set at 1 ml/min with injection volume of 20 µl.

For validating analytical procedures, the recommended protocol in the international conference of harmonized procedures which includes the limit of detection (LOD), limit of quantification (LOQ), linearity, precision, and accuracy was used (CEC, 1996).

The 3 replications in a day on 3 consecutive days were used to check for precision and accuracy. Three concentrations of 1, 2.5, and 10 µg/ml of stock solutions were prepared from melamine. Then 1 ml of each concentration was transferred to 3 test tubes and 9 ml of acetonitrile was then added to each of the 9 test tubes, shaken for 2 min, and dried with nitrogen at 35°C. 1 ml of mobile phase (30% distilled water + 70% ethanol) was added to the mixture and shaken for 2 min. The resultant mixture was then exposed to ultrasonic waves for 3 min and again shaken for 2 min. Finally, the mixture was injected into the HPLC column for analysis. For this method standard deviation must be <20% to accept its precision.

### Sample preparation

Four Iranian standard brands of melamine-wares were purchased from the market. These brands were well known and commonly available. Three different tests were designed to examine the effect of acidity on melamine migration to food simulant. Therefore, 16 unique samples were prepared for injection and analysis in the HPLC column. 4×3=12 (4= number of melamine-wares; 3= condition tests).

Melamine wares were washed with distilled water, and dried in an air oven at 30°C. The food-simulating solvent was preheated to 90°C and poured to 1 cm below the upper edge of the wares. The samples were then placed in an oven to maintain the desired temperature of the food simulant for 30 minutes. Then, 1 ml of the sample was transferred to a test tube to which 9 ml acetonitrile was added; the mixture was dried by gas flow at 25°C. After this, 1 ml HPLC mobile phase (30% water + 70% ethanol) was added to the sample and thoroughly shaken for 2 min and then placed in an ultrasonic device for 2 min. The mixtures were then transferred to vials and prepared for injection.

### Injection to the HPLC

The injections were performed according to the HPLC manufacturer's instructions. The flow rate was set at 6 min based on 3 min retention time. The other specifications were: 100 µl injection volume, 220 nm wavelength, mobile phase of 30% water + 70% ethanol and 6 min injection time.

### Data analysis

SPSS (v.21) and Excel 2013 were used for data analysis. ANOVA test was also carried out.

## Results

To obtain the calibration curve, the ratios of 6 different melamine standard concentrations (0.5, 1, 2, 2.5, 5 and 10 µg/ml) diluted with deionized distilled water were plotted against responses of the HPLC detector. The results are shown in Figure 1.

Standard chromatogram of melamine and chromatogram of samples are shown in Figures 2 and 3.

### Validation of method

The LOD and LOQ of HPLC method were 0.145 and 0.435 ppm, respectively. A signal-to-noise ratio (S/N) was used to validate the LOD and LOQ. Correlation coefficient (R<sup>2</sup>) between concentration and response time was 0.9909, thus showing a linear relationship between the variables. Relative standard deviation was <20%, which was acceptable. Validation results are in Table 1.

### Migration test

Quantification of melamine migration was conducted as previously described (see sample preparation section). The results of mean melamine migration (average of 3 repetitions) and significance comparison of the type of material (distilled water, acid and ethanol) and samples are shown in Tables 2 and 3.

## Discussion

Since there are no common and routine methods to measure melamine migration from melamine-ware in food

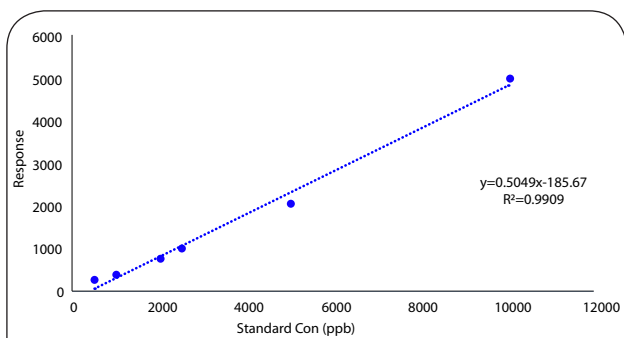


Figure 1. HPLC calibration curve.

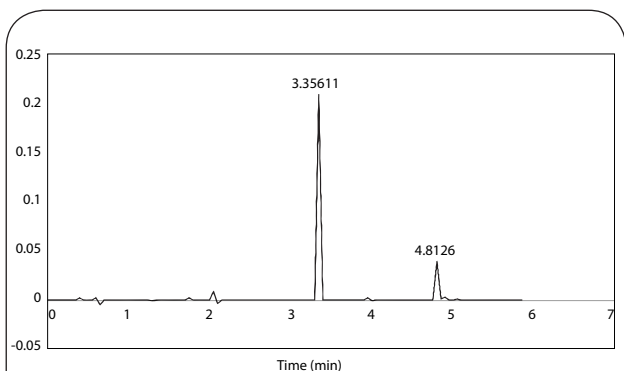


Figure 2. Standard chromatogram of melamine.

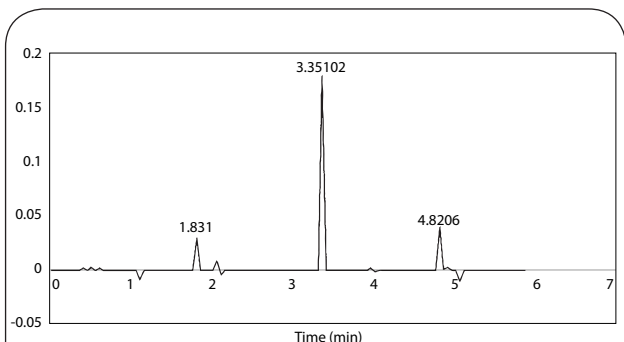


Figure 3. Separation chromatogram of samples.

Table 1. Validation results.

Parameter	Result
Retention Time	3.2 min
Accuracy (% Recovery)	94.9 %
Precision	95.3%
Slope	0.5049
Intercept	-185.67
Linearity range (µg/ml)	0.5–10
Standard equation regression	$y = 0.5049x - 185.67$
Correlation Coefficient	$R^2 = 0.9909$
LOD (µg/ml)	0.145
LOQ (µg/ml)	0.435

Table 2. Mean melamine migration of samples (average of 3 repetitions).

Sample	Test	Mean Result ± SD (ppm)	p-value
Sample 1	Water 30°C – 90 min	2.14252 ± 0.00057735	<0.001
	Acetic acid (3%) 30°C – 90 min	2.84767 ± 0.000416333	
	Etanol (15%) 30°C – 90 min	5.4008 ± 0.0019615	
Sample 2	Water 30°C – 90 min	1.33437 ± 0.005445487	<0.001
	Acetic acid (3%) 30°C – 90 min	2.37823 ± 0.005795113	
	Etanol (15%) 30°C – 90 min	1.22344 ± 0.003695042	
Sample 3	Water 30°C – 90 min	2.20392 ± 0.001078579	<0.001
	Acetic acid (3%) 30°C – 90 min	4.38275 ± 0.001249	
	Etanol (15%) 30°C – 90 min	1.17591 ± 0.000493288	
Sample 4	Water 30°C – 90 min	2.86153 ± 0.003415162	<0.001
	Acetic acid (3%) 30°C – 90 min	3.70930 ± 0.02988650	
	Etanol (15%) 30°C – 90 min	1.94048 ± 0.001692139	

control laboratories in Iran, it was vital to design a valid method using HPLC to resolve this challenge. Validation results of 94.9% accuracy and 95.3% precision showed that HPLC analysis is a reliable technique to determine melamine migration and can consequently be applied and developed for use in food control laboratories in Iran. The analysis of melamine migration confirmed and indicated that the designed method for this study was significant at  $p < 0.001$ .

With this method, melamine migration was detected in all samples at values less than 30 mg/kg, which is

the European Union standard. The results of the study also indicated that under the same conditions (30°C and 90 min) acidity affected melamine migration, hence higher values were obtained for acidic foods. The mean differences (using ANOVA test) in melamine migration were significant among acidic, alcoholic and neutral food stimulants. The  $p$ -values were significant at levels of less than 0.001. Migration to alcoholic food simulant was less because melamine does not dissolve completely in alcohol. Our finding was consistent with studies of other authors (LU *et al.*, 2009; Chao-Yi Chien *et al.*,

**Table 3.** Significance comparison of the type of material (distilled water, acid and ethanol).

Brand	Temperature and time	Simulant (I)	Simulant (J)	Mean difference (I-J)	p value	95% Confidence interval for differences	
						Upper bound	Lower bound
Sample 1	30°C - 90 min	Water	Acetic acid	1.219*	0	1.430	1.008
			Ethanol	-0.468*	0	-.257	-.679
		Acetic acid (3%)	Water	1.687*	0	1.898	1.476
			Ethanol	0.468	0	.679	.257
		Ethanol (15%)	Water	-1.219*	0	-1.008	-1.430
			Acetic acid	-1.687*	0	-1.476	-1.898
Sample 2	30°C - 90 min	Water	Acetic acid	-0.368*	0	-0.156	-0.579
			Ethanol	-0.162	0.196	0.049	-0.373
		Acetic acid (3%)	Water	0.206	0.059	0.417	-0.006
			Ethanol	0.368*	0	0.579	0.156
		Ethanol (15%)	Water	-0.206	0.059	0.006	-0.417
			Acetic acid	0.162	0.196	0.373	-0.049
Sample 3	30°C - 90 min	Water	Acetic acid	0.378*	0	0.590	0.167
			Ethanol	-0.492*	0	-0.281	-0.704
		Acetic acid (3%)	Water	0.871*	0	1.082	0.660
			Ethanol	0.492*	0	0.704	0.281
		Etanol (15%)	Water	-0.871*	0	-0.660	-1.082
			Acetic acid	-0.378*	0	-0.167	-0.590
Sample 4	30°C - 90 min	Water	Acetic acid	-0.047	1.000	0.164	-0.258
			Ethanol	0.525*	0	0.736	0.314
		Acetic acid (3%)	Water	0.047	1.000	0.258	-0.164
			Ethanol	0.572*	0	0.783	0.361
		Etanol (15%)	Water	-0.572*	0	-0.361	-0.783
			Acetic acid	-0.525*	0	-0.314	-0.736

2011; Chik *et al.*, 2011). Chik *et al.* measured melamine migration from 41 samples of food serving dishes to food simulants. In that study, samples were exposed to two types of food simulants (3% acetic acid and distilled water) under three test conditions (25, 70 and 100 °C) for 30 min, using LC-MS/MS device. The results of their study suggested that excessive heat and acidity may directly affect melamine migration from melamine-ware products. Melamine migration observed in all samples was less than the specific migration limit (SML). In addition, Lu *et al.* examined melamine migration from dairy products packaged in 37 samples. The simulating solutions were distilled water, 3% acetic acid, n-hexane and 15% ethanol. It was found that the migration in 15% (v/v) ethanol aqueous solution and 3% (w/v) acetic acid aqueous solution were greater than in distilled water (Lu *et al.*, 2009). In a similar study, Chao-Yi Chien *et al.* measured melamine migration from different material-made tableware by LC-MS/MS device. Test samples were filled with pre-warmed distilled water and 3% acetic acid as the simulant at temperatures ranging from 20 to 90 °C for 15 to 30 min. They reported high melamine migration levels from the melamine-made samples containing 3% acetic acid in a water bath of 90 °C for 30 min, whereas melamine was not

detected in other material-made samples under the same conditions (Chao-Yi Chien *et al.*, 2011).

## Conclusion

All over the world, there is growing public concerns about the safety of food contact materials. This study investigated a method to measure melamine migration from melamine-ware to food and showed that under experimental conditions acidity affected melamine migration towards higher levels but there were low levels of melamine migration (less than specific migration limit) from melamine-ware samples to simulants. However, long term exposure to melamine and its effect on public health should be considered. Therefore, precautions should be taken with regard to choosing melamine wares for exposure to food stuff.

## REFERENCES

- Chien C, Wu C, Liu C, Chen BH, Huang, SP, Chou, YH. (2011). High melamine migration in daily-use melamine-made tableware. *J Hazard Mater* **188**(1–3): 350–6.

- Commission of the European Communities (CEC). (1996). Proceedings of the International Conference on Harmonization, [http://www.fda.gov/Drugs/Guidance/Compliance\\_Regulatory\\_Information/Guidances/ucm265700.htm](http://www.fda.gov/Drugs/Guidance/Compliance_Regulatory_Information/Guidances/ucm265700.htm).
- Chik Z, Haron DE, Ahmad ED, Taha H, Mustafa AM. (2011). Analysis of melamine migration from melamine food contact articles. *Food Addit Contam Part A Chem Anal Control Expo Risk Assess.* **28**(7): 967–73.
- FDA. (2007). Interim Melamine and Analogues Safety/Risk Assessment, US Food and Drug Administration, May 25, 2007. Available at: <http://www.cfsan.fda.gov/~7Edms/melamra.html>. Accessed December 18, 2008.
- Jacaab micronized melamine J-40 technical data sheet [Internet]. (2007). JACAAB L.L.C. Manufacturing & Repackaging of Specialty Chemicals; [cited 2007 June 1]. Available from: <http://www.jacaab.com/msds/Jacaab%20Melamine%20J-40%20TDS.pdf>
- Jeong WI, Do SH, Jeong DH, Chung JY, Yang HJ, Yuan DW, Hong IH, Park JK, Goo MJ, Jeong KS. (2006). Canine renal failure syndrome in three dogs. *J Vet Sci* **7**(3): 299–301.
- Johannes KF. (2005). Reactive polymers fundamentals and applications: a concise guide to industrial polymers. Norwich (NY): William Andrew Publishing/Plastic Design Library
- Hau AK, Kwan TH, Li PK. (2009). Melamine Toxicity and the Kidney. *J Am Soc Nephrol.* **20**(2): 245–50.
- Lokensgard E, Richardson TL. (2003). Industrial plastics: theory and application. 3rd ed. Clifton Park (NY): Delmar Learning.
- Lu J, Xiao J, Yang DJ, Wang ZT, Jiang DG, Fang CR, Yang J. (2009). Study on migration of melamine from food packaging materials on markets. *Biomed Environ Sci.* **22**(2): 104–8
- Risk Assessment Studies (RAS). (2010). Report No. 42, Chemical Hazard Evaluation. (2010). Safety of Melamine-ware Available for Use on Local Food Premises. Centre for Food Safety Food and Environmental Hygiene Department the Government of the Hong Kong Special Administrative Region.
- WHO. (2009). Toxicological and health aspects of melamine and cyanuric acid. Report of a WHO Expert Meeting in collaboration with FAO supported by Health Canada. Geneva: World Health Organization.

ORIGINAL ARTICLE

# Alteration in MDA, GSH level and hematological changes due to thiamine deficiency in *Mus musculus*

Anupama SHARMA, Renu BIST

Bioscience and Biotechnology Department, Banasthali University, Banasthali-304022, Rajasthan, India

ITX110418A10 • Received: 16 June 2017 • Accepted: 17 March 2018

## ABSTRACT

It is known that thiamine deficiency may lead to Alzheimer's diseases in humans. The present study has thus been conducted to understand the role of thiamine deficiency with respect to alteration in the peripheral blood of Swiss albino mice. For this purpose, adult Swiss albino mice (6–8 week old) were divided into three groups. The first group was control; the second (group II) and the third group (group III) were made thiamine deficient for 08 and 10 days respectively. Thiamine deficiency was induced in mice by injecting pyrithiamine (5 µg/10 g bwt) and feeding a thiamine deficient diet. The erythrocytes, leukocytes count, hemoglobin, hematocrit value, mass cell volume, mean corpuscular hemoglobin in blood of mice were determined by hematoanalyzer. Malondialdehyde (MDA) and reduced glutathione (GSH) level was also determined in serum of treated and non-treated groups. A significant reduction in leukocyte and erythrocyte count was observed in both the thiamine deficient groups as compared to control. Levels of hemoglobin and hematocrit value were also declined in the thiamine deficient groups. Enhancement in mass cell volume (MCV) level and decline in mean corpuscular hemoglobin (MCH) levels were observed in both thiamine deficient groups with respect to control. Inter-group comparison of all parameters also showed a significant value at  $p < 0.01$ . In comparison with the control group, elevation in MDA and decline in GSH level was observed in both thiamine deficient groups which were statistically significant. These data indicate that thiamine deficiency leads to significant alterations in the hematological parameters as well as in MDA and GSH level.

**KEY WORDS:** blood; hematological alterations; thiamine deficiency; Alzheimer's diseases

## Introduction

Nutrition is one of the basic needs for proper functioning of various organ systems. Early malnutrition may have harmful effects not only on the immune function but also on the development of the nervous system, gastrointestinal tract, and it can cause metabolic syndrome (He *et al.*, 2009). Thiamine (vitamin B1) is a water soluble vitamin and cannot be synthesized. Thiamine is essential in the body for energy metabolism, specifically 0.33 mg of thiamine is required for generation of 4400 kJ of energy (Smithline *et al.*, 2012). The primary active form of thiamine is thiamine diphosphate (ThDP). It is a cofactor of several multienzyme complexes related to glucose metabolism, *i.e.* pyruvate dehydrogenase

complex (PDHC),  $\alpha$ -ketoglutarate dehydrogenase complex, and transketolase. Thiamine deficiency (TD) provides a pertinent experimental system to understand the neurodegenerative disorder in which mitochondrial dysfunction attributes to the failure of tricarboxylic citric acid (TCA) cycle enzymes (Sheu *et al.*, 1998; Sharma *et al.*, 2013).

Further, blood is a protective, regulatory, and homeostatic connective tissue and consists of blood cells and plasma (Nasyrova *et al.*, 2006; Eze *et al.*, 2010). It is an essential medium which circulates around the body within the cardiovascular system and acts as a transportation system for many substances, such as O<sub>2</sub>, CO<sub>2</sub>, drugs, hormones and xenobiotics. In blood, transportation of oxygen is achieved through the presence of hemoglobin (Ashton, 2013). Blood profiles in living beings determine the internal environment and recognizing the causes of impairment in homeostasis as corroborated by marked fluctuations in physiological indices in different internal and external environmental conditions (Koubkova, 2002; Sattar & Mirza, 2009). Blood values are used for

Correspondence address:

**Dr. Anupama Sharma, MSc., PhD.**

Department of Bioscience and Biotechnology

Banasthali University, Banasthali-304022, India

TEL.: +391-9414933057

E-MAIL: anupamasharma.biotech@gmail.com

determining the level of stress as well as the well-being of the animal. Hematological examination is a manifestation of an animal's responses to its external and internal environments (Koubkova *et al.*, 2002; Carlota *et al.*, 2015), nutritional deficiencies and stress (Agarwal *et al.*, 2016). The hematological parameters are biological tools to assess alterations in the health and physiological status which could not be detected during physical examinations (Kronfeld & Medway, 1969). Thiamine deficiency might affect hematopoiesis and various other organ systems. Further, erythrocytes are the most important blood cells in the human body. The main function of red blood cells (RBCs) is to carry oxygen to the cells during respiration (Johnston & Morris, 1996; Chineke *et al.*, 2006). Decrease in the level of RBC's causes anemia (Tejashwini & Padma, 2015), White blood cells are an important part of the body's immune system. They protect against certain bacteria, viruses, cancer cells, infectious diseases. Low white blood cell counts (WBC) may indicate that a person is in risk of infection, whereas high WBC counts generates antibodies in phagocytosis and high degree of resistance to diseases (Soetan *et al.*, 2013) and might indicate an existing infection and tissue damage (Tejashwini & Padma, 2015).

Additionally, hemoglobin (Hb) is the oxygen-carrying protein in blood, providing an indication of the capacity of the blood to oxygenate the tissue for oxidation of ingested food to release energy for the other body functions as well as to transport carbon dioxide out of the body (Ugwuene, 2011; Omiyale *et al.*, 2012; Isaac *et al.*, 2013; Soetan *et al.*, 2013). Further, thiobarbituric acid reactive substance (TBARS) is the end product of lipid peroxidation (LPO), which is an important event induced by oxidative stress related to the pathogenesis of several diseases (Halliwell & Gutteridge, 1969; Reznick & Packer, 1993). Increased reactive oxygen species (ROS) production in thiamine deficiency can trigger cell membrane damage, including LPO and alterations in the functional integrity of ion channels and transporters (Jhala & Hazell, 2011). GSH acts as a direct scavenger and is a major intracellular redox tampon system (Blokina *et al.*, 2003). It is a tripeptide containing cysteine that has a reactive sulfhydryl group with reductive potency, and thus it plays a critical role in detoxification of ROS (Urso & Clarkson, 2003; Jozefczak *et al.*, 2012). It has facile electron donating capacity linked to its sulfhydryl group (Kidd, 1997). GSH removes the free radicals overproduced and decreases its cellular concentration offering a defense against oxidative stress. Glutathione is one of the major outcomes of free radical-mediated injury leading to the production of a range of quite stable end products that are capable to initiate LPO (Ferreiro *et al.*, 2012). Previous studies suggest that thiamine deficiency reduces the concentration of thiamine in the spleen (Fitzsimons *et al.*, 2005; Ketola *et al.*, 2008). In this perspective, the present study was conducted to identify the effect of thiamine deficiency in hematological variables, as well as the MDA and GSH level in Swiss albino mice.

## Materials and methods

### Chemicals

Pyriethamine hydrobromide was procured from Sigma (MO, USA). 5, 5'-dithiobis-2-nitrobenzoic acid, (DTNB), ethylene diamine tetraacetic acid (EDTA), tris hydrochloride, trichloroacetic acid (TCA), 2-thiobarbituric acid (TBA) were purchased from Sisco research laboratories (Mumbai, India). All other chemicals were used of analytical grade.

### Animal care and monitoring

Swiss albino Male mice (6–8 week old) were procured from C.C.S. Haryana Agricultural University, Hisar. They were fed pelleted diet (Hindustan Uniliver Limited) and water *ad libitum*. After 7 days of adaptation, the mice were used for experimental purpose. Maintenance and treatment of animals was done in accordance with the Committee for the Purpose of Control and Supervision of Experimentation on Animals (CPCSEA), New Delhi.

### Experimental design

The animals were divided into three groups with minimum of six animals in each group and treated as follows:

- |           |  |
|-----------|--|
| Group I   | Control                                |
| Group II  | Thiamine deficient for 08 days (TD 08) |
| Group III | Thiamine deficient for 10 days (TD 10) |

### Induction of thiamine deficiency (TD)

Mice were made thiamine deficient by injecting the pyriethamine hydrobromide (5 µg/10 g of body weight) intraperitoneally daily for 8 and 10 days and fed with thiamine deficient pelleted diet (MP Biomedical, Mumbai, India). Control animals were fed a normal diet.

### Determination of hematological parameters

After the 8 and 10 days exposure to thiamine deficient diet and pyriethamine hydrobromide, blood was collected from retro-orbital sinus of mice. 20 µl of blood of different experimental groups were kept in EDTA vial and 500 µl sample diluent was added. The samples were loaded on the hematoanalyzer (PocH-100i). Hematological parameters such as RBC, WBC count, hemoglobin (Hb), hematocrit value (HCT), mass cell volume(MCV) and mean corpuscular hemoglobin(MCH) were determined in control and treated groups.

### Estimation of malondialdehyde (MDA) and GSH level

#### Serum separation

After exposure duration, whole blood samples were drawn from retro orbital sinuses of control and treated mice. Blood samples were collected and allowed to clot for half an hour and centrifuged at 3500 rpm for 10 min at 4°C. Serum was isolated and used for determination of oxidative stress markers: thiobarbituric acid reactive substances (TBARS) and reduced glutathione (GSH).

#### Estimation of MDA level

MDA assay has been widely used to measure LPO. MDA is one of the end products derived from the breakdown

of polyunsaturated fatty acids and related esters. MDA (LPO product) reacts with TBA and forms MDA-TBA adduct which gives a characteristically pink color in high temperature with acidic environment. The LPO product was read at 512 nm spectrophotometrically (Ohkawa *et al.*, 1979).

#### Assessment of reduced glutathione (GSH) level

GSH level served as an index for determining the extent of oxidative stress. GSH was determined by Ellman's method. First, the serum sample is made protein free and then reduced glutathione reacts with DTNB and forms 5-mercapto-2-nitrobenzoic acid giving a light yellow color. Spectrophotometrically reduced glutathione level was measured at 412 nm (Ellman's 1959).

#### Data analysis and statistics

The data were represented as Mean±SEM. The statistical analysis was done by using one-way analysis of variance (ANOVA) (Statistical Package of Social Science editor 16). Intergroup comparisons were made by *post-hoc* comparison analysis and significant level was measured at 99%.

## Results

The data on erythrocyte count, Hb level and MCH level indicated a significant decline in all three parameters in both 8- and 10-day thiamine deficient mice in comparison to control (Figure 1). The hematocrit value also showed a similar pattern of changes (Figure 2) as erythrocyte count and Hb level. The decline in MCH level was more pronounced in 10-day thiamine deficient mice with respect to 8 days and this difference was statistically significant (Figure 2). Whereas MCV was increased significantly in 8 and 10 days thiamine deficient groups as compared to non-thiamine deficient group (Figure 2).

The leukocyte count declined significantly ( $p < 0.01$ ) in thiamine deficient groups for 8 and 10 days with respect to control group. The decline was more pronounced in 10-day thiamine deficient mice with respect to 8 days, which was statistically significant (Figure 3).

GSH level was considerably decreased ( $p < 0.01$ ) in both the thiamine deficient groups as compared to control group (Figure 4). Maximum reduction of GSH level was observed in 10-day thiamine deficient group as compared to the 8-day thiamine deficient group and non-treated group which was statistically non-significant.

The level of MDA was significantly ( $p < 0.01$ ) higher in the serum of both the treated groups as compared to control group. The elevation of MDA level was more pronounced ( $p < 0.01$ ) in the mice of 10-day thiamine deficient group with respect to 8-day deficient mice (Figure 5).

## Discussion

Thiamine is an essential water-soluble vitamin and its availability is a prerequisite for normal cellular

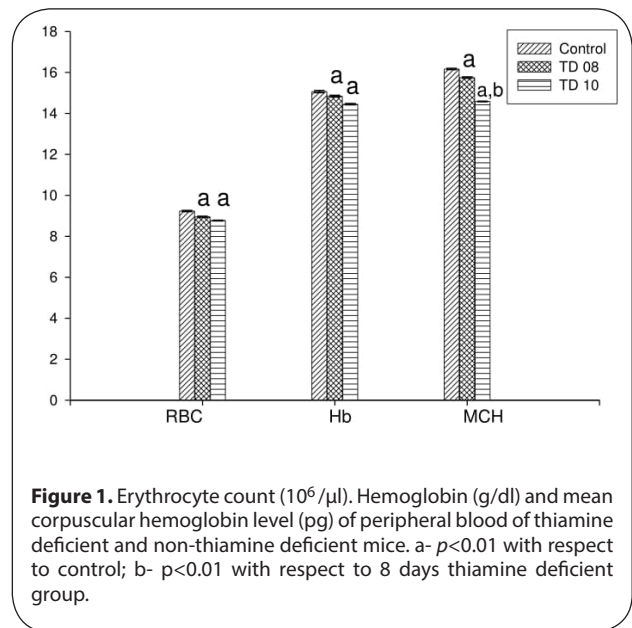


**Figure 1.** Erythrocyte count ( $10^6/\mu\text{l}$ ), Hemoglobin (g/dl) and mean corpuscular hemoglobin level (pg) of peripheral blood of thiamine deficient and non-thiamine deficient mice. a-  $p < 0.01$  with respect to control; b-  $p < 0.01$  with respect to 8 days thiamine deficient group.

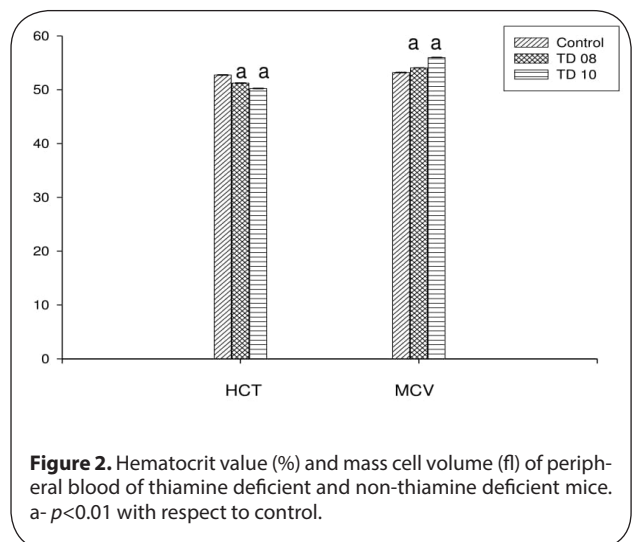


**Figure 2.** Hematocrit value (%) and mass cell volume (fl) of peripheral blood of thiamine deficient and non-thiamine deficient mice. a-  $p < 0.01$  with respect to control.

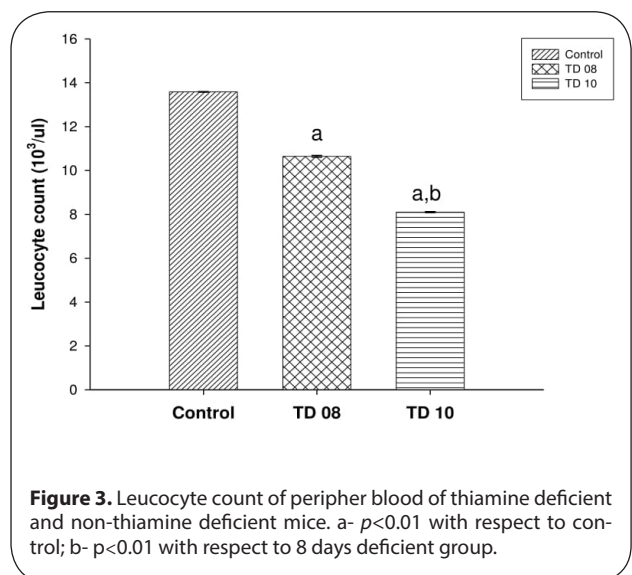


**Figure 3.** Leucocyte count of peripher blood of thiamine deficient and non-thiamine deficient mice. a-  $p < 0.01$  with respect to control; b-  $p < 0.01$  with respect to 8 days deficient group.

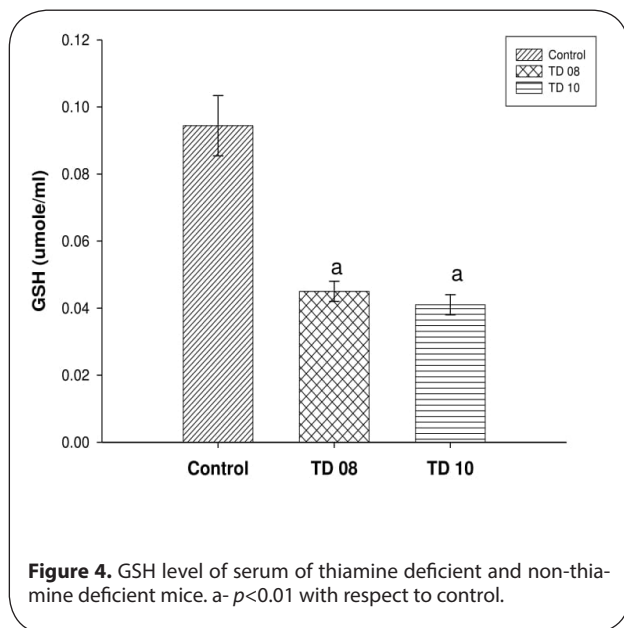


**Figure 4.** GSH level of serum of thiamine deficient and non-thiamine deficient mice. a-  $p < 0.01$  with respect to control.

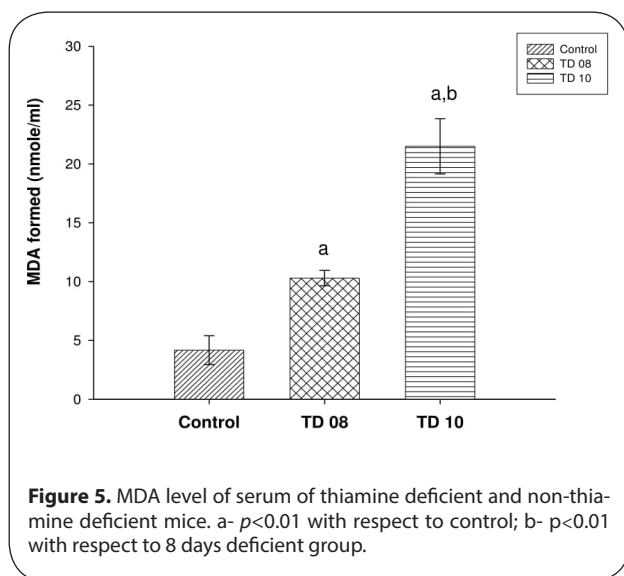


**Figure 5.** MDA level of serum of thiamine deficient and non-thiamine deficient mice. a-  $p < 0.01$  with respect to control; b-  $p < 0.01$  with respect to 8 days deficient group.

metabolism of the brain (Liu *et al.*, 2016) and needed for various other physiological functions of the body. It serves as a specific cofactor of certain enzymes involved in energy metabolism of cells and its deficiency may affect enzymes of the TCA cycle (Sharma *et al.*, 2013; Sharma & Bist, 2014). Thiamine deficiency may also be associated with brain degenerative conditions such as Parkinson's and Alzheimer's disease (Hazell & Butterworth, 2009; Hazell, 2009; Karuppagounder *et al.*, 2009; Hirsch & Parrott, 2012). Blood is a loose connective tissue which is first to be affected by a stress introduced into the body and therefore proposes an insightful and consistent indicator, which could be effectively used to assess the magnitude of oxidative stress (Lakshmanan *et al.*, 2013). The results showed alterations in the erythrocyte and leukocyte count, Hb, HCT, MCH, MCV in peripheral

blood of thiamine deficient groups as compared to control. The decline in erythrocyte count may be due to inhibition of pyrimidine 5-nucleotidase that results in an accumulation of nucleotides in the erythrocyte. This enzyme inhibition and nucleotide accumulation affect erythrocyte membrane stability and survival by alteration of cellular energetics. Falahtakar *et al.* (2014) reported another reason for the reduction in RBC and Hb level as due to altered hematopoiesis. It directly affects the blood forming organs which results in the excessive destruction in RBC synthesis (Badraoui *et al.*, 2011). The decline in RBC count in peripheral blood generates free radicals and causes oxidative stress (Stoys, 1990; Fibach *et al.*, 2008), supporting the present study by observing the elevation in MDA and decline in GSH level in the serum of thiamine deficient groups.

Further, decrease in leukocyte count was observed in the thiamine deficient group and Hb, MCH hematocrit value was also decreased in exposed animals with thiamine deficiency. It may reflect anemia which is often mainly due to destruction of erythrocytes. Nevertheless, the decline in erythrocyte count is ~3% (TD 08 days) and ~5% (TD 10 days) as compared to reduction in leukocyte count, which was 21.6% (TD 08 days) and 40.3% (TD 10 days) with respect to control group, indicating more pronounced changes in leukocyte count than erythrocyte count.

The data of the present study show the elevation in MDA level and reduction in GSH level in thiamine deficient mice which may act as key markers of oxidative stress. Several previous reports showed an increase in MDA level due to thiamine deficiency in different organs, such as heart (Shangari *et al.*, 2003), liver and brain of thiamine deficient mice (Sharma *et al.*, 2013; Sharma & Bist, 2014), exhibiting the conditions of stress. As the thiamine deficiency increases MDA level which represents the direct relation with dose and duration. GSH level in serum was found to be reduced in thiamine deficient exposed group as compared to control. These results are in agreement with earlier findings of Sharma *et al.* (2013; 2014) regarding the reduction in GSH level in brain mitochondria as well as liver tissue in thiamine deficient mice. Earlier, Shangari *et al.* (2003) also reported a reduction in cellular GSH level in rat hepatocytes under thiamine-deficient conditions. Glutathione is involved in various cellular functions, ranging from the control of physical and chemical properties of cellular proteins and peptides to the detoxification of free radicals. Reduction in GSH level and increase in MDA level promotes stress in serum of thiamine deficient group, which acts as a key marker of oxidative stress.

## Conclusion

The current study concluded that thiamine deficiency alters the changes in hematological parameters and induces oxidative stress in Swiss albino mice, which may lead to neurodegeneration.

## Acknowledgments

The authors are thankful to the Vice Chancellor, Head of Department (Bioscience and Biotechnology), Banasthali University for providing the facilities to carry out the study. The financial support from the Indian Council of Medical Research, New Delhi, India, in the form of Senior Research Fellowship (45/19/2011-CMB/BMS) to AS is gratefully acknowledged. I am highly thankful to Dr. Sunil Kumar (Scientist G & Director-In-Charge, NIOH, Ahmedabad) for helping in preparation of the manuscript.

## REFERENCES

- Agarwal S, Chaudhary B, Bist R. (2016). Bacoside A and bromelain relieve dichlorvos induced changes in oxidative responses in mice serum. *Chemico-biological Interactions* **254**: 173–178.
- Ashton N. (2013). Physiology of red and white blood cells. *Anaesth Intensive Care* **14**(6): 261–266.
- Badraoui R, Abdelmoula NB, Rebai T. (2011) Erythrocytes oxidative damage and hematological effects of 2, 4, 4' 5-tetrachlorodiphenyl sulfone in rats. *Experimental and Toxicologic Pathology* **63**(5): 479–482.
- Blokhina O, Virolainen E, Fagerstedt KV. (2003). Antioxidants, oxidative damage and oxygen deprivation stress: a review. *Annals of Botany* **91**(2): 179–194.
- Chineke CA, Ologun AG, Ikeobi CON. (2006). Haematological parameters in rabbit breeds and crosses in humid tropics. *Pak J Biol Sci.* **9**(11): 2102–2106.
- Ellman GL. (1959). Tissue sulfhydryl groups. *Arch Biochem Biophys* **82**: 70–77.
- Eze JI, Onunkwo JI, Shoyinka SVO, Chah FK, Ngene AA, Okolinta N, Onyenwe IW. (2015). Haematological profiles of pigs raised under intensive management system in South-Eastern Nigeria. *Nigerian Veterinary Journal* **31**(2): 115–123.
- Falahatkar B, Akhavan SR, Poursaeid S, Hasirbaf E. (2014). Use of sex steroid profiles and hematological indices to identify perinucleolus and migratory gonadal stages of captive Siberian sturgeon *Acipenser baeri* (Brandt, 1869) females. *Journal of Applied Ichthyology* **30**(6): 1578–1584.
- Ferreiro E, Baldeiras I, Ferreira IL, Costa RO, Rego AC, Pereira CF, Oliveira CR. (2012). Mitochondrial-and endoplasmic reticulum-associated oxidative stress in Alzheimer's disease: from pathogenesis to biomarkers. *International Journal of Cell Biology* **2012**: 1–23.
- Fibach E, Rachmilewitz E. (2008). The role of oxidative stress in hemolytic anemia. *Current Molecular Medicine* **8**(7): 609–619.
- Fitzsimons JD, Williston B, Amcoff P, Balk L, Pecor C, Ketola HG, Honeyfield DC. (2005). The effect of thiamine injection on upstream migration, survival, and thiamine status of putative thiamine-deficient coho salmon. *Journal of Aquatic Animal Health* **17**(1): 48–58.
- Halliwell B, Gutteridge JMC. (1985). Oxygen radicals and the nervous system. *Trends in Neurosciences* **8**: 22–26.
- Hazell AS. (2009). Astrocytes are a major target in thiamine deficiency and Wernicke's encephalopathy. *Neurochemistry International* **55**(1): 129–135.
- Hazell AS, Butterworth RF. (2009) Update of cell damage mechanisms in thiamine deficiency: focus on oxidative stress, excitotoxicity and inflammation. *Alcohol & Alcoholism* **44**(2): 141–147.
- He Z, Sun Z, Liu S, Zhan, Q, Tan Z. (2009). Effects of early malnutrition on mental system, metabolic syndrome, immunity and the gastrointestinal tract. *Journal of Veterinary Medical Science* **71**(9): 1143–1150.
- Hirsch JA, Parrott J. (2012). New considerations on the neuromodulatory role of thiamine. *Pharmacology*. **89**(1–2): 111–116.
- Isaac LJ, Abah G, Akpan B, Ekaett, IU (2013) Haematological properties of different breeds and sexes of rabbits. In *Proceedings of the 18th Annual Conference of Animal Science Association of Nigeria*, 24–27.
- Jhala SS, Hazell AS. (2011). Modeling neurodegenerative disease pathophysiology in thiamine deficiency: consequences of impaired oxidative metabolism. *Neurochemistry International* **58**(3): 248–260.
- Johnston JK, Morris DD (1996) Alterations in blood proteins. In B. P. Smith (Ed.), *International Animal Medicine* (2nd ed.). USA: Mosby Publishers.
- Jozefczak M, Remans T, Vangronsveld J, Cuypers A. (2012). Glutathione is a key player in metal-induced oxidative stress defenses. *International Journal of Molecular Sciences* **13**(3): 3145–3175.
- Karuppagounder SS, Xu H, Shi Q, Chen LH, Pedrin, S, Pechman D, Gibson GE. (2009). Thiamine deficiency induces oxidative stress and exacerbates the plaque pathology in Alzheimer's mouse model. *Neurobiology of Aging* **30**(10): 1587–1600.
- Ketola HG, Isaacs GR, Robins JS, Lloyd RC. (2008). Effectiveness and retention of thiamine and its analogs administered to steelhead and landlocked Atlantic salmon. *Journal of Aquatic Animal Health* **20**(1): 29–38.
- Kidd PM. (1997). Glutathione: systemic protectant against oxidative and free radical damage. *Altern Med Rev* **2**(3): 155–176.
- Koubkova M, Haertlova H, Knizkova I, Kunc P, Flusser J, Dolezal O. (2002). Influence of high environmental temperatures and evaporative cooling on some physiological, hematological and biochemical parameters in high-yielding dairy cows. *Czech Journal of Animal Science-UZPI* **47**(8): 309–318.
- Kronfeld DS, Medway W. (1969). In A textbook of veterinary clinical pathology. Edited by W. Medway, J. E. Prier, and J. S. Wilkinson. The Williams and Wilkins Co., Baltimore.
- Lakshmanan SA, Rajendran CS. (2013). Impact of Dichlorvos on tissue glyco-gen and protein content in freshwater fingerlings, *Oreochromis mossambicus* (Peters). *International Journal of Research in Environmental Science and Technology* **3**(1): 19–25.
- Liu D, Ke Z, Luo J. (2017). Thiamine deficiency and neurodegeneration: the interplay among oxidative stress, endoplasmic reticulum stress, and autophagy. *Molecular Neurobiology* **54**(7): 5440–5448.
- Nasyrova DI, Sapronova AY, Nigmatullina RR, Ugrumov MV. (2006) Changes in blood plasma volume in rats during ontogenesis. *Russian Journal of Developmental Biology* **37**(5): 301–305.
- Ohkawa H, Ohshi N, Yagi K. (1979). Assay of lipid peroxides in animal tissues by thiobarbituric acid reaction. *Anal Biochem* **95**: 351–358.
- Omiyale CA, Yisa AG, Ali-Dankrah LA. (2012). Haematological characteristics of Yankasa sheep fed Fonio (*Digitaria iburua*) straw based diets. In *Proceeding of the 37th Annual Conference of the Nigerian Society for Animal Production* **37**: 108–110.
- Reznick AZ, Packer L. (1993) Free radicals and antioxidants in muscular and neurological diseases and Disorders. In *Free radicals: from basic science to Medicine* 425–437.
- Sattar A, Mirza RH. (2009) Haematological parameters in exotic cows during gestation and lactation under subtropical conditions. *Pakistan Veterinary Journal* **29**(3): 129–132.
- Shangari N, Bruce WR, Poon R, O'Brien, PJ. (2003). Toxicity of glyoxals—role of oxidative stress, metabolic detoxification and thiamine deficiency. *Biochemical Society Transactions* **31**(Pt 6): 1390–1393.
- Sharma A, Bis R. (2014). Thiamine deprivation disturbs cholinergic system and oxidative stress in liver of *Mus musculus*. *Int J Pharmacol Pharm Sci* **6**: 139–143.
- Sharma A, Bist R, Bubber P. (2013). Thiamine deficiency induces oxidative stress in brain mitochondria of *Mus musculus*. *Journal of Physiology and Biochemistry* **69**(3): 539–546.
- Sheu KF, Calingasan NY, Lindsay JG, Gibson GE. (1998). Immunochemical characterization of the deficiency of the alpha ketoglutarate dehydrogenase complex in thiamine-deficient rat brain. *J Neurochem* **70**(3): 1143–1150.
- Smithline HA, Donnino M, Greenblatt DJ. (2012). Pharmacokinetics of high-dose oral thiamine hydrochloride in healthy subjects. *BMC Clinical Pharmacology* **12**(1): 4.
- Soetan KO, Akinrinde AS, Ajibade TO. (2013). Preliminary studies on the haematological parameters of cockerels fed raw and processed guinea corn (*Sorghum bicolor*). In *Proceedings of 38th Annual Conference of Nigerian Society for Animal Production* pp. 49–52.
- Stohs SJ. (1990). Oxidative stress induced by 2, 3, 7, 8-tetrachlorodibenzo-p-dioxin (TCDD). *Free Radical Biology and Medicine* **9**(1): 79–90.
- Tejashwini M, Padma MC. (2015). Counting of RBC's and WBC's Using Image Processing Technique. *International Journal on Recent and Innovation Trends in Computing and Communication* **3**(5): 2948–2953.
- Ugwuene MC. (2011). Effect of dietary palm kernel meal for maize on the haematological and serum chemistry of broiler turkey. *Nigerian Journal of Animal Science* **13**: 93–103.
- Urso ML, Clarkson PM. (2003). Oxidative stress, exercise and antioxidant supplementation. *Toxicology* **189**(1): 41–54.